

**The Systems Biology of the Circadian
Control of Freezing Tolerance in
*Arabidopsis thaliana***

Jack Keily

Submitted for the degree of Doctor of Philosophy in Biological
Sciences

December 2012

The Systems Biology of the Circadian Control of Freezing Tolerance in *Arabidopsis thaliana*

Jack Keily

December 2012

Submitted to the University of Exeter as a thesis for the degree of Doctor
of Philosophy in Biological Sciences

This thesis is available for Library use on the understanding that it is
copyright material and that no quotation from the thesis may be published
without proper acknowledgement.

I certify that all material in this thesis which is not my own work has been
identified and that no material has previously been submitted and
approved for the award of a degree by this or any other University.

Signature.....

Abstract

The *Arabidopsis thaliana* circadian clock is involved in regulating several plant systems including light signalling, germination and the cold signalling pathway. The role of the circadian clock in regulating far-red and red light induced dormancy and germination, however, is not well understood. In this thesis it is shown that the circadian clock does not seem to be involved in regulating far-red light induction of dormancy, but that the *TIMING OF CAB EXPRESSION 1 (TOC1)* gene is vital for red light induced germination to occur.

In *Arabidopsis thaliana*, the transcription factors, C-REPEAT BINDING FACTORS (CBFs) are key components of the cold acclimation pathway. The expression of the *CBFs* has recently been shown to be regulated by the circadian clock; however, our understanding of how the *CBFs* are regulated by the clock is far from complete.

In the main focus of this thesis a systems biology approach was utilised to try and better understand the circadian regulation of plant cold responses, specifically the manner by which the circadian clock regulates the cold acclimation pathway *C-REPEAT BINDING FACTOR 3 (CBF3)* gene. Freezing tolerance assays were carried out to increase our knowledge of the clock regulation of the cold signalling pathway. Circadian clock mutant lines without previously reported freezing tolerance phenotypes were identified in the *TOC1* mutant, *toc1-101*, and the *EARLY FLOWERING 3 (ELF3)* and *LUX ARRHYTHMO (LUX)* mutants *elf3-1* and *lux*. The freezing assay data was used to influence model designs for the circadian regulation of *CBF3* expression. Several potential models of *CBF3* regulation were created. The models were then optimised against publically available microarray gene expression data. Model selection using a Corrected Akaike Information Criterion (AICc) was utilised to establish models that best fit biological data. Predictions made by the models were then tested, thus leading to the establishment of new circadian clock mechanisms of *CBF3* being discovered.

The modelling procedure predicted the involvement of the Evening Complex (EC) and TOC1 in regulating *CBF3* expression as well as the already reported regulation by LATE ELONGATED HYPOCOTYL (LHY) and CIRCADIAN CLOCK ASSOCIATED1 (CCA1); the PSEUDO-RESPONSE REGULATORS (PRRs) which had been predicted as direct regulators of the CBFs were not needed to produce correct *CBF3* expression in any of the potential models.

The direct TOC1 and Evening Complex regulation of *CBF3* promotion was then confirmed by chromatin immunoprecipitation.

Contents

The Systems Biology of the Circadian Control of Freezing Tolerance in <i>Arabidopsis thaliana</i>	3
Abstract	4
Contents	10
List of Figures	12
List of Tables	13
Abbreviations	14
Publications	18
1 Introduction	19
1.1 Circadian clocks	19
1.1.1 Introduction to circadian clocks	19
1.1.2 Circadian clocks are found throughout nature	21
1.2 The <i>Arabidopsis</i> circadian clock	22
1.2.1 <i>Arabidopsis</i> as a model plant organism	22
1.2.2 Transcriptional regulation of <i>Arabidopsis</i> circadian clock system .	23
1.2.3 Posttranscriptional regulation of the <i>Arabidopsis</i> circadian clock .	27
1.2.4 Inputs of the <i>Arabidopsis</i> circadian clock	29
1.2.5 Outputs of the <i>Arabidopsis</i> circadian clock	29
1.2.6 Circadian control of pathogen responses	34
1.3 Modelling biological systems	35
1.3.1 What is systems biology?	35
1.3.2 Mathematical modelling of gene expression	36

Contents

1.3.3	The Development of the <i>Arabidopsis</i> circadian clock mathematical model	43
1.4	The cold acclimation pathway	49
1.5	Temperature, light and seed physiology	57
1.6	Thesis aims and objectives	59
2	Materials and Methods	61
2.1	Mutant lines	61
2.2	Growth media for plants	61
2.3	Plant growth and seed harvest	61
2.4	Seed sterilisation	63
2.5	Germination assays	63
2.5.1	Red light germination assay	63
2.5.2	Far-red light germination assay	64
2.5.3	Low temperature cold stratification period assay	64
2.6	Freezing tolerance assay	65
2.7	Molecular biology	65
2.7.1	Purification of total RNA from plant tissue	66
2.7.2	cDNA synthesis	67
2.7.3	qRT-PCR	67
2.7.4	ChIP	70
2.8	Modelling	74
2.9	Model creation in CellDesigner	74
2.10	Model optimisation in SBSIVisual	77
2.11	AICc in Matlab	77
2.12	Perturbations to the models	79
2.13	<i>CBF3</i> promoter region analysis	79
3	Results: Light, and clock regulation of germination and dormancy	80
3.1	Determination of protocol for assay on light effect on germination	81
3.1.1	How does growth media affect germination in different ecotypes of <i>Arabidopsis thaliana</i> react to different light conditions?	82
3.1.2	How does cold stratification affect the germination of <i>Arabidopsis</i> seeds of different ecotypes?	85
3.2	Do the core clock genes have a role in light regulated germination?	88
3.2.1	Far-red light sensitivity is not lost in clock mutants	88

Contents

3.2.2	The effects of red light on germination	92
3.3	The role of clock genes in regulating germination under low temperature conditions	96
3.4	Discussion	98
3.4.1	Circadian clock genes and their role in light regulated germination	98
3.4.2	The role of clock genes in regulating germination under low temperature conditions	102
3.4.3	Chapter 03 summary	103
4	Results: Connecting the circadian clock to the cold acclimation pathway	104
4.1	The temperature at which a plant is grown and the temperature at which a plant is frozen has varying effects on plant survivability	106
4.2	Additional circadian genes are shown to have a role in freezing tolerance	110
4.2.1	Survival rates when frozen at -3°C	111
4.2.2	Survival rates when frozen at -5°C	113
4.3	<i>CBF1</i> expression can be altered by long term exposure to different temperatures	118
4.4	Discussion	121
4.4.1	Circadian clock components involved in freezing tolerance	121
4.4.2	<i>CBF1</i> expression can be altered by long term exposure to different temperatures	126
4.4.3	Chapter 4 summary	128
5	Results: Modelling the circadian clock regulation of <i>CBF3</i> expression	130
5.1	Model construction and selection	131
5.1.1	Model construction	131
5.1.2	Model optimisation	132
5.1.3	Model selection	135
5.2	The Pokhilko 2010 circadian clock model to regulate simulated <i>CBF3</i> expression	136
5.2.1	Several potential models of <i>CBF3</i> regulation by the circadian clock were created	136
5.2.2	<i>CBF3</i> inhibition by TOC1 gives the best fit to biological data	139
5.2.3	Model simulations under different day length periods can be used to eliminate potential models	140

Contents

5.2.4	The models can be made to simulate <i>CBF3</i> expression in circadian clock mutants	142
5.2.5	Predictions made by the models	144
5.3	The Pokhilko 2012 circadian clock model to regulate simulated <i>CBF3</i> expression	146
5.3.1	The potential models tested for <i>CBF3</i> regulation by the circadian clock	148
5.3.2	LHY up-regulation combined with TOC1 and EC inhibition of <i>CBF3</i> expression gives the best fit to biological data	149
5.3.3	<i>CBF3</i> Expression profiles in the new models	151
5.3.4	Day length alters peak <i>CBF3</i> expression in model simulations	155
5.3.5	How well do the models recreate known mutations from the literature?	157
5.3.6	Simulations of perturbations to the clock	160
5.4	Testing the predictions made by the model	162
5.4.1	Plants with the <i>toc1-101</i> mutation have increased peak <i>CBF3</i> expression	162
5.4.2	Plants with the <i>lux-5</i> mutation have decreased peak <i>CBF3</i> expression	162
5.4.3	The <i>CBF3</i> promoter region contains both TOC1 and LUX binding sites	164
5.4.4	TOC1 binds directly to the <i>CBF3</i> promoter region	167
5.4.5	Components of the Evening Complex bind directly to the <i>CBF3</i> promoter region	169
5.4.6	In models where <i>CBF3</i> expression is up-regulated by LHY/CCA1 and inhibited by TOC1 and the Evening Complex, gating of cold signalling is possible	171
5.5	Discussion	173
5.5.1	Modelling <i>CBF3</i> transcriptional regulation by the circadian clock	173
5.5.2	Model construction and selection	175
5.5.3	The Pokhilko 2012 circadian clock model to regulate simulated <i>CBF3</i> expression	177
5.5.4	Testing the predictions made by the model	182
5.5.5	Chapter 5 summary	184

6	General discussion and future work	186
6.1	The circadian clock gene <i>TOC1</i> is required for normal red light induced germination to occur	186
6.2	More circadian clock genes are involved in regulating freezing tolerance than previously thought	187
6.3	Modelling the circadian clock regulation of the cold acclimation pathway gene <i>CBF3</i>	188
6.3.1	Modelling methodology	188
6.3.2	Model validation	189
6.3.3	Further additions to the <i>Arabidopsis</i> circadian clock model of <i>CBF3</i> regulation	191
6.3.4	Modelling temperature effects	193
6.4	Further validation of the role of <i>TOC1</i> in directly regulating <i>CBF3</i> mRNA transcription	195
6.5	A systems biology approach to problem solving	195
6.6	Thesis summary	196
	Acknowledgements	198
	Appendix	199
	Bibliography	234

List of Figures

1.1	Features of a circadian rhythm	21
1.2	The <i>Arabidopsis</i> circadian clock	22
1.3	Early model of the circadian clock connecting <i>LHY/CCA1</i> and <i>TOC1</i>	25
1.4	The basic structure of systems biology	36
1.5	Three loop circadian clock model	45
1.6	The Pokhilko 2010 circadian clock model	47
1.7	Cold acclimation pathway	48
1.8	<i>CBF</i> self-regulation	54
2.1	CellDesigner	76
3.1	Red and far-red light effects on wild-type seeds imbibed on either MS agar or water agar	84
3.2	Red and far-red light effects on wild-type seeds with or without cold stratification	87
3.3	Far-red light germination rates of clock mutants	91
3.4	Red light germination rates of clock mutants	95
3.5	Germination rates of low temperature matured clock mutant seeds	97
4.1	Columbia freezing tolerance at different freezing temperatures	107
4.2	Columbia freezing tolerance of plants grown at different temperatures	109
4.3	Clock mutant freezing tolerance when frozen at -3°C	112
4.4	Clock mutant freezing tolerance when frozen at -5°C	117
4.5	<i>CBF1</i> expression when grown at different ambient temperatures	120
5.1	Microarray data of <i>CBF3</i> expression	134
5.2	<i>CBF3</i> simulated versus biological expression in different day lengths using the P2010 circadian clock model	141

List of Figures

5.3	<i>lhy</i> and <i>prp5 prp7 prp9</i> simulated <i>CBF3</i> expression in models created using the P2010 circadian clock model	143
5.4	<i>toc1 CBF3</i> simulated expression in models created using the P2010 circadian clock model	145
5.5	Difference between the P2010 and the P2012 circadian clock model . . .	147
5.6	<i>CBF3</i> simulated versus biological expression in different day lengths using the P2012 circadian clock model	153
5.7	<i>CBF3</i> simulated versus biological expression in different day lengths in the four models of best fit using the P2012 circadian clock model	154
5.8	Simulated changes in <i>CBF3</i> peak expression in different day lengths . . .	156
5.9	Mode of <i>CBF3</i> regulation by the four models of best fit	158
5.10	<i>lhy</i> and <i>prp5 prp7 prp9</i> simulated <i>CBF3</i> expression in models created using the P2012 circadian clock model	159
5.11	<i>toc1</i> and <i>lux CBF3</i> simulated expression in models created using the P2012 circadian clock model	161
5.12	<i>CBF3</i> expression in <i>lux-5</i> and <i>toc1-101</i>	164
5.13	T1ME and LBS location on the <i>CBF3</i> promoter region	167
5.14	TOC1 binding affinity for the <i>CBF3</i> promoter	168
5.15	LUX binding affinity for the <i>CBF3</i> promoter	170
5.16	ELF3 binding affinity for the <i>CBF3</i> promoter	171
5.17	Cold gating in the model of best fit	173
5.18	Final architecture of the model of <i>CBF3</i> regulation by the circadian clock	174
5.19	Simulated protein concentrations in the model of best fit	177
5.20	Simulated protein accumulation in the model of best fit in <i>lux</i> and <i>toc1</i> .	181

List of Tables

2.1	Mutant <i>Arabidopsis</i> alleles	62
2.2	Primers	69
2.3	ChIP Extraction Buffer 1	70
2.4	ChIP Extraction Buffer 2	71
2.5	ChIP Nuclei Lysis Buffer	71
2.6	ChIP Dilution Buffer	71
2.7	ChIP Low Salt Wash Buffer	72
2.8	ChIP High Salt Wash Buffer	72
2.9	ChIP LiCl Wash Buffer	73
2.10	ChIP TE Buffer	73
3.1	Significance test of far-red light germination with or without cold stratification	90
3.2	Significance test of red light germination with or without cold stratification	93
4.1	Significant differences in Columbia survival when grown at different temperatures	110
4.2	Significant differences in clock mutant survival when frozen at -3°C	112
4.3	Significant differences in clock mutant survival when frozen at -5°C	114
4.4	Significant differences between prr mutant freezing tolerance	115
5.1	Model equations of <i>CBF3</i> regulation in the P2010 model	138
5.2	AICc scores for potential models of <i>CBF3</i> regulation in models using the P2010 circadian clock model	139
5.3	Model equations of <i>CBF3</i> regulation in the P2012 model	150
5.4	AICc scores for potential models of <i>CBF3</i> regulation in models using the P2012 circadian clock model	151
5.5	Known binding sites in the <i>CBF3</i> promoter region	166

Abbreviations

Abbreviation	Definition
8L:16D	Short day conditions; 8 hours of light followed by 16 hours of darkness
12L:12D	Normal day conditions; 12 hours of light and 12 hours of darkness
16L:8D	Long day conditions; 16 hours of light and 8 hours of darkness
24L:0D	Constant light conditions; 24 hours of light
ABA	Abscisic acid
<i>ACT2</i>	<i>ACTIN2</i>
agris	<i>Arabidopsis</i> Gene Regulatory Information Server
AIC	Akaike Information Criterion
AICc	Corrected akaike Information Criterion
AP2	APETALA2
BIC	Bayesian Information Criterion
CAMTA	Calmodulin binding transcription activator
<i>CBF</i>	<i>C-REPEAT BINDING FACTOR</i>
<i>CBF1</i>	<i>C-REPEAT BINDING FACTOR 1</i>
<i>CBF2</i>	<i>C-REPEAT BINDING FACTOR 2</i>
<i>CBF3</i>	<i>C-REPEAT BINDING FACTOR 3</i>
CBS	CCA1-binding site
<i>CCA1</i>	<i>CIRCADIAN CLOCK ASSOCIATED 1</i>
cDNA	Complementary deoxyribonucleic acid
CHE	CCA1 HIKING EXPEDITION
Col	Columbia
<i>CRR1</i>	<i>COLD AND CIRCADIAN REGULATED 1</i>
<i>CRR2</i>	<i>COLD AND CIRCADIAN REGULATED 2</i>
ChIP	Chromatin immunoprecipitation
<i>CO</i>	<i>CONSTANTS</i>
<i>COP1</i>	<i>CONSTITUTIVE PHOTOMORPHOGENIC 1</i>

Continued on next page

List of abbreviations

Abbreviation	Definition
<i>COR</i>	<i>COLD-REGULATED</i>
<i>COR15a</i>	<i>COLD-REGULATED 15a</i>
<i>COR15b</i>	<i>COLD REGULATED 15b</i>
<i>COR47</i>	<i>COLD-REGULATED 47</i>
CRT	C-repeat
CS	Cold stratification
Ct	Cycle threshold
CT	Circadian time
dCt	adjusted input Ct - ChIP sample Ct
DIC	Deviance Information Criterion
DF	Dilution factor
DRE	Dehydration Response Element
<i>DREB</i>	<i>DEHYDRATION RESPONSE ELEMENT-BINDING</i>
<i>DREB1A</i>	<i>DEHYDRATION RESPONSE ELEMENT-BINDING 1A</i>
<i>DREB1B</i>	<i>DEHYDRATION RESPONSE ELEMENT-BINDING 1B</i>
<i>DREB1C</i>	<i>DEHYDRATION RESPONSE ELEMENT-BINDING 1C</i>
EC	Evening complex
EDTA	Ethylenediaminetetraacetic acid
EE	Evening element
<i>ELF3</i>	<i>EARLY FLOWERING 3</i>
<i>ELF4</i>	<i>EARLY FLOWERING 4</i>
ERF	ETHYLENE RESPOSNSIVE FACTOR
FD	bZIP transcription factor 14
FIC	Focused Information Criterion
<i>FKF1</i>	<i>FLAVIN-BINDING KELCH REPEAT F-BOX 1</i>
<i>FRO1</i>	<i>FROSTBITE 1</i>
<i>FT</i>	<i>Flowering Locus T</i>
GA	gibberellic acid
GFP	Green fluorescent protein
<i>GI</i>	<i>GIGANTEA</i>
<i>HFR1</i>	<i>LONG HYPOCOTYL IN FAR-RED 1</i>
<i>HOS1</i>	<i>HIGH EXPRESSION OF OSMOTICALLY RESPONSIVE GENE 1</i>

Continued on next page

List of abbreviations

Abbreviation	Definition
<i>ICE</i>	<i>INDUCER OF CBF EXPRESSION</i>
<i>ICE1</i>	<i>INDUCER OF CBF EXPRESSION 1</i>
<i>KIN1</i>	<i>KINASE 1</i>
LBS	LUX binding site
Ler	Landsberg Erecta
<i>LHY</i>	<i>LATE ELONGATED HYPOCOTYL</i>
LiCl	Lithium chloride
LOV	Light-Oxygen-Voltage
<i>LUX</i>	<i>LUX ARRHYTHMO</i>
MgCl ₂	Magnesium chloride
MYB	Myeloblastosis
MYB15	MYB DOMAIN PROTEIN 15
MS	Murashige and Skoog
NaCl	Sodium chloride
NCS	No cold stratification
NI	Night Inhibitor
NOX	BROTHER OF LUX ARRHYTHMO
NP	Nonyl phenoxyethoxyethanol
ODE	Ordinary differential equation
P2010	Pokhilko 2010 model of the circadian clock (Pokhilko et al., 2010)
P2012	Pokhilko 2012 model of the circadian clock (Pokhilko et al., 2012)
<i>PCC1</i>	<i>PATHOGEN AND CIRCADIAN CONTROLLED 1</i>
<i>PER</i>	<i>PERIOD</i>
PGA	Parallel genetic algorithm
phyB	phytochrome B
PI	Protease inhibitor
<i>PIF3</i>	<i>PHYTOCHROME-INTERACTING FACTOR3</i>
<i>PIF4</i>	<i>PHYTOCHROME-INTERACTING FACTOR4</i>
<i>PIF5</i>	<i>PHYTOCHROME-INTERACTING FACTOR5</i>
<i>PIF7</i>	<i>PHYTOCHROME-INTERACTING FACTOR7</i>
PMSF	phenylmethanesulfonyl fluoride
<i>PRR</i>	<i>PSEUDO RESPONSE REGULATOR</i>

Continued on next page

List of abbreviations

Abbreviation	Definition
<i>PRR5</i>	<i>PSEUDO RESPONSE REGULATOR 5</i>
<i>PRR7</i>	<i>PSEUDO RESPONSE REGULATOR 7</i>
<i>PRR9</i>	<i>PSEUDO RESPONSE REGULATOR 9</i>
psbD	PHOTOSYSTEM II REACTION CENTER PROTEIN D
qRT-PCR	Real-time reverse-transcription polymerase chain reaction
RAV	ETHYLENE RESPONSE DNA BINDING FACTOR
RNA	Ribonucleic acid
ROS	reactive oxygen species
SBML	Systems Biology Mark-up Language
SDS	Sodium dodecyl sulfate
SIG5	SIGMA FACTOR5
T.E.	Tris-ethylenediaminetetraacetic acid
TIME	TOC1 morning element
<i>TOC1</i>	<i>TIMING OF CAB EXPRESSION 1</i>
Tris-HCl	Tris-Hydrochloride
UTR	Un-translated region
WA	Water agar
WS	Wassilewskija
ZT	Zeitgeber time
<i>ZTL</i>	<i>ZEITLUPE</i>

Publications

Keily, J., Macgregor, D. R., Smith, R. W., Millar, A. J., Halliday, K. J. and Penfield, S. (2013). Model selection reveals control of cold signalling by evening-phased components of the plant circadian clock. *The Plant Journal* 76, 247-57.

The model will be made publicly available as well as uploaded to the PLASMO data base (www.plasmo.ed.ac.uk).

1 Introduction

1.1 Circadian clocks

1.1.1 Introduction to circadian clocks

The rotation of Earth about its axis results in environmental changes throughout the course of a day, such as changes in light levels and temperature. Over time organisms have evolved circadian clocks to help them predict the daily changes in the environment in order that they can alter their behaviour and physiology appropriately for the different conditions that are present at the different times of the day.

The term “circadian” was coined in 1959 by Franz Halberg and refers to a behavioural or physiological mechanism which oscillates with the approximate period of 24 hours (Halberg, 1959). The circadian clock refers to the mechanism responsible for driving circadian rhythms; biological processes with an oscillation of approximately 24 hours which is both endogenous and entrainable. The first scientific recording of circadian rhythms was carried out almost 300 years ago by the French scientist Jean-Jacques d’Ortous de Mairan who noted a sustained rhythmical movement of *Mimosa* leaves, even when the plants were moved into areas without light (Gardner et al., 2006) and since then a wide variety of processes in a wide variety of living organisms have been shown to be circadian (Czeisler et al., 1999).

There are four basic characteristics that are required for a physiological rhythm to be classified as “circadian” (Harmer, 2009). Firstly, the rhythm needs to keep to an approximately 24 hour cycle. Secondly, this cycle should continue, even when the entraining conditions are switched to free running, unvarying, conditions, however, the cycle is usually not exactly 24 hours after the change to constant conditions. The third characteristic of circadian rhythms is that altering the appropriate environmental cues

1 Introduction

can be used to reset circadian rhythms. Finally, classically in the literature, circadian rhythms are temperature compensated with the same periodicity independent of the temperature in which they are located, so 24 hour periodicity of rhythms should occur whatever the temperature (Harmer, 2009).

The benefits to fitness that a circadian clock provides are well recorded. Plants with wild-type clock periods have increased chlorophyll levels, increased growth rate and fix more carbon than plants with periods that do not match the environment they are in (Dodd et al., 2005). *Drosophila* with *PERIOD* (*PER*) null mutant, *per-01*, have increased susceptibility to oxidative stress and accelerated functional decline compared to wild-type *Drosophila* (Krishnan et al., 2009). The reproductive fitness of cyanobacteria is increased in strains of cyanobacteria with normal circadian clocks compared to competing cyanobacteria with altered clock periods (Ouyang et al., 1998). In mice abnormal circadian clocks have been shown to alter energy management, resulting in obese mice with several obesity related ailments (Turek et al., 2005). In humans abnormal fasting/eating cycles and sleep/wake cycles have been linked to numerous ailments, such as altered glucose tolerance, carbohydrate metabolism and detrimental effects on endocrine function (Spiegel et al., 1999). Maintaining a working circadian clock is therefore highly useful for biological organisms.

Circadian rhythms often take the form of sinusoidal waves that have a number of characteristics that can be used to describe their appearance (**Figure 1.1**). The three main components of the sinusoidal wave are the phase, amplitude and the period. The phase refers to a specific point of time on the wave in which an event occurs; the amplitude is half the distance between the peak and trough of an oscillation and the period is the amount of time taken for one oscillation to occur (Harmer, 2009).

When discussing circadian clocks there are two periods of time that are often discussed; circadian time (CT) and zeitgeber time (ZT). ZT refers to the time after exposure to a circadian synchronising stimuli, such as light, so that ZT0 would be the time at which the stimuli was received and ZT12, for example, would be 12 hours after exposure; whereas CT time refers to free running conditions, where CT0 would be the time at which circadian synchronising stimuli would occur if the plant were not in free running conditions (Harmer, 2009).

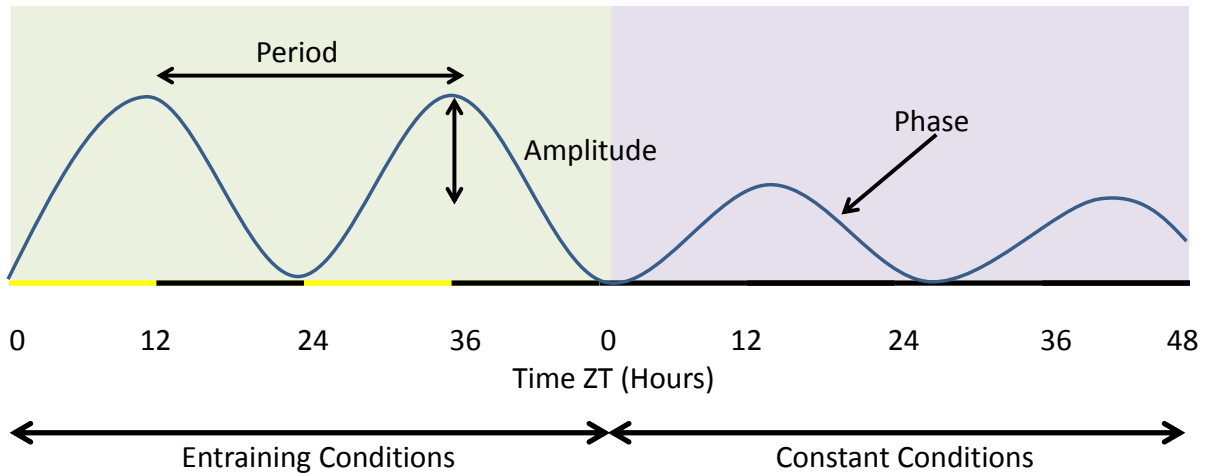


Figure 1.1: The main features of a circadian rhythm. Under the entraining conditions (in this case light and dark cycles) there is a 24 hour clock period as shown. Under constant conditions the amplitude is changed, and the period of the oscillation also changes (in this case to a 25 hour free-running period). The phase refers to a specific point at which an event occurs, and in circadian clocks it usually refers to the peak of an oscillation (such as peak gene expression time). Adapted from Harmer, 2009.

1.1.2 Circadian clocks are found throughout nature

Originally, the most studied organisms for investigating circadian clocks were *Drosophila* and *Neurospora*, however, the clocks of many other organisms have since been studied in detail, such as the plant, mammalian and cyanobacterial circadian clock (Leloup and Goldbeter, 1998; Berson et al., 2002; Turek et al., 2005; Vinh et al., 2013). The molecular components of circadian clocks are not conserved between the different kingdoms, yet the basic circadian physiology is largely similar. As described above, there are certain criteria that is required to be met for a rhythm to be considered circadian that is present in disparate organisms. As well, there is a commonality between organisms that the circadian clock is cell autonomous with robust circadian rhythms occurring in single isolated cells from both multicellular and unicellular organisms (Mihalcescu et al., 2004; Nagoshi et al., 2004).

1.2 The *Arabidopsis* circadian clock

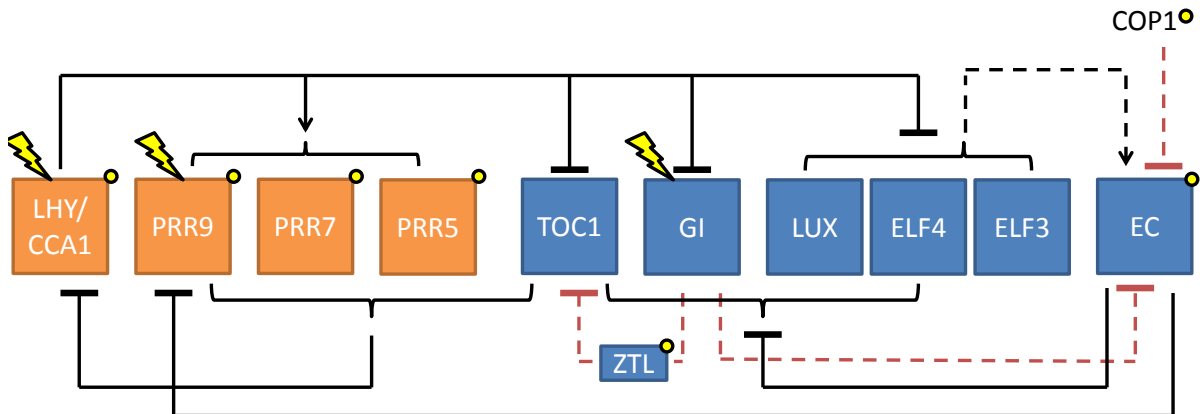


Figure 1.2: A cartoon of the core *Arabidopsis* circadian clock. LHY/CCA1 promotes *PRR* expression whilst *LHY/CCA1* expression is inhibited by the PRRs and TOC1. LHY/CCA1 also inhibits the expression of the evening genes *TOC1*, *GI*, *LUX*, *ELF4* and *ELF3*. *GI*, *LUX*, and *ELF4* expression is inhibited by the Evening Complex (EC) which is a complex composed of LUX-ELF4-ELF3. *PRR9* expression is also inhibited by the EC. Transcriptional regulation is shown by solid black lines. The dashed black lines represent Evening Complex formation from LUX, ELF4 and ELF3. The dashed red lines represent post-translational regulation of the EC by COP1 and GI. GI also stabilises ZTL protein in the presence of light resulting in post-translational regulation of *TOC1* by ZTL, also indicated by a dashed red line. Flashes represent acute light induced responses and the yellow dots attached to components of the clock indicate that post-translational regulation by light. Components of the morning loop are shown in orange boxes. Components of the evening loop are shown in blue boxes. Figure adapted from Pokhilko *et. al.*, 2012.

1.2.1 *Arabidopsis* as a model plant organism

Over the past 30 years, *Arabidopsis thaliana* has become the most thoroughly studied plant organism with over 3500 papers based on *Arabidopsis* getting added to the PubMed data base (<http://www.ncbi.nlm.nih.gov/pubmed>) in 2008 alone, compared to the only seven titles that were added in 1979 (Koornneef and Meinke, 2010). This rise

in popularity is likely due to its relatively small genome size which has been fully sequenced (The Arabidopsis Genome Initiative, 2000), thus allowing extensive genetic research to occur with the species. *Arabidopsis* also has a short germination time and life cycle and a robust growth ability and small size which makes the plant easy to grow for experiments and resulted in the proposal of *Arabidopsis* as a model organisms for plant genetic research (Laibach, 1943; Somerville and Koornneef, 2002). The circadian clock of plants has primarily been developed in *Arabidopsis* due to its popularity, and as such was the ideal choice of plant species to work with.

1.2.2 Transcriptional regulation of *Arabidopsis* circadian clock system

The circadian core oscillators of *Arabidopsis thaliana* consist of two interlocked transcriptional feedback loops. The first loop is the “morning loop” and consists of *LHY*, *CCA1*, *PSEUDO RESPONSE REGULATOR 5 (PRR5)*, *PSEUDO RESPONSE REGULATOR 7 (PRR7)* and *PSEUDO RESPONSE REGULATOR 9 (PRR9)* as seen in **Figure 1.2** (Schaffer et al., 1998; Wang and Tobin, 1998; Matsushika, 2000; Nakamichi et al., 2010). The morning loop forms a negative feedback loop with an “evening loop” which consists of *TOC1*, *GIGANTEA (GI)*, *ELF3*, *EARLY FLOWERING4 (ELF4)* and *LUX* **Figure 1.2** (Somers et al., 1998; Park, 1999; Matsushika, 2000; Covington, 2001; Nusinow et al., 2011).

LATE ELONGATED HYPOCOTYL and CIRCADIAN CLOCK ASSOCIATED1

The first components of the clock to be described consisted of *LHY* (Schaffer et al., 1998), *CCA1* (Wang and Tobin, 1998) and *TOC1* (Somers et al., 1998), wherein the myeloblastosis-related transcription factors *LHY* and *CCA1* negatively regulate *TOC1* expression and *TOC1* positively regulates *LHY* and *CCA1* expression, as seen in (**Figure 1.3**) (Alabadi et al., 2001), although, as discussed below, this positive regulation of *LHY* and *CCA1* transcription has recently been questioned. *CCA1* and *LHY* expression peaks at dawn with *LHY* and *CCA1* protein production occurring 2-3 hours later when these two transcription factors associate with the *TOC1* promoter resulting in a repression of *TOC1* expression (Alabadi et al., 2001). The morning expressed genes, *LHY* and *CCA1* produce proteins that negatively regulate evening

1 Introduction

expressed genes, such as *TOC1* and *LUX* by binding to the Evening Element (EE, nucleotide sequence AAAATATCT) that is found in their promoters (Harmer et al., 2000; Alabadí et al., 2001; Hazen et al., 2005). This inhibition of evening expressed genes means that their expression is repressed during the day, when LHY and CCA1 are present, but allows for expression during the evening/night, when LHY and CCA1 concentration decreases. LHY and CCA1 are also involved in promoting morning gene expression via interactions with the CCA1-binding site (CBS, nucleotide sequence AAAAATCT) (Farré et al., 2005).

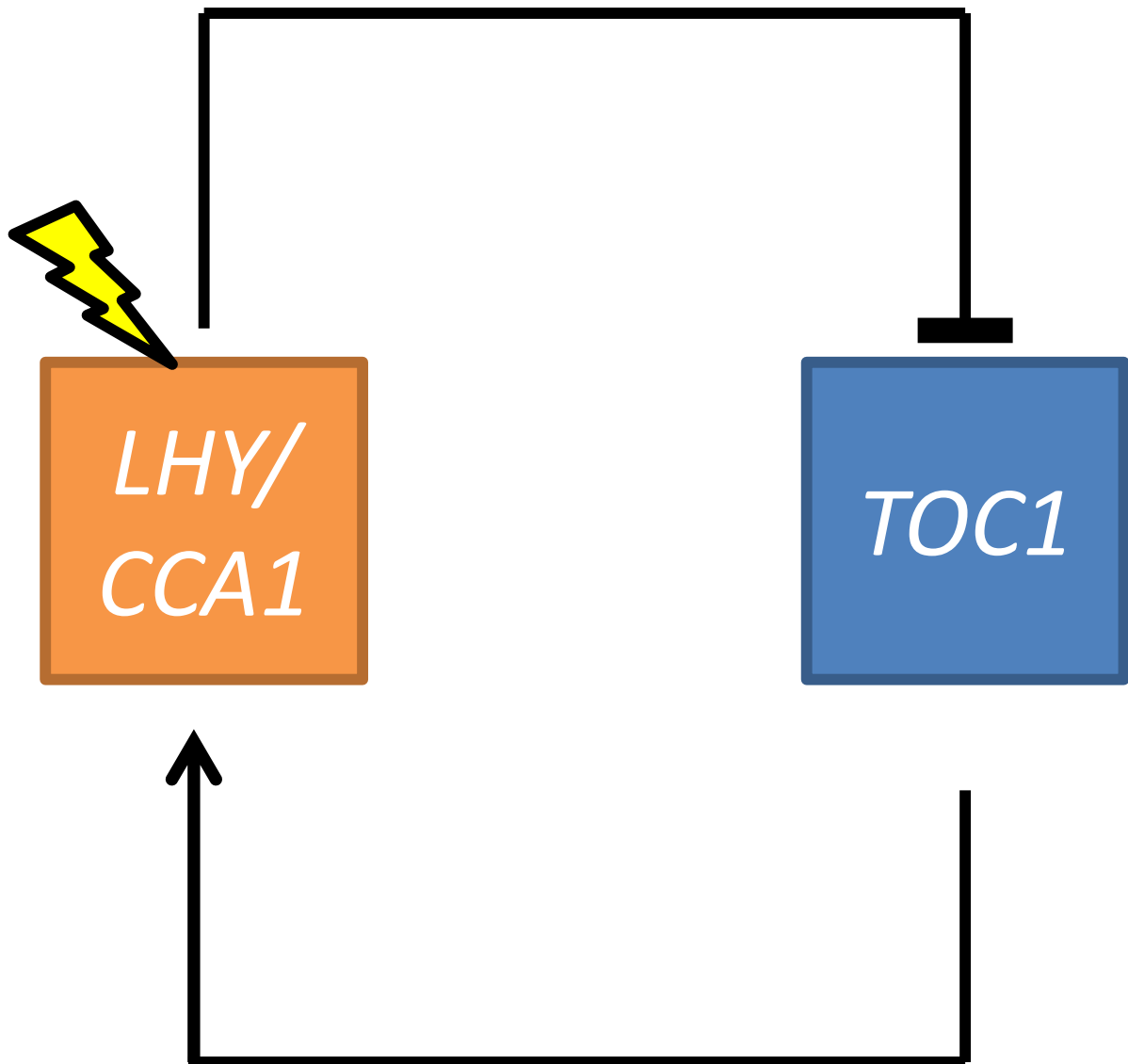


Figure 1.3: An early model of the *Arabidopsis* circadian clock model. In this model, the morning genes *LHY* and *CCA1* produce proteins that negatively regulate *TOC1* expression. *TOC1*, meanwhile, produces TOC1 which is involved in up-regulating *LHY/CCA1* expression. Orange boxes represent morning genes and blue boxes represent the evening gene with a lightning arrow to indicate light input into the model.

TIMING OF CAB EXPRESSION1

TOC1 is one of the core genes in the *Arabidopsis* circadian clock. In luminescence assays, *toc1-1* mutants have been shown to have short periods compared to wild-type plants under various light conditions (Millar and Kay, 1996). The mode of action of TOC1 in the circadian clock is currently being questioned. TOC1 was previously thought to promote the morning myeloblastosis (MYB) genes *LHY* and *CCA1* (Alabadi et al., 2001). This promoter effect of TOC1 was elucidated through *toc1* mutant studies; *toc1-2* plants have reduced *CCA1* messenger ribonucleic acid (mRNA) and *LHY* mRNA expression compared to wild-type plants (Alabadi et al., 2001). The mechanism for TOC1 activation of *LHY* and *CCA1* was unknown, but *CCA1* HIKING EXPEDITION (CHE), a TOC1 interacting protein that is regulated by *CCA1* and which binds to the *CCA1* promoter was, suggested as a possible mechanism of action (Pruneda-Paz et al., 2009). Recently, however, this mode of action has been questioned and new experimental studies and mathematical modelling suggests that TOC1 is in fact a repressor of *LHY/CCA1* rather than an activator (Huang et al., 2012; Pokhilko et al., 2012). With TOC1 acting as a repressor of *LHY/CCA1* rather than an activator, recently published observations can be explained such as the increased TOC1 concentration observed in *ZEITLUPE* (*ZTL*) mutants that coincides with reduced expression of *LHY*, *CCA1*, *PRR7* and *PRR9* (Más et al., 2003b; Baudry et al., 2010).

PSEUDO RESPONSE REGULATORS

The *PSEUDO-RESPONSE REGULATORS* encompass several genes in the circadian clock, *TOC1* (*PRR1*), *PRR3*, *PRR5*, *PRR7* and *PRR9*. The pseudo-response regulators *PRR7* and *PRR9* are morning genes involved in the *Arabidopsis* circadian clock. Luminescence experiments with *prr7-11* and *prr9-1* mutants showed a lengthening of clock period under constant white light and no change in period under constant dark, compared to wild-type plants, indicating a light signalling role for *PRR7* and *PRR9* (Farré et al., 2005). *LHY* and *CCA1* positively affect *PRR7* and *PRR9* expression as shown by the decrease in *PRR7* and *PRR9* in *lhy* and *cca1* mutants (Farré et al., 2005). In a separate study to that of Farre et al (2005), *prr5*, *prr7* and *prr9* single mutants were created as well as *prr5 prr7*, *prr5 prr9* and *prr7 prr9* double mutants and the *prr5 prr7 prr9* triple mutant (Nakamichi et al., 2005). In

the Nakamichi (2005) study the necessity of having these three genes function correctly for normal circadian clock period to occur was reinforced through a number of *prp* mutant experiments which showed abnormal circadian clock periods. The *PRRs* have different peak expression periods, with *PRR9* peak expression occurring at dawn, *PRR7* peak expression occurring in the morning and *PRR5* peak expression occurring at mid-day with *TOC1* (*PRR1*) peak expression occurring in the evening (Matsushika, 2000). Whilst *PRR5*, *PRR7* and *PRR9* are functionally redundant, the fact that the different *PRRs* are expressed throughout the day in a sequence of expression allows them to regulate proper clock timekeeping throughout the day, as confirmed by the loss of proper clock rhythmicity seen in the *prp5 prp7 prp9* triple mutants (Nakamichi et al., 2005).

Evening Complex

Three other genes and their corresponding proteins are important components of the circadian clock needed for normal rhythmic oscillations and the correct expression of *TOC1* and *LHY/CCA1: ELF3; ELF4* and *LUX* (Hazen et al., 2005; Onai and Ishiura, 2005; McWatters et al., 2007; Kolmos et al., 2009; Dixon et al., 2011; Helfer et al., 2011). In a recent study these three proteins have been shown to form a complex, named the Evening Complex (EC), in which *LUX* has been shown to bind directly to the promoter sequence of *PRR9* at the *LUX* binding sites [(LBS), GATWCG; W represents either A or T] (Helfer et al., 2011).

As well as the genes that are involved in the transcriptional regulation of the circadian clock, there are other genes, and environmental factors that are involved in regulating the plant circadian clock.

1.2.3 Posttranscriptional regulation of the *Arabidopsis* circadian clock

The transcriptional regulatory feedback loops that form the core of the *Arabidopsis* circadian clock are also subject to posttranscriptional regulation (Harms et al., 2004; Mehra et al., 2009). The protein kinase, CK2, phosphorylates the circadian clock protein *CCA1* (Sugano et al., 1998), with CK2 overexpression in *Arabidopsis* resulting in *CCA1* losing its circadian oscillator function (Daniel et al., 2004). Proteolysis and

phosphorylation have also been observed in the Pseudo-response Regulator proteins, PRR5, PRR7, PRR9 and TOC1 (Fujiwara et al., 2008). ZTL is an important clock associated protein that is responsible for the post transcriptional regulation of the clock proteins PRR5 and TOC1 by targeting them for degradation (Más et al., 2003b; Kiba et al., 2007). The F-box protein, ZTL, also has an N-terminal Light-Oxygen-Voltage (LOV) domain by which blue light is perceived. ZTL activity is mediated by blue light, which activates ZTL, to target TOC1 and PRR5 for degradation (Más et al., 2003b; Kiba et al., 2007). *ZTL* mRNA is constitutively expressed yet ZTL protein concentration levels are rhythmically expressed. The oscillation of ZTL concentration has been shown to be caused and sustained by blue light-enhanced interaction with GI that results in stable ZTL, thus explaining why *ZTL* mRNA levels are constitutively expressed yet the protein concentration oscillates (Kim et al., 2007). This light enhanced interaction with GI results in stable ZTL which allows ZTL to target TOC1 and PRR5 for degradation, thus ensuring they have robust oscillations that are dependent on the time of day (Kim et al., 2007). The ubiquitin E3 ligase CONSTITUTIVE PHOTOMORPHOGENIC1 (COP1) interacts with the circadian clock Evening Complex protein ELF3 to mediate GI degradation (Yu et al., 2008).

Alternative splicing and the circadian clock

Recently, the idea of alternative splicing as a mechanism to link the circadian clock to cold tolerance has been introduced (James et al., 2012; Hofmann, 2012). The posttranscriptional alternative splicing of a gene allows for the production of more than one protein (sometimes with different functions) to be produced from a single gene, thus increasing diversity in the transcriptome and proteome. A genome wide study of *Arabidopsis* revealed *CCA1* (along with up to 42% of *Arabidopsis* genes) to be alternatively spliced (Filichkin et al., 2010). The two splice variants of *CCA1* were identified and named, *CCA1 α* and *CCA1 β* . *CCA1 β* accumulates in high light conditions and decreases in accumulation in cold conditions (Filichkin et al., 2010). *CCA1 α* and *CCA1 β* are both capable of forming homodimers and heterodimers with themselves and another morning gene product, LHY (Seo et al., 2012). *CCA1 β* represses the action of *CCA1 α* and LHY by forming non-functional *CCA1 α /CCA1 β* and *CCA1 β /LHY* heterodimers (Seo et al., 2012). Splice variation is inhibited by cold treatment where *CCA1 β* production is eliminated in the cold. *35S:CCA1 α* plants had

enhanced freezing tolerance compared to wild-type plants, whereas *35S:CCA1 β* plants had reduced freezing tolerance. This shows an important role for alternative splicing in regulating CCA1 and LHY circadian activity, as well as regulating freezing tolerance (Seo et al., 2012; Dong et al., 2011). CCA1 is not the only circadian clock related gene known to undergo alternative splicing. *CCA1*, *LHY*, *TOC1*, *PRR3*, *PRR5*, *PRR7*, *PRR9*, *ZTL* and *GI* are all shown to be alternatively spliced showing just how widespread this mechanism is (Sanchez et al., 2010; James et al., 2012; Seo et al., 2012).

1.2.4 Inputs of the *Arabidopsis* circadian clock

Due to the daily rotation of the Earth about its axis, there are daily changes in light and temperature levels. Plants have adapted to use these cues to reset their circadian clocks each day to make sure that their clocks are always up-to-date with the changes that are occurring in the environment and such cues are often referred to as “zeitgebers” (“time-givers”). Entrainment to environmental conditions is important as it allows plants to have a functioning circadian clock throughout the year as the daily environmental cycles change throughout the year. In plants the two core environmental stimuli that entrain the circadian clock are temperature and light.

Light is important for the circadian clock. The effects of light stimulation of the clock alter throughout the day. Pulses of light in the early morning are known to result in advances in the clock. Pulses of light in the evening delay the clock. This allows for the clock to adjust to changes in day light lengths (Devlin and Kay, 2001).

1.2.5 Outputs of the *Arabidopsis* circadian clock

A large percentage of *Arabidopsis* genes are circadian regulated, with approximately 6% of *Arabidopsis* genes cycling expression throughout the day (Harmer et al., 2000). The circadian clock is involved with several plant processes and pathways such as hormone signalling (Covington and Harmer, 2007; Robertson et al., 2009), regulation of growth (Dowson-Day and Millar, 1999; Nozue et al., 2007), starch and sugar mobilisation (Harmer et al., 2000; Morcuende et al., 2005), flowering time (Hayama, 2003), pathogen responses (Zhang et al., 2013) and photosynthesis (Dodd et al., 2013).

Plant cold response pathways are also known to be regulated by the circadian clock, and this output is discussed in detail in **section 1.4**.

Circadian regulation of growth and hormone signalling

In *Arabidopsis* the circadian clock is important in regulating growth and hormonal signalling.

In light dark cycles hypocotyl elongation occurs shortly before dawn (Dowson-Day and Millar, 1999), whereas in constant light conditions hypocotyl elongation occurs at the end of the subjective day period (Nozue et al., 2007). The light pathway and the circadian clock interact to control stem elongation under normal light/dark cycles via the transcriptional and postranscriptional regulation of two transcription factors, *PHYTOCHROME-INTERACTING FACTOR4* (*PIF4*) and *PHYTOCHROME-INTERACTING FACTOR5* (*PIF5*) (Nozue et al., 2007). Growth is initiated late at night by the clock mediated induction of *PIF4* and *PIF5* transcription and is subsequently ceased during the morning by the light induced degradation of *PIF4* and *PIF5* (Nozue et al., 2007). The circadian clock protein *CCA1* associates with the *ELF3* promoter to inhibit *ELF3* expression, and *ELF3* associates with the promoter of *PRR9* to repress *PRR9* expression, with *PRR9* also being responsible for inhibiting *CCA1* expression, thus forming a negative feedback loop of gene expression (Lu et al., 2012) and *ELF3* has recently been shown to inhibit *PIF4* and *PIF5* expression (Lu et al., 2012); this data, in association with the observation that *elf3* mutant plants and *CCA1 OX* mutant plants have higher *PIF4* and *PIF5* expression (Lu et al., 2012) and elongated hypocotyl lengths (Lu et al., 2012), compared to wild-type plants, presents a potential pathway for the circadian regulation of *Arabidopsis* growth via PIFs. The targets of *PIF4* and *PIF5* which are thought to confer growth is the hormone signalling pathway. The expression of *PIF4* has been shown to change gibberellic acid (GA) sensitivity in *Arabidopsis*, making the GA hormonal pathway a possible mediator of the circadian clock regulated *PIF4*-controlled daily growth cycles that are observed (de Lucas et al., 2008) as GA is important for plant growth (Brian, 1959).

The circadian clock is also involved in regulating auxin signal transduction (Covington and Harmer, 2007). Auxin is another plant hormone that is important for growth with the hormone having a role in many developmental stages such as lateral root and leaf initiation, embryogenesis and apical dominance (Casimiro et al., 2003; Fleming, 2005;

Jenik and Barton, 2005). Plant sensitivity to auxin changes throughout the day, with peak sensitivity occurring in the early morning (Covington and Harmer, 2007). Recent evidence points to *PIF5* as a modulator of auxin sensitivity as demonstrated by the fact that numerous auxin pathway genes are regulated by PIF5 (Nozue et al., 2011) and *pif5* mutant plants show altered sensitivity to exogenous auxin compared to wild-type plants (Nozue et al., 2011). However, it should be noted that PIF5 growth control is not simply through the control of auxin levels as *PIF5-OX* mutant plants show greater de-regulation of growth than that witnessed in auxin over-producing plants (Nozue et al., 2011). This implies that auxin levels are not directly regulated by PIF5, and as such it is possible that PIF5 is not directly regulating auxin, but that PIF5 regulates the expression of another gene, which in turn produces a protein that regulates auxin levels (Nozue et al., 2011). *HFR1* (*LONG HYPOCOTYL IN FAR-RED 1*) is thought to be a good candidate as HFR1 is known to affect auxin responses and *HFR1* expression is regulated by PIF5 (Hornitschek et al., 2009; Nozue et al., 2011).

Circadian regulation of photosynthesis

Circadian involvement in the regulation of light harvesting has been known for several years now, first getting described in marine algae in 1961 (Sweeney and Haxo, 1961). Having a circadian clock that is involved in regulating photosynthesis increases photosynthesis and results in a doubling of *Arabidopsis* productivity (Dodd et al., 2005). The chloroplast are essential for photosynthesis in *Arabidopsis* and transcript profiles show that 70% of chloroplast genes that encode proteins can be regulated by the circadian clock (Michael et al., 2008). A recent study, (Noordally et al., 2013), shows that the circadian clock regulates chloroplast transcription using a nuclear-encoded timing signal, SIGMA FACTOR5 (SIG5), which targets the chloroplast gene *PHOTOSYSTEM II REACTION CENTER PROTEIN D* (*psbD*) (Nagashima et al., 2004). SIG5 regulates transcription from the *psbD* blue light-responsive promoter of the *psbDC* operon in mature chloroplasts (Tsunoyama et al., 2004). Delayed fluorescence, the emission of photons from photosynthetic components of plants upon transfer into darkness, shows circadian oscillations in *Arabidopsis* (Gould et al., 2009), and can be used as a system for investigations into the circadian regulation of photosynthesis. Delayed fluorescence experiments in two *sig5* mutants, *sig5-2* and *sig5-3*, were carried out to investigate the regulation of photosystem II by the circadian clock regulated protein SIG5 (Noordally et al., 2013).

In both *sig5-2* and *sig5-3* peak delayed fluorescence occurred 4 and 5.9 hours early, respectively, compared to wild-type plants and in *sig5* mutant plants, circadian oscillations in the abundance of transcripts encoded by the chloroplast *psbDC* operon was not observed, unlike in wild-type plants, (Noordally et al., 2013), further adding evidence of the importance of SIG5 in regulating circadian control of photosynthesis. ChIP experiments using wild-type and *sig5-2* mutant plants show that SIG5 may contribute to the circadian rhythm of additional photosystem I and photosystem II reaction centre genes (Noordally et al., 2013). SIG5 is important for mediating the circadian regulation of photosynthesis, but as there is functional redundancy in some sigma factors in *Arabidopsis*, (Hanaoka et al., 2012), future work is required on the remaining sigma factors to determine their role as well in the circadian regulation of photosynthesis.

Circadian regulation of starch mobilisation

Daytime growth as a result of photosynthetic carbon fixing is also accompanied by nocturnal metabolism and growth. Starch is often accumulated throughout the day and is broken down during the night to provide sugars for nocturnal growth and metabolism. The rate at which starch degradation in *Arabidopsis* occurs adjusts dependant on the onset time of night so as to allow the plant to have access to starch reserves throughout the night without running out too fast, or having too excess levels remaining at the start of the morning (Lu et al., 2005). When *Arabidopsis* plants were grown in 16 hour of light followed by 8 hours of darkness and then transferred to darkness after only eight hours of light, the starch degradation rate is reduced compared to that of the previous evenings (Lu et al., 2005). Plants grown in short day (only 8 hours of light) conditions which were then exposed to 16 hours of light before darkness had an increased rate of starch degradation compared to previous evenings (Lu et al., 2005). It has been thought that the circadian clock was important for regulating the rate of starch accumulation during the day (Ni et al., 2009), however, it is now thought that the circadian clock instead acts as the timer that matches the utilisation of starch to the predicted night length (Graf et al., 2010). *lhy cca1* mutants have fast running circadian clocks with a free-running period of approximately 17 hours in constant light (Mizoguchi et al., 2002; Locke et al., 2005b). In days consisting of 12 hours of light followed by 12 hours of darkness *lhy cca1* double mutant plants used up their starch reserves 35% faster than in the wild-type plants (Graf et al.,

2010). When *lhy cca1* mutant plants were exposed to 8.5 hours of light and 8.5 hours of darkness starch degradation was more linear, with the plants almost using all their starch reserves by the morning, much like wild-type plants exposed to 12 hour nights (Graf et al., 2010). The full mechanism by which the circadian clock regulates the rate of starch degradation for metabolism is not yet fully elucidated.

Circadian regulation of flowering time

The circadian clock in plants is responsible for regulating photoperiodism in plants. Having flowering induction in response to day length allows for the synchronising of flowering to the changing seasons. In *Arabidopsis* the circadian clock regulated flowering pathway contains three key genes to promote flowering, *GI*, *CONSTANS* *CO* and *Flowering Locus T (FT)* (Mizoguchi et al., 2005). Experiments using *lhy cca1* double mutants, *35S:GI* over-expression mutants and *gi* mutants show that *GI* acts between the circadian clock and the promotion of flowering by regulating *CO* and *FT* expression (Mizoguchi et al., 2005). *CO* mRNA expression levels are reduced in *gi* mutants which lead to the idea that *GI* has either a direct or indirect role in promoting *CO* transcription (Suárez-López et al., 2001) and it was later confirmed that *CO* mRNA expression is regulated by *GI* and FLAVIN-BINDING KELCH REPEAT F-BOX 1 (FKF1) which form a complex in a light-dependent manner to regulate *CO* transcription (Sawa et al., 2007). *GI* expression is regulated directly by the circadian clock where LHY/CCA1 acts to regulate the *GI-CO-FT* pathway in light/dark cycles (Mizoguchi et al., 2002; Más, 2005; Mizoguchi et al., 2005). *CO* directly activates the expression of *FT* and the expression of *CO* is regulated by the circadian clock, peaking in mRNA expression 16 hours after dawn (Valverde et al., 2004) and regulated differently under different light conditions (Wang et al., 2001; Jang et al., 2008). Under short days, *CO* expression peaks in the dark and *CO* is rapidly targeted for degradation by COP1 which results in flowering being inhibited in these conditions, whereas in long days, peak expression occurs during the day resulting in a build-up of *CO* and results in flowering taking place (Wang et al., 2001; Jang et al., 2008) as exposure to light is also required to activate *CO* protein function (Valverde et al., 2004). *FT* promotes flowering in *Arabidopsis*; *FT* is transported to the shoot apical meristem via the phloem (Corbesier et al., 2007; Mathieu et al., 2007) at which point it interacts with a transcription factor protein bZIP transcription factor 14 (FD) to promote the activation of floral identity genes which induce flowering (Abe et al., 2005;

Wigge et al., 2005).

1.2.6 Circadian control of pathogen responses

Understanding of the molecular mechanisms of the circadian control of pathogen responses in plants is still relatively new but the idea that the circadian clock is involved in regulating plant innate immunity is not, due to the circadian expression of plant defence genes (Sauerbrunn and Schlaich, 2004; Roden and Ingle, 2009; Wang et al., 2011). Perturbations to clock genes such as *CCA1* (Bhardwaj et al., 2011) and *GI* (Oliverio et al., 2007) can lead to reduced resistance against the bacterial pathogen *Pseudomonas syringae* and/or the oomycete pathogen *Hyaloperonospora arabidopsis*. Some pathogens can enter plants through wounds and stomata, and the circadian defence against pathogens comes in some part through the circadian regulation of stomata aperture as demonstrated by the enhanced susceptibility of *Arabidopsis* plants to spay-infection of *Pseudomonas syringae* at night in *lhy cca1* double mutants compared to wild-type plants as a result of a decrease in *lhy cca1* plants ability to close stomatal apertures (Zhang et al., 2013). The defence gene *COLD AND CIRCADIAN REGULATED 2 (CCR2)* (Lauvergeat et al., 2001) acts downstream of *CCA1* and *LHY* to regulate stomatal defence against pathogens (Zhang et al., 2013). *cca1 lhy* double mutants also showed increased susceptibility to *Hyaloperonospora arabidopsis* which does not enter plants through stomata, rather it produces hyphae that penetrates epidermal cells to enter the intracellular space which suggests that there are other pathways through which *LHY* and *CCA1* are required for wild-type defence levels of *Arabidopsis* to be achieved (Zhang et al., 2013). The circadian clock controlled *PATHOGEN AND CIRCADIAN CONTROLLED 1 (PCC1)* gene is a possible candidate for this non-stomatal regulation. *CCA1-OX* plants show that *PCC1* is regulated by the circadian clock (Sauerbrunn and Schlaich, 2004). Over-expression of *PCC1* are more resistant to normally virulent oomycetes than wild-type plants (Sauerbrunn and Schlaich, 2004). Jasmonate and salicylate are important for plant defence with both involved in up-regulating a number of defence genes in *Arabidopsis* (Reymond and Farmer, 1998). Jasmonate and salicylate have their accumulation circadian-regulated: jasmonate accumulation peaks in the middle of the subjective morning whereas salicylate accumulation peaks in the middle of the subjective night (Goodspeed et al., 2012). This adds yet another plant defence pathway that is regulated by the circadian clock.

As can be seen from the above sections, the *Arabidopsis* circadian clock is vital for a great many different physiological processes throughout the plant, without which plants would be far less fit.

1.3 Modelling biological systems

1.3.1 What is systems biology?

Systems biology can broadly be characterised as the integration of computational modelling and laboratory experimentation (Kitano, 2002). Biological data is used to create models that are then used to make biological predictions. These predictions can then be tested in the laboratory and the results used to help improve on the model system (**Figure 1.4**). For example, a systems biology approach was used in this study when investigating the clock regulation of *CBF* expression: biological data was used to create mathematical models of *CBF3* regulation by the clock. The different models were then tested experimentally to ascertain which model most accurately replicates what is observed biologically. Biological predictions were then made using this model and then tested experimentally in the laboratory to confirm the model predictions. Through this process our understanding of *CBF3* regulation by the circadian clock was increased (this work is shown in Chapter 5).

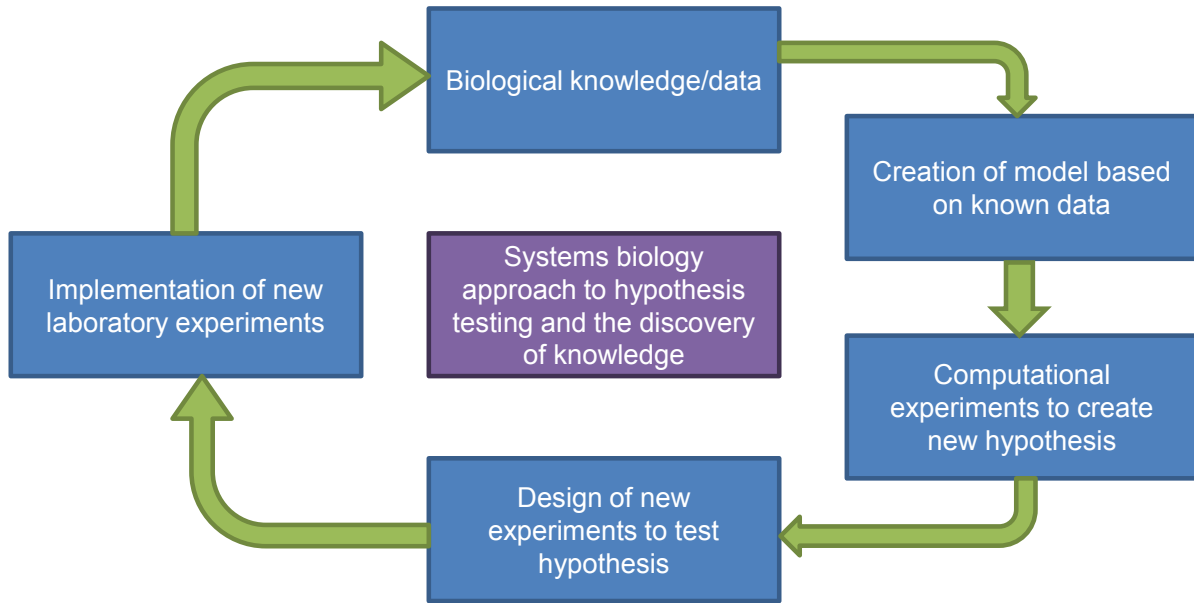


Figure 1.4: The basic structure of systems biology, wherein the mathematical models based on known biological data are used to create hypothesis about the biological system that would not otherwise be apparent. These hypotheses are then tested experimentally in the laboratory and the results of these tests are then used to update the models to make them more accurate and the cycle repeats.

1.3.2 Mathematical modelling of gene expression

Ordinary differential equation models of the *Arabidopsis* circadian clock

There are several different types of models that can be used to mathematically simulate systems of gene expression, such as ordinary differential equation models, partial differential equation models, stochastic equation models and rule-based formalisms (De Jong, 2002). Ordinary differential equations (ODEs) are amongst the most widely used mathematical models for dynamic systems (De Jong, 2002) and have been used in the creation of *Arabidopsis* circadian clock models.

Many biological systems, such as transcriptional networks, require that the model can represent a multicomponent, temporally changing system and for this differential equation models excel. In *Arabidopsis* circadian ODE models of regulatory networks

1 Introduction

are represented by a series of differential equations, in which the components (protein concentration, mRNA concentration) interact with one-another by a strict set of rules defined in terms of rate equations (Ay and Arnosti, 2011). Each equation in the model will calculate the levels of a protein or mRNA as a function of the other components of the model, as set out in their corresponding equation. The Pokhilko 2012 circadian clock model (hereafter referred to as the P2012 model), for example, can be described by a series of 28 ordinary differential equations (9 ODEs for mRNA concentration levels and 19 ODEs for protein levels). The models will take into account time and/space variables, such as the protein concentration, and will incorporate parameters such as the production and degradation of said components, as is exemplified in several of the *Arabidopsis* circadian clock models that will be discussed below (Locke et al., 2005b; Pokhilko et al., 2010). *Arabidopsis* circadian models also take into account light input. In the P2012 model, for example, light enters from two sources: 1) a light-sensitive activator protein which allows for the modelling of the acute light activation of *LHY/CCA1*, *PRR9* and *GI* and 2) a light function L , where lights on is modelled as $L = 1$ and lights off is modelled as $L = 0$. When creating ODE models of circadian clocks the parameter values for mRNA and protein concentrations can either be constrained from previous, available, data or fitted to newly created time series data as described below in the **Parameter value estimations** section. Several clock models use Michaelis-Menten kinetics with Hill functions to describe the enzyme activity in their models (Pokhilko et al., 2010; Pokhilko et al., 2012), and are used in this study to describe *CBF3* regulation by circadian proteins. In Michael-Menten equations enzyme reaction rates are calculated as a function of the substrate concentration and follow the structure of [1.1]

$$\text{Reaction rate} = \frac{V_{max}(x)}{K_m+x} \quad [1.1]$$

Where V_{max} is the maximum rate velocity that can be achieved by the system as the substrate concentration gets larger. K_m is the substrate concentration at which the reaction rate is half that of V_{max} and x is substrate concentration (Motulsky and Christopoulos, 2003).

In the Pokhilko circadian clock models, and this study, Michaelis-Menten kinetics can be applied to gene activation and repression where the mRNA levels of a gene can be modelled (Pokhilko et al., 2010; Pokhilko et al., 2012). The change in concentration of gene “A” mRNA over time is either repressed or activated by protein “X”. This can be represented using Michaelis-Menten kinetics as seen in [1.2] for activation and [1.3] for

1 Introduction

repression. A Hill coefficient is also commonly incorporated into the Michaelis-Menten equations to allow for ligand inhibition or promotion of ligand binding as also shown in [1.2] and [1.3].

Activation:

$$\frac{dc_A^m}{dt} = n_c \left(\frac{X^h}{k^h + X^h} \right) - m_c c_A^m \quad [1.2]$$

Repression:

$$\frac{dc_A^m}{dt} = n_c \left(\frac{k^h}{k^h + X^h} \right) - m_c c_A^m \quad [1.3]$$

Where c_A^m is the concentration of A mRNA, n_c and m_c represent the rate constants for transcription and degradation respectively, X represents protein “X” concentration, k represents a Michaelis-Menten constant and h represents a Hill coefficient (where $h > 1$ corresponds to promoting ligand binding, $h < 1$ corresponds to inhibit ligand binding and $h = 1$ corresponds to non-cooperative ligand binding where ligand binding does not relate to the number of prior bound ligands). In *Arabidopsis* circadian clock models, Hill functions are often set to the value of 2, which corresponds to the dimerization of plant clock components (Fujiwara et al., 2008; Wang et al., 2010; O’Neill et al., 2011).

Parameter value estimations

Once the equations for the models have been created, the different parameter values for the different components of the newly created models need to be determined. This is the process whereby values are selected for the individual parameters so that they produce outputs that match experimental biological data as best as possible. This is often done using an objective function so that the model performance can be compared to the experimental data, usually the sum of the squares of residuals between the data and the simulation.

One can carry out parameter optimisation by hand, selecting values for the parameters using prior knowledge of the system. After running the model using a hand selected parameter, new parameter values can be selected to see if the model can be improved upon (Mendes and Kell, 1998). Whilst this trial-and-error approach has the advantage of not requiring the set-up and use of optimisation algorithms and programs and is computer un-intensive it does come with several drawbacks; obtaining parameter

values that result in models that mimic the data well can be hard to obtain, the process can be extremely time consuming and even if good results are obtained it is hard to establish if there are better parameter values that can be obtained (or if no good fit can be found it is hard to determine if there are parameter values that will give a good match). This manual optimisation and basic computational iterative optimisation, such as hill climbing, also share the same problem that some more advanced techniques also have in that a search may find a local optimum value but not a global optimum value (Kirkpatrick et al., 1983). As such global parameter optimisation algorithms are often used to obtain parameter values for models. There are several optimisation algorithms used in systems biology to create parameter values. The use of global parameter value estimation techniques is used to establish several parameter values simultaneously for a given model and are therefore of great use for biological systems (Mendes and Kell, 1998).

There are many different types of parameter value optimisations that are used in systems biology such as the manual optimisation mentioned above and the popular techniques mentioned below.

Simulated annealing

Simulated annealing is a probabilistic meta-heuristic for global optimisation of a given function in a large search space first proposed in 1983 (Kirkpatrick et al., 1983). Simulated annealing works by mimicking the physical process of annealing in metallurgy where a metal is heated and then cooled to reduce defects (Bertsimas and Tsitsiklis, 1993). In simulated annealing, the cooling effect represents a decrease in the probability of accepting worse solutions over time as the search space is explored (Bertsimas and Tsitsiklis, 1993). Simulated annealing can be useful if there are several non-optimal solutions that may be found. However, there can be problems if the process of simulated annealing completes before the most optimal solution is found, giving a false optima. Simulated annealing has the disadvantage that it is quite computationally intensive, although as computers become more powerful, this issue will become less important (Radenski, 2012).

Particle swarm

Particle swarm optimisation is a meta-heuristic swarm intelligence optimisation technique. In particle swarm optimisation, a set of randomly generated solutions, termed the “swarm”, propagates in the design space towards the optimal solution over a given number of iterations based on information shared by all the members of the

swarm (Valle et al., 2008). Particle swarm optimisation has a few advantages over similar optimisation algorithms, such as genetic algorithms (which are discussed below); they can be easier to implement than other techniques with low computational effort in comparison to other techniques (Valle et al., 2008). Particle swarm optimisation also has a more efficient search history than other techniques as previous best results are remembered, however they have the disadvantage of not guaranteeing that an optimal solution will be obtained (Valle et al., 2008).

Genetic algorithms

Parallel genetic algorithms (PGA) were used in this study to optimise the parameter values of the models created. Genetic algorithms are global search heuristics based on the idea of Darwinian evolution, in which a stochastic search algorithm eliminates bad traits whilst keeping and re-combining good traits in order to find the optimal solution (Mitchell, 1998; Kumar et al., 2010). Whilst stochastic search algorithms are less likely to find a global optima for parameter values than deterministic approaches, they have been shown to function well with a high number of unknown values (Moles et al., 2003). Genetic algorithms encode the variables of a search problem into strings of alphabets which represent possible solutions to the problem (Mitchell, 1998). In genetic algorithms, the strings are referred to as “chromosomes” and the alphabets as “genes” and the individual value of the gene is termed the “allele” (Goldberg, 1989). So, in this study, a chromosome would represent a set of potential parameter values. A population of chromosomes is created in genetic algorithms which, over time, reproduce and undergo selection and mutation to evolve better chromosomes/parameter values (Mitchell, 1998). There are several steps to the process of evolution in genetic algorithms (Goldberg, 1989; Mitchell, 1998; Leardi, 2007):

1. **Creation of population** - the initial population of candidate solutions are generated.
2. **Evaluation** - the fitness of the candidate solutions is calculated.
3. **Reproduction** - the chromosome with the best solutions are propagated to the next generation.
4. **Crossover** - Crossover occurs at the gene level. Locus are chosen at random and sequences of the chromosome before and after the locus are exchanged between two chromosomes to create two new offspring.

1 Introduction

5. **Mutation** - Mutation occurs at the allele level. Individual alleles are changed at random to create new, mutated, strings.
6. The new solutions replace the original parent population.
7. Steps 2-6 are repeated until a termination condition is met. The most common termination conditions used are: a predefined number of generations, a fitness threshold is met or a maximum evolution time is met (Leardi, 2007).

The PGA algorithm used in this study used a chi-squared least-squares objective function shown in equation [1.4] which is evaluated for each data point in the experimental data (Adams et al., 2013):

$$(cal_y - dat_y)^2 * \frac{norm}{weight} \quad [1.4]$$

Where cal_y is the simulation at a time point and dat_y is the corresponding experimental measurement for the given time point. The normalisation factor, $norm$, and weight factor, $weight$, were set at 1 in this study. In SBSI, the individual costs are summed over all of the data points in the data set and divided by the number of data points to give an average cost across the data set.

Unlike traditional random searches, in genetic algorithms are not examined at a single point at a time, rather several points are considered simultaneously (Rojas, 1996). The function for all elements of the population must be calculated, as well as new populations created thus leading to genetic algorithms being computationally intensive in comparison to simple random search algorithms (Rojas, 1996). The issue of genetic algorithms being computationally intensive is constantly decreasing over time as computers become more powerful. Genetic algorithms do have advantages over local search methods though as they will not necessarily remain trapped in sub-optimal local maximum or minimum of the target function, also as bad proposals are simply discarded from one generation to another, bad results do not effect the end solution negatively (Rojas, 1996). Genetic algorithms are also useful when there is no information about the gradient of the function to be evaluated and even in cases where there are several local maxima or minima, genetic algorithms can still obtain good results (Rojas, 1996). Genetic algorithms can have a tendency to converge to local optima rather than global optima, however, there are steps that can be taken to overcome this issue by altering mutation rates or maintaining a diverse population of solutions (Taherdangkoo et al., 2012).

As stated above, this study uses PGAs. PGAs differ from normal genetic algorithms in that the optimisation process takes place over multiple computer processors to speed up the calculations. Parallel genetic algorithms were used in this study to optimise the model parameter values for several reasons. The computational cost was not an issue here as calculations were done off-site using the SBSI servers at the University of Edinburgh (Adams et al., 2013). Studies have shown annealing procedures are only slightly better at finding global minima compared to genetic algorithms but are more computationally intensive than genetic algorithms (Kathryn Blackmond Laskey, 2003). The slightly increased ability of simulated annealing to find global minima compared to genetic algorithms was not deemed great enough to warrant the increased computational run-time. The large number of parameters that are being optimised in the different models also made genetic algorithms suitable for this study as they are capable of handling large numbers of parameters in their search space (Mitchell, 1998).

Model selection

When there are several potential possible models that can be simulated to try and represent a biological system, and the correct model of regulation is unknown, then model selection techniques need to be used to help establish which of the potential models best represents the biology.

There are a number of different model selection techniques such as the Akaike Information Criterion (AIC), the Bayesian Information Criterion (BIC), the Deviance Information Criterion (DIC) or even the Focused Information Criterion (FIC), that can be used to assess model fitness (Akaike, 1974; Schwarz, 1978; Claeskens and Hjort, 2003).

The two most common techniques used are the AIC and BIC and whilst they have some similarities, such as a penalty term that punishes large numbers of parameters to reduce the likelihood of over-fitting (Akaike, 1974; Schwarz, 1978), there is a fundamental philosophical difference between the two different techniques that makes AIC the more favourable of the two. The AIC, unlike BIC, does not aim to find the “true” model (Burnham and Anderson, 2004). Famously George E. P. Box is quoted as saying that “Essentially, all models are wrong, but some are useful” and at this point in time our understanding of the biological mechanisms being modelled in this thesis are

such that of the potential models being proposed here none of them will be the “true” model that contains all of the biological processes of *CBF3* regulation. It is the case that when comparing different potential models to each other, and the biological data, in order to find which of the potential models best fits the data, none of the models are likely to be a final, correct model encompassing all the possible biological regulation of the genes. Because of this reason in the modelling carried out in this thesis, BIC was ruled out as a potential statistical technique for model identification, and AIC was used instead.

The AIC is calculated as [1.5]

$$AIC = -2\log(L_{MLE}) + 2K \quad [1.5]$$

where $LMLE$ is the maximum likelihood estimate of the likelihood function and K is the number of independently adjusted parameters within the model (Akaike, 1974).

in this thesis a corrected version of the AIC (AICc) is used, in which a better approximation of the Kullback-Leibler divergence, which is explained below, is obtained (Hurvich and Tsai, 1989) The AICc is calculated as [1.6]

$$AICc = -2\log(L_{LME}) + \frac{2q(K+1)}{q-k-2} \quad [1.6]$$

where q is the total number of data points used in the analysis. The second term of [1.6] always has to be positive so that the first term is correctly “penalised” by the number of parameters in the model, i.e. $q > K + 2$

The Kullback-Leibler divergence is central to the AIC in that it is the measure of the difference between two probability distributions (in this case the observed biological data and the model simulation), and so, the better the Kullback-Liebler divergence approximation, the more accurate the AIC result (Kullback and Leibler, 1951).

1.3.3 The Development of the *Arabidopsis* circadian clock mathematical model

In 2005, a mathematical model for a basic feedback loop involved in the plant circadian clock was created to help further knowledge of the plant circadian clock (Locke et al., 2005b). To form a model of LHY-CCA1-TOC1 interaction that is at the centre of the *Arabidopsis* circadian clock, seven coupled differential equations

1 Introduction

were constructed. As *LHY* and *CCA1* were indistinguishable from one another, for the purposes of modelling, the authors retained only one of the genes in their model, *LHY* (Locke et al., 2005b). Michaelis-Menten kinetics were used to describe enzyme action in the model, as had been done in previous circadian clock models (Leloup et al., 1999; Kurosawa et al., 2002; Leloup and Goldbeter, 2003) and used Hill functions to describe the transcriptional activation term for *LHY* and *TOC1* mRNA (Locke et al., 2005b). The authors created their own cost function which allowed them to qualitatively assess the fit of the models to the biological data using the different parameter values they obtain from their parameter searches, rather than quantitatively assess the fit to the biological data as there was too little data available at the time for quantitative comparisons to be made. This “basic” mathematical model of the circadian clock was capable of simulating *LHY* and *TOC1* expression throughout the day and peak expression of *TOC1* and *LHY* was kept near to biologically observed times in 24 hour dark and 24 hour light conditions (**Figure 1.3**). However, this model was not capable of matching the observed short period phenotype seen in *toc1* or *lhy* mutants with reduced gene expression, and in fact gave an opposite long period shift in the model mutant simulations (Locke et al., 2005b).

This original *Arabidopsis* mathematical circadian clock model that incorporated the *LHY*, *CCA1* and *TOC1* genes was later improved upon by the authors in the same year (Locke et al., 2005a). This newer model needed to address some of the issues of the older model, such as the period phenotype in the *toc1/lhy* mutant simulations as well as the fact that an approximately 12 hour delay is needed between *TOC1* transcription and *LHY/CCA1* activation (Locke et al., 2005b). A second transcriptional feedback loop was added which included new non-experimentally deduced components X and Y. The new additions to the model enabled the correction of the earlier error in *toc1* and *lhy* mutant periods (Locke et al., 2005b). The authors of this new model also proposed X as a mechanism to add delay to their model to allow for the gap between *TOC1* and *LHY* expression of 12 hours. The authors suggest that X may take the form of a gene with the product of X activating *LHY* transcription (Locke et al., 2005a). Y, however, forms a second loop with *TOC1* and is included to help explain the short period oscillation that is present in the *lhy cca1* double mutant plants. *GI* has been suggested as the best candidate for Y by the authors as *GI* is required for normal amplitude and period length in both *LHY* and *CCA1* (Locke et al., 2005a).

The model was then refined even further (Locke et al., 2006) to include a feedback loop

between *PRR7* and *PRR9* and *LHY/CCA1* (**Figure 1.5**) (Farré et al., 2005). With the addition of *PRR7* and *PRR9* in this model the rhythmic phenotypes of *toc1* mutants (short period rhythms) could now be correctly simulated as could the *gi* mutant short period rhythms, assuming *Y* as *GI*. The long period phenotypes of the *prp7 prp9* double mutant were also correctly simulated in the new model. This circadian clock model, however, still lacked certain known clock components, such as *LUX* and *ELF4*.

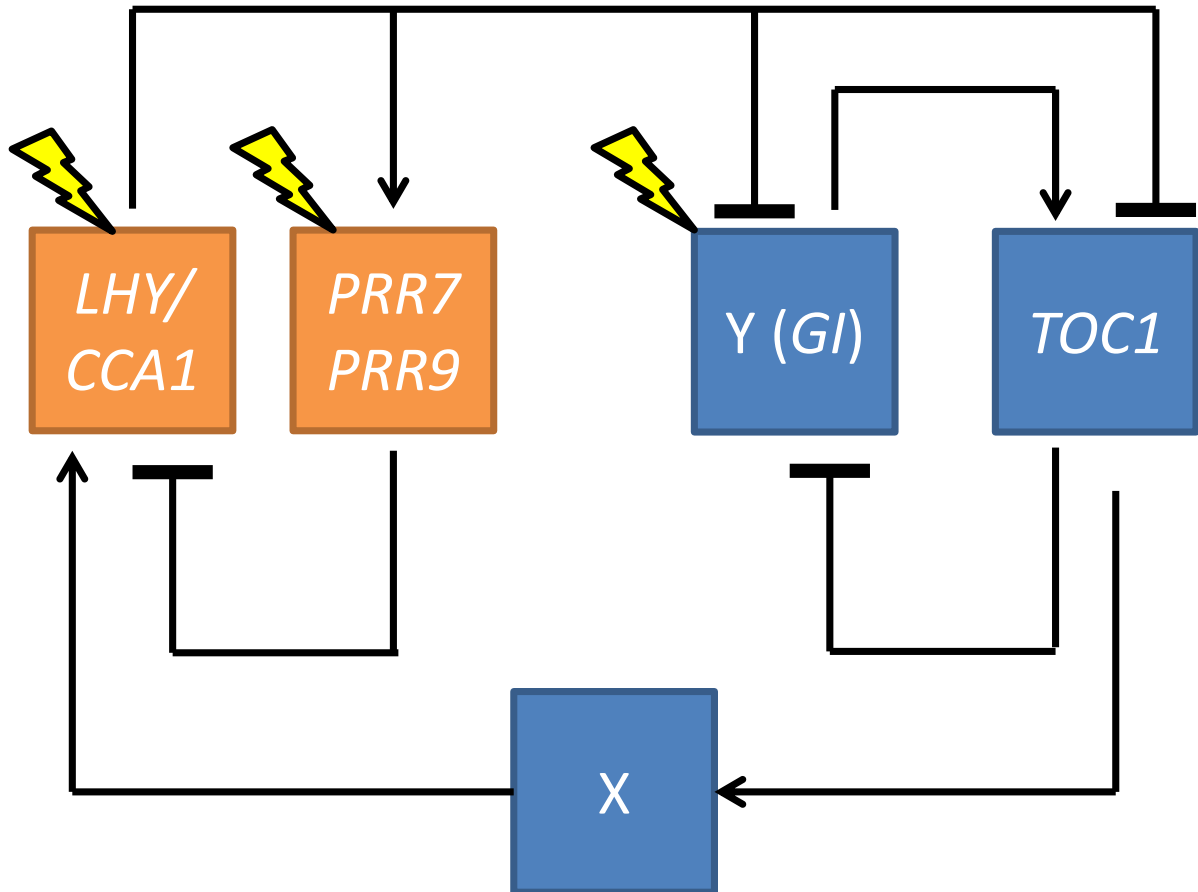


Figure 1.5: The three-loop *Arabidopsis* circadian clock model. Orange boxes represent morning genes and blue boxes represent the evening genes with a lightning arrow to indicate light input into the model. Figure adapted from Locke *et al.*, 2006.

In 2010, a new model of the circadian clock was created which included numerous recent experimental findings that were not included in the previous Locke 2006 model, especially with regards to post-transcriptional regulation of the clock (Pokhilko et al.,

1 Introduction

2010). This model, like its predecessors, was based on a series of ordinary differential equations using Michaelis-Menten kinetics to describe enzyme action in the model, with parameter values for the different components of the model either being constrained based on experimental data, or fitted to multiple time series data sets. The new model included GI stabilisation of ZTL, and the ZTL regulated targeted degradation of TOC1 (**Figure 1.6**). In addition to *PRR7* and *PRR9*, a new Night Inhibitor (NI) component was also included in the Pokhilko 2010 (P2010) model with *PRR5* being suggested as a possible candidate for NI due to the similar repressive role that it has on *LHY/CCA1* expression that is shared with PRR5 (Pokhilko et al., 2010; Nakamichi et al., 2010). The component X was removed from the model and instead replaced with posttranscriptionally modified TOC1 protein. This model addressed questions that had arisen since the Locke 2006 circadian clock model was published, based on new experimental data. GI in the Locke 2006 model was considered as part of the component Y, an activator of *TOC1* transcription, however, newer evidence showed *GI* affecting *TOC1* at the protein level, not at the transcriptional level (Kim et al., 2007). This led to the separation of *Y* and *GI* in this model which addressed this issue as well as the issue of the reduction in *TOC1* expression in *gi* mutants (Locke et al., 2006).

This model still had several unanswered questions, mostly in regards to the component *Y*, the *TOC1* transcriptional activator (Pokhilko et al., 2010). The inclusion of components such as *ELF4* and *LUX* still had not been incorporated into the model. With the P2010 circadian clock model a large number of parameter values that had previously been mathematically derived were constrained using biological data, 35 of the 90 (Dixon et al., 2011). This resulted in a model that was more biologically accurate under normal conditions and better able to mimic biological outputs of perturbations to the clock than the previously created models.

Earlier this year, the Pokhilko 2012 model of the Arabidopsis circadian clock was created which incorporates all of the transcriptional components seen in **Figure 1.2**. The latest clock model has several changes and improvements over the prior models. The main change was the inclusion of the Evening Complex genes, *ELF3*, *ELF4* and *LUX*. In the P2010 model (and earlier clock models) the evening loop of the clock included the hypothetical component Y which was included as a transcriptional activator of *TOC1* (Locke et al., 2006; Pokhilko et al., 2010). The component Y is removed from the P2012 circadian clock and instead is replaced by the Evening Complex genes. The EC genes are capable of providing oscillations in the circadian

clock even in *lhy/cca1* mutants due to the negative feedback loop that they form with the *PRRs* (Pokhilko et al., 2012). Importantly the EC inhibits *TOC1* transcription where previously component Y would promote transcription; GI still promotes transcription. The inclusion of an inhibitory effect of the GI on the EC improved *gi* mutant simulations compared to the older model.

Published data had shown decreased *LHY* and *CCA1* mRNA levels in mutants that had increased levels of TOC1 protein (Somers et al., 2004; Kang et al., 2011). By running the *ztl* single and *prp7 prp9* double mutant simulations in the model the authors concluded the reversal of the mode of action of TOC1, changing it from a promoter of *LHY/CCA1* to an inhibitor (Pokhilko et al., 2012). The model was also able to predict that the Evening Complex was responsible for regulating the expression of *LHY* and *CCA1* through the *PRRs* (Pokhilko et al., 2012).

By using a combination of biological experiments to influence model design, predictions were possible to make using the models that both confirmed hypotheses about how the circadian clock was regulated and also provided new hypotheses that may not have been thought of were it not for the development of the models.

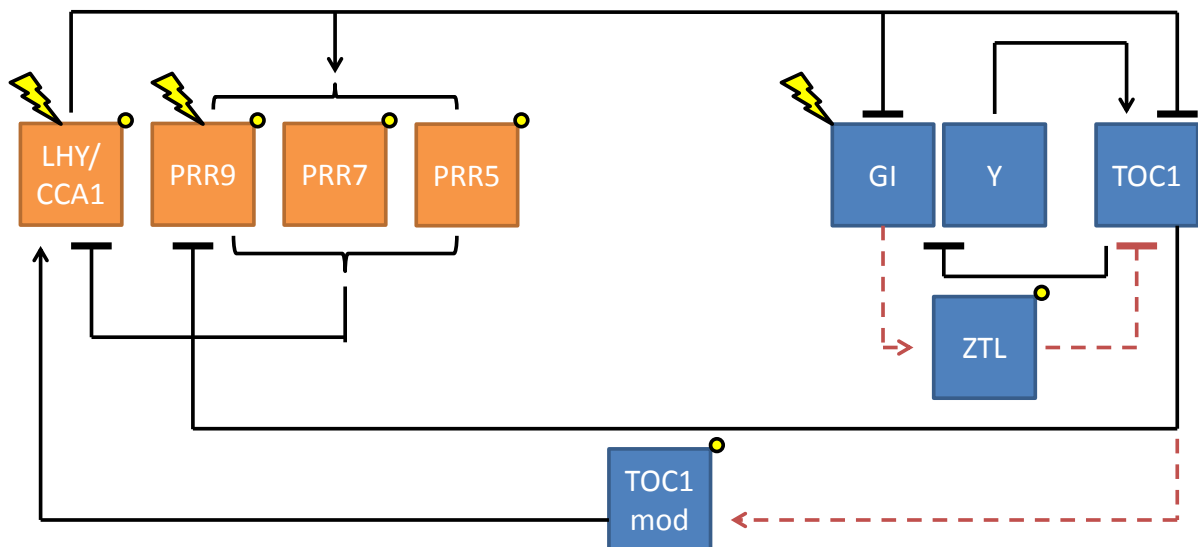


Figure 1.6: The Pokhilko 2010 model. Orange boxes represent the morning components of the circadian clock and the blue boxes represent evening components. Transcriptional regulation is shown by solid lines. Dashed red lines represent post translational regulation. Flashes represent light responsive gene expression and yellow dots are post transcriptional regulation by light. Figure adapted from Pokhilko *et al.*, 2010.

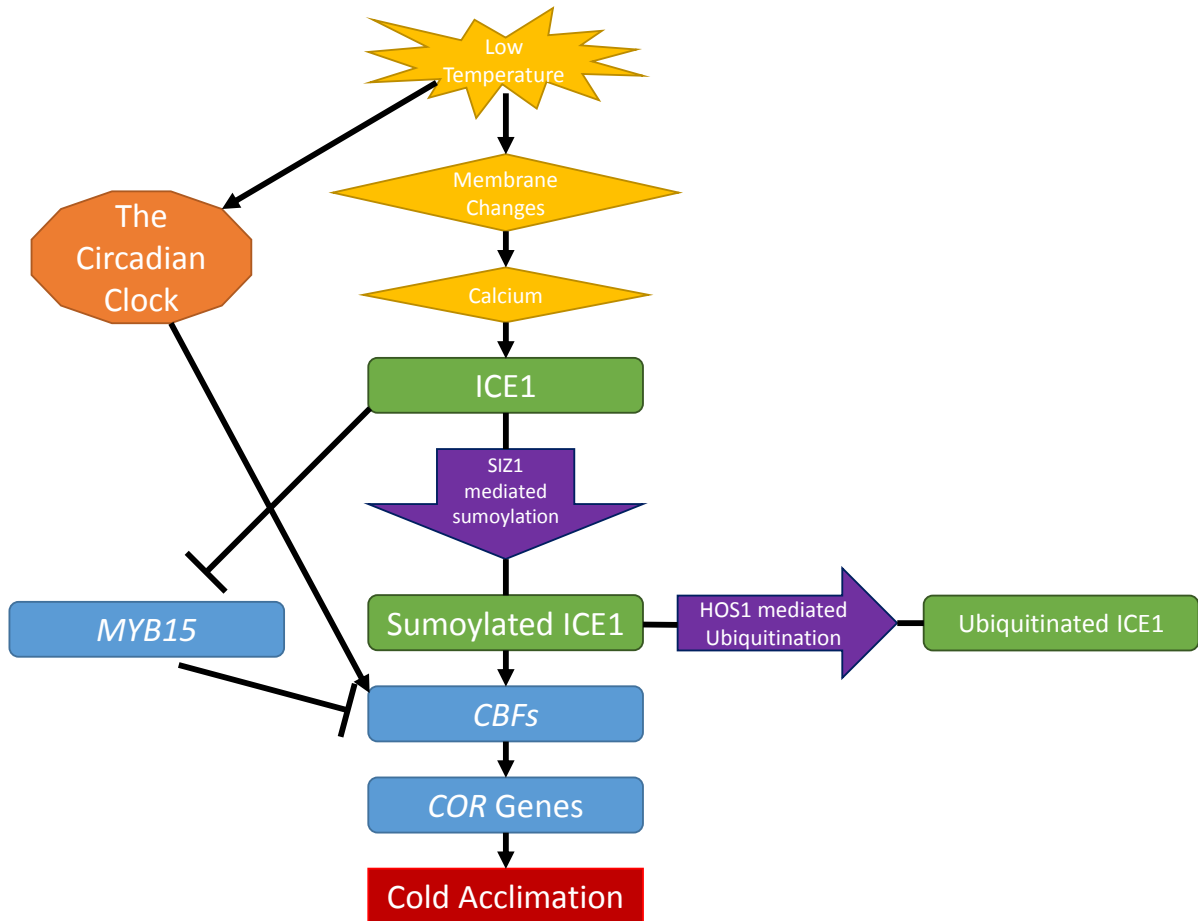


Figure 1.7: The cold acclimation pathway. Two pathways of cold acclimation are represented in this figure. In one pathway, low temperatures result in alterations to the structure of cellular membranes. This cold induced membrane alteration is thought to induce changes in cellular calcium which act as the first stage of cold acclimation pathway leading to SIZ1 mediated sumoylation of ICE1 which is needed for ICE1 to activate *CBF* gene expression. The expression of the *CBFs* is negatively regulated by MYB15. HOS1 ubiquitinates ICE1 and negatively regulates the expression of the *CBFs*. *CBFs* are responsible for regulating *COR* gene expression. *COR* proteins are responsible for physiological changes to plant cells which prevent freezing damage. In the other pathway cold temperatures directly affect the circadian clock, which in turn promotes the expression of the *CBFs*. Arrows represent positive regulation and barred lines represent negative regulation. Figure adapted from Chinnusamy *et al.*, 2007.

1.4 The cold acclimation pathway

Cold stress has many detrimental effects for plant growth and development, and if the temperatures are low enough can result in plant death. Cold acclimation is used by many temperate plants to acquire freezing tolerance from exposure to low, but non-freezing temperatures. Transcriptional regulation of the cold acclimation pathway is regulated by INDUCER OF CBF EXPRESSION 1 (ICE1) and the CBF transcriptional cascade resulting in the expression of the *COLD REGULATED (COR)* genes (**Figure 1.7**).

CBF genes

The three *CBFs* (also known as *DEHYDRATION RESPONSE ELEMENT-BINDING (DREBs)*) of interest to this study which are involved in the *CBF* mediated cold acclimation pathway are *C-REPEAT BINDING FACTOR1 (CBF1)*, *C-REPEAT BINDING FACTOR2 (CBF2)* and *CBF3*. In plants overexpressing *CBF1* there is increased *COR6*, *COR15a*, *COR47* and *COR78* transcripts in plants not exposed to low temperatures as well as increased freezing tolerance (Jaglo-Ottosen et al., 1998). Our knowledge of the *CBF* family was extended from just *CBF1* (also known as DREB1B) to include *CBF2 (DREB1C)* and *CBF3 (DREB1A)* which are located in tandem on chromosome 4 (Gilmour et al., 1998; Liu et al., 1998; Shinwari et al., 1998). *CBF1*, *CBF2* and *CBF3* share more than 84% sequence similarity to each other (Medina, 1999). These three *CBFs* have increased expression after 15 minutes of exposure to cold temperatures (Gilmour et al., 1998). Similar to *CBF1*, increased *CBF2* and *CBF3* expression results from *Arabidopsis* exposure to cold temperatures (Gilmour et al., 1998).

CBF transcription factors

The *CBF* transcription factors belong to the APETALA2/ETHYLENE RESPONSIVE FACTOR (AP2/ERF) DNA binding domain super-family (Gilmour et al., 1998). The AP2/ERF super-family consists of 147 genes and is split into four smaller families of genes: AP2, ERF, ETHYLENE RESPONSE DNA BINDING FACTOR (RAV) and At4g13040 (Nakano et al., 2006). The ERF family is then

divided into two subfamilies consisting of the ERF and the DREB/CBF proteins (Sakuma et al., 2002). DREB/CBF transcription factors bind to the C-repeat/Dehydration response element (CRT/DRE) sequence, a cis-element containing the conserved CCGAC sequence (Yamaguchi-Shinozaki and Shinozaki, 1994; Stockinger, 1997). Interestingly *DREB2* gene expression is induced by drought and salt stress but not low temperatures, whereas *CBF1*, *2*, and *3* (*DREB1B*, *C* and *A* respectively) have their gene expression induced by low temperature but not drought or salt stress (Gilmour et al., 1988; Sakuma et al., 2002). The CBF proteins can be characterised by a conserved amino acid signature located immediately downstream (DSAWR) and upstream (PKKP/RPAGR_xKFxETRHP) of the AP2/ERF domain which also differentiates the CBFs from other AP2/ERF proteins (Jaglo et al., 2001). Deletion of the PKKP/RPAGR_xKFxETRHP sequence removes the ability of CBF1 to bind to its target genes (Canella et al., 2010). CBF1, CBF2 and CBF3 have a predicted molecular mass of approximately 24 KD (Stockinger, 1997) and contain a C-terminal sequence which is required for CBFs to act as transcriptional activators (Wang et al., 2005) and a NH₃-terminal sequence which is thought to be important for CBF localisation (Raikhel, 1992; Wang et al., 2005). The AP2 domain of AP2/ERF proteins consists of a three-strand β -sheet followed by an α -helix (Allen et al., 1998). Amino acids 14 and 19 of the β -sheet have been described as important for the proteins to bind to their target DNA (Allen et al., 1998). In the CBFs amino acids 14 and 19 of the AP2 β -sheet represent valine and glutamic acid respectively (Gilmour et al., 1998), but mutant analysis of CBF1 shows that only valine is required for binding specificity (Sakuma et al., 2002). CBF-like proteins are found in several species that cold acclimate such as *Brassica napus*, wheat and rye (Jaglo et al., 2001). CBF-like proteins are even present in species of plants that are not capable of cold acclimation, such as tomatoes (Jaglo et al., 2001) who do not have as varied CBF regulon in comparison to *Arabidopsis* (Zhang et al., 2004).

COR genes

The *Arabidopsis* *COR* (*COLD-RESPONSIVE*) genes have an active role in cold acclimation, their over-expression resulting in increased freezing tolerance as shown by decreased electrolyte leakage when frozen compared to wild-type plants (Jaglo-Ottosen et al., 1998). The regulation of the *COR* genes is, therefore, vital for plants to be able to respond to adverse cold temperatures correctly. Many *COR* genes contain a

C-repeat/Dehydration Response Element (DRE) consisting of a 5 bp essential core sequence of CCGAC which is involved in both dehydration and cold responses (Yamaguchi-Shinozaki and Shinozaki, 1994).

Calcium in cold sensing

The mechanism through which cold sensing occurs is less well known than the downstream reactions to said cold temperatures, however, a role for calcium is often suggested to be important. Calcium is involved in several plant signalling pathways such as red light induced photomorphogenesis or stomatal closure (Gilroy et al., 1990; Shacklock et al., 1992). Low temperature exposure of plants results in rapid increases in cytosolic levels of calcium from cellular and extracellular stores (Knight et al., 1996). Calcium influx is also required for the cold induction of *KIN1* (Kurkela and Franck, 1990; Knight et al., 1996), a *CBF* regulon member. A link between calcium and the cold acclimation pathway was established when calmodulin binding transcription activator (CAMTA) factors were discovered to bind to a regulatory element of the *CBF2* gene promoter region (Doherty et al., 2009). Calcium influx is dependent on alterations in membrane cytoskeletal structure with changes in the actin cytoskeleton thought to be responsible for activating the channels by which calcium influx occurs (Orvar et al., 2000). Interestingly, increased calcium levels are heat shock activated similar to that of cold shock activation (Ming Gong, 1998). Changes in membrane fluidity/rigidity have been suggested as a possible solution to the cold/heat induced calcium influx dilemma. Membrane fluidity/rigidity is used to induce either heat or cold induced MAP kinase pathways respectively, offering a possible cytoskeletal /membrane dynamic that could allow for determination of heat or cold responses for calcium pathways (Sangwan et al., 2002; McClung and Davis, 2010). Reactive oxygen species (ROS) are also thought to affect cold signalling through calcium signatures; the *Arabidopsis fro1* (*frostbite1*) mutant, for example, alters calcium signalling under low temperature conditions through its increased levels of ROS (Lee, 2002).

***CBF* regulation by the cold acclimation pathway**

Due to the speed at which *CBF* transcripts start to accumulate after cold exposure, the possibility of a temperature sensing (thermostat) transcription factor was proposed that would be present at warm temperatures, bind to the *CBF* promoters to activate

1 Introduction

expression quickly when temperatures drop, which was putatively named INDUCER OF CBF EXPRESSION (ICE) (Gilmour et al., 1998). The CBFs themselves were ruled out for this role by Gilmour et al as *CBF1* over expression did not have an effect on *CBF3* levels (Gilmour et al., 1998).

An upstream transcription factor that regulates *CBF* in the cold was identified and called INDUCER OF CBF EXPRESSION 1 (ICE1) (Chinnusamy et al., 2003). The gene was identified using *CBF3-LUC Arabidopsis* lines exposed to cold conditions that showed low luminescence; one such line was designated *ice1* which showed low levels of luminescence compared to wild-type plants (Chinnusamy et al., 2003). The *ice1* mutation conferred a decrease in *CBF1*, *CBF2* and *CBF3* expression, with the greatest impairment in expression observed in *CBF3* (Chinnusamy et al., 2003). Several *COR* genes downstream of *CBFs* such as *COR15a* and *COR47a* also had decreased expression in the *ice1* mutants (Chinnusamy et al., 2003). ICE1 is a basic helix-loop-helix transcriptional activator protein that is capable of binding to the promoter region of the *CBF3* promoter to induce expression (Chinnusamy et al., 2003). ICE1, whilst being constitutively expressed and localised to the nucleus, only induces *CBF* expression in cold stress conditions which implies a posttranscriptional modification being required for ICE1 to necessitate downstream gene activation (Chinnusamy et al., 2003). SIZ1-mediated sumoylation of ICE1 is involved in regulating *CBF3* expression (Miura et al., 2007). *siz1* mutant plants do not have altered *ICE1* expression, yet cold induced *CBF3* expression is severely reduced in *siz1* mutant plants (Miura et al., 2007). *siz1* mutant plants also have reduced cold-induction of the *CBFs* and the downstream *COLD-REGULATED 15a (COR)* genes *COR15A*, *COLD-REGULATED 47 (COR47)* and *KINASE 1 KIN1* compared to wild-type plants (Miura et al., 2007). *siz1* mutant plants also have increased cold induced accumulation of MYB DOMAIN PROTEIN 15 (MYB15), a protein that binds directly to *CBF* promoter regions and inhibits their expression, compared to wild-type plants (Agarwal et al., 2006; Miura et al., 2007). MYB15 also physically interacts with ICE1, and *MYB15* is negatively regulated by ICE1 (Agarwal et al., 2006). HIGH EXPRESSION OF OSMOTICALLY RESPONSIVE GENE 1 (HOS1) is an inhibitor of *CBF* expression via posttranscriptional degradation of ICE1 (Lee et al., 2001; Miura et al., 2007). HOS1 was identified as a negative regulator of the *CBF* regulon in *Arabidopsis*, wherein *CBFs* and downstream cold induced genes such as *RD29A*, *COR15a*, *COR47* and *KIN1* all have increased cold induction in *hos1* mutants (Ishitani et al., 1998; Lee et al., 2001). HOS1 encodes a RING finger protein

1 Introduction

that mediates ubiquitination and degradation of the cold responsive pathway protein ICE1 (Lee et al., 2001; Dong et al., 2006). HOS1 physically interacts with ICE1 and is required for ICE1 ubiquitination (Dong et al., 2006). Cold induced degradation of ICE1 is inhibited in *hos1* mutants and overexpression of HOS1 results in reduced *CBF* expression and freezing tolerance makes *HOS1* an important component of the Arabidopsis cold signalling pathway (Dong et al., 2006).

As well as regulation by ICE1 and HOS1, CBF gene expression is also regulated by the CBFs themselves (Novillo et al., 2004; Novillo et al., 2007). *cbf2* mutants have increased *CBF1* and *CBF3* expression suggesting that CBF2 acts as an inhibitor of these two genes as shown in **Figure 1.8** (Novillo et al., 2007). The reduced expression of *CBF3* in *ice1* mutants is accompanied by an increase in *CBF2* expression, suggesting a possible inhibitory role of CBF3 on CBF2 (Chinnusamy et al., 2003). *CBF1* and *CBF3* expression precedes that of *CBF2* when induced by cold temperatures and this resulted in the suggestion that CBF1 and CBF3 may positively regulate *CBF2* expression in response to cold, however this was later dismissed by the same authors (Novillo et al., 2004; Novillo et al., 2007).

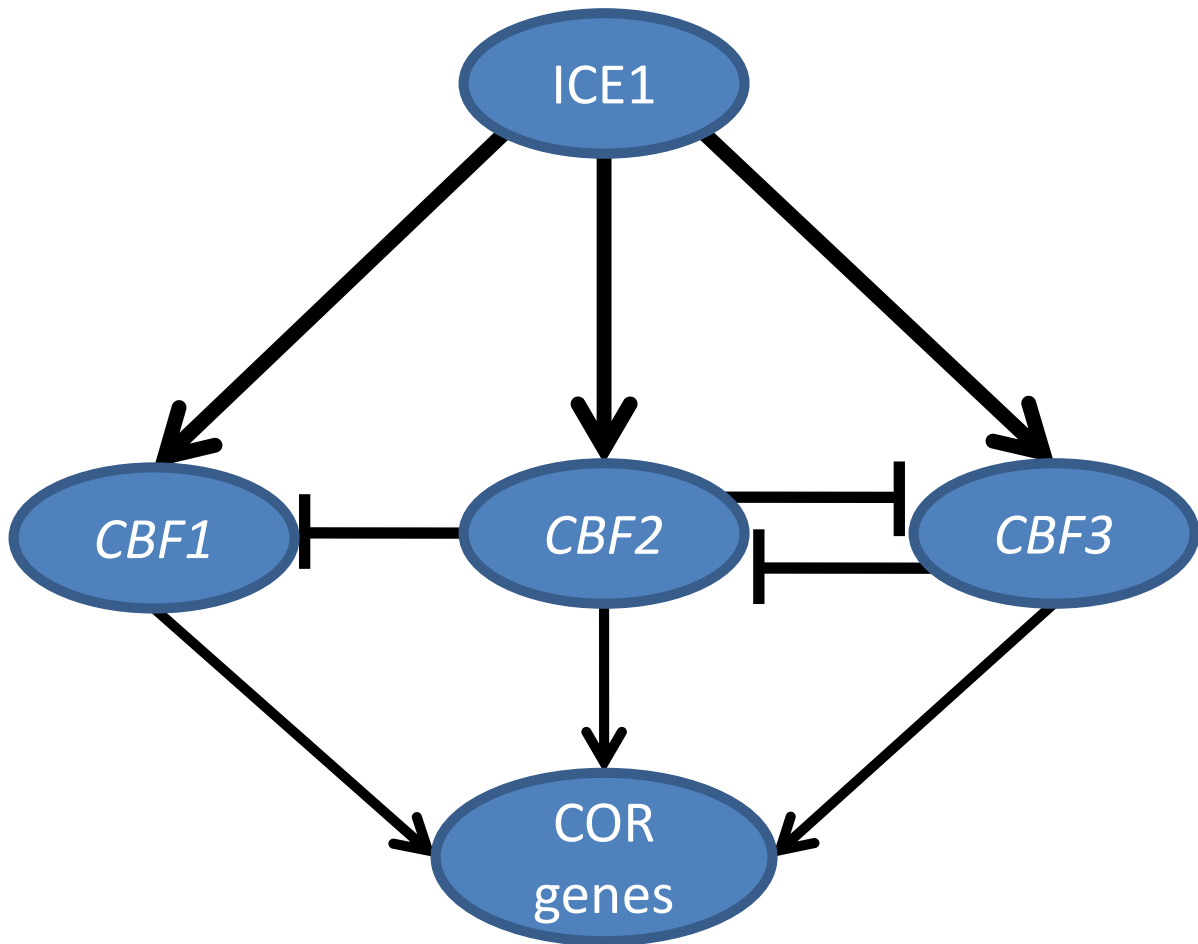


Figure 1.8: CBF regulation of CBF expression. CBF2 inhibits the expression of *CBF1* and *CBF3* as shown by increased *CBF1* and *CBF3* expression in *cbf2* mutants. CBF3 also possibly acts as an inhibitor of *CBF2* expression as suggested by increased CBF2 expression in *ice1* mutants that have decreased CBF3 levels. Adapted from Novillo *et. al.*, 2004.

Circadian regulation of the cold response pathway

The circadian clock interacts with the cold response pathway in *Arabidopsis*; temperature can affect the expression of certain genes with circadian expression, and the circadian clock itself is involved in regulating temperature responses. The cold-regulated *COLD AND CIRCADIAN REGULATED 1 (CCR1)* and *CCR2* genes of *Arabidopsis*, for example, are regulated by the circadian clock with peak expression occurring 11 h after dawn (Carpenter *et al.*, 1994). Low temperature causes a small

1 Introduction

increase in transcript levels for *CCR1* and *CCR2* both in peak expression levels and trough expression levels and cold pulses during free-running conditions result in a delay to the phase of cycling of *CCR1* and *CCR2* transcript levels (Carpenter et al., 1994). Microarray data showed that a number of cold regulated genes, such as *COR15a* and *COLD REGULATED 15b COR15b* mRNA levels were cycling in expression with a peak 8 hours after dawn (Harmer et al., 2000). *CBF3* was also shown in the same study to be oscillating with a peak at midday as well, leading the authors to first suggest a circadian role for the regulation of the *CBFs* (Harmer et al., 2000). This circadian oscillation of *CBF3* expression at warm temperatures led to further studies into the interactions between the circadian clock and the *CBF* cold response pathway (Fowler et al., 2005). In this study the authors showed strong evidence for the circadian clock involvement in regulating the *CBF* mediated cold response pathway (Fowler et al., 2005). In response to the observation that *CBF* transcript levels oscillate at warm temperatures, the authors of the study wanted to establish whether the time of day at which a plant was exposed to cold conditions affected the level of induction of the *CBFs*. Plants were grown at warm temperatures (24°C) in 12L:12D light conditions and then transferred to either 4°C or maintained at 24°C at ZT4 or ZT16 to see if time of day affected *CBF1*, *CBF2* or *CBF3* gene induction (Fowler et al., 2005). At both ZT4 and ZT16 there was no increase in *CBF* expression in plants maintained at 24°C. Higher levels of *CBF1*, *CBF2* and *CBF3* transcripts were observed in plants transferred to 4°C at ZT4 than plants that were transferred to 4°C at ZT16, although there was still a small increase in *CBF* transcript accumulation at ZT16 in plants transferred to 4°C compared to 16°C (Fowler et al., 2005). Increases in *CBF* transcripts when moved to 4°C was observed as quickly as 1 hour after transfer to lower temperatures, and the peak in expression occurred 4 hours after temperature transfer. These results were repeatable in constant light conditions, showing that the change in transcript levels were not due to light changes. The importance of the clock in regulating the cold gating of *CBF1* *CBF2* and *CBF3* transcript accumulation was further highlighted by the observation that in *CCA1-OX* arrhythmic plants, no cold gating was observed at the times tested (Fowler et al., 2005).

Further evidence has been provided to show that the circadian clock is important for regulating the *CBF* cold response pathway. Freezing tolerance is altered in a number of different circadian clock mutant plants. In the *lhy-21 cca1-1* double mutant, *lhy-21* single mutant and *cca1-11* single mutant, there is a decrease in *CBF1*, *CBF2* and

1 Introduction

CBF3 expression compared to wild-type plants (Espinoza et al., 2010; Dong et al., 2011). As well as a decrease in *CBF3* expression in *lhy cca1* double mutants, there was also a decrease in freezing tolerance in comparison to wild-type plants (Dong et al., 2011). The assumption, therefore, that LHY, CCA1 or both, are required for induction of *CBF* expression is backed up by the fact that CCA1 was also shown to directly bind to the promoter region of *CBF1*, *CBF2*, and *CBF3* (Dong et al., 2011). The *PRR* genes have also been shown to be important regulators of *CBF* expression with the *prp5-10 prp7-10 prp9-11* triple mutant having an increase in *CBF3* and *CBF2* expression throughout the day, and an increase in *CBF1* expression in the morning and afternoon compared to wild-type plants (Nakamichi et al., 2009). The *prp* triple mutants were also shown to have significantly increased survival in freezing conditions compared to wild-type plants when exposed to 24 hours of -5°C, further linking these genes to a regulatory role of the *CBFs*. *gi-3* mutants have also been shown to have increased electrolyte leakage in freezing conditions compared to wild-type plants, and *GI* expression is cold induced, however, *gi-3* mutants showed no change in *CBF1*, *CBF2* or *CBF3* expression levels compared to wild-type plants, suggesting that *GI* is not involved in regulating freezing tolerance through the *CBFs* (Cao et al., 2005).

The evening gene *TOC1* has been suggested as a possible regulator for downstream oscillations of *CBF1* and *CBF2* expression through PHYTOCHROME-INTERACTING FACTOR7 (PIF7). PIF7 binds to the G-box promoter regions of *CBF1* and *CBF2*, but has weak binding to the *CBF3* promoter (Kidokoro et al., 2009). PIF7 is actively regulated by *TOC1* (Nakamichi et al., 2009) and thus this has been proposed as a circadian regulatory pathway for the regulation of *CBF1* and *CBF2* (Kidokoro et al., 2009).

As discussed in detail previously, recent evidence on alternative splicing has provided further evidence that the circadian clock and the cold acclimation pathway are closely linked, with temperature induced alternative splicing of *CCA1* resulting in altered freezing tolerance compared to wild-type plants in *Arabidopsis* (Hofmann, 2012; James et al., 2012).

1.5 Temperature, light and seed physiology

Plants have adapted to grow in environments where temperature can vary widely over the course of a year, or even day. As a result of these changes plants have evolved a number of mechanisms to allow them to adapt, such as the cold acclimation pathway or drought resistance pathway (Thomashow, 1999; Zhu, 2002). Plants prepare for the freezing temperatures of winter by exposure to cold, non-freezing, temperatures in the lead up to the colder season, without which the plants would die (Thomashow, 1999). Plants use of temperature to predict future environmental conditions is also important for a number of other biological processes such as determining the change from one life stage to another (Lee et al., 2007) or the regulation of seed germination (Finch-Savage et al., 2007; Kurtar, 2010) as well as many other aspects of their lives. This use of current environmental conditions to predict future conditions is vital for plant survival as it means that the plant is able to prepare for changes in its environment, rather than having to constantly adapt at the time of change, by which point it may take too long and the plant could die. Our understanding of the separate pathways involved in plant adaptation, while extensive, is not complete, and in the case of how separate pathways interact with one another, such as the cold acclimation pathway and the circadian clock, even less is known. Gaining an understanding of how plants adapt, and how these separate pathways help to regulate one-another is of great importance for helping us to understand how plants will adapt and cope with current and future environmental change. An understanding of how plants will adapt, or not, to environmental change is important for agricultural reasons, but gaining a greater understanding should also allow us to engineer crops that can be grown in more regions than is currently possible, or will be possible in the future.

Seed dormancy

The regulation of seed dormancy is essential for ensuring that a seed germinates in as favourable conditions as possible. One of the key environmental signals that regulate seed germination is temperature. Seeds that are matured at high temperatures will have low levels of dormancy and high germination rates whereas seeds matured at lower temperatures will have higher levels of dormancy and low germination rates (Schmuths et al., 2006; Donohue et al., 2008; Chiang et al., 2009). Temperature plays a large role in regulating dormancy in seeds in order for them to germinate in the

1 Introduction

right season in which they will have the greatest chance of survival.

The term “dormancy” or “dormant seed” is applied to a seed which is both intact, viable under normally favourable conditions for germination, yet the seed does not germinate (Finch-Savage and Leubner-Metzger, 2006). There are two different types of dormancy; primary dormancy and secondary dormancy. Primary dormancy is induced and maintained via abscisic acid (ABA). As the seed matures, the level of ABA increases as does the level of dormancy within it until the seed is fully matured and disperses from the mother plant; the seed now has primary dormancy (Finch-Savage and Leubner-Metzger, 2006). Following the dispersal of the seeds they start to lose their primary dormancy through a process known as after-ripening if they are in a dry state. If the seed is imbibed then dormancy release factors such as cold stratification or the detection of components of smoke (such as karrikins), will lead to a reduction in dormancy (Holdsworth et al., 2008; Nelson et al., 2009). If there are no dormancy breaking stimuli on imbibed seeds (or if after-ripening occurs in a dry seed) and there are not environmentally favourable conditions present to stimulate germination (such as light), then the seed will become dormant again in a process called secondary dormancy. Secondary dormancy prevents germination from occurring in unfavourable environmental conditions and can be introduced and lost repeatedly, often in sync with seasonal changes, until the right conditions present themselves (Finch-Savage and Leubner-Metzger, 2006).

Germination can be split into three different stages, related to the uptake of water by the seed (Finch-Savage and Leubner-Metzger, 2006; Holdsworth et al., 2008). In phase 1 (imbibition) there is a rapid uptake of water by the dry seed, in phase 2 the water intake plateaus and in the third phase, in which the embryo breaks through the seed coat, there is another increase in the uptake of water and germination is complete. Two key hormones involved in germination and dormancy are ABA and gibberellin (GA). ABA-insensitive/deficient mutants have precocious germination, even under conditions that are usually unfavourable (Bewley, 1997). Whilst ABA is predominantly associated with the maintenance of dormancy, GA is mostly associated with germination.

There are numerous environmental stimuli which can affect the germination and dormancy of seeds. Light, for example, is important for germination and dormancy; in the presence of red light, seed germination is stimulated, whereas far-red light acts as a block to germination (Borthwick et al., 1952), a likely adaptation to the fact that as light travels through canopy cover it becomes far-red shifted and seeds do not want to

germinate if direct sunlight is being blocked by other plants. The effects of red and far-red light are reversible with the final light input acting as the final indicator of whether the seed will germinate or not (Bae and Choi, 2008). Temperature is another important environmental factor that can affect germination/dormancy. Periods of cold stratification can drastically reduce the level of dormancy within seeds, and the temperature at which seeds mature can also have an effect on the level of dormancy in the seed (Heschel et al., 2007; Nordborg and Bergelson, 1999). As well as environmental factors having a direct effect on germination and dormancy, there is also evidence that suggests that germination and dormancy is linked to the circadian clock and that light signalling is also linked to the circadian clock. Circadian clock mutants, for example, have been shown to have differing germination frequencies when compared to wild type seeds (Penfield and Hall, 2009).

1.6 Thesis aims and objectives

There were several aims to this project.

The main aim was to try and understand the role of the circadian clock in temperature responses in *Arabidopsis*, in the regulation of cold acclimation and seed germination.

Previous studies had shown that the circadian clock was involved in regulating a number of signalling pathways that were involved in regulating dormancy and germination in seeds (Penfield and Hall, 2009), and the circadian clock had been shown to be involved in light signalling pathways (Kim et al., 2007) however the role of the clock in the light signalling regulation of seed dormancy and germination had not been investigated. Germination experiments were carried out using seeds with mutations to different components of the circadian clock with the aim of finding seeds that had altered sensitivity to red and far-red light in Chapter 3, with the identification of TOC1 as a key protein in regulating red light mediated regulation of germination.

The focus of this study then moved away from the circadian regulation of seed dormancy, and instead looked the role of the circadian clock in regulating the cold acclimation pathway and modelling said regulation: this consists of the majority of this thesis.

The regulation of the cold signalling pathway by the circadian clock is vital for allowing plants to prepare for future cold conditions that are more likely to occur at certain times of the day, such as during the night. However, our knowledge of the

1 Introduction

circadian transcriptional regulation of the cold acclimation pathway is largely unknown. This thesis aimed to discover new circadian clock genes with a role in regulating the cold response pathways in plants, and in Chapter 4 role for the *TOC1* gene in freezing tolerance regulation.

As well as the discovery of potential new circadian genes involved in the regulation of freezing tolerance in *Arabidopsis* this project aimed to create a mathematical model connecting the circadian clock to the cold signalling pathway with the hope of increasing our understanding of how the circadian clock regulates the transcription of the *CBF* genes and to test the predicted regulatory mechanisms suggested by the freezing tolerance assays.

This study shows that the use of publically available microarray mRNA data for model optimisation, as opposed to creating new RT-PCR time series data, is capable of producing biologically relevant models of transcriptional regulation. In Chapter 5 a model of *CBF3* regulation by the circadian clock is created in which *CBF3* transcription is promoted by LHY/CCA1 and inhibited by both TOC1 and the Evening Complex. This success should hopefully allow for the future modelling of the control of numerous circadian outputs for which microarray data is already publicly available (Harmer et al., 2000; Mockler et al., 2007).

This study uses a systems biology approach to understanding the circadian clock regulation of freezing tolerance via *CBF3* and aims to demonstrate the benefits of a systems approach over that of a lab-based only approach.

2 Materials and Methods

2.1 Mutant lines

Four wild-type ecotypes of *Arabidopsis thaliana* were used: Columbia-0 (Col-0, Col), C24, Wassilewskija (WS) and Landsberg Erecta (Ler). Mutant plants from Col, Ler and C24 were used in this thesis (Table 2.1).

2.2 Growth media for plants

Two types of growth media were used; Murashige & Skoog agar (MS), and water agar (WA). Both agar types were 0.9% agar with a pH of 5.7-5.8. MS-agar had the addition of 0.45% Murashige and Skoog. Where the pH was lower than 5.7-5.8, potassium hydroxide was added to obtain the correct pH. Standard 9 cm diameter petri dishes were used and sealed with micropore tape after the addition of seeds to the media.

2.3 Plant growth and seed harvest

Arabidopsis plants were grown on compost (Everiss and Levington F2 Seeds and Modular) treated with Intercept Greenhouse Insecticide (Bayer Inc.) in trays of 24 pots, 1 pot per plant. General growth of plants for bulk seed collection was carried out in the University of York greenhouse, and later the University of Exeter Greenhouse. As seeds developed, the plants were wrapped in paper bags to collect the seeds. Each seed batch was size fractionated using a 200 mm mesh sieve (Fisher Scientific) to separate out unfit seeds. Specific environmentally controlled experiments were carried

Table 2.1: Mutant *Arabidopsis* plants used in this study, the ecotype background for each mutant and the effect on function of the mutation.

Mutant	Background	Effect on function	Reference
CCA1 OX	Col	Over-expression	(Wang and Tobin, 1998)
<i>elf3-1</i>	Col	Null mutant	(Zagotta et al., 1996)
<i>gi-201</i>	Col	Null mutant	(Martin-Tryon et al., 2007)
LHY OX	Ler	Over-expression	(Schaffer et al., 1998)
<i>lhy-11 cca1-1</i>	Col	Null mutant	(Nakamichi et al., 2007)
<i>lhy-20</i>	Col	Loss of function	(Michael et al., 2003)
<i>lux-5</i>	Col	Loss of function	(Hazen et al., 2005)
<i>prrr5-1</i>	Col	Loss of function	(Eriksson et al., 2003)
<i>prrr5-11 prrr7-11</i>	Col	Null mutant	(Nakamichi et al., 2005)
<i>prrr5-11 prrr7-11 prrr9-10</i>	Col	Null mutant	(Nakamichi et al., 2005)
<i>prrr5-11 prrr9-10</i>	Col	Null mutant	(Nakamichi et al., 2005)
<i>prrr7-11 prrr9-10</i>	Col	Null mutant	(Nakamichi et al., 2005)
<i>prrr7-3</i> (Also known as <i>prrr7-11</i>)	Col	Null mutant	(Michael et al., 2003; Yamamoto et al., 2003)
<i>prrr9-1</i>	Col	Null mutant	(Zeilinger et al., 2006)
TOC1 MG	C24	Over-expression	(Mas, Alabadi, et al., 2003)
<i>toc1-101</i>	Col	Loss of function	(Kaczorowski, 2004)
<i>toc1-2 prrr5-11 prrr7-11 prrr9-10</i>	Col	Null mutant	(Yamashino et al., 2008)
<i>ztl-3</i>	Col	Null mutant	(Somers et al., 2004)

out in Panasonic MLR Plant Growth Cabinets, with the growth conditions explained in the specific experimental methods sections below.

2.4 Seed sterilisation

All seeds that were imbibed on MS-agar and water agar were first sterilised. 6 Klorsept-17 Effervescent Disinfectant Tablets dissolved in 100 ml of sterile water was used for bleach. The bleach was then used to create a bleach/ethanol solution of 95% ethanol, 5% bleach. 1 ml of 100% ethanol was added to seeds in Eppendorf tubes and inverted to wash followed by ethanol removal. A ten minute wash of 1 ml ethanol/bleach solution was then carried out followed by a further two washes of 1 ml 100% ethanol. Seeds were then left to dry in a sterile flow hood.

2.5 Germination assays

These assays were carried out to determine the rates of germination of circadian clock mutant seeds under different light treatments, as well as to assess dormancy levels of clock mutant seeds matured at low temperatures.

2.5.1 Red light germination assay

For the germination assays assessing germination rates after exposure to different periods of red light exposure, seeds were first sterilised then imbibed on either water-agar or MS-agar depending on the experiment. In experiments with a cold stratification period, seeds were now cold stratified for three days at 4°C; if no cold stratification was to take place then move straight on to the next step. Seeds were exposed to white light at $100 \mu\text{mol photons/m}^{-2}/\text{s}^{-1}$ for one hour to promote germination. Seeds were then exposed to five minutes of far-red ($30 \mu\text{mol photons/m}^{-2}/\text{s}^{-1}$) light to block germination followed by either 0, 10, 30 or 60 seconds of red light ($30 \mu\text{mol photons/m}^{-2}/\text{s}^{-1}$). Seeds were then incubated for five days at 22°C in the dark after which the percentage of seeds germinated was recorded.

This experiment was carried out in complete darkness, or with seeds wrapped in three layers of tinfoil, unless light exposure is required as stated above.

2.5.2 Far-red light germination assay

For the germination assays assessing germination rates after exposure to different periods of far-red light exposure seeds were first sterilised then placed onto either water-agar or MS-agar depending on the experiment. In experiments with a cold stratification period, seeds were now cold stratified for three days at 4°C; if no cold stratification was to take place then move straight on to the next step. Seeds were then exposed to white light ($100 \mu\text{mol photons/m}^{-2}/\text{s}^{-1}$) for one hour to promote germination. Seeds were then exposed to either 0, 10, 30 or 60 seconds of far-red light ($30 \mu\text{mol photons/m}^{-2}/\text{s}^{-1}$). Seeds were then incubated for five days at 22°C in the dark after which the percentage of seeds germinated was recorded.

This experiment was carried out in complete darkness, or with seeds wrapped in three layers of tinfoil, unless light exposure is required as stated above.

2.5.3 Low temperature cold stratification period assay

To assess the effect of different cold stratification periods on plants that were grown at low temperatures, plants were grown at 22°C in 12 hours $100 \mu\text{mol photons/m}^{-2}/\text{s}^{-1}$ white light and 12 hour dark conditions until the first flowers started to develop. At this point the temperature conditions were altered to 12°C so that the seeds would mature entirely at 12°C. The seeds were harvested, sterilised and plated onto WA plates. The agar plates were then cold stratified at 4°C in the dark for either 0, 1, 2 or 3 days. After the cold stratification period the plates were moved to 22°C, 12 hours $100 \mu\text{mol photons/m}^{-2}/\text{s}^{-1}$ white light, 12 hours dark for five days to allow for germination to occur, at which point the number of dormant and germinated seeds were scored.

2.6 Freezing tolerance assay

This assay was used to establish circadian clock mutant plants that had altered freezing tolerance phenotypes. The assay was developed by Dr Dana Macgregor at the University of Exeter, adapted from Franklin and Whitelam, 2007 (Franklin and Whitelam, 2007).

Seeds were sown on compost (Everiss and Levington F2 Seeds and Modular) treated with Intercept Greenhouse Insecticide (Bayer Inc.) in trays split into 24 compartments with approximately 16-20 seeds per compartment. The seeds were then cold stratified for three days at 4°C in the dark. The trays were then transferred to growth cabinets set to 22°C with 12 hours of approximately 100 $\mu\text{mol photons/m}^{-2}/\text{s}^{-1}$ white light per day for seven days to allow for germination to occur. After one week's growth they were then transferred to the test temperatures for either 17 days at 12°C; 11 days at 17°C or 9 days at 22°C to allow for four true leaves to grow. Plants were then frozen at either -5°C for 24 hours or at -3°C for 24 hours in the dark as heat from the cabinet lights prevented the consistent and accurate maintenance of the freezing temperatures. A period of one day at a recovery temperature of 4°C in the dark (heat from lights prevented maintenance of low temperatures) was then allowed before moving the plants back to their test conditions for a period of time to allow the plants that are still alive to continue growing; five days at 17°C/22°C or seven days at 12°C. Survival was assessed by checking to see if any further leaves had grown since the plants exposure to freezing temperatures.

2.7 Molecular biology

Genomic sequences were obtained from The *Arabidopsis* Information Resource (TAIR), (www.arabidopsis.org). Primers were designed using Primer3 (<http://frodo.wi.mit.edu/>), and then checked for validity using the NCBI primer-BLAST (<http://www.ncbi.nlm.nih.gov/tools/primer-blast/>).

2.7.1 Purification of total RNA from plant tissue

RNA purification from plant tissue was carried out using the RNeasy Plant Mini Kit (Qiagen, Valencia, CA). Buffer RLT, Buffer RPE and Buffer RW1 are supplied with the kit. Before using the RNeasy Plant Mini Kit, 10 μ l of 2-mercaptoethanol per 1 ml Buffer RLT needs to be added to the Buffer RLT. Before using the RNeasy Plant Mini Kit, 4 volumes of 100% ethanol needs to be added to Buffer RPE to dilute as the buffer is supplied as a concentrate.

Frozen plant tissue was ground in liquid nitrogen with a pestle and mortar and transferred to a RNase-free 2 ml microcentrifuge tube and the liquid nitrogen was allowed to evaporate.

To samples of approximately 100 mg ground plant tissue, 450 μ l Buffer RLT (with 2-mercaptoethanol added) was added and mixed vigorously. The lysate was then transferred to a QIAshredder spin column placed in a 2 ml collection tube and centrifuged at full speed for 2 minutes. Without disrupting the pellet of plant material the supernatant was transferred to a new microcentrifuge tube. A 0.5 volume (225 μ l) of 100% ethanol was then added to the lysate, mixed by pipetting. The sample is then transferred to an RNeasy spin column placed in a 2 ml collection tube. The samples were then spun in the centrifuge for 15 minutes at 8000 g and the flow through was discarded. 700 μ l of Buffer RW1 was then added to the RNeasy spin column and centrifuged once more for only 15 seconds at 8000 g. The flow through was once more discarded and 500 μ l of Buffer RPE was added to the RNeasy spin column and centrifuged once more for 15 seconds at 8000 g followed by discarding the flow through. Another wash of 500 μ l Buffer RPE for 2 minutes at 8000 g, after discarding the flow through the sample was spun for another minute at 8000 g. 40 μ l of RNase-free water was then added and the sample spun once more in a new clean 1.5 ml collection tube for 1 minute at 8000 g. The elute was then re-added to the spin column and spun for another 1 minute at 8000 g and the flow through kept. Ribonucleic acid (RNA) concentration was then established using a NanoDrop (Thermo Scientific). Complementary deoxyribonucleic acid (cDNA) was then synthesised from the samples.

2.7.2 cDNA synthesis

First strand cDNA was synthesised by using 1 μl of Oligo-dt (Invitrogen) added to 5 micrograms (μg) of purified RNA in 10 μl of RNase free water and denatured for 10 minutes at 70°C. 9 μl of cDNA synthesis master mix (4 μl 5X FS reaction buffer (Invitrogen), 2 μl dithiothreitol 0.1 M (Invitrogen), 2 μl deoxynucleotide triphosphates 10 μM , and 1 μl Superscript II Reverse Transcriptase (Invitrogen)) was then added to each sample and incubated for one hour at 42°C. The samples were then diluted in up to 200 μl of sterile water. Real-time reverse-transcription polymerase chain reaction (qRT-PCR) was then carried out to assess mRNA expression levels in the samples.

2.7.3 qRT-PCR

Standard curves were created using an undiluted sample, a 1:10, 1:100, 1:1000, and a 1:10000 dilution in sterile water. A water sample and a “No Template Control” were also used. A master mix of nuclease free water (up to a final volume of 16 μl), 10 μl of SYBR Green Master Mix [2X SYBR Green Master Mix (Invitrogen) was used in time-series qRT-PCRs, later chromatin immunoprecipitation (ChIP) experiments used Brilliant III Ultra-Fast SYBR Green QPCR Master Mix (Agilent)], 1 μl of Forward primer (200-500 nM) and 1 μl of reverse primer (200-500 nM) and 0.3 μl of reference dye (Invitrogen). The master mix was added to the required wells in the 96 well plate and 4 μl of (0.5 pg - 100 ng) of cDNA was added to the master mix in their wells. The 96 well plates were then spun to collect and mix the samples and master mix in the bottom of each well and were run on a MXP 3005P qPCR machine (Agilent Technologies). qRT-PCR thermal profile for the MXP 3005P qPCR consisted of three minutes at 95°C for one cycle, 40 cycles of 15 seconds at 95°C followed by 15 seconds at 60°C and one final cycle of 1 minute at 95°C followed by 30 seconds at 55°C with a final step of 30 seconds at 95°C.

For **Figure 4.5** and **Figure 5.12** the mRNA quantity of a gene of interest as well as a control gene was calculated. In these experiments *ACTIN2* (*ACT2*) was used as the control gene. The individual samples were first automatically normalised against the reference dye and the average quantity for the gene of interest and control gene were calculated. For **Figure 4.5** and **Figure 5.12** three biological samples were used for

2 Materials and Methods

each data point. The quantity for the gene of interest was then normalised against the control gene quantity to give a final normalised quantity. For **Figure 4.5** a standard curve was used with sample ZT64 17°C as the undiluted sample with a value set to 1; for **Figure 5.12** sample Col CT0 was used as the undiluted sample with a value set to 1.

For the qRT-PCR carried out for the ChIP experiments (**Figure 5.14**, **Figure 5.15**, **Figure 5.16**) the same MXO 3005P qPCR settings were used as described above. Standard curves were created for each ChIP sample and qRT-PCR was carried out on three biological samples. The analysis of the qRT-PCR is described below in the section **Analysis of Chip results**.

Primers for amplification used can be seen in **Table 2.2**.

Table 2.2: Primers
qRT-PCR Time Series Primers

Primers	Sequence	Use
Actin (ACT2) F	5'-CGTTTCGGCTTTCCTTAGTGTTA-3'	qRT-PCR Control Gene
Actin (ACT2) R	5'-AGCGAACGGATCTAGAGACTC-3'	qRT-PCR Control Gene
CBF1 F	5'-TGGCTGAAGGCATGCTTTTA-3'	Check CBF1 Expression
CBF1 R	5'-ACAAAATGGAACGACTATCGAAT-3'	Check CBF1 Expression
CBF3-F-2012	5'-AATATGGCAGAAGGATGCT-3'	Check CBF3 expression
CBF3-R-2012	5'-ACTCCATAACGATACGTCGT-3'	Check CBF3 expression
TOC1 F	5'-TCTTCGCAGAAATCCCTGTGAT-3'	Check TOC1 expression
TOC1 R	5'-GCTGCACCTAGCTTCAAGCA-3'	Check TOC1 expression
LUX F	5'-GACGATGATCTGTGATGATAAGG-3'	Check LUX expression
LUX R	5'-CAGTTTATGCACATCATATGGG-3'	Check LUX expression
qRT-PCR ChIP Primers		
Primers	Sequence	Use
Actin (ACT2) F	5'-CGTTTCGGCTTTCCTTAGTGTTA-3'	Negative control
Actin (ACT2) R	5'-AGCGAACGGATCTAGAGACTC-3'	Negative control
TGTG F	5'-TCTCTGGACACATGGCAGAT-3'	Check binding at putative TOC1 binding site
TGTG R	5'-TGTCCTCTGGTAATGCCACGTA-3'	Check binding at putative TOC1 binding site
LUX-F-I	5'-TTTAGCAACAGAAAGCCACAAA-3'	Check binding at putative LUX binding site 1
LUX-R-I	5'-AGTGAAGTCAAAAATAAAGCA-3'	Check binding at putative LUX binding site 1
LBSHF	5'-GTTTAAACACAGCAGGAAGTAAATAT-3'	Check binding at putative LUX binding site 2
LSBIIR	5'-TCGGAAGTCAAAAATAAAGCA-3'	Check binding at putative LUX binding site 2
LHYprChIP (G-box)F	5'-TTCTGGCTCGTAGAGAAAGCAA-3'	Positive control for TOC1 binding
LHYprChIP (G-box)R	5'-CTGGAACAGCACCAAGGGTA-3'	Positive control for TOC1 binding
2012-03-05 II-F	5'-CATAAATTGGCTCGTCTCGAA-3'	Negative control
2012-03-05 II-R	5'-TTGGTTGTCTCGTACGGATTTG-3'	Negative control

2.7.4 ChIP

ChIP buffers and solutions were prepared in the lab on the day of use (**Table 2.3-2.10**). Protease inhibitors (ROCHE complete cocktail) were added just before use.

20 ml of Milli-Q water was first added to 50 ml conical centrifuge tubes, with needle holes in the cap. To the conical centrifuge tubes, seedlings were added until the volume of Milli-Q water and sample reached 30 ml. After emptying the water, 20 ml of 1.0% formaldehyde was added. The seedlings were then vacuum infiltrated in a vacuum pump desiccator for 10 minutes to cross link. The samples were quenched by adding 1.3 ml of 2 M glycine to the tube and vacuum infiltrated for a further five minutes after which the samples were rinsed three times with Milli-Q water after which the water was removed and the samples were frozen in liquid nitrogen and stored at -80°C . The tissue was ground in liquid nitrogen in a mortar and pestle and added to 30 ml of Extraction Buffer 1 (**Table 2.3**) in a 50 ml conical tube.

Table 2.3: **ChIP Extraction Buffer 1**

ChIP Extraction Buffer 1	For 100 ml	
0.4 M Sucrose	20 ml	2 M
10 mM Tris-Hydrochloride (Tris-HCl) pH 8	1 ml	1 M
5 mM 2-mercaptoethanol	35 μl	14.3 M
1 mM phenylmethanesulfonylfluoride (PMSF)	1 ml	0.1 M
Protease Inhibitors (PI)	2 tablets	
	H_2O to volume	

After filtering the solution through two layers of Miracloth into a Nalgene Oak Ridge Centrifuge Tube (Thermo Scientific) they were centrifuged for 20 minutes at 3000 g at 4°C . After removing the supernatant, the pellet was re-suspended gently using a paintbrush in 1 ml of Extraction Buffer 2 (**Table 2.4**) and transferred to a 1.5 ml Eppendorf tube and left on ice for 10 minutes. The sample was then centrifuged at 14,000 g for ten minutes at 4°C followed by the removal of the supernatant. The remaining pellet was then re-suspended in 500 μl of Nuclear Lysis Buffer (**Table 2.5**).

The chromatin was sheared to between 100 and 1,000 bp using a Bioruptor UCD 200 (Diagenode) set to high intensity (320 W) for ten minutes (cycles of 30 seconds on and 30 seconds off) at 4°C . 20 μl was removed and mixed with 80 μl of

2 Materials and Methods

Table 2.4: **ChIP Extraction Buffer 2**

Extraction Buffer 2	for 10 ml	
0.25 M Sucrose	1.25 ml	2 M
10 mM Tris-HCl pH 8	100 μ l	1 M
10 mM magnesium chloride ($MgCl_2$)	100 μ l	1 M
1% Triton X-100	100 μ l	100%
5 mM 2-mercaptoethanol	3.5 μ l	14.3 M
1 mM PMSF	100 μ l	0.1 M
PI	400 μ l	25 X
	H_2O to volume	

Table 2.5: **ChIP Nuclei Lysis Buffer**

Nuclei Lysis Buffer	for 5 ml	
50 mM Tris-HCl pH 8	0.25 ml	1 M
10 mM ethylenediaminetetraacetic acid (EDTA)	100 μ l	0.5 M
1% sodium dodecyl sulfate (SDS)	0.5 ml	10%
1 mM PMSF	50 μ l	0.1 M
PI	200 μ l	25 X
	H_2O to volume	

Tris-ethylenediaminetetraacetic acid (T.E.) and stored at $-80^\circ C$ to be used as the input DNA control; Immunoprecipitation was carried out on the remaining chromatin. 25 μ g chromatin was transferred to a 50 ml tube and diluted with 10 X ChIP Dilution Buffer (Table 2.6).

Table 2.6: **ChIP Dilution Buffer**

ChIP Dilution Buffer	for 10 ml	
1.1% Triton X-100	110 μ l	100%
1.2 mM EDTA	24 μ l	0.5 M
16.7 mM Tris-HCl pH 8	167 μ l	1 M
167 mM sodium chloride (NaCl)	334 μ l	5 M
	H_2O to volume	
1 mM PMSF	100 μ l	
PIs	400 μ l	25 X

75 μ l (25 μ l for pre-clean and 50 μ l for later stages) Magnetic Protein A agarose beads were equilibrated with ChIP Dilution Buffer. The chromatin sample was pre-cleaned by adding 25 μ l of protein A beads and rotating for 1 hour. A magnet was used to attract the beads, and the supernatant was transferred to a clean tube. The antibody (Green

2 Materials and Methods

fluorescent protein [GFP] Abcam ab290 1:1000) was added and the sample incubated at 4°C overnight on a rotating mixer wheel. The remaining 75 μ l of beads were added and incubated for a further 2 hours on a rotating mixer wheel at 4°C. A magnet was then used to pellet the beads and recover in 1 ml of Low Salt Wash Buffer (**Table 2.7**) and transfer to a new 1.5 ml Eppendorf tube and wash for 5 minutes at 4°C.

Table 2.7: **ChIP Low Salt Wash Buffer**

Low Salt Wash Buffer	for 50 ml	
150 mM NaCl	1.5 ml	5 M
0.2% sodium dodecyl sulfate (SDS)	1 ml	10%
0.5% Triton X-100	0.25 ml	100%
2 mM EDTA	200 μ l	0.5 M
20 mM Tris-HCl pH 8	1 ml	1 M
	<i>H₂O</i> to volume	

Further washes were carried out with 1 ml of each of the following for five minutes each at 4°C: High Salt Wash Buffer (**Table 2.8**), four times; lithium chloride (LiCl) Wash Buffer (**Table 2.9**), once; T.E. (**Table 2.10**), two washes. After removing the residual T.E. the sample needs to have the cross-linking reversed and the DNA needs to be purified; 100 μ l of 10% Chelax resin and vortex. Reverse the protein DNA cross-links by boiling the sample for 10 minutes. Add 1 μ l of 20 mg/ml Proteinase K and incubate for 30 minutes at 50°C followed by boiling for another 10 minutes. After centrifuging for 5 minutes at full speed the supernatant was collected and 100 μ l of T.E. was added to the pellet and then vortexed and centrifuged once more. Both supernatants were then combined in a single tube and clean up the DNA using a QIAquick PCR purification Kit (Qiagen).

The ChIP samples and input samples had qRT-PCR carried out as described in section 2.7.3 and the percent input was calculated as described below.

Table 2.8: **ChIP High Salt Wash Buffer**

High Salt Wash Buffer	for 50 ml	
500 mM NaCl	5 ml	5 M
0.2% SDS	1 ml	10%
0.5 Triton X-100	0.25 ml	100%
2 mM EDTA	200 μ l	0.5 M
20 mM Tris-HCl pH 8	1 ml	1 M
	<i>H₂O</i> to volume	

Table 2.9: **ChIP LiCl Wash Buffer**

Lithium Chloride (LiCl) Wash Buffer	for 50 ml	
0.25 M LiCl	3.125 ml	4 M
0.5% nonyl phenoxypolyethoxylethanol (NP)-40	0.25 ml	100%
0.5% sodium deoxycholate	0.25g	
1 mM EDTA	100 μ l	0.5 M
10 mM Tris-HCl pH 8	0.5 ml	1 M
	<i>H₂O</i> to volume	

Table 2.10: **ChIP TE Buffer**

TE Buffer	for 50 ml	
10 mM Tris-HCl pH 8	0.5 ml	1 M
1 mM EDTA	100 μ l	0.5 M
	<i>H₂O</i> to volume	

Analysis of ChIP results

Percent input was calculated for the ChIP experiments to show the percentage of DNA that was precipitated by the GFP Abcam ab290 antibodies.

To calculate the percent input several steps were carried out on the qRT-PCR data. The dilution factor (DF) was first calculated.

$$DF = \log_2(\text{chromatin } \mu\text{l}/\text{input } \mu\text{l})$$

The input sample cycle threshold (Ct) data obtained from the qRT-PCR for both the ChIP samples and the input samples was adjusted using the DF.

$$\text{input Ct} - DF$$

The ChIP sample Ct was subtracted from the adjusted input Ct to give the dCT.

$$dCT = (\text{adjusted input Ct} - \text{ChIP sample Ct})$$

Before the percent input was calculated, the primer efficiency was first calculated.

$$\text{Primer efficiency} = 10^{(-1/\text{slope of the standard curve})}$$

Using the primer efficiencies, the percent input was then calculated.

$$\text{Percent input} = 100 \times (2^{-dCT})$$

The percent input of the three biological samples for each data point was then averaged and the standard error shown for **Figure 5.14**, **5.15** and **5.16**.

2.8 Modelling

Three different programs were used to create the different models, CellDesigner 4.1 (<http://www.celldesigner.org>), SBSIVisual (<http://www.sbsi.ed.ac.uk/>) and Matlab R2012a (<http://www.mathworks.co.uk/products/matlab/>). The three different programs each had a specific role to play for the creation of the models. CellDesigner was used to create the model files, SBSIVisual was used to optimise the model parameter values and Matlab was used to run the AICc.

2.9 Model creation in CellDesigner

CellDesigner was used to create the models in the Systems Biology Markup Language (SBML) (Hucka et al., 2003). CellDesigner takes SBML code and represents it visually as a network (**Figure 2.1**), the model can then be edited and re-saved as SBML code.

To create the new models discussed in this thesis the original circadian clock model without *CBF3* regulation (in this case either the Pokhilko 2010 or 2012 circadian clock model) is opened in CellDesigner. CellDesigner will create a cartoon of the model which makes it easier to visualise (**Figure 2.1**).

To add *CBF3* mRNA expression to the model the following steps were taken. A new “Generic Protein” compartment was added to the image to represent *CBF3* as shown in the red box in **Figure 2.1**. A degradation rate for the *CBF3* mRNA needs to be added and this was done by inserting a “degraded” box connected to the gene box via a “state transition” arrow (with the arrow facing the “degraded” box) as shown in the red box in **Figure 2.1**. By right clicking on the state transition arrow and selecting “edit kinetic law” the mathematical equation for the degradation of *CBF3* can be added. The *CBF3* compartment needs to be connected to the different regulatory components of the clock and this is done by adding a “degraded” box and connecting it to the *CBF3* compartment, but this time with the “state transition” arrow pointing to the

CBF3 box. A “catalyst” arrow was used to connect the clock components to the “state transition” arrow, as shown in the orange box in **Figure 2.1** where the example is of *CBF3* expression being regulated by TOC1. By right clicking on the “Catalyst” arrow, the equation for *CBF3* transcription and transcriptional regulation by the clock can be added.

At this point *CBF3* transcriptional regulation has thus been added to the circadian clock model, however, the model still needs to be told what new parameters have been added and the corresponding parameter values.

The parameters used in the ordinary differential equations need to be entered into the parameters tab. The model can then be saved again as SBML code and SBSIVisual was then used to optimise the parameter values that were entered so that they best match the biological data.

The different equations used for the different potential models are discussed and can be found in Chapter 5, Table 5.1 and Table 5.3.

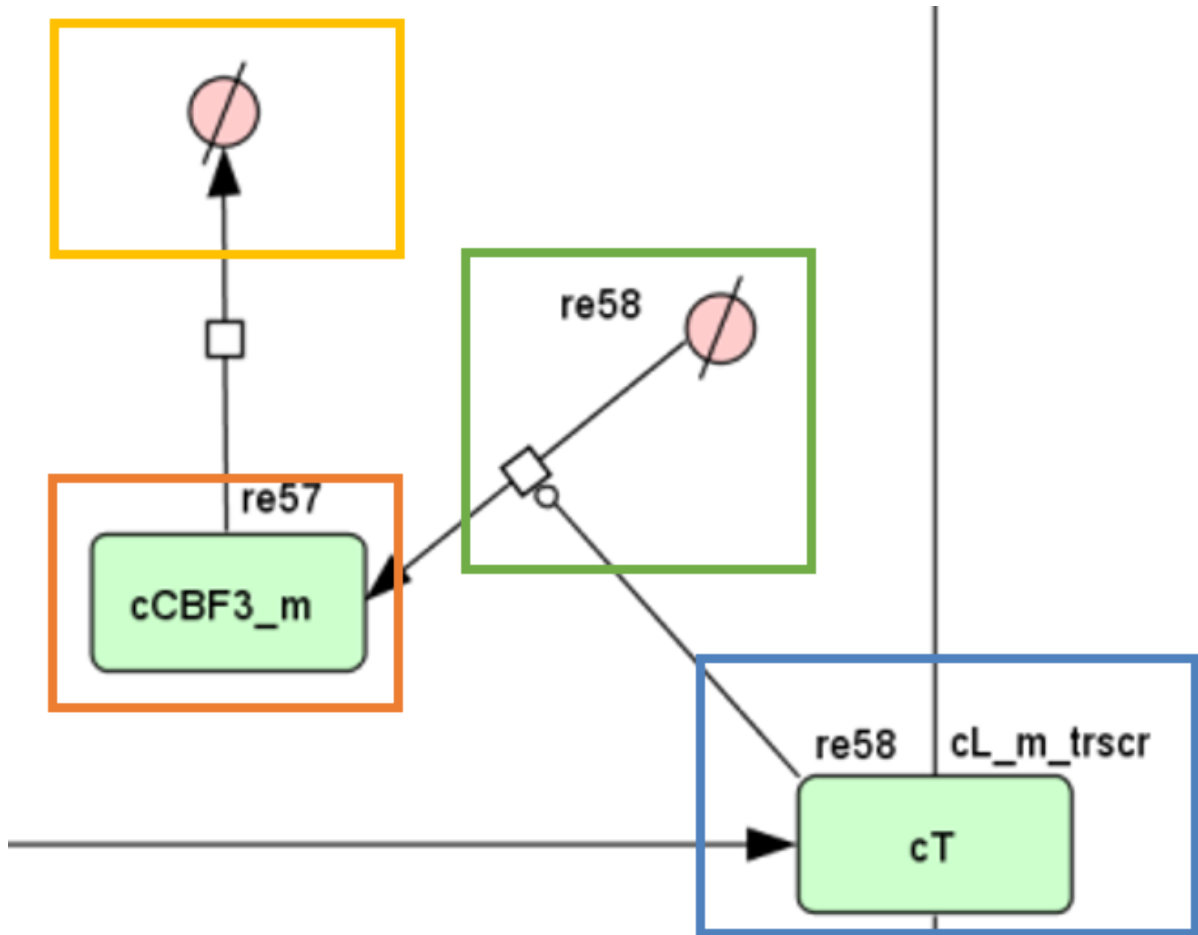


Figure 2.1: Screenshot of CellDesigner. Shown is a section of a circadian clock model, visualised in CellDesigner, which has had *CBF3* regulation by TOC1 added. In the orange box *CBF3* mRNA, labelled as “cCBF3_m” is visualised, with the degradation rate highlighted in the yellow box and the regulation by TOC1 highlighted in a green box. TOC1, labelled as “cT” is highlighted in a blue box. “re57” labels the reaction of *CBF3* degradation, “re58” labels the promotion of *CBF3* by TOC1 and “cL_m_trscr” labels the regulation of LHY/CCA1 by TOC1. The arrow pointed at TOC1 represents TOC1 production. CellDesigner is useful for non-mathematicians to create and edit models as it allows for the models to be represented as a visual diagram that can be more easily understood than pure code.

2.10 Model optimisation in SBSIVisual

Parameters had to be optimised against known data so that they best match the known oscillation of *CBF3* mRNA. The models were optimised using SBSIVisual version 1.4.5, optimising the simulated models to 12 hours of light followed by 12 hours of dark (12L:12D) diurnal cycles data of *Arabidopsis thaliana* grown at 22 °C, obtained from the DIURNAL website (diurnal.cgrb.oregonstate.edu (Mockler et al., 2007)) using a parallel genetic algorithm in SBSIVisual. The parameter values for the Pokhilko 2010 and Pokhilko 2012 model ODEs were fixed at the published values and only the new *CBF3* parameters were optimised. The parameter values of the new model components were constrained to 0 - 0.5 nM or nM/hr.

The parameter values for the new models can be seen in Appendix Table 1 for the Pokhilko 2010 models and Appendix Table 2 for the Pokhilko 2012 model.

A parallel genetic algorithm was used to fit the models to the biological data. Optimisation took place on the SBSI Dispatcher Web Server at the University of Edinburgh. The number of generations for the genetic algorithms was set to 5,000 as was the maximum number of generations. The population size was set to 100 and the target cost function was set to 0.01. The reporter interval was set to 0.1 with the maximum time setting set to 1000000 and the solver interval set to 0.01. The Chi-squared cost function was used for the cost function.

2.11 AICc in Matlab

AICc program files

A corrected akaike information criterion (AICc) program package was supplied by Robert Smith of the Halliday lab at the University of Edinburgh.

Microarray data for CBF expression of *Arabidopsis thaliana* grown at 22°C in four different day length conditions was obtained from the DIURNAL website (diurnal.cgrb.oregonstate.edu (Mockler et al., 2007)):

1. Short day conditions; 8 hours of light followed by 16 hours of darkness (8L:16D)

2 Materials and Methods

2. Normal day conditions; 12 hours of light and 12 hours of darkness (12L:12D)
3. Long day conditions; 16 hours of light and 8 hours of darkness (16L:8D)
4. Constant light conditions; 24 hours of light (24L:0D)

The AICc Matlab code is split into four separate programs and the code is shown in the Appendix. The AICcU_PROB and Akaike files required no alteration to get them to work for the *CBF3* modelling. The other files had to be modified slightly in order for them to work. The Information Criterion file had to have the location of the *CBF3* data files entered so that it could read the data, as did the Cost file and the loaded data had to be designated. The Akaike_Weights file had to have the different locations of the 13 different *CBF3* simulations entered so that they could be loaded correctly. In the Akaike_Weights file, the number of parameter values and the corresponding model name had to be entered for all the models so that the information criterion could be properly calculated. The number of models was also altered in the Akaike_Weights file so that the program knew that there were 13 models to test.

As well as the AICc program files, the biological data files and the simulation data files also need to be added to Matlab for the AICc to run. For the biological data, four files were created, one for each of the different day length conditions. The files consist of a matrix with the first column as the time in hours, and the proceeding columns as biological expression values for the different time points. For the simulation files, a matrix was created for each model, with the first column consisting of the time in hours, and then a column with the 08L:16D data, a column with the 12L:12D data, a column with the 16L:8D data and the final column consisting of the 24L:0D data. The program files then have to be directed to these files as indicated above.

The AICc was run in Matlab R2012a. Three folders were used: one folder contained the *CBF3* expression data from the Diurnal website; one folder contained the *CBF3* simulation data; one folder contained the AICc program files.

With all the data files correctly entered the AICc was run by typing in the command:

$$[a \ c] = \text{Akaike_Weights}(4,0)$$

Matlab then calculates and displays the AICc values for the different models and the AICc weights of the different models.

2.12 Perturbations to the models

Null mutants

Perturbations to the model to simulate mutants were created by setting the transcription rate to zero for the gene that was to be mutated.

LHY/CCA1 pulse

Using the models created, the COPASI plugin is required to simulate the models. The Change Amount functionality of CellDesigner does not work with COPASI, so a work-around was required. The selected model was run for 168 days in CellDesigner in 12L:12D light conditions, using the COPASI solver plugin (www.copasi.org). At the end of the 12L:12D simulation the concentration of all the species of the model was recorded. These concentrations were then added to a new model file as the starting concentrations and the light conditions were changed to 24L:0D. The new 24L:0D model was then run for 4 hours and 16 hours and the final concentrations of all the species recorded once more. These concentrations were then added as the starting concentrations in a new 24L:0D model but with the difference of changing the LHY/CCA1 protein level to 5 nM. The model was then simulated for a further 20 or 8 hours (depending on when the LHY/CCA1 pulse occurred) to get a total of two 24 hour simulations with a LHY/CCA1 pulse occurring at either ZT4 or ZT16.

2.13 *CBF3* promoter region analysis

The Ohio State University *Arabidopsis* Gene Regulatory Information Server (**agris**, <http://arabidopsis.med.ohio-state.edu/>), AtcisDB - Arabidopsis cis-regulatory element database, was used to search for known binding sites in the *CBF3* promoter region. The sequence viewer in The *Arabidopsis* Information Resource website (<http://www.arabidopsis.org/>) was used to obtain the DNA sequence for the *CBF3* promoter region so that a manual search of the sequence could be carried out to look for TOC1 binding site (T1ME) motifs and LUX binding site motifs.

3 Results: Light, and clock regulation of germination and dormancy

The ability of dormant seeds to germinate is greatly dependent on a number of environmental conditions such as temperature, light or even seed after-ripening to promote germination. The role of the circadian clock in regulating seed dormancy has only recently started to be understood. Circadian clock mutant seeds can have altered germination phenotypes when compared to wild-type seeds (Penfield and Hall, 2009). Mutations in at least five different clock genes have been shown to alter germination phenotypes in *Arabidopsis* plants; *lhy*, *cca1*, *gi*, *ztl* and *lux* show strong clock regulation of dormancy control (Penfield and Hall, 2009). The clock is also important for the regulation of hormone signalling with regards to germination, with *toc1* mutant plants having altered hormone induced germination phenotypes (Penfield and Hall, 2009).

Light exposure can determine whether or not a seed will remain dormant or germinate; exposure to red light will result in germination being stimulated, whereas exposure to far red light will inhibit germination (Borthwick et al., 1952). Light is also involved in regulating the circadian clock, such as the light regulated translation of the morning-loop LHY protein as well as being involved in regulating growth rates via the clock (Kim et al., 2003; Miyata et al., 2011). Light is also known to act through other components of the circadian clock such as *TOC1* and *GI* (Más et al., 2003b; Mizoguchi et al., 2005).

The role of the circadian clock in regulating seed germination has previously been studied, however, not in regards to the role of the circadian clock in controlling light signalling as a regulator of germination and dormancy in seeds. A series of germination assays were devised to test whether the circadian clock was involved in regulating light induced germination in fresh, imbibed, *Arabidopsis* seeds.

As well as investigating the role of the clock in regulating light signalling for dormancy regulation in seeds, the role of temperature was also investigated. Temperature is an important regulator of dormancy/germination levels in plant seeds, and the circadian clock is an important component of the cold signalling pathway in plants (Cao et al., 2005; Fowler et al., 2005; Seo et al., 2012). The role of the circadian clock in controlling low temperature regulation of germination in seeds was investigated; as such, the germination frequency of cold matured seeds was investigated in a number of *Arabidopsis* mutant seeds.

3.1 Determination of protocol for assay on light effect on germination

In order to test the effect of red and far-red light on the regulation of germination, an appropriate and repeatable procedure had to be developed and tested to determine the correct experimental conditions needed to provide the data required.

In order to test which protocol, if any, was the best for ascertaining seed germination frequency under red and far-red light, a number of experiments were carried out to look into the effect of light on germination on wild type plants and plants that had known altered germination rates. A series of experiments were created to answer the following questions; is water agar sufficient to investigate germination rates or would MS need to be added? In the germination assays will a cold stratification period be required to gain useful germination information?

When investigating the role of far-red light, seeds were first exposed to 1 hour of white light in order to induce germination in the seeds, followed by the different periods of far-red light exposure to inhibit germination. When investigating the effects of red light, the seeds were exposed to 1 hour of white light to induce germination, but were then exposed to five minutes of far-red light to inhibit germination in the seeds, and as such germination would be induced by the different periods of red light only. For more detail, see the Methods chapter.

3.1.1 How does growth media affect germination in different ecotypes of *Arabidopsis thaliana* react to different light conditions?

Different ecotypes of *Arabidopsis* have evolved in different geological regions of the world and as such have altered physiological responses to the environment in which they are found. In order to try and establish which ecotypes of *Arabidopsis* will provide the best results for the purpose of investigating germination in circadian clock mutant plants, four commonly used ecotypes were tested for their ability to germinate on either water agar or MS-agar under different light conditions. Getting a base understanding of the germination phenotypes of the different ecotypes when tested in our laboratory set-up will allow for the monitoring of any phenotypic changes in mutant ecotypes as well as establish which ecotype will be best used for the experiments in order to obtain as much information as possible.

The first experiment looked into whether it was necessary to use MS-agar to test for germination of seedlings under varying light conditions or whether simple water agar would be sufficient. As such, wild-type Col, C24, Ler and WS seeds were germinated on either water agar or MS-agar after exposure to different red/far-red light treatments. On both growth materials the seeds were exposed to either 0, 10, 30, 60 or 300 seconds of red light at $30 \mu\text{mol}/\text{m}^{-2}/\text{s}^{-1}$, or far-red light at $30 \mu\text{mol}/\text{m}^{-2}/\text{s}^{-1}$. In the red light experiments seeds were first exposed to one hour of white light at $100 \mu\text{mol}/\text{m}^{-2}/\text{s}^{-1}$ to promote germination followed by five minutes of far-red light at $30 \mu\text{mol}/\text{m}^{-2}/\text{s}^{-1}$ to inhibit germination. The far-red light experiments first had exposure to white light at $100 \mu\text{mol}/\text{m}^{-2}/\text{s}^{-1}$ for one hour prior to the far-red light treatment. The seeds were then stored in the dark for five days at 22°C at which point the seeds were observed to see how many of each data set had germinated. Each data point obtained is the average of five biological replicates showing the percentage of seeds that had germinated, each of which consisted of between (on average) 20-30 seeds, and the results, along with the standard error for each data point, can be seen in **figure 3.1**.

Germination rates were initially tested on seeds imbibed on water agar (WA) plates. Freshly harvested and imbibed seeds of Col, C24, Ler and WS ecotypes had low germination rates when grown on water agar (**Figure 3.1A**). After exposure to red light for up to 300 seconds, only Col seeds were able to germinate to a frequency

3 Results: Light, and clock regulation of germination and dormancy

greater than 10%, peaking at 34.2% germination frequency. As expected, all lines had low (<10%) germination rates when exposed to far-red light. Imbibing the seeds on MS agar, however, allows for the observation of increased germination rates in the lines tested (**Figure 3.1B**). Again, far-red light exposed seeds had low (<10%) germination rates; however, Col and Ler plants were able to obtain germination frequencies of 83.6% and 57.5% respectively when exposed to red light. WS and C24 seeds, however, were not able to obtain germination levels greater than 12.5% and 10.4% respectively after red light exposure on MS agar. Whilst imbibing seeds on MS agar will therefore allow for the investigation of clock mutant line germination frequencies in mutant plants of Col and Ler backgrounds, it would be difficult to do so in mutant plants of C24 and WS backgrounds. As such further tests were carried out on seeds that were either cold stratified to break dormancy, or not cold stratified.

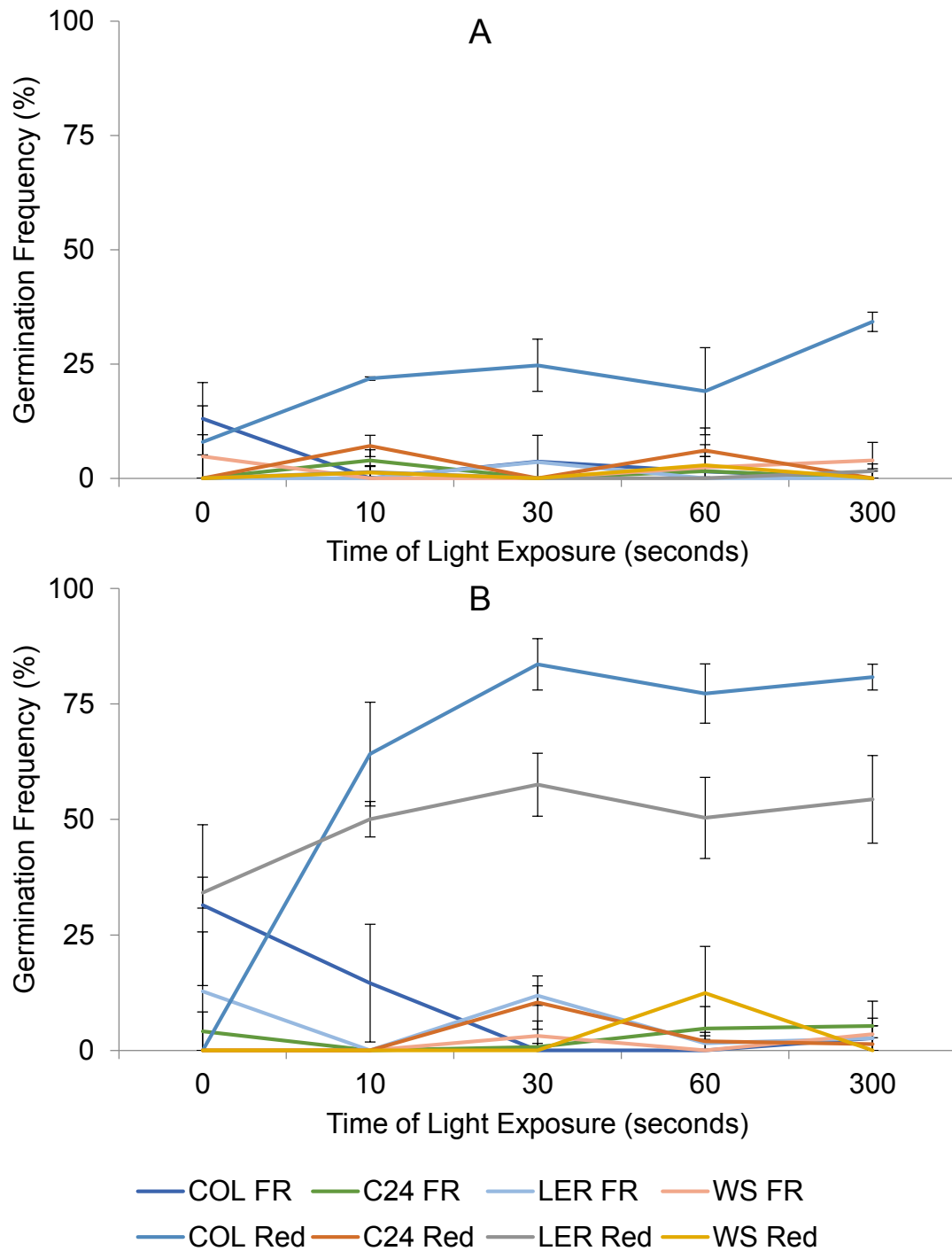


Figure 3.1: The Effects of far-red light and red light on seeds imbibed on either (A) Water Agar, or (B) MS Agar. Germination rates are low after exposure to far-red light, on either growth medium. After exposure to red light germination only occurs to high levels in Col and Ler seeds imbibed on MS-agar. Values are the average of five biological experiments, each consisting of 20-30 seeds, with the standard error shown. FR indicated far-red light exposure and Red indicates red light exposure.

3.1.2 How does cold stratification affect the germination of *Arabidopsis* seeds of different ecotypes?

Exposure to a short period of cold temperature (cold stratification) breaks the dormancy of fresh seeds, thus allowing them to germinate; a period between three-five days at 4°C is often used for a cold stratification treatment (Penfield et al., 2005; Donohue et al., 2008; Kendall et al., 2011). Applying a cold stratification period of three days at 4°C should, hopefully, result in increased levels of germination of C24 and WS seeds which would allow for the investigation of mutant clock seeds from these backgrounds to be investigated for altered germination frequencies.

The next experiment looked into the effects of cold stratification on the wild-type seeds. As such, wild-type Col, C24, Ler and WS seeds were germinated on MS-agar after either a three day cold stratification period at 4°C or without a cold stratification period, followed by exposure to different red/far-red light treatments. After the exposure to the cold stratification period, or not, the seeds were exposed to either 0, 10, 30 or 60 seconds of red light at $30 \mu\text{mol}/\text{m}^{-2}/\text{s}^{-1}$, or far-red light at $30 \mu\text{mol}/\text{m}^{-2}/\text{s}^{-1}$. In the red light experiments seeds were first exposed to one hour of white light at $100 \mu\text{mol}/\text{m}^{-2}/\text{s}^{-1}$ to promote germination followed by five minutes of far-red light at $30 \mu\text{mol}/\text{m}^{-2}/\text{s}^{-1}$ to inhibit germination. The far-red light experiments first had exposure to white light at $100 \mu\text{mol}/\text{m}^{-2}/\text{s}^{-1}$ for one hour prior to the far-red light treatment. The seeds were then stored in the dark for five days at 22°C at which point the seeds were observed to see how many of each data set had germinated. Each data point obtained is the average of five biological replicates showing the percentage of the seeds that germinated, each of which consisted of between (on average) 20-30 seeds, and the results, along with the standard error for each data point, can be seen in **figure 3.2**.

Seeds that were not exposed to a cold stratification period of three days at 4°C had low germination frequencies when exposed to both far-red (**Figure 3.2A**) and red light (**Figure 3.2B**). After exposure to far-red light, germination rates of non-cold stratified seeds dropped from 35.3% and 26.1% for C24 and Ler respectively down to 3% and 0% respectively. Col and WS seeds that were not cold stratified never achieved greater than 10% germination when not cold stratified under any light regiment (**Figure 3.2**). After a three-day cold stratification period, the four *Arabidopsis* ecotypes had germination frequencies greater than 85% before far-red exposure (*Figure*

3 Results: Light, and clock regulation of germination and dormancy

3.2A). After cold stratification and far-red light exposure, C24 germination frequency dropped from 100% to a low of 57%; Ler dropped from 95.3% to 51% germination after 60 seconds of far-red light, but the greatest changes were in the WS and Col ecotypes which dropped from 97.1% and 88.6% respectively down to 4.7% and 2.4% germination frequencies respectively after 60 seconds of far-red light exposure.

With no cold stratification, but exposure of up to 60 seconds of red light C24, WS and Col all had less than 5% germination frequencies (**Figure 3.2B**). Ler, with no cold stratification period was able to increase its germination frequency from no germination after no red light exposure, up to 28% after 60 seconds of red light treatment (**Figure 3.2B**). After a dormancy period of three days at 4°C, all four ecotypes of *Arabidopsis* were able to respond to the red light stimuli. Cold stratified Col seeds increased their germination rates from an initial 14.2% with no red light stimuli to 92.9% after 60 seconds of red light. Cold stratified WS seeds increased their germination rates from 3.4% up to 89%; C24 increased from 56.2% to 98.5% and Ler increased from 78% to 98% after red light exposure of 60 seconds (**Figure 3.2B**).

It was decided that two different experiments would be required to investigate germination phenotype mutants, seeds that are cold stratified and seeds that are not cold stratified. This would allow for the observation of seeds that have either increased sensitivity to re and far-red light signalling, as well as decreased sensitivity.

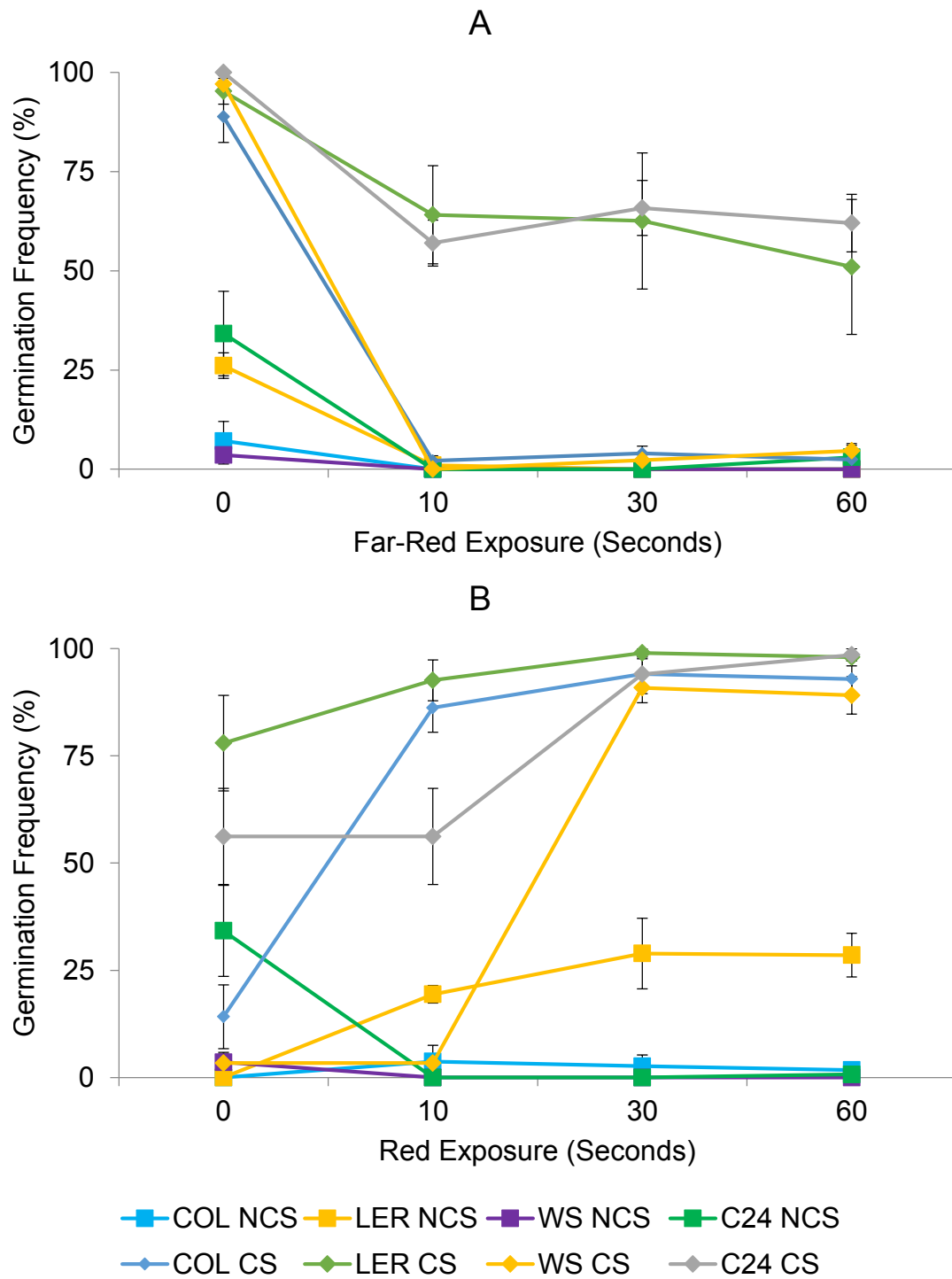


Figure 3.2: The effects of (A) far-red and (B) red light on seeds exposed to a three day cold stratification (CS) period and seeds that were not exposed to a cold stratification period (NCS). Seeds that were exposed to a cold stratification period had greater levels of germination than the seeds which were not exposed. Values are the average of five biological experiments, each consisting of 20-30 seeds, with the standard error shown.

3.2 Do the core clock genes have a role in light regulated germination?

With the production of a working protocol to test red/far-red light signalling in fresh, imbibed, *Arabidopsis* seeds, the investigation into the role of the circadian clock in regulating light effects on seed dormancy and germination could take place.

Experiments would take place with clock mutant seeds that were either cold stratified or not cold stratified in order to detect any clock mutant lines that had either increased or decreased sensitivity to the light stimuli and thus provide a role for the clock in the regulation of light signalling with regards to germination in seeds.

3.2.1 Far-red light sensitivity is not lost in clock mutants

Freshly harvested seeds containing mutations to the circadian clock were tested to see if they had altered germination rates under far-red light compared to wild-type plants in order to try and ascertain whether the clock has a role in maintaining dormancy in seeds via the light signalling pathway.

Seeds with perturbations to components of the circadian clock were germinated on MS-agar after either a three day cold stratification period at 4°C or without a cold stratification period, followed by exposure to different far-red light treatments. After the exposure to the cold stratification period, or not, the seeds were exposed to either 0, 10, 30 or 60 seconds of far-red light at 30 $\mu\text{mol}/\text{m}^{-2}/\text{s}^{-1}$. The seeds were first exposed to white light at 100 $\mu\text{mol}/\text{m}^{-2}/\text{s}^{-1}$ for one hour prior to the far-red light treatment. The seeds were then stored in the dark for five days at 22°C at which point the seeds were observed to see how many of each data set had germinated. Each data point obtained is the average of five biological replicates showing the percentage of the seeds that germinated, each of which consisted of between (on average) 20-30 seeds, and the results, along with the standard error for each data point, can be seen in figure 3.3. The results were also assessed to determine which results, if any, were significantly different to that of the wild-type seeds using two-tailed students t-test with a significance level of ($P < 0.05$) as can be seen in **table 3.1**.

No cold stratification

In seeds that were not exposed to a three day cold stratification period, there is less than 10% germination frequency in seeds from the Col ecotype background, with what little germination is present being completely inhibited by any far-red light exposure (**Figure 3.3A**). C24 seeds and the C24 mutant *TOC1 MG* (a *TOC1* over-expressing line: *TOC1 Mini Gene*) seeds had a germination rate of 34.2% and 54.2% before far-red light exposure, which was then also inhibited by far-red light stimuli (**Figure 3.3A**). In the seeds with no cold stratification exposure, only the *LHY OX* seeds had a significantly altered germination frequency to that of their wild-type, Ler, seeds (t-test, $P < 0.05$, **Table 3.1**) before far-red light exposure, but this was lost when Ler seed germination frequency dropped to the same as that of *LHY OX* after far-red light treatment (**Figure 3.3**).

With cold stratification

After a cold stratification period, *LHY OX* seeds were still not germinating, resulting in a significant reduction in germination frequency compared to the wild-type Ler seeds at 0, 10 and 30 seconds of far-red light exposure (**Table 3.1** and **Figure 3.3**). By 60 seconds of far-red light exposure, however, Ler germination frequency had been reduced enough that there was no significant difference in germination rates between them and the *LHY OX* seeds (**Figure 3.3B**). At no time was the germination rate of *TOC1 MG* significantly different to that of its wild-type C24 seeds after a cold stratification period and exposure to far-red light (**Table 3.1** and **Figure 3.3B**). It is interesting to note that seeds from the C24 ecotype and the Ler wild-type seeds all showed low sensitivity to far-red light compared to the seeds from the Col ecotype background with none dropping below 50% germination rates, even after 60 seconds of exposure to far-red light (**Figure 3.3B**). The circadian clock mutant seeds in the Col background did not have significantly different germination rates compared to wild-type when exposed to 10, 30 or 60 seconds of far-red light (**Table 3.1**) with all seeds having germination inhibited by far-red light. Prior to far-red light exposure, however, *gi-201*, *lhy-11 cca1-1* and *prr5-11 prr7-11 prr9-10* had significantly reduced germination rates (**Table 3.1** and **Figure 3.3B**).

These data clearly show that there is no apparent difference in circadian clock

3 Results: Light, and clock regulation of germination and dormancy

Table 3.1: Two tailed Students t-test comparing the germination rates of different circadian clock mutants seeds to wild-type seeds when exposed to far-red light, with or without exposure to cold stratification. Red boxes are not statistically significant and green boxes are statistically significant ($P < 0.05$). * indicates that there was no germination in either the wild-type or the mutant lines, as such there was no significant difference.

Far-red light no CS period of light exposure (seconds)				
	0	10	30	60
<i>prp5-11 prp7-11 prp9-10</i>	0.57	0.39	*	*
<i>toc1-2 prp5-11 prp7-11 prp9-10</i>	0.75	*	*	*
<i>toc1-101</i>	0.24	*	*	*
TOC1 MG	0.29	*	*	0.94
CCA1 OX	0.24	*	*	*
LHY OX	0.00	0.39	*	*
<i>gi-201</i>	0.30	*	*	*
<i>lhy-11 cca1-1</i>	0.32	*	*	*
Far-Red Light with CS Period of light exposure (seconds)				
	0	10	30	60
<i>prp5-11 prp7-11 prp9-10</i>	0.03	0.45	0.11	0.18
<i>toc1-2 prp5-11 prp7-11 prp9-10</i>	0.53	0.49	0.21	0.18
<i>toc1-101</i>	0.61	0.18	0.11	0.18
TOC1 MG	0.39	0.24	0.34	0.08
CCA1 OX	0.50	0.58	0.11	0.18
LHY OX	0.00	0.01	0.04	0.06
<i>gi-201</i>	0.03	0.18	0.11	0.18
<i>lhy-11 cca1-1</i>	0.04	0.18	0.11	0.18

mutant's ability to sense and react to far-red light compared to wild-type plants, with the possible exception of **LHY OX**.

3 Results: Light, and clock regulation of germination and dormancy

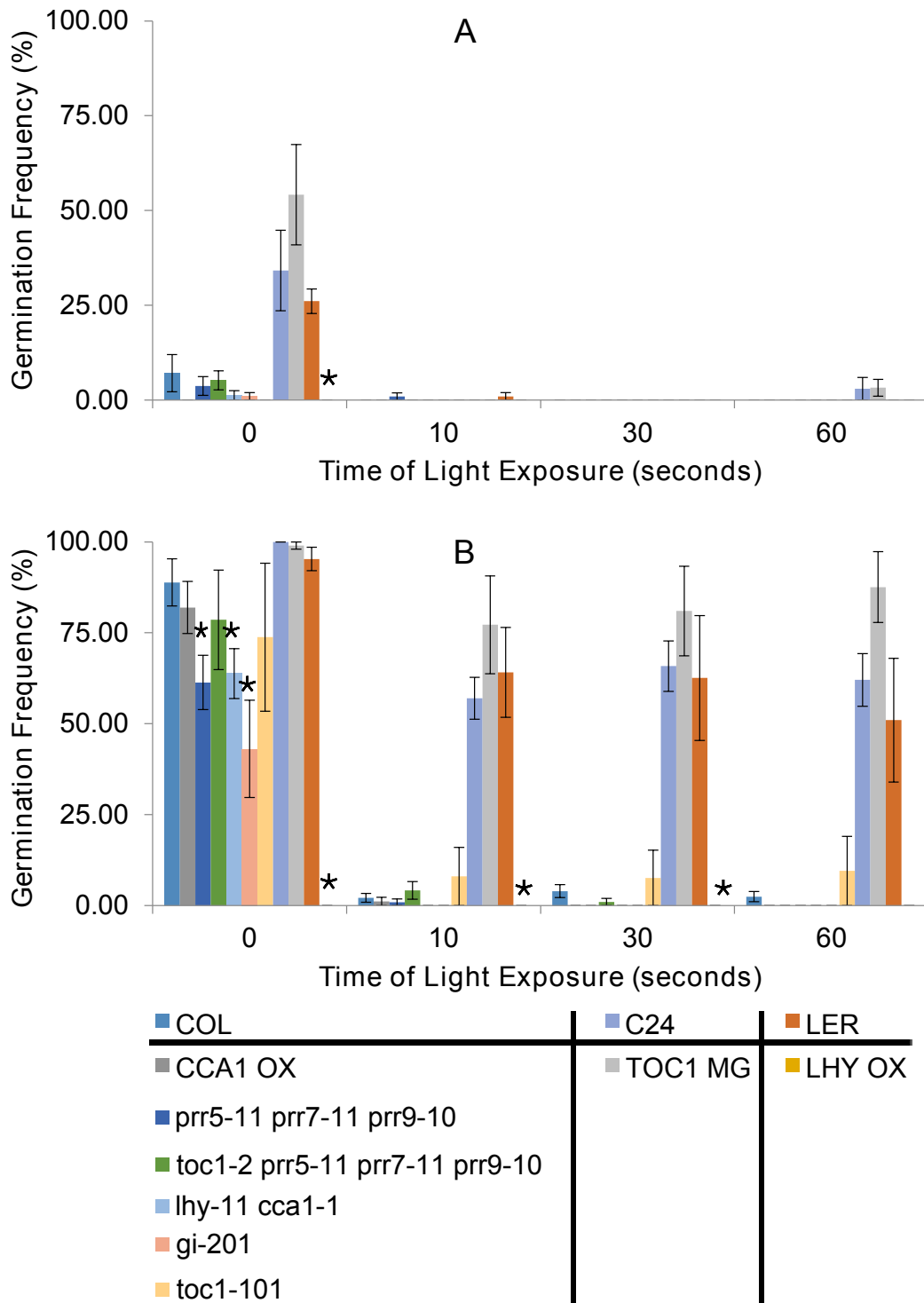


Figure 3.3: Germination rates for circadian clock mutant seeds one week after (A) far-red light exposure with no cold stratification period or (B) far-red light exposure with three days of 4°C cold stratification. Significant results indicated by *, ($P < 0.05$); significant results only occurred in LHY OX seeds which failed to germinate in any conditions. Values are the average of five biological experiments, each consisting of 20-30 seeds, with the standard error shown.

3.2.2 The effects of red light on germination

Freshly harvested seeds containing perturbations to circadian clock components were tested to see if they had altered germination rates under red light compared to wild-type plants in order to try and ascertain whether the clock has a role in maintaining dormancy in seeds via the light signalling pathway.

Seeds with perturbations to components of the circadian clock were germinated on MS-agar after either a three day cold stratification period at 4°C or without a cold stratification period, followed by exposure to different red light treatments. After the exposure to the cold stratification period, or not, the seeds were exposed to either 0, 10, 30 or 60 seconds of red light at $30 \mu\text{mol}/\text{m}^{-2}/\text{s}^{-1}$, or far-red light at $30 \mu\text{mol}/\text{m}^{-2}/\text{s}^{-1}$. The seeds were first exposed to one hour of white light at $100 \mu\text{mol}/\text{m}^{-2}/\text{s}^{-1}$ to promote germination followed by five minutes of far-red light at $30 \mu\text{mol}/\text{m}^{-2}/\text{s}^{-1}$ to inhibit germination. The seeds were then stored in the dark for five days at 22°C at which point the seeds were observed to see how many of each data set had germinated. Each data point obtained is the average of five biological replicates showing the percentage of the seeds that germinated, each of which consisted of between (on average) 20-30 seeds, and the results, along with the standard error for each data point, can be seen in **figure 3.4**. The results were also assessed to determine which results, if any, were significantly different to that of the wild-type seeds using two-tailed students t-test with a significance level of ($P < 0.05$) as can be seen in **table 3.2**.

No cold stratification

With no cold stratification period, all seeds tested had low germination rates, with none achieving greater than 50% germination, even after 60 seconds of red light exposure (**Figure 3.4A**). Again, the only mutant line with a significant difference in germination rate (**Table 3.2**) to the wild-type seeds was *LHY OX* which showed no germination (**Figure 3.4A**). The seeds in the Col background never achieved germination rates greater than 10%. C24 and the C24 mutant *TOC1 MG* both showed increased germination after red light exposure (although not significantly different from one-another, **Table 3.2**), where germination frequencies peaked at 20.2% for C24 and 44.5% for *TOC MG* after 60 seconds of red light (**Figure 3.4A**).

Table 3.2: Two tailed Students t-test comparing the germination rates of different circadian clock mutants seeds to wild-type seeds when exposed to red light, with or without exposure to cold stratification. Red boxes are not statistically significant and green boxes are statistically significant (P<0.05). * indicates that there was no germination in either the wild-type or the mutant lines.

Far-red light no CS period of light exposure (seconds)				
	0	10	30	60
<i>prp5-11 prr7-11 prr9-10</i>	*	0.39	0.44	0.76
<i>toc1-2 prr5-11 prr7-11 prr9-10</i>	*	0.97	0.55	0.37
<i>toc1-101</i>	*	0.39	0.18	0.18
TOC1 MG	0.39	0.27	0.61	0.19
CCA1 OX	*	0.39	0.18	0.18
LHY OX	*	0.00	0.04	0.01
<i>gi-201</i>	*	0.39	0.27	0.44
<i>lhy-11 cca1-1</i>	*	0.39	0.18	0.18

Far-Red Light with CS Period of light exposure (seconds)				
	0	10	30	60
<i>prp5-11 prr7-11 prr9-10</i>	0.18	0.04	0.05	0.20
<i>toc1-2 prr5-11 prr7-11 prr9-10</i>	0.39	0.49	0.27	0.35
<i>toc1-101</i>	0.15	0.00	0.00	0.00
TOC1 MG	0.18	0.14	0.19	0.39
CCA1 OX	0.15	0.34	0.57	0.52
LHY OX	0.01	0.00	0.00	0.00
<i>gi-201</i>	0.17	0.05	0.01	0.08
<i>lhy-11 cca1-1</i>	0.15	0.21	0.07	0.22

With cold stratification

With the addition of a cold stratification period *LHY OX* was still not able to germinate to rates greater than 10%, even after red light exposure (**Figure 3.4B**) resulting in significantly reduced germination rates to the wild-type Ler seeds (**Table 3.2**). The C24 and the C24 circadian clock mutant *TOC1 MG* seeds both showed similar high initial levels of germination, which were further increased by red light stimuli (**Figure 3.4B**). Wild-type Col seeds, and Col clock mutant seeds had germination frequencies less than 15% prior to red light stimulation, with no significant difference in germination between the seeds. After as little as 10 seconds of red light exposure, Col germination rates increased 71.3 percentage points to 86.2% from 14.9%, peaking at 94% after 30 seconds of red light. Of the clock mutants in the Col background, only *toc1-101* had constitutively significantly reduced germination

frequency compared to wild-type seeds after all red light treatments (**Table 3.2**) with the seeds never achieving greater than 10% germination rates. Of the circadian clock mutant seeds from the Col background, only the *prr* triple mutant after 10 seconds of red light and *gi-201* after 30 seconds of red light had a significant reduction in germination rates compared to wild-type seeds.

3 Results: Light, and clock regulation of germination and dormancy

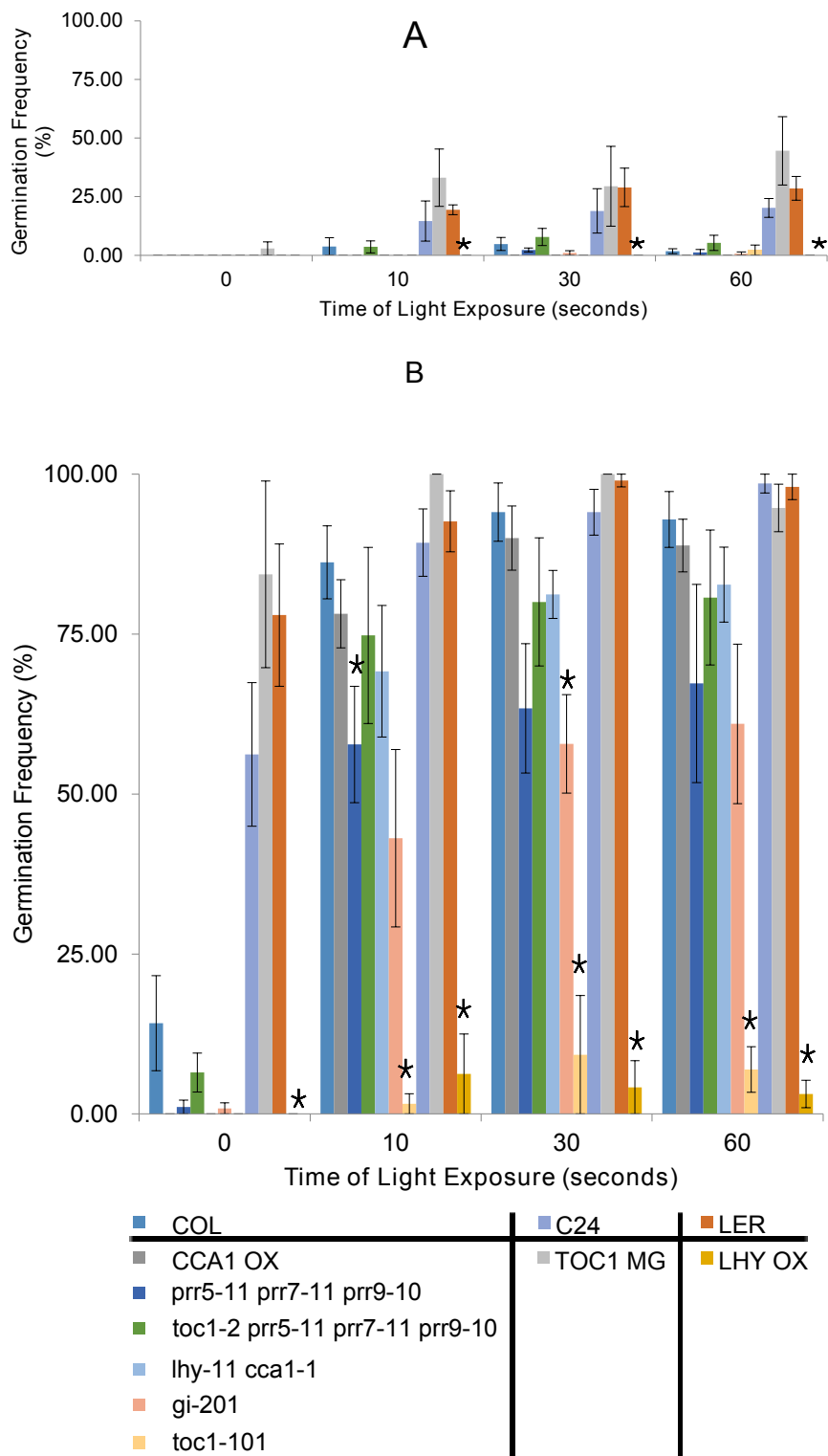


Figure 3.4: Germination rates for circadian clock mutant seeds one week after (A) red light exposure with no cold stratification period or (B) red light exposure with three days of 4°C cold stratification. Significant results indicated by *, ($P < 0.05$). Values are the average of five biological experiments, each consisting of 20-30 seeds, with the standard error shown.

3.3 The role of clock genes in regulating germination under low temperature conditions

The effects of cold stratification periods and after-ripening temperature has been shown to be regulated by the circadian clock (Penfield and Hall, 2009). *lhy cca1* double mutants have increased germination frequency after 2-3 days of cold stratification, whereas *gi* has decreased germination after 2-4 days of cold stratification and *ztl* has decreased germination rates after 1-2 days of cold stratification compared to wild-type plants (Penfield and Hall, 2009). The effects of altered seed imbibition temperature in different clock mutants was also investigated in the study, showing that different clock mutants had altered germination rates under different imbibition temperatures (Penfield and Hall, 2009). The effects of low temperature during the maturation of the seeds themselves have not been investigated, however.

In order to obtain seeds that had matured at low temperatures plants with circadian clock mutations were grown at 22°C in 12L:12D light conditions until flowers started to develop. At the point at which flowers were starting to develop the temperature at which the plants were growing was reduced to 12°C so that seeds would mature at this lower temperature. For each wild-type plant and mutant line, five plants were grown and harvested for seeds. The freshly harvested seeds were then cold stratified for a period of 0-3 days at 4°C, after which they were allowed to germinate at 22°C in 12L:12D white light ($100 \mu\text{mol}/\text{m}^{-2}/\text{s}^{-1}$) conditions and germination rates were assessed one week after cold stratification had finished. For each data point the average of four biological replicates is shown, along with the standard error for the data (**figure 3.5**).

A *CBF1-rrnai* line was included as the *CBFs* are involved in temperature signalling and have recently been shown to affect dormancy in *Arabidopsis* seeds (Kendall et al., 2011); it was therefore of interest to see the effects of a *CBF* mutant in germination of seeds matured at low temperatures. If the circadian clock genes were involved in the temperature regulation of dormancy levels in seeds, then this can be detected by altered germination rates between wild-type and circadian clock mutant seeds when matured at low temperatures compared to the germination phenotypes observed in seeds matured at warmer temperatures, as already reported in the literature. As the dormancy levels of the wild-type seeds is so high in seeds matured at 12°C it was not

3 Results: Light, and clock regulation of germination and dormancy

possible to ascertain any mutant line that had a significantly reduced germination rate (t-test, $P < 0.05$) with the exception of *lux-5* and *ztl-3* which did not germinate, even after three days of cold stratification (Figure 3.5). Neither did any of the lines show a significant increase in germination rates compared to wild-type seeds when matured at 12°C.

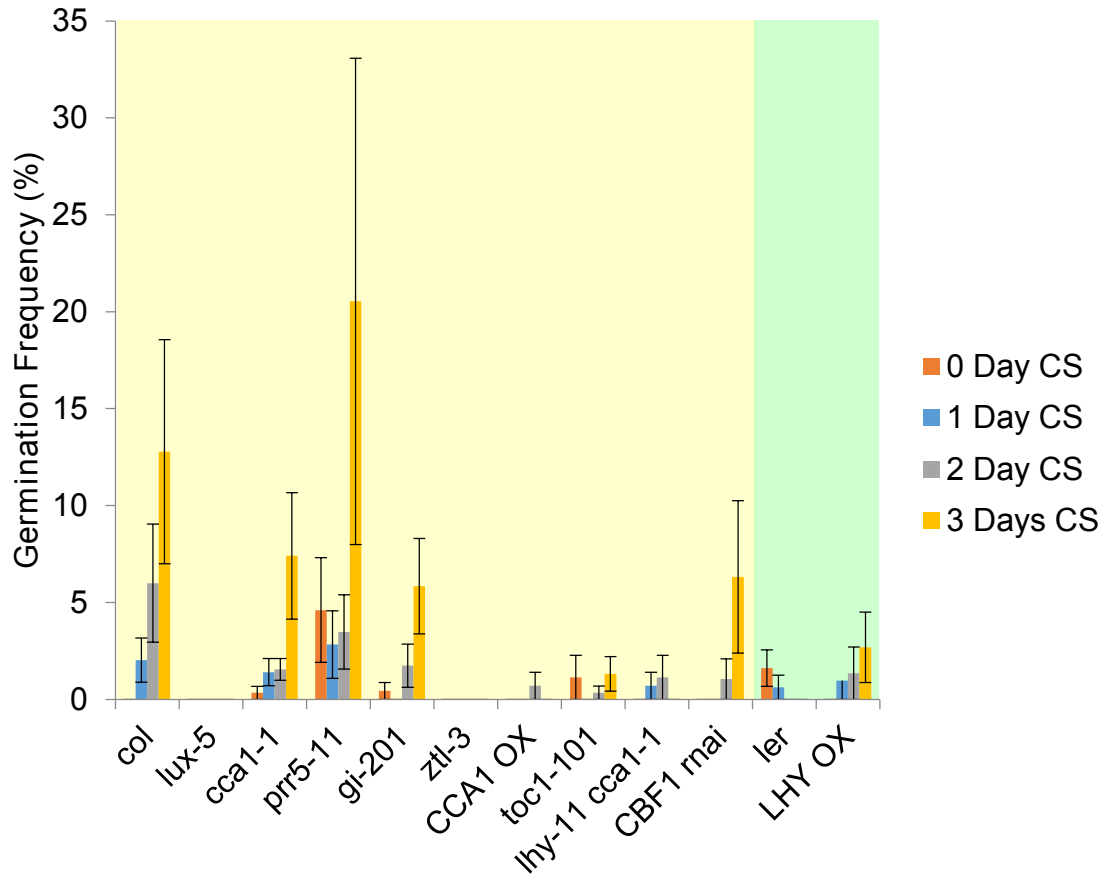


Figure 3.5: Germination rates of circadian clock mutant seeds matured at 12°C and then exposed to different cold stratification periods at 4°C. Germination was scored one week after imbibition. Results are clustered by seed background; the yellow background represents seeds derived from Col wild-type and the green background represents seeds derived from Ler wild-type. Values are the average of four biological experiments, each consisting of 20-30 seeds, with the standard error shown.

3.4 Discussion

3.4.1 Circadian clock genes and their role in light regulated germination

In this chapter the circadian clock was investigated to see what role it plays (if any) in light regulation of germination in *Arabidopsis* seeds. Several different mutant seeds with perturbations to components of the circadian clock were investigated to see what role they play in the light regulation of germination.

***GI* and light regulation of germination**

gi mutants have been shown to have reduced germination rates after three days of cold stratification compared to wild-type plants (Penfield and Hall, 2009) as is also observed in this study in the *gi-201* null mutant seeds (**Figure 3.4**). This reduced germination rate compared to wild-type plants also occurs even after exposure to red light; however, not always at a significantly reduced rate. This data suggests that whilst *GI* is important for seeds to germinate correctly, the reduction in germination can be attributed to the previously described role of *GI* in regulating normal ABA and GA responses in seeds (Penfield and Hall, 2009) and not to a perturbed red/far-red light signalling pathway.

***PRRs* and light regulation of germination**

The *prp* mutant *TOC1 MG* seeds showed no difference in observed germination rates compared to wild-type C24 seeds when exposed to red or far-red light with or without cold stratification. This is similar to reported *TOC1 MG* germination reported in the literature where *TOC1 MG* and wild-type seeds grown on water agar with a cold stratification treatment showed no significant difference in germination (Penfield and Hall, 2009).

Unlike previous reports where there was no observed difference between *toc1* mutant seeds and wild-type seed germination (Penfield and Hall, 2009), this study showed a significant reduction in germination rates between *toc1-101* loss-of-function seeds and

wild-type Col seeds when cold stratified exposed to red light (**Table 3.2**). The *toc1-101* seeds used in this study are capable of germinating with relatively high frequency under favourable conditions, as when exposed to 1 hour of white light and no other light inputs they were able to germinate to a rate of 72.81% of all the seeds after one week imbibition at 22°C in the dark (**Figure 3.4B**, 0 seconds exposure to far-red light). This means that the *toc1-101* seeds that did not germinate after exposure to different red light treatments were not able to respond to, or sense, the red light stimuli that they were exposed to after an initial 5 minutes of exposure to far-red light. Previous *toc1* mutant investigations had shown that some alleles have no light dependent defect phenotypes (Somers et al., 1998; Ito et al., 2007). Other studies, however, show a role for *TOC1* in the red light dependent control of circadian gene expression as *toc1-2* mutant plants have arrhythmic circadian expression when grown in red light (Más et al., 2003a). *TOC1 MG* plants are hypersensitive to red light with regards to photomorphogenesis with decreased hypocotyl length in seedling grown in red light compared to wild-type plants (Más et al., 2003a). The opposite effect is observed in the *toc1-2* allele plants, where they display hyposensitivity to red light with increased hypocotyl length when grown in red light compared to wild-type plants (Más et al., 2003a). It is not completely surprising therefore to find that *toc1-101* loss-of-function seeds are also hyposensitive to red light stimuli with regards to germination promotion as shown in this study. The hypersensitivity observed in the literature of *TOC1 MG* plants to far-red light in relation to hypocotyl growth was not reproduced in this study. This was largely due to the already high levels of germination that are observed in the C24 wild-type plants that prevent a significant increase in germination from being observed. However, when there was no-cold stratification applied to the seeds, there was a slight increase in the germination rates of the *TOC1 MG* seeds compared to wild-type seeds when exposed to red light, but not to a significant amount and often with overlapping error-bars **Figure 3.4**. *TOC1* is therefore an important component of several red light signalling pathways in *Arabidopsis* and without this circadian clock gene germination under red light is impaired.

TOC1 has been shown to interact directly with PHYTOCHROME-INTERACTING FACTOR3 (PIF3) (Makino et al., 2002), which is required for normal phytochrome B (PhyB) level modulation (Leivar et al., 2008). *phyB* is responsible for mediating germination in dark or red light conditions, as demonstrated by the substantial decrease in germination that occurs in these conditions in *phyB* mutant plants

compared to wild-type plants (Leyser and Day, 2009). It is possible that the reduction in germination observed in *toc1-101* plants in red light conditions is due to a breakdown of phyB regulation by the circadian clock via PIF3.

As well as investigating *PRR1/TOC1*, the role of *PRR5*, *PRR7* and *PRR9* in the circadian regulation of germination was also studied. Early photomorphogenesis experiments looking at *prr5 prr7 prr9* triple mutant seedling sensitivity to red light show that they are hyposensitive (“blind”) to red light (Nakamichi et al., 2005; Kato et al., 2007). *prr5 prr7 prr9* mutant seedlings grown under red light show the same levels of hypocotyl growth as wild-type plants when grown in the dark; however, whereas wild-type seedlings have hypocotyls approximately half as long when grown in red light compared to darkness, there is no observable decrease in *prr5 prr7 prr9* hypocotyl length (Nakamichi et al., 2005). Hyposensitivity of *prr5 prr7 prr9* to far-red light was also reported where again these *prr* triple mutant seedlings have increased hypocotyl length compared to wild-type plants when grown in far-red light (Nakamichi et al., 2005).

The data collected in this study showed no hyposensitivity to far-red light with both the *toc1-2 prr5-11 prr7-11 prr9-10* and the *prr5-11 prr7-11 prr9-10* mutant seeds which had similar levels of germination inhibition as the wild-type plants. The *prr* triple and quadruple mutant data collected in this study shows a reduction in germination frequency compared to wild-type plants when exposed to red light; however, whilst germination levels were reduced the observed reduction in germination frequency is only significant in *prr5-11 prr7-11 prr9-10* seeds when exposed to 10 seconds of red light (Table 3.2). The observed reduction in red light sensitivity seen in the *prr* triple mutant compared to wild-type plants is similar to the reported red light hyposensitivity reported in the literature with regards to hypocotyl de-etiolation (Nakamichi et al., 2005; Kato et al., 2007).

The above shows that the *PRRs* are involved in mediating the red light induction of germination, and that *TOC1* in particular is essential for this process.

CCA1, LHY and light regulation of germination

lhy cca1 double mutant seeds have a small, but still significant, increase in levels of germination frequency relative to wild-type plants (Penfield and Hall, 2009) which was not observed in any of the experiments carried out in this study (**Figure 3.3** and

Figure 3.4). Likewise, *lhy cca1* mutant plants from the WS background have a reported hypersensitivity to cold treatment compared to wild-type plants, with an increase in germination rates after 1-3 days of cold stratification and germination under white light conditions (Penfield and Hall, 2009) This increased sensitivity to cold treatment was not observed in the *lhy-11 cca1-1* null mutant seeds from the Col background used in this study (**Figure 3.4**). An increased sensitivity to cold treatment was not observed in this study after cold stratification compared to wild-type plants after exposure to any of the red light treatments. Plants from different backgrounds can have very different germination and dormancy phenotypes (Vaistij et al., 2013) as also seen here. This highlights an issue where data obtained from plants of different backgrounds are not easily comparable to one another and shows why, where possible, the plants in this study were from the same (Col) background.

Of the results obtained, the most striking was that of the *LHY-OX* mutant seeds. *LHY-OX* seeds have previously reported germination phenotypes in that they are insensitive to germination promotion by alternating warm day temperature and cold evening temperature and have low germination rates when imbibed at 22°C and 27°C (Penfield and Hall, 2009). Under all of the conditions that these seeds were tested in this study only a very low level of germination occurred. As there was no germination in these seeds to be inhibited by far-red light exposure this possess the problem that with low germination rates in all test conditions, one is unable to ascertain whether this is due to hypersensitivity to far-red light and reduced sensitivity to red light, or whether the low levels of germination are a result of other factors that are not related to light sensitivity.

In conclusion, mutations to the circadian clock did not alter seed far-red light sensitivity. TOC1, which has been shown to be involved in red light signalling pathways also is necessary for dormancy regulation via red light stimuli in seeds, however, the rest of the clock mutant seeds tested did not appear to significantly alter red light sensitivity.

3.4.2 The role of clock genes in regulating germination under low temperature conditions

When maturing seeds at low temperatures, strong dormancy was observed in seeds, even after three days of cold stratification. In all of the *Arabidopsis* seeds tested with mutations to components of the circadian clock, dormancy levels were not significantly altered from that of the wild-type seeds.

Clock mutant *lhy cca1* seeds matured in warm greenhouse conditions reported to have an increase in germination rates compared to wild-type seeds after 1-3 days of cold stratification (Penfield and Hall, 2009). No significant (t-test, $P < 0.05$) difference was seen in *lhy cca1* mutants in this study in seeds matured at 12°C compared to wild-type seeds grown in the same conditions. Unfortunately, due to the low germination rates of the wild-type seeds when matured at 12°C, it was not possible to obtain significantly decreased levels of germination (t-test, $P < 0.05$) in any of the mutant lines, even in *ztl-3* and *lux-5* which showed no germination (Figure 3.5). If one ignores significance, we see that *lhy-11 cca1-1* seeds matured at the lower temperatures have increased dormancy compared to wild-type seeds (Figure 3.5), a result opposite that of the seeds when matured at warmer temperatures. LHY expression at 12°C has greater amplitude and peak expression compared to plants that are grown at warmer temperatures (Gould et al., 2006) showing altered clock functionality in plants growing at different temperatures, and here showing different functionality of the circadian clock in seeds matured at different temperatures.

The fact that the *gi-201* mutant was able to germinate when matured at 12°C, yet shares the same mutant phenotype as *lhy-20* with regards to expression levels in plants grown at 12°C suggests that the *lhy-11 cca1-1* phenotype observed here is compounded by the inclusion of a concurrent null mutation to *CCA1* as well.

The null mutant *ztl-3* does repeat the decrease in germination that is observed at warmer temperatures (Penfield and Hall, 2009) suggesting that unlike LHY and CCA1, ZTL functionality remains constant in seeds irrelevant of maturation temperature.

The *lux-5* mutant data was interesting as there was no observed germination in any of the seeds with this mutation when matured at 12°. *lux-5* mutant seeds are capable of germinating when matured at warm temperatures, such as the *lux-5* mutant plants

matured at 22° in this study those matured in greenhouses as reported in the literature (Penfield and Hall, 2009). This shows that *LUX* is required to break the strong levels of dormancy that occurs in seeds that are matured at 12°.

3.4.3 Chapter 03 summary

This study wanted to establish which circadian clock genes were involved in regulating dormancy in seeds via the red light signalling pathway. To do this it was decided that MS-agar should be used for the experiment as Col and Ler seeds were able to germinate to greater levels when exposed to red light and grown on MS-agar compared to when they were grown on water agar. It was decided that where possible the seeds used in this study were to be from the Col background. Also, to establish clock mutant lines that have either increased or decreased sensitivity to light signalling it was decided to test both seeds that had been exposed to a cold stratifying period of three days and seeds that had not had a cold stratification period.

Exposure of circadian clock mutant seeds to far-red light did not result in the discovery of any seeds with a loss of sensitivity to far-red light when compared to wild-type seeds. Exposure of the clock mutant seeds to red light stimuli, however, showed a lack of red light sensitivity for *toc1-101* seeds which had significantly reduced germination rates compared to wild-type seeds, similar to the red light hyposensitivity reported in *toc1* mutants with regards to photomorphogenesis (Más et al., 2003a). Low levels of germination was observed for *LHY OX* seeds in all conditions, likely a result of the perturbation to the clock, as reported previously (Penfield and Hall, 2009), rather than due to reduced red/far-red light sensitivity.

Seeds matured at low temperatures (12°C) showed high dormancy, even after three days of cold stratification. None of the circadian clock mutant seed had significantly different levels of germination frequency compared to wild-type plants, however it should be noted that the low levels of wild-type germination made the establishment of significant reductions in germination not detectable, even in lines that had no germination.

4 Results: Connecting the circadian clock to the cold acclimation pathway

Three *CBF* transcription factors (*CBF1*, *CBF2* and *CBF3*) are core components of the cold acclimation pathway. The *CBFs* are activated by low temperature (as well as drought) and are responsible for initiating a transduction cascade which results in *COR* gene transcription (Stockinger, 1997; Gilmour et al., 1998; Jaglo-Ottosen et al., 1998). The *COR* genes produce proteins that enhance freezing survival (Thomashow, 1998). *CBF* expression is circadian, with a peak in expression occurring 7-8 hours after dawn (Harmer et al., 2000; Nakamichi et al., 2009). The cold induction of *CBFs* is also circadian gated, with the time at which a plant is exposed to cold temperatures affecting the extent to which *CBF* expression is increased (Fowler et al., 2005). As well as the *CBFs* being circadian in expression and gated by the clock, the expression of *CBFs* and the ability of plants to survive at freezing temperatures, is also altered in some circadian clock mutant plants (Dong et al., 2011; Seo et al., 2012). *lhy cca1* double mutant plants have decreased resistance to cold temperatures as well as a decrease in *CBF* expression (Dong et al., 2011) and the *prr5 prr7 prr9* T-DNA insertion, loss of function plants have a decreased sensitivity to the cold and an increase in *CBF* expression (Nakamichi et al., 2010). Because of this, *LHY* and *CCA1* have been suggested as up-regulators of *CBF* expression and *PRR5*, *PRR7* and *PRR9* as inhibitors of *CBF* expression; however, only *CCA1* has been shown to directly bind to *CBF* promoter regions (Dong et al., 2011). A question of interest, therefore, is: in the *prr5 prr7 prr9* triple mutant, are all three mutations required to result in the increased freezing tolerance phenotype, or are single/double mutations sufficient to reproduce the increase in freezing survival rates? As well as the previously reported genes that have been shown to be involved in regulating freezing tolerance there may be other circadian clock genes involved that have not previously been reported as having a role in this pathway. As such, to model the *CBF3* regulation by the circadian clock, other clock

4 Results: Connecting the circadian clock to the cold acclimation pathway

genes were investigated to see if they had a role in the freezing tolerance pathway.

In order to answer the above questions a freezing assay was developed and used. In the freezing assay a number of plants with perturbations to different circadian clock components were frozen and the survival rates of the plants were assessed.

A freezing tolerance protocol for circadian clock mutants was developed in the Penfield Laboratory by Dr Dana Macgregor and was used here for the following freezing tolerance experiments. In developing the protocol the average time for different clock mutants to grow four true leaves at the different temperatures was ascertained and incorporated into the protocol: all plants were exposed to seven days at 22°C to allow for equal germination, followed by a further 10 days growth for plants grown at 22°C, 11 days growth for plants grown at 17°C or 15 days for plants grown at 12°C to allow for four true leaves to grow in the majority of the clock mutant plants (as established previously by Dr Dana Macgregor). The plants were then exposed to 24 hours of -3°C freezing followed by 24 hours at 4°C to allow the plants to thaw. Whether or not a plant continues to grow was used to determine whether a plant had died or not and in developing the protocol Dr Macgregor established that five days back at either 22°C or 17°C after thawing was enough time to establish whether a plant has died or not, and that seven days was required for plants growing at 12°C as they grow at a slower rate. All plants were transferred between environmental conditions at the same time point, CT0.

Establishing which mutant plant lines have an increased or decreased survival rate allows for a better understanding of whether or not a gene is involved in regulating freezing tolerance. Previous freezing assays were used to show that *lhy*, *cca1* single and double mutants, and *prr5 prr7 prr9* triple mutants had an altered freezing phenotype compared to their wild-type counterparts (Nakamichi et al., 2009; Dong et al., 2011). Here, a greater number of clock mutants were investigated to try to establish a better image of how the clock is involved in regulating plant freezing tolerance.

4.1 The temperature at which a plant is grown and the temperature at which a plant is frozen has varying effects on plant survivability

To carry out a freezing tolerance assay on *Arabidopsis* circadian clock mutant plants in order to discover freezing tolerance phenotypes, the freezing tolerance of wild-type plants was first established under the laboratory conditions available for this study. Clock mutant seeds from the Columbia ecotype background were obtained, thus reducing the number of different wild-type ecotype plants to test, as well as making comparisons between mutant phenotypes easier. Columbia seed freezing tolerance under laboratory conditions were tested to establish which freezing temperatures would allow for the best chance of discovery of mutant plants with either a decreased or increased freezing tolerance phenotype.

To test the freezing tolerance of wild-type Col plants six pots, each containing approximately 15-20 seeds, were cold stratified for three days at 4°C. After the cold stratification period the seed pots were moved to 22°C for 14 days in white light (100 $\mu\text{mol}/\text{m}^{-2}/\text{s}^{-1}$) 12:12 conditions. After the 14 days of growth the pots were exposed to one of six freezing temperatures (-1, -2, -3, -4 -5 and 0°C) for 24 hours followed by 24 hours at 4°C and then moved back to 22°C for a further five days, at which point survival rates were assessed. Three biological replicates of this experiment were carried out and the average survival rates at the different temperatures, along with the standard error, can be seen in **figure 4.1**.

Columbia plants were able to survive with zero fatalities when exposed to 24 hours of 0, -1 and -2°C. At -3°C there is an average survival rate of 84.7% which decreases to only 5.7% average survival rates when the temperature was reduced to -5°C. Based on these observations it was concluded that carrying out a freezing tolerance assay with plants frozen at -5°C would allow for the discovery of plants that have an increased survival rate compared to that of Columbia, wild-type, plants. Conversely, carrying out a freezing assay with plants frozen at -3°C will allow for the discovery of plants that have a decreased survival rate compared to that of the Columbia, wild-type, plants. Thus it was decided to test freezing tolerance at two temperatures, -5°C and -3°C, rather than just one temperature.

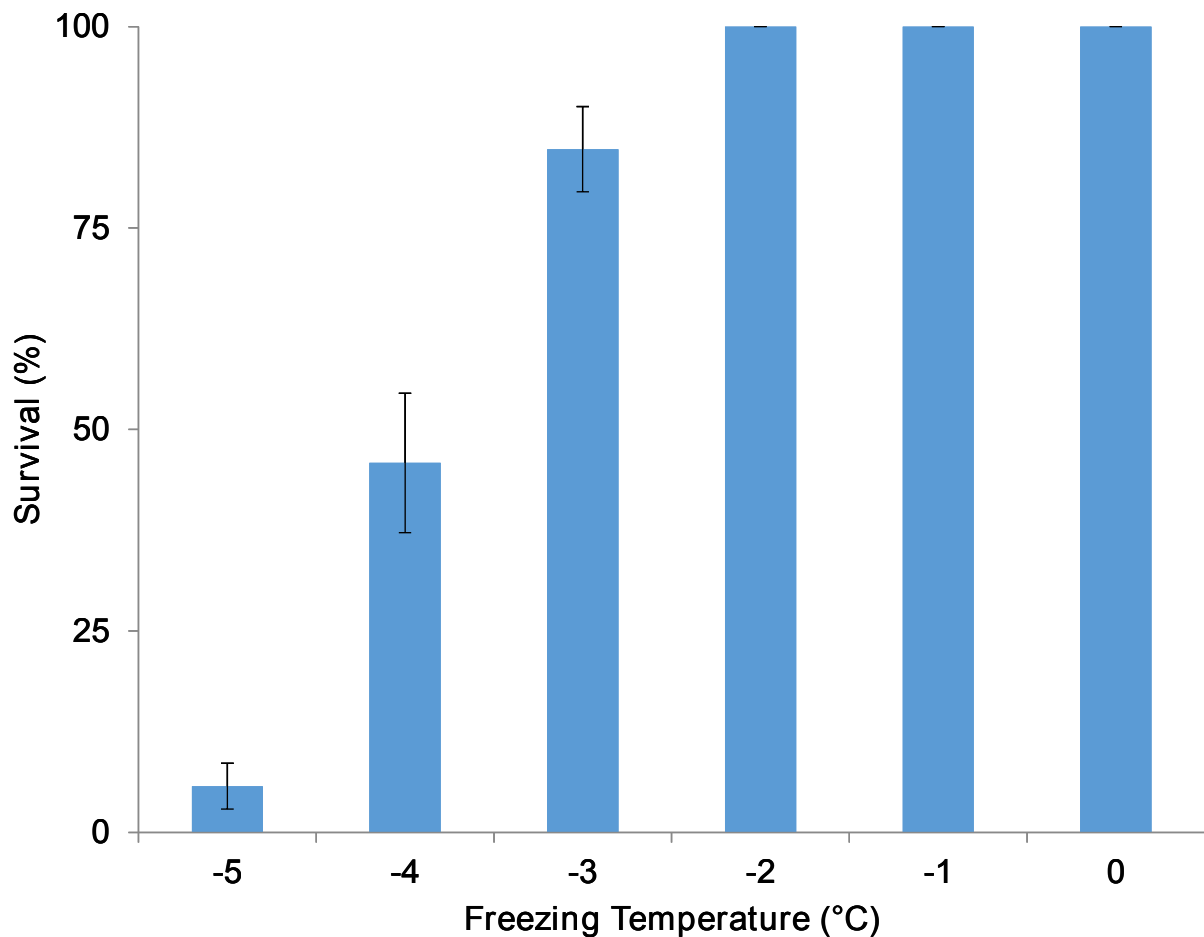


Figure 4.1: Wild-type Columbia plants frozen at 0, -1 and -2°C for 24 hours showed no deaths as a result of exposure to the freezing conditions but as the freezing temperature decreases from -3°C to -5°C the death rate increases rapidly until less than 10% of plants survive 24 hours of exposure to -5°C. Values are the average of three biological experiments, with each experiment comprising 15-20 plants for each temperature condition. The standard error is shown.

Knowledge of how the circadian clock is involved in regulating freezing tolerance in plants that are exposed to short term freezing conditions has recently made great advances (Dong et al., 2011; Seo et al., 2012; James et al., 2012), but is still incomplete. It is also known that the circadian clock is regulated differently at different temperatures (Gould et al., 2006). Therefore, this study aimed to not only investigate further the role of the individual *PRRs* in freezing tolerance and ascertain whether other clock genes were involved in regulating freezing tolerance, but also to determine how temperature induced changes to the circadian clock affects a plant's freezing

tolerance.

To determine whether the different growth temperatures affected the clock regulation of freezing tolerance, the difference in wild-type survival in plants grown at different temperatures was first tested to confirm that differences in freezing tolerance in wild-type plants grown at different temperatures could be observed using the laboratory set-up available for this study.

Columbia seeds were cold stratified in pots, each containing approximately 15-20 seeds, for three days at 4°C. After the cold stratification period the seed pots were moved to 22°C in white light ($100 \mu\text{mol}/\text{m}^{-2}/\text{s}^{-1}$) 12:12 conditions for one week to allow germination to occur. After one week's growth they were then transferred to the test temperatures for either 17 days at 12°C; 11 days at 17°C or 9 days at 22°C to allow for four true leaves to grow. Plants were then frozen at either -5°C for 24 hours or at -3°C for 24 hours in the dark as heat from the cabinet lights prevented the consistent and accurate maintenance of the freezing temperatures. A period of one day at a recovery temperature of 4°C in the dark (heat from lights prevented maintenance of low temperatures) was then allowed before moving the plants back to their test conditions for a period of time to allow the plants that are still alive to continue growing; five days at 17°C/22°C or seven days at 12°C. Three biological replicates of this experiment were carried out and the average survival rates at the different temperatures, along with the standard error, can be seen in **figure 4.2**.

Columbia plants frozen at -5°C had significantly lower survival levels than plants that were frozen at only -3°C (Students t-test, $P < 0.05$; **Table 4.1**). The plants that were frozen at -3°C showed no significant difference in the survival rates of the plants that were grown at different temperatures (Students t-test, $P < 0.05$; **Table 4.1**). The plants that were frozen at -5°C had no significant difference in the observed survival rates between the plants that were grown at 17°C and 22°C, but there was a significant greater survival rate in the plants that were grown at 12°C compared to those that were grown at either 17°C or 22°C (Students t-test, $P < 0.05$; **Table 4.1**). From the data collected here two freezing temperatures to use for the freezing tolerance assay were established, -5°C and -3°C, which would detect mutant plants with either a decrease or increase in freezing sensitivity. It was also confirmed that under the test conditions available, growing plants at either 12°C, 17°C or 22°C would allow for the identification of circadian clock mutant plants that had altered sensitivity to growth temperature compared to wild-type plants.

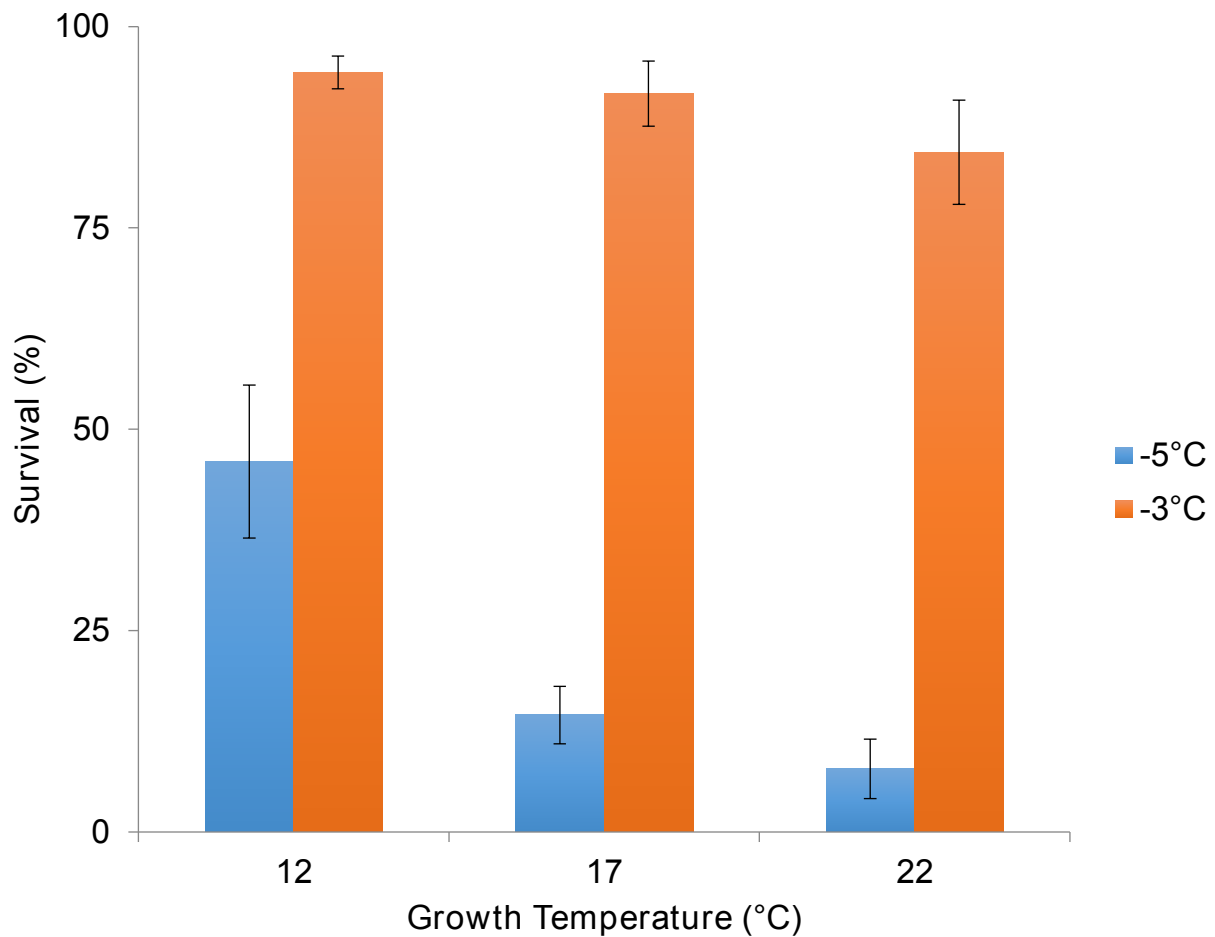


Figure 4.2: Wild-type Columbia plants grown at 12°C, 17°C or 22°C show little change in their freezing tolerance when frozen at -3°C for 24 hours. Columbia plants frozen at -5°C have larger differences in survival rates at the different growth temperatures with a decrease in survival rate going from 45.9% survival in plants grown at 12°C to only 7.9% in plants grown at 22°C. Orange bars represent average survival rates for plants frozen at -3°C and blue bars are the average survival rates of plants frozen at -5°C. Values are the average of three experiments, with each experiment comprising of 15-20 plants for each temperature condition. The standard error is shown.

Table 4.1: Statistics of difference in Columbia survival when frozen at either -3°C or -5°C after growth at either 12, 17 or 22°C. Plants frozen at -5°C have significantly different survival rates than those frozen at -3°C. The plants frozen at -3°C had no significant difference in survival rates in any of the different growth temperatures, whereas the plants frozen at -5°C had significantly different survival rates in plants that were grown at 12°C compared to the other two growth temperatures. Two-tailed Students t-test; green boxes show significant differences and red boxes show none-significant differences, $P < 0.05$.

Plants grown at -5°C versus plants grown at -3°C			
Growth temperature	12°C	17°C	22°C
P-value	0.00	0.00	0.00
Plants frozen at -3°C			
Growth temperature comparison	12°C against 17°C	12°C against 22°C	17°C against 22°C
P-value	0.62	0.21	0.38
Plants frozen at -5°C			
Growth temperature comparison	12°C against 17°C	12°C against 22°C	17°C against 22°C
P-value	0.00	0.00	0.30

4.2 Additional circadian genes are shown to have a role in freezing tolerance

Components of the circadian clock are known to affect freezing tolerance in *Arabidopsis*; for example triple *PRR* mutants (*prrr5 prrr7 prrr9*) have an increase in freezing tolerance when exposed to -5°C for 24 hours (Nakamichi et al., 2009), whereas plants with *lhy*, *cca1* and *lhy cca1* double mutants have decreased freezing survival after freezing exposure and the *lhy cca1* double mutant has increased electrolyte leakage after freezing exposure (Espinoza et al., 2010; Dong et al., 2011). *gi-3* mutant plants have also been shown to have an increase in electrolyte leakage compared to wild-type plants in freezing conditions indicating decreased freezing tolerance (Cao et al., 2005). In the following two sections it is shown that there are further genes involved that are both components of the core circadian clock as well as involved in regulating freezing tolerance that had yet to be described as such.

The same protocol was used as in section 4.1 to investigate the freezing tolerance of wild-type *Arabidopsis* plants, as well as plants with perturbations to their circadian clock. Seeds were cold stratified in pots, each containing approximately 15-20 seeds, for three days at 4°C. After the cold stratification period the seed pots were moved to

22°C in white light ($100 \mu\text{mol}/\text{m}^{-2}/\text{s}^{-1}$) 12:12 conditions for one week to allow germination to occur. After one week's growth they were then transferred to the test temperatures for either 17 days at 12°C; 11 days at 17°C or 9 days at 22°C to allow for four true leaves to grow. Plants were then frozen at either -5°C for 24 hours or at -3°C for 24 hours in the dark as heat from the cabinet lights prevented the consistent and accurate maintenance of the freezing temperatures. A period of one day at a recovery temperature of 4°C in the dark (heat from lights prevented maintenance of low temperatures) was then allowed before moving the plants back to their test conditions for a period of time to allow the plants that are still alive to continue growing; five days at 17°C/22°C or seven days at 12°C. Three biological replicates of this experiment were carried out and the average survival rates at the different temperatures, along with the standard error, can be seen in **figure 4.3** and **figure 4.4**.

4.2.1 Survival rates when frozen at -3°C

As mentioned earlier, two freezing temperatures were selected, -5°C to ascertain any circadian clock mutants with increased freezing tolerance, and -3°C to ascertain any clock mutant plants with decreased freezing tolerance. In this section an investigation into whether any of the clock mutant plants tested have decreased freezing tolerance is carried out.

The greatest variation in survival rates observed was in plants that were grown at 22°C with several of the mutant plants showing altered survival rates compared to that of the wild-type plants (**Figure 4.3**). *lux-5*, *lhy-20*, *prp7-3* and *elf3-1* all showed significantly reduced survival rates at least at one growth temperature when compared to wild-type plants. Of the clock mutant plants grown at 22°C *elf3-1*, *lux-5*, *lhy-20* and *prp7-3* had significantly decreased survival rates compared to wild-type plants ($P < 0.05$, **Table 4.2**). In plants grown at 12°C, there was no significant difference between the survival rates of the mutant plants and that of the wild-type plants with the noticeable exception of the *lux-5* and *elf3-1* plants which had significantly reduced survival rates ($P = 0.02$ for *lux-5* and $P = 0.03$ for *elf3-1*; **Figure 4.3**). In the plants grown at 17°C there was no significant difference in the survival rates of any of the plants, with none of the plants that had mutations to the clock having a statistically significant decrease in survival rates (t-test, $P < 0.05$, **Table 4.2**).

4 Results: Connecting the circadian clock to the cold acclimation pathway

Table 4.2: A one tailed Students t-test comparing the survival differences between wild-type plants and clock mutant plants that were frozen at -3°C for 24 hours. Red boxes are not statistically significant and green boxes are statistically significant ($P < 0.05$). A one tailed test was carried out as I was only interested in looking for significance in one direction not two. *elf3-1* was shown to be significantly decreased when grown at 22°C and *prp5-1* was shown to be significantly increased when grown at 12°C as it had 100% survival.

Mutant	Growth Temperature		
	12°C	17°C	22°C
<i>toc-101</i>	0.02	0.16	0.08
<i>lux-5</i>	0.02	0.38	0.01
<i>lhy-20</i>	0.16	0.20	0.05
<i>prp5-1</i>	0.00	0.05	0.07
<i>prp7-3</i>	0.35	0.07	0.03
<i>prp9-1</i>	0.38	0.05	0.49
<i>prp5-11 prp7-11 prp9-10</i>	0.26	0.05	0.46
<i>elf3-1</i>	0.03	0.44	0.01
<i>gi-201</i>	0.21	0.19	0.14

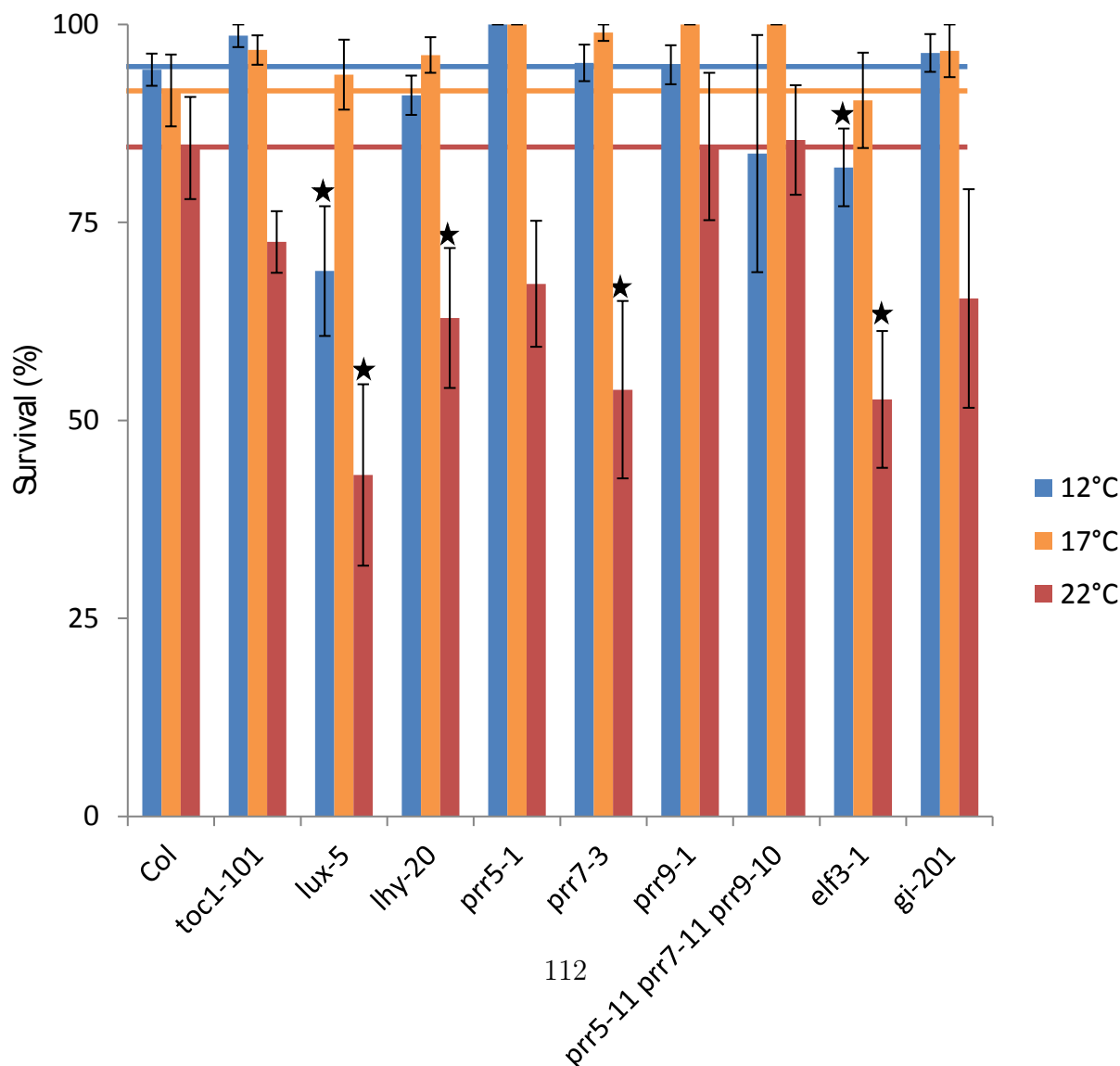


Figure 4.3: Survival rates of different *Arabidopsis* plants with circadian clock mutations grown at either 12°C , 17°C or 22°C after being frozen at -3°C for 24 hours,

4.2.2 Survival rates when frozen at -5°C

To establish circadian clock mutants that have increased freezing tolerance compared to wild-type plants the same protocol was followed as used in the previous section, with the exception that plants were frozen at -5°C rather than -3°C. The only line which had a decrease in survival rate when exposed to -5°C freezing conditions was the *lux* mutant line when grown at 12°C (**Figure 4.4**). We know from the literature already that the *prp5 prp7 prp9* loss of function T-DNA plant has significantly increased survival rates when grown at 22°C and exposed to 24 hours of -5°C freezing temperatures (Nakamichi et al., 2009). The increased freezing tolerance phenotype compared to wild type plants of the *prp5 prp7 prp9* triple mutant is again seen in this data set in plants not just grown at 22°C (as seen in the Nakamichi 2009 paper) but also in plants that were grown at 12°C and 17°C, with all three growth temperatures resulting in significantly increased survival rates compared to wild type plants (T-test $P < 0.05$, **Figure 4.4** and **Table 4.3**). Survival rates of the *prp* triple mutants that were grown at 17°C were significantly lower compared to the plants that were grown at 12°C (t-test $P = 0.00$) or 22°C (t-test $P = 0.00$); there was no significant difference in survival rates between the *prp* triple mutant plants that were grown at 12°C and 22°C when frozen at -5°C (t-test $P = 0.09$).

This study has shown that the *prp* triple loss of function can have a large effect on the survival rates of plants that are frozen at -5°C in plants grown at 12°C, 17°C and 22°C. It has not been established, however, whether all three of the PRRs are acting together to produce this phenotype or if the same freezing phenotypes can be reproduced with single gene mutations. The single mutant *prp5* has a significant increase in the survival rates of the plants when grown at all three temperatures (t-test, $P < 0.05$, **Table 4.3**) and when grown at 12°C and 17°C there is no significant difference in the survival rates between the *prp5-1* mutant and the *prp* triple mutant (t-test, $P > 0.05$, **Table 4.4** and **Figure 4.4**). When grown at 12°C there is a 10 percentage point decrease in survival rate in *prp5* compared to the *prp5 prp7 prp9* triple mutant (81.7% survival versus 91.7% survival respectively). The *prp7* single mutant has a similar survival rate to that of the *prp5* single mutant when grown at 12°C (77.7%) as does the *prp9* single mutant (78%), however, unlike *prp5* and *prp9*, *prp7* is not significantly different to wild type plants when grown at 12°C ($P < 0.01$, **Table 4.3**). When grown at 12°C, *prp5-1*, *prp7-3* and *prp9-1* did not have significantly different survival rates compared to the *prp* triple mutant (t-test, $P > 0.5$, **Table 4.4**).

Table 4.3: A one tailed t-test comparing the survival rates between wild type plants and clock mutant plants that were frozen at -5°C for 24 hours to try and determine if any had a significant increase in survival. In comparison to the -3°C freezing experiment, there are several mutant lines that have significantly altered survival rates when frozen at -5°C. Red boxes are not statistically significant and green boxes are statistically significant (P<0.05).

Mutant	Growth Temperature		
	12°C	17°C	22°C
<i>toc-101</i>	0.00	0.00	0.00
<i>lux-5</i>	0.01	0.10	0.26
<i>lhy-20</i>	0.13	0.00	0.06
<i>prp5-1</i>	0.00	0.00	0.00
<i>prp7-3</i>	0.06	0.00	0.00
<i>prp9-1</i>	0.00	0.02	0.02
<i>prp5-11 prp7-11</i>	0.03	0.00	0.05
<i>prp5-11 prp9-10</i>	0.00	0.00	0.04
<i>prp7-11 prp9-10</i>	0.17	0.01	0.00
<i>prp5-11 prp7-11 prp9-10</i>	0.00	0.00	0.00
<i>elf3-1</i>	0.32	0.01	0.43
<i>gi-201</i>	0.06	0.00	0.05

When grown at 17°C survival rates are slightly higher in the *prp5* mutant than in the triple mutant (69.3% survival versus 62.2% survival respectively), whereas *prp7* and *prp9* both have a decrease in survival (50.7% and 53.3% respectively) compare to the *prp* triple mutant. All three *prp* single mutants have an increase in survival rates compared to wild type plants when grown at 17°C (P<0.05, **Table 4.3**). In the *prp5-1*, *prp7-3* and *prp9-1* mutants there is no significant difference in the survival rates of the plants when grown at 17°C and frozen at -5°C compared to the *prp* triple mutant (t-test, P>0.05, **Table 4.4**).

When grown at 22°C, all three *prp* single mutants have significantly increased survival rates compared to wild-type plants (P<0.05, **Table 4.3**). When grown at 22°C there is significantly lower survival rate compared to the *prp* triple mutant in the *prp5* mutant (53.1% survival rate versus 86.1% survival rate respectively; t-test, P<0.05, **Table 4.4**). The *prp7-3* mutant also had a significantly lower survival rate compared to the *prp* triple mutant when grown at 22°C and frozen at -5°C (47% survival rate compared to 86.1%; t-test, P<0.05, **Table 4.4**).

This study aimed to try and determine which *PRRs* or which combination of *PRRs*

Table 4.4: There is little significant differences in survival phenotypes between the *pr* single/double mutants and the *pr* triple mutant. A two-tailed t-test comparing the survival rates of the *pr* single and double mutants compared to the *pr* triple mutant plants after freezing at -5°C. Red boxes are not statistically significant and green boxes are statistically significant (P<0.05).

Mutant	Growth Temperature		
	12°C	17°C	22°C
<i>pr</i> 5-1	0.29	0.33	0.00
<i>pr</i> 7-3	0.43	0.24	0.00
<i>pr</i> 9-1	0.07	0.53	0.07
<i>pr</i> 5-11 <i>pr</i> 7-11	0.12	0.78	0.28
<i>pr</i> 5-11 <i>pr</i> 9-10	0.19	0.16	0.53
<i>pr</i> 7-11 <i>pr</i> 9-10	0.12	0.02	0.87

were required for the observed phenotype in the triple mutant, and as such investigating the freezing phenotypes of the *pr* double mutants, not just the single mutants, would help greatly with this as the observed phenotype of the triple mutant may not require mutations to all three of the *PRRs*. When grown at 12°C and frozen at -5°C, the *pr*5-11 *pr*7-11 and the *pr*5-11 *pr*9-10 double mutants had significantly increased survival rates compared to wild-type plants (t-test, P<0.05; **Figure 4.4** and **Table 4.3**). When grown at 17°C and frozen at -5°C all three of the *pr* double mutants had significantly increased survival rates compared to wild-type plants, and when grown at 22°C, also, all of the double mutants had significantly increased survival compared to wild-type plants (t-test, P<0.05; **Figure 4.4** and **Table 4.3**). There was no significant difference in survival rates between the *pr* double mutants and the *pr* triple mutant when grown at all temperatures and frozen at -5°C, except in the *pr*7-11 *pr*9-10 double mutant when grown at 17°C which had significantly lower survival rates (**Table 4.4**).

The *pr* mutant plants were not the only ones to have significantly altered freezing phenotypes when compared to wild-type plants. When grown at 12°C and 22°C *elf3-1* mutants had no significant difference in survival when exposed to -5°C freezing temperatures, however, in the plants that were grown at 17°C survival rates were significantly greater than in wild-type plants grown at the same temperature (**Table 4.3** and **Figure 4.4**). Like *lef3-1*, *gi-201* mutants also had significantly increased survival rates compared to wild-type when grown at 17°C, but not at the other two temperatures.

4 Results: Connecting the circadian clock to the cold acclimation pathway

The most interesting results, however, was those of the *toc1-101* mutant plants. The *toc1-101* mutants had a significant increase in survival rates in all three of the growth temperatures compared to wild-type plants, with the plants grown at 12°C having almost no fatalities. *toc1-101* mutant plants grown at 12°C had 98% survival rates compared to that of 45.1% for the wild-type plants. When grown at 17°C this had dropped to only 56.8% survival rates for the *toc1-101* mutant plants, but this was still significantly greater than the Columbia wild-types (t-test, $P < 0.05$, **Table 4.3**) and when grown at 22°C *toc1-101* survival was 45.2% compared to the wild-type 9.3% (**Figure 4.4**).

4 Results: Connecting the circadian clock to the cold acclimation pathway

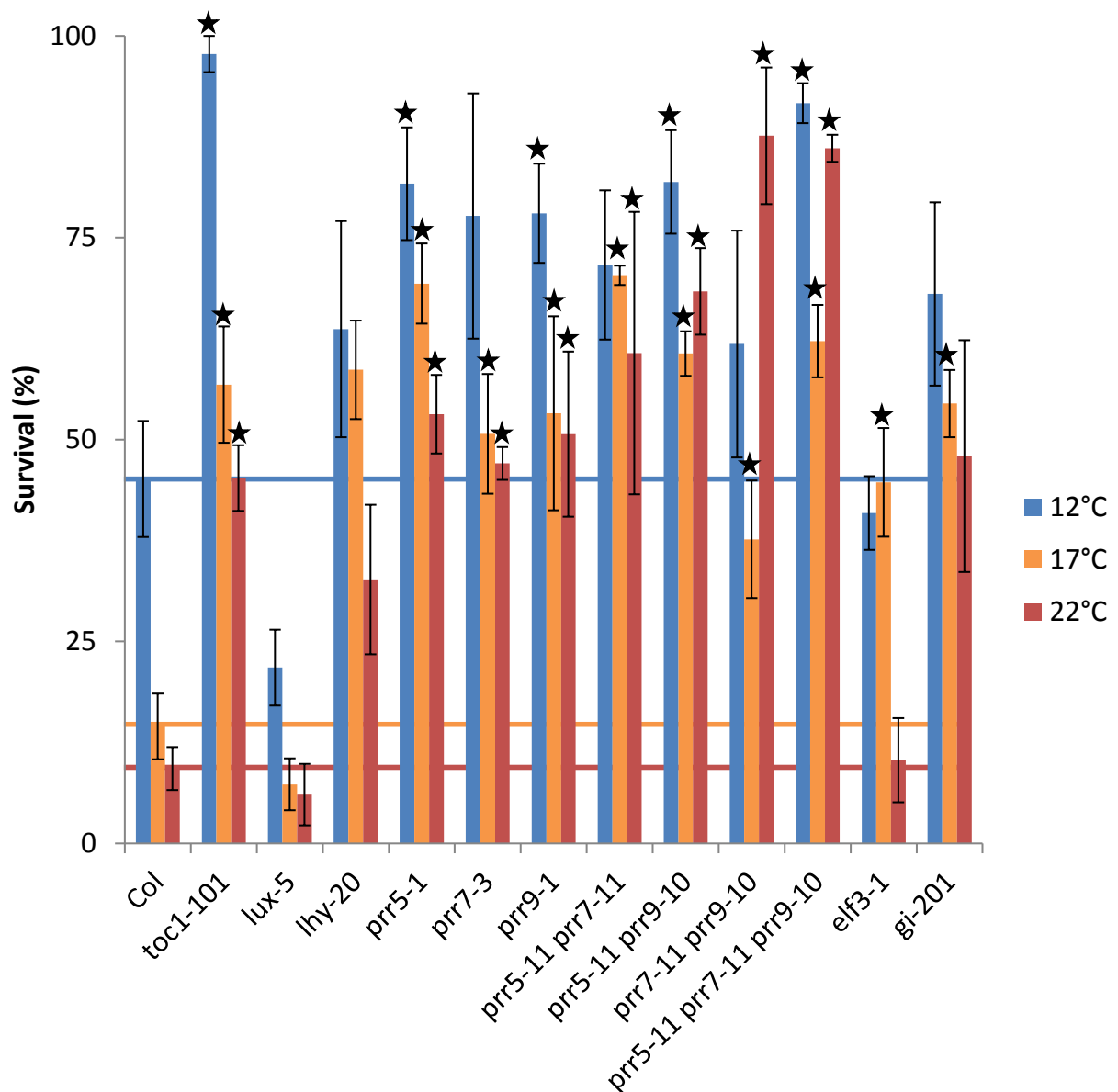


Figure 4.4: Survival rates of different *Arabidopsis* plants with circadian clock mutations grown either at 12°C, 17°C or 22°C after being frozen at -5°C for 24 hours, followed by 24 hours at 4°C. Survival was assessed either after five days back at their original temperature (for plants grown at 17°C and 22°C) or seven days back at their original growth temperature (for plants grown at 12°C). Horizontal lines represent the average survival of the Columbia plants at the different temperatures and are included to make comparisons to mutant survival easier. Significant **increases** in survival rates are indicated by a black star, ($P < 0.05$). Values are the average of five biological experiments, with each experiment comprising of 15-20 plants. Standard error shown.

4.3 *CBF1* expression can be altered by long term exposure to different temperatures

It was known from the literature that *CBF* gene expression occurs throughout the day (though at low levels) with a peak in expression occurring at approximately eight hours after subjective dawn, and is increased when a plant is exposed to a cold shock (Fowler et al., 2005). How *CBF* expression levels are altered by longer term exposure to varying growth temperatures, however, is not known. In order to test how *CBF* expression changed over long term exposure to different temperatures, *CBF1* expression over a period of three days was assessed in plants exposed to four different environmental temperatures.

RNA samples were provided by Doctor Aurora Pinas-Fernandez at the University of Edinburgh enabled the investigation of *CBF1* expression in *Arabidopsis* plants grown at different temperatures. The RNA samples were from *Arabidopsis* plants that were grown for seven days under entraining conditions of 22°C, 12 hours light, 12 hours dark followed by transfer to constant light conditions at either 12°C, 17°C, 22°C or 27°C with samples collected every four hours from ZT 48 to ZT 120. These RNA samples were assessed by qRT-PCR to look at the expression of *CBF1* in the samples to see how the expression changed not just over the period of days, but also between the different growth temperatures (**Figure 4.5A**). **Figure 4.5A** shows the average expression of *CBF1* in three biological samples normalised to *ACTIN2* expression. Unfortunately, the individual data points, before averaging, were lost, so no standard error is shown.

Figure 4.2 shows that even small changes in growth temperature can have a large effect on a plant's freezing tolerance. As *CBFs* are positive regulators of certain *COR* genes' expression (Gilmour et al., 1998; Jaglo-Ottosen et al., 1998) we can predict that plants grown at different temperatures would have different levels of *CBF* expression in order to facilitate this change in freezing tolerance.

Plants grown at 22°C and then transferred to constant conditions have been shown to have a peak in expression at 8 hours after relative dawn for the first two days after transfer into continuous conditions (Kidokoro et al., 2009). The plants grown at 17°C and 22°C have peak *CBF1* expression four hours later than the normal 8 hours after subjective dawn, peaking 12 hours after subjective dawn instead (**Figure 4.5A**). 12°C grown plants lose their rhythmicity of *CBF1* whereas the plants that were grown at

4 Results: Connecting the circadian clock to the cold acclimation pathway

27°C have decreased expression of *CBF1* but maintain a peak in expression 8 hours after subjective dawn in the period of 120-172 hours after transfer to constant conditions. The 22°C grown plants are the only plants that maintain a single clear peak per day in *CBF1*, with the plants that were grown at the other temperatures displaying several peaks in expression throughout the day (**Figure 4.5A**).

To get an easier understanding of how the overall expression levels of *CBF1* are altered in the different temperatures the average expression of the plants from all of the different time points at the different temperatures was calculated and graphed so that the change in total mRNA production between the different temperatures could be easily observed (**Figure 4.5B**). Growth at the different temperatures has an effect on the overall expression levels of *CBF* with an analysis of variance (ANOVA) showing that there is significant difference in expression between the different growth temperatures ($P=0.02$). Individual t-tests show that there is a significant difference in expression between the plants that were grown at the following temperatures: 12°C and 17°C; 17°C and 27°C; 22°C and 27°C as indicated by arrows on **Figure 4.5B** ($P<0.05$).

4 Results: Connecting the circadian clock to the cold acclimation pathway

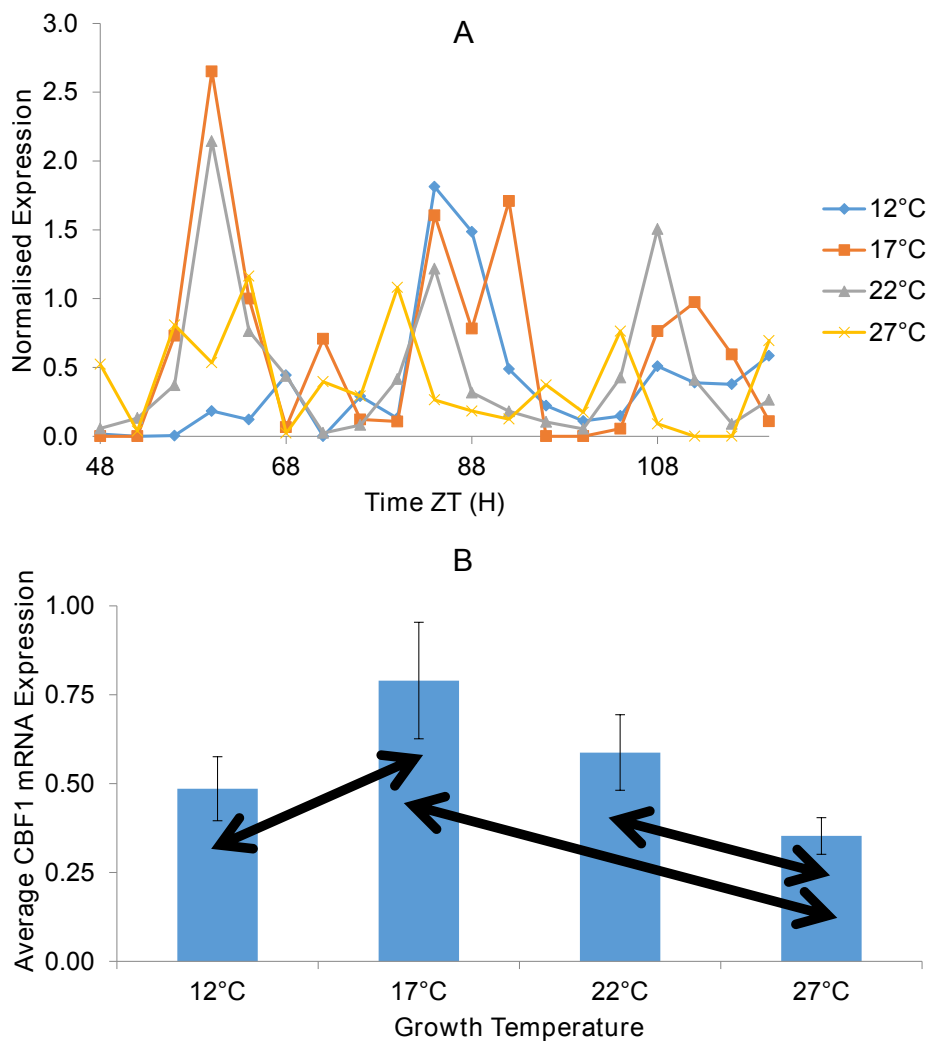


Figure 4.5: *CBF1* mRNA expression in *Arabidopsis* plants grown at four different temperatures and moved to constant light conditions. A) The four time series with a four hour resolution showing *CBF1* expression relative to *ACT2* under circadian conditions in plants grown at either 12°C (blue line), 17°C (orange line), 22°C (grey line) or 27°C (yellow line). Results are the average of three biological experiments. B) The average *CBF1* expression from over the whole time series. The temperature at which the plants are grown clearly affects the amount of *CBF* that is expressed throughout the day. Arrows indicate significantly different expression (t-test, $P < 0.05$), and error bars are standard error.

4.4 Discussion

In this chapter, plants with perturbations to components of the circadian clock were used to investigate the role of the circadian clock in regulating freezing tolerance in *Arabidopsis thaliana*.

4.4.1 Circadian clock components involved in freezing tolerance

The circadian clock is important for regulating cold response pathways in *Arabidopsis* (Fowler et al., 2005; Nakamichi et al., 2009; Dong et al., 2011), however, the mechanisms of the clock regulation of the cold response pathway are still largely unknown. There are several clock genes that have been shown to be important for regulating freezing tolerance in *Arabidopsis*, such as *LHY*, *CCA1* and *PRR5*, *PRR7* and *PRR9*. Here freezing tolerance assays in a number of circadian clock mutants were carried out to try and discover any new genes of importance for regulating freezing tolerance, as well as to gather more information on known genes of interest.

It has been shown that clock genes such as *LHY*, *CCA1* or *TOC1* are expressed differently in plants at different temperatures (Gould et al., 2006). Mutations to the circadian clock can also have different effects on circadian clock gene expression at different temperatures, such as the effect of the *gi* mutation on *TOC1* expression: *TOC1* expression levels are almost identical to wild-type in *gi-11* mutants grown at 17°C but at 27°C *TOC1* expression does not increase like in wild-type plants and is almost constant in expression (Gould et al., 2006).

If the circadian clock is responsible for regulating freezing tolerance, then one would predict that mutations to the circadian clock can result in different freezing tolerance phenotypes in plants grown at different temperatures.

Freezing assays at two different temperatures (-5°C and -3°C) were carried out on plants grown at either 12°C, 17°C or 22°C, where freezing plants at -5°C was used to try and identify plants with decreased freezing sensitivity (increased freezing survival rates) and -3°C was used to identify plants with increased freezing sensitivity (plants with decreased freezing survival rates).

LHY and its importance in freezing tolerance

LHY is involved in positively regulating *CBF* expression (Dong et al., 2011). As such, one would predict a decrease in freezing tolerance in plants that lack functional *LHY* genes due to the corresponding reduction in the expression of the freezing tolerance *CBF* genes. Plants that were grown at 22°C and frozen at -3°C had a significant decrease in freezing tolerance similar to the *lhy cca1* double mutant phenotype reported in the literature (Dong et al., 2011). When *lhy-20 Arabidopsis* plants were grown at 12 and 17°C, however, there was no significant decrease in freezing tolerance as one may have predicted. This implies that the role of LHY in regulating freezing tolerance may vary at different temperatures. At 12 and 17°C *LHY* mRNA expression levels are greater than in plants that are grown at 27°C (Gould et al., 2006) so one may hypothesise that the effect of perturbing *LHY* at 12 and 17°C would be greater than in plants grown at warmer temperatures. The fact that this is not the case in the *lhy-20* loss-of-function mutant may be a product of the mutant allele used, and perhaps a full *lhy* null mutant would show a reduction in freezing tolerance that is not observed here. The reason for no significant difference in freezing tolerance in wild-type and *lhy-20* plants grown at 12 and 17°C may also be due to compensation from other clock components involved in regulating freezing tolerance at these temperatures. For example, as discussed below, *TOC1* appears to be involved in negatively regulating freezing tolerance; *toc1* mutant plants have increased freezing tolerance. If there was decreased *TOC1* levels in plants grown at 12 and 17°C then this may be compensating for the loss of *LHY* function. *TOC1* mRNA levels are decreased at 12 and 17°C compared to plants that are grown at 27°C, however there is not data for plants grown at 22°C (Gould et al., 2006). The decreased *TOC1* expression levels seen at the lower temperatures may be compensating for *lhy* mutation at these temperatures, but not at warmer temperatures where there is increased *TOC1* expression.

Evening Complex components and their importance in freezing tolerance

The Evening Complex is made up of LUX, ELF3 and ELF4 proteins and is capable of binding the promoters of clock genes, such as *PRR9* and *LUX* to regulate expression (Dixon et al., 2011; Helfer et al., 2011; Nusinow et al., 2011). When grown at 12°C and 22°C and frozen at -3°C, plants with the *elf3-1* mutation had significant reductions in survival rates compared to wild-type plants, but not when grown at 17°C

and frozen at -3°C (**Figure 4.3**). A significant decrease in survival in plants grown at 12°C or 22°C and then frozen at -3°C was also observed in the *lux-5* mutant plants. When grown at 12°C or 22°C and frozen at -5°C , plants with the *elf3-1* null mutation had no significant change in their freezing tolerance compared to wild-type plants, but when grown at 17°C there was a significant increase in survival compared to wild-type plants (**Figure 4.4**). The effect of the *elf3-1* mutant on freezing tolerance, therefore, depends not only on the temperature at which the plants are grown, but also the severity of the freezing exposure. *ELF3* is involved in temperature regulated timing of flowering time; *elf3-7* mutants have partial suppression of the normal, wild-type, delay in flowering time that is observed in plants grown at low temperatures (Strasser et al., 2009). Not only is *ELF3* important for temperature dependant flowering time, but microarray and gene enrichment analysis identified 2473 temperature-regulated genes and 478 *elf3* regulated genes at 23°C , 235 of which were identified in both groups (Strasser et al., 2009). At 16°C of the 1263 *elf3* regulated genes identified, 341 were also temperature responsive (Strasser et al., 2009). *ELF3* would appear to be an important circadian clock gene for regulating low temperature and freezing temperature responses in *Arabidopsis* and is an interesting candidate for the modelling of *CBF3* regulation by the circadian clock that will be discussed in **Chapter 5**. Whilst *CBF3* was not identified as *elf3* and temperature regulated in the Strasser et al. (2009) microarray data this does not completely rule out a role for *ELF3* in regulating *CBF3* expression as there are other known *CBF3* regulatory factors that may act to compensate for the loss of *ELF3* seen in this microarray data. The above shows a possible role *ELF3* in regulating freezing tolerance, possibly through the actions of the Evening Complex as discussed in more detail in **Chapter 5**.

The *PRRs* are important for freezing tolerance in *Arabidopsis thaliana*

This study aimed to establish if the freezing survival phenotype observed in the *prp5 prp7 prp9* triple mutant (Nakamichi et al., 2009) was requisite on all three of these *prp* mutations being present in the plants or whether single or double mutants were able to replicate the increased survival rates seen in the triple mutant. The increased survival is present when a plant is grown at either 12°C , 17°C or 22°C which shows that the phenotype is present under a wide variety of temperatures. The increased survival phenotype, whilst present at all three growth temperatures, still appears to have some temperature dependence, however, as plants that were grown at 17°C and frozen at

-5°C had significantly reduced survival rates compared to the plants that were grown at either 12°C or 22°C (**Table 4.4**).

There are few cases, under the conditions tested, where the *prp* single or double mutants have significantly different survival rates when frozen at -5°C compared to the *prp* triple mutant (**Table 4.4**). In the plants that were grown at 12°C, none of the *prp* single or double mutants had significantly different survival rates; when grown at 17°C only the *prp7-10 prp9-11* double mutant was significantly different to the *prp* triple mutant and when grown at 22°C only the *prp5-1* and *prp7-3* single mutants had significantly different survival rates compared to the *prp* triple mutant when frozen at -5°C. Also, in all of the growth temperatures, only *prp7-3* and the *prp7-10 prp9-11* mutant plants did not have significantly increased freezing tolerance. In the case of the *prp7-3* mutant this may be due to the relatively large standard-error observed in these two data sets that is preventing a significant difference in survival rates compared to wild-type plants from being observed. The above data suggests that the individual *PRRs* are equally important for maintaining wild-type freezing tolerance at 12°C and 17°C, but as the temperature increases to 22°C, different *PRRs* start to have larger roles in maintaining wild-type freezing tolerance.

The *PRRs* are partially redundant with regards to maintaining normal circadian rhythms, but are expressed in sequence so that a tight control is maintained over the clock throughout the day (Salomé and McClung, 2005). The fact that mutations to the individual *PRRs* are capable of producing similar phenotypic differences in freezing tolerance compared to the *prp5 prp7 prp9* triple mutant plants is likely a result of the genes acting throughout the day to regulate freezing tolerance in a similar partially redundant manner to that of regulating circadian rhythms; thus the *PRRs* maintain normal freezing tolerance throughout the day.

In the future, it would be interesting to develop a time dependent freezing assay to establish whether the time of day at which the *prp* mutants are frozen affects the freezing tolerance observed, as is discussed further in the **Future work** section of **Chapter 6**.

Plants containing the *toc1-101* mutation had significantly increased freezing survival rates compared to wild-type plants at all three of the tested growth temperatures when frozen at -5°C; this increase strongly suggesting an inhibitory role of TOC1 in the regulation of freezing tolerance. This phenotype could either be due to the result of the mutations having a direct or indirect effect on the cold acclimation pathway. One

mechanism through which the *toc1* mutant may have an indirect effect on the cold acclimation pathway is through the *lhy* and *cca1* regulation of the *CBFs*. *lhy cca1* single and double mutants have decreased freezing survival and *CCA1* has been shown to directly bind to the *CBF* promoter regions (Dong et al., 2011). *TOC1* has an inhibitory effect on *LHY* and *CCA1* expression (Pokhilko et al., 2012). Therefore, in a *toc1* mutant the inhibitory effect of the *TOC1* protein on *LHY* and *CCA1* expression is absent, resulting in increased *LHY/CCA1* expression. As *LHY/CCA1* are up-regulators of *CBF* expression one would hypothesise that an increase in *CBF3* expression in *toc1* mutant plants is likely the cause of the increased freezing tolerance of the *toc1* mutants.

Another hypothesis is that *TOC1* directly affects the cold acclimation pathway by directly binding to the promoter of a cold pathway component altering its expression, thus affecting freezing tolerance in the plants. *TOC1* can form a complex with *PIF7* and *PIF7* binds to the G-box element of the *CBF1* and *CBF2* promoter region (Kidokoro et al., 2009). This provides a possible mechanism for *TOC1* regulation of *CBF1* and *CBF2* that could result in increased freezing tolerance in the *toc1-101* mutant plants; however, the *CBF3* promoter region does not contain a G-box element for binding to occur (Kidokoro et al., 2009). The direct role of *TOC1* in freezing tolerance is discussed further below when the direct inhibitory role of *TOC1* on *CBF3* transcription is discussed, as this explains why a *toc1-101* mutant (which lacks the inhibitory effect on *CBF3* transcription) would have increased freezing tolerance.

Loss of *GI* function does not adversely affect freezing tolerance in *Arabidopsis* in this study

Plants with the *gi-201* null mutation had significantly increased survival rates when grown at 17°C and frozen at -5°C, but not when grown at the other two temperatures (t-test, $P < 0.05$; **Table 4.3**). *GI* has been shown to be important for temperature compensation with regards to maintaining rhythmicity of the circadian clock as temperatures diverge from 17°C down to 12°C or up to 27°C (Gould et al., 2006). The effect of *gi* mutations to the regulation of the circadian clock alters at different temperatures, with altered *CCA1* and *TOC1* expression compared to wild-type plants when temperatures start to either decrease or increase away from 17°C. We see the opposite effect here in regards to freezing tolerance, with no difference seen compared

to wild type plants when grown at either 12°C or 22°C, but a significant increase in survival rates when grown at 17°C and frozen at -5°C, and in the plants frozen at -3°C there is no significant difference in survival rates between the *gi* mutant plants and the wild-type plants. As *CCA1* expression levels are lower in *gi* mutant plants grown at 12°C compared to wild-type plants (Gould et al., 2006) and *CCA1* has been shown to be a positive regulator of the cold response *CBF* genes (Dong et al., 2011), one may have predicted that there would be a decrease in freezing tolerance due to a decrease in *CBF* induction; however, this is not observed, indicating that other factors are involved in compensating for the loss of *gi* function. However, this result would add further credence to the hypothesis suggested by the *toc1-101* results discussed above that *TOC1* acts to inhibit *CBF3* expression. There is decreased *TOC1* in *gi* mutant plants grown at 12°C (Gould et al., 2006), which would result in a decrease in *CBF3* inhibition which may be what is counterbalancing the effects of increased *CCA1* expression. A previous study reports a decrease in plant freezing tolerance in *gi-3* mutant *Arabidopsis* plants that was not replicable in this study (Cao et al., 2005). Whilst plants grown at 22°C and frozen at -3°C had decreased survival rates compared to wild-type plants, this decrease in survival was not significant and all other data collected in this study showed the same levels of survival or greater than wild-type plants. The younger seedlings used in the Cao *et. al.* (2005) study and the differences in experimental techniques as well as the different *gi* mutant plants used here may go some way to explain the differences observed between this study and the results published in the literature.

4.4.2 *CBF1* expression can be altered by long term exposure to different temperatures

This study has shown that the circadian clock is involved in the freezing tolerance of plants grown at different ambient temperatures, and based on knowledge from the literature this is likely through the regulation of the cold acclimation pathway genes, the *CBFs*.

The *CBFs* had been shown to have their expression levels altered by short term cold treatment (Fowler et al., 2005) but the effects of long term exposure to different temperatures on *CBF* expression in have not been studied. Here, we show that longer term exposure to different, non-chilling, temperatures results in altered *CBF1*

expression in *Arabidopsis* (**Figure 4.5**). Plants grown at different temperatures have different peak expression levels of the central clock genes (Gould et al., 2006). If the clock is indeed involved in regulating the expression levels of the *CBFs* then the change in the expression level of the core clock genes at the different temperatures studied in the literature (Gould et al., 2006) are likely to be a cause of the change in the *CBF1* expression levels that is seen in this data.

When grown at 27°C the levels of *LHY* expression decreases compared to that of plants that are grown at 17°C (Gould et al., 2006). A corresponding decrease in *CBF1* mRNA expression is also seen in *Arabidopsis* plants that are grown at 27°C compared to plants that are grown at 17°C as one may expect as *LHY* and *CCA1* are important in promoting *CBF* expression (Dong et al., 2011). The opposite is seen in *TOC1* and *GI* mRNA expression levels when comparing plants grown at 27°C to those grown at 17°C where *TOC1* and *GI* mRNA expression levels increase (Gould et al., 2006). The decrease observed in *CBF1* expression can, therefore, be attributed to the decreased induction of *CBF1* by *LHY/CCA1* as well as a the possibility that *CBF1* expression is inhibited by *TOC1* in a similar manner to that of *CBF3* as shown in this study.

As temperatures decreased from 17°C to 12°C *LHY* and *CCA1* amplitude and peak expression increases (Gould et al., 2006). The levels of *CBF1*, however, decrease in plants grown at 12°C compared to plants that are grown at 17°C (**Figure 4.5**). A decrease in *CBF1* expression is not what one may expect when there is an increase of *LHY/CCA1* which promote *CBF* expression, however, if *TOC1* acts as an inhibitor of *CBF1* in the same way as it does *CBF3*, as shown in this study, then the increase in *TOC1* may explain the decrease in *CBF1* levels in plants grown at 12°C rather than 17°C. Recent evidence, however, suggests that *TOC1* may not act as an inhibitor of *CBF1* expression as a recent study has shown that unlike *CBF3* and *CBF2*, *toc1-101* loss-of-function mutants do not have significantly increased levels of *CBF1* mRNA unlike *CBF2* and *CBF3* (Keily et al., 2013). *Arabidopsis* acclimates rapidly to cold temperatures with enhanced freezing tolerance being observed within a day of cold exposure (Gilmour et al., 1988; Kurkela et al., 1988). One could hypothesise, therefore, that the plants that are grown at the lower temperatures are already more cold acclimated than those plants that are grown at warmer temperatures, and therefore the need for *CBFs* to adapt to sudden cold periods is reduced.

4.4.3 Chapter 4 summary

To increase understanding of the clock's role in regulating freezing tolerance in *Arabidopsis thaliana*, plants with clock mutants were frozen at different temperatures to ascertain any phenotypic differences in survival rates compared to wild-type plants. First, though, the test conditions were established. Freezing wild-type plants at -3°C resulted in only small levels of mortality with 84.8% of wild-type plants surviving. Therefore, freezing at -3°C was decided upon as a good test temperature to look for mutant plants with increased sensitivity to freezing. Freezing wild-type plants at -5°C resulted in large levels of mortality with only 5.7% of plants surviving, thus establishing -5°C as a good test temperature to ascertain mutants with decreased sensitivity to freezing conditions. Growing plants at 12°C , 17°C , or 22°C would also allow for the role of clock genes in regulating temperature signalling at different ambient temperatures to be further investigated.

Survival rates of clock mutant plants when exposed to -3°C showed no difference to wild-type plants when grown at 17°C . When moving away from 17°C growth conditions to 12°C or 22°C significantly decreased survival rates were observed in *lux-5* and *elf3-1* mutants. The *lhy-20* plants showed a significant decrease in freezing tolerance when grown at 22°C and frozen at -3°C as one would expect if LHY was to act as a promoter of *CBF* expression as has been reported (Dong et al., 2011). The *prp7-3* mutant plants showed significant decreases in survival rate compared to wild-type plants when grown at 22°C and frozen at -3°C , which is surprising given the increase in freezing tolerance seen when *prp7-3* was frozen at -5°C . The remaining plants tested showed no difference to wild-type survival.

When frozen at -5°C several clock mutant plants lines showed significantly increased freezing survival phenotypes compared to wild-type plants. The *prp* single, double and triple mutants all showed significantly increased survival rates in at least two growth temperatures, with most showing increased survival at all three growth temperatures showing that the reported *prp* triple mutant decreased sensitivity to freezing temperatures phenotype (Nakamichi et al., 2009) can be replicated in the individual *prp* mutants. *lux-5* and *lhy-20* were the only mutant lines tested to not have any significantly altered survival rates at any of the growth temperatures when frozen at -5°C . The freezing tolerance assays identified *TOC1* as an important gene for regulating freezing tolerance in *Arabidopsis*. *toc1-101* showed consistently significantly

4 Results: Connecting the circadian clock to the cold acclimation pathway

increased survival rates compared to wild-type plants when frozen at -5°C .

Here it is shown that the ambient growth temperature that *Arabidopsis* is grown at affects non-stress induced *CBF1* expression levels; *CBF1* mRNA decreasing in amplitude and peak expression as ambient temperatures increased or decreased away from 17°C .

5 Results: Modelling the circadian clock regulation of *CBF3* expression

In chapter 4 possible regulatory mechanisms for clock regulated control of freezing tolerance were investigated with new circadian components, such as the Evening Complex, being implicated as possible regulators of the cold acclimation pathway. One of the core objectives of this thesis is to create a model of this circadian regulation of the cold response pathway and in Chapter 5 the creation and testing of said model is discussed.

A model of the circadian clock is required, onto which regulation of the cold signalling pathway can be incorporated. Fortunately several mathematical models of the circadian clock have been developed over the last 10 years (Locke et al., 2005b; Locke et al., 2005a; Gould et al., 2006; Zeilinger et al., 2006) which means that a model of the circadian clock does not need to be created from new as an existing model can be used. At the start of the modelling process, the newest and most detailed model of circadian regulation available for use was the Pokhilko 2010 (hereafter referred to as P2010) model (Pokhilko et al., 2010) which built on previous Locke models (Locke et al., 2005b; Locke et al., 2005a; Locke et al., 2006). As this was the most recent model that had been published, as well as the most advanced published model, it was decided that this would act as the circadian clock model onto which regulation of the cold signalling pathway would be added. As well as the circadian components of the model, the clock needs to be connected to the cold signalling pathway. Rather than build a complete cold signalling pathway model, this study instead focused on connecting the circadian clock to one of the core cold signalling pathway components that is regulated by the clock, the *CBFs*. The *CBFs* are central to the cold acclimation pathway and, as has been previously mentioned their expression is circadian gated suggesting a direct link between the circadian clock and the cold acclimation pathway through these genes (Fowler et al., 2005). Therefore, it was decided that *CBF*

regulation by the circadian clock would be the focus of the modelling efforts in this study. There are several *CBF* genes that have varying roles in stress regulation, but core to the cold acclimation pathway are *CBF1*, *CBF2* and *CBF3* which are known to be responsible for regulating cold responsive (COR) genes, thus resulting in altered freezing tolerance in plants (Stockinger, 1997; Liu et al., 1998; Medina, 1999; Novillo et al., 2004). *CBF1*, *CBF2* and *CBF3* all have highly similar sequences (www.arabidopsis.org) and expression profiles as well as similar circadian gating of cold induction (Nakamichi et al., 2009; Kidokoro et al., 2009). *CBF2*, however, is thought to have a slightly different role than *CBF3* and *CBF1* in that it is a negative regulator of *CBF1* and *CBF3* expression (Novillo et al., 2004). *CBF3* also has the most robust expression under ambient conditions (Mockler et al., 2007). Because of the above, and because of prior success in the Penfield and Halliday laboratories with *CBF3* primers, it was decided to focus experiments and modelling on the *CBF3* gene, rather than try to model all three *CBFs* separately.

5.1 Model construction and selection

5.1.1 Model construction

The P2010 and P2012 circadian clock models that are to act as the base onto which *CBF3* mRNA regulation by the clock will be incorporated is based on a series of differential equations (Pokhilko et al., 2010; Pokhilko et al., 2012). As such the models created here consist of ordinary differential equations (ODEs), using Michaelis-Menten kinetics to describe the enzymatic control of *CBF3* mRNA expression over time. The potential models of *CBF3* mRNA regulation by clock proteins will therefore have the following basic equation structure [1] where *CBF3* mRNA levels are dependent on transcription of *CBF3* mRNA being up-regulated and/or down-regulated by circadian clock proteins, and the degradation of *CBF3* mRNA.

$$\frac{dc_{CBF3}^m}{dt} = n_{CBF3} \left(\frac{gC1^{aC}}{gC1^{aC} + cA^{aC}} \right) \left(\frac{cB^{bC}}{gC2^{bC} + cB^{bC}} \right) - m_{CBF3} c_{CBF3}^m \quad [1.1]$$

Wherein n_{CBF3} is the transcription rate constant for *CBF3* mRNA synthesis and m_{CBF3} is the rate constant for *CBF3* mRNA degradation. $\frac{dc_{CBF3}^m}{dt}$ is the concentration of *CBF3* mRNA. $gC1$ and $gC2$ are Michaelis-Menten constants and aC and bC are Hill coefficients. cA is the concentration of inhibitory protein “A” and cB is the

concentration of promoter protein “B”.

CellDesigner version 4.1 (<http://www.celldesigner.org/>) was used to create the different model codes. CellDesigner was used, as it is a simple way for people with a non-programming background to create and edit existing mathematical models and was used here to create all the pre-optimised models.

***CBF3* experimental data sets used for model optimisation and model validation**

The biological data for *CBF3* expression was obtained from the DIURNAL website (diurnal.cgrb.oregonstate.edu (Mockler et al., 2007)) which stores microarray data for diurnal and circadian gene expression data from several array experiments (Mockler et al., 2007). Data for *CBF3* expression in 8L:16D, 12L:12D, 16L:8D and 24L:0D day length conditions were available from the DIURNAL database. *CBF3* mRNA shows a peak 8 hours after dawn in this dataset, and low and invariant expression at other time-points. This background expression was not significantly different to zero and was thus the lowest expression value for *CBF3* expression in each time-series was assumed to be zero and other data-points normalised to 1 accordingly (**Figure 5.1**).

5.1.2 Model optimisation

Once the model files had been created, the new parameters had to be optimised against known data so that they best match the known oscillation of *CBF3* mRNA.

The models were optimised using SBSIVisual version 1.4.5, optimising the simulated models to the 12L:12D diurnal cycles data obtained from the DIURNAL database using a parallel genetic algorithm (PGA) in SBSIVisual. Model equations were solved and simulated using the differential equation solver CVODES (Hindmarsh et al., 2005; Serban and Hindmarsh, 2005).

Model optimisation is computer resource intensive and therefore can take time, even when using the SBSI computer servers at the University of Edinburgh, to optimise the models. Calculating the AICc, however, is not computer resource intensive and results are obtained as soon as the AICc is executed. Therefore, the optimisation process was kept as simple and streamlined as possible to reduce the time taken for the optimisation to occur, whereas this was not an issue for the AICc. Because *CBF3*

expression is extremely similar under all four of the available day length condition data available, only the 12L:12D data was used for the optimisation of each model so that models weren't optimising to several different data sets. As time was not an issue for the AICc calculations it was decided to run the AICc against all four of the different day length data sets available.

Parameter constraints

The models that were created in this thesis were either built on the Pokhilko 2010, or the Pokhilko 2012 *Arabidopsis* circadian clock model. None of the models that were created here had CBF3 feeding back into the circadian clock model and therefore the clock is un-altered by the inclusion of *CBF3* as an output; as such the parameter values for the Pokhilko 2010 and Pokhilko 2012 model ODEs were fixed at the published values and only the new *CBF3* parameters were optimised. Previous circadian clock models had constrained parameter values to a range of 0 - 10 nM or nM/hr (Locke et al., 2005b; Locke et al., 2006; Pokhilko et al., 2010); however, whilst optimising the procedure for this study it was found that increasing the range above 0 - 0.5 nM or nM/hr offered no benefit to model fitting. Combined with a decreased computational run-time, it was decided to constrain the parameter values of the new model components to 0 - 0.5 nM or nM/hr .

The newly created parameter values for the *CBF3* equations can be seen in **Appendix Table 1** for the Pokhilko 2010 models and **Appendix Table 2** for the Pokhilko 2012 model. SBSIVisual can be used to edit the model components and to simulate ordinary differential equations in order to quickly visualise the outputs of the different models using the differential equation solver CVODES (Serban and Hindmarsh, 2005).

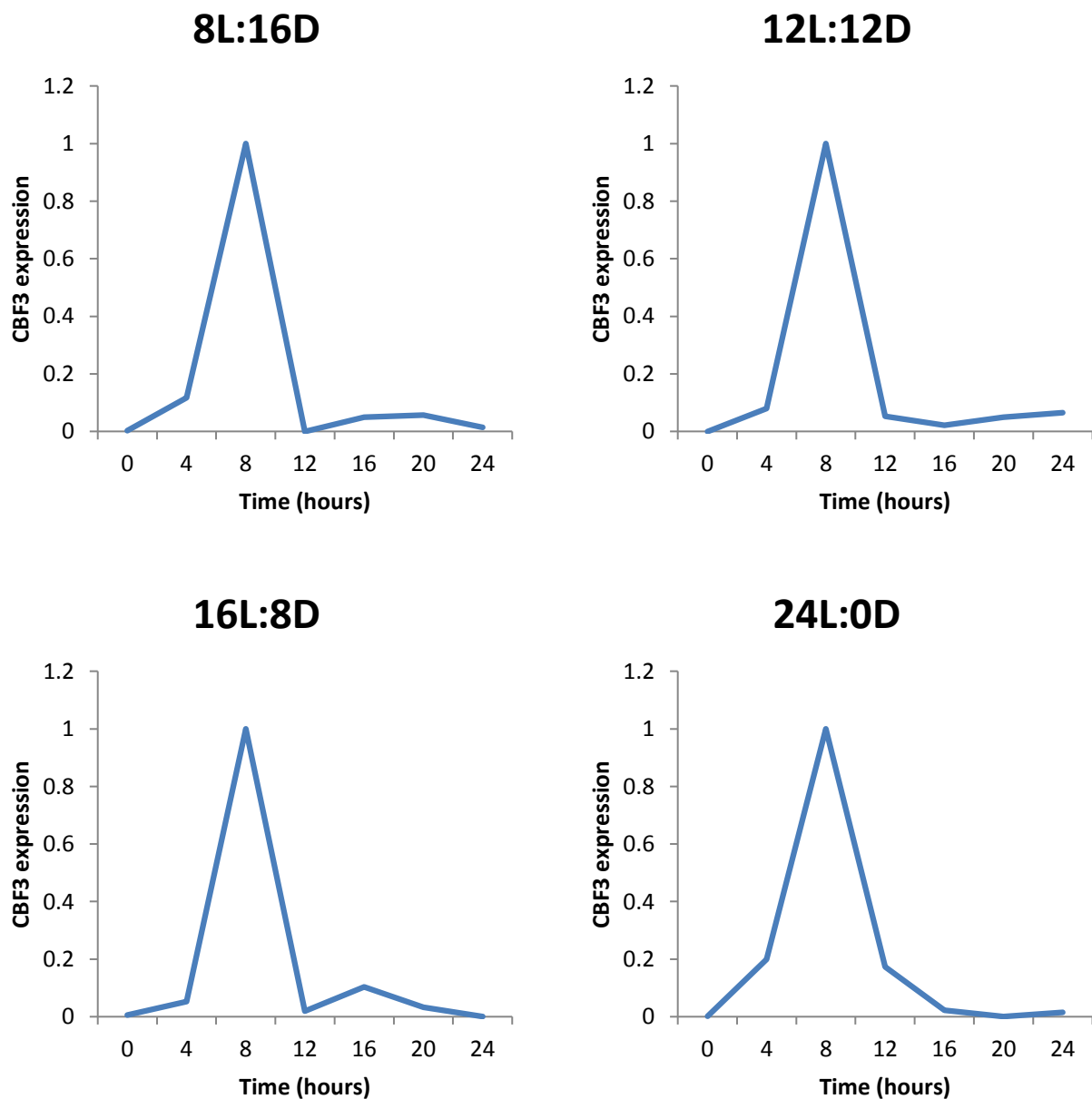


Figure 5.1: Microarray data obtained from the DIURNAL website (Mockler et al., 2007) showing *CBF3* expression in *Arabidopsis thaliana* grown under four different day length conditions: 8L:16D, 12L:12D, 16L:8D and 24L:0D. Peak expression has been normalised to a value of 1. Expression of *CBF3* remains low throughout the day, with a sharp peak in expression occurring 8 hours after dawn in all four of the different day length conditions at which data was collected.

5.1.3 Model selection

After creating the potential models and optimising the parameter values against the microarray data, the different models were then statistically assessed to determine which models were best able to fit their *CBF3* expression simulations to the biological data. The use of model selection techniques provides objective, numerical metrics against which to balance the priority of which model construction best fits the data. The common techniques used for model selection are AIC and BIC and whilst they have some similarities, such as a penalty term that punishes large numbers of parameters to reduce the likelihood of over-fitting (Akaike, 1974; Schwarz, 1978), there is a fundamental philosophical difference between the two different techniques that makes AIC the more favourable of the two. The AIC, unlike BIC, does not aim to find the “true” model (Burnham and Anderson, 2004) as here it is likely that none of the potential models will be the “true” model that contains all of the biological processes of *CBF3* regulation. It is the case that we want to compare the different potential models to each other and the biological data in order to find which of the potential models best fits the data, not which one of the models is the final, correct model. Because of this reason the BIC was ruled out as a potential statistical technique for model identification, and AIC was used instead.

A corrected version of the AIC (AICc) was used in which a better approximation of the Kullback-Leibler divergence is obtained (Hurvich and Tsai, 1989). The AICc ranks the different models in the order that they best fit the biological data. In this case the biological data sets used were the *CBF3* microarray expression data in four different day length conditions: 8L:16D, 12L:12D, 16L:8D and 24L:0D. The AICc are scored so that the lowest score has the best fit to the data sets. As multiple photoperiods are used to form the AICc, the summation of the different photoperiod scores are divided by the number of photoperiods, in this case 4, to give a single value. A Matlab package created and provided by Robert Smith of the Halliday laboratory at the University of Edinburgh was used to calculate the AICc score. The package also calculates the AICc weight for all of the models. Akaike Weights use the AICc scores to provide a probability measure for a model variant from the set of models (Burnham and Anderson, 2004). Thus, the higher the probability for a given model, the more likely it fits the data without over-fitting occurring.

5.2 The Pokhilko 2010 circadian clock model to regulate simulated *CBF3* expression

A number of potential models were simulated, testing possible connections between the circadian clock and the cold acclimation gene *CBF3*. By modelling the different interactions and simulating them mathematically, models that don't fit the biological data can be dismissed and the models that have the best fit to the biological data can be followed up on experimentally. As the modelling process was initiated the most up-to-date and detailed model of the *Arabidopsis* circadian clock was the P2010 model (Pokhilko et al., 2010). As such the P2010 model was used as the circadian component of the models created herein.

5.2.1 Several potential models of *CBF3* regulation by the circadian clock were created

Several different models were created based on prior knowledge from the literature and knowledge presented here. To model all of the possible interactions is unrealistic as there are too many possible combinations of interactions between the clock components of the P2010 model and *CBF3* regulation that could occur. The core components of the clock were therefore tested; *LHY/CCA1*, *TOC1*, *X*, *NI*, *PRR7* and *PRR9* with their roles of interaction explained below. There is data from the literature showing an increase in *CBF3* expression in the *prp5 prp7 prp9* triple mutant, suggesting an inhibitory role of the *PRRs* on *CBF3* expression resulting in the inhibition by the *PRRs* being simulated (Nakamichi et al., 2009). *LHY/CCA1* has been shown to directly bind the *CBF3* promoter and electrolyte leakage assays of *lhy cca1* double mutants show increased leakage as well as decreased *CBF3* mRNA expression in the *lhy cca1* double mutant strongly suggesting an up-regulatory role of *LHY/CCA1* on *CBF3* expression; hence *LHY CCA1* was modelled as an up-regulator of *CBF3* (Dong et al., 2011). As discussed in **Chapter 4**, *toc1* mutants have increased freezing survival suggesting that *TOC1* acts to inhibit *CBF* expression. Due to the increased freezing tolerance of *toc1* plants, *TOC1* was modelled as an inhibitor in several of the potential models. Similarly, there is data in the literature that suggests a role for *TOC1* as an inhibitor of *CBF* expression through regulation of *PIF7*, further reason for including this regulatory connection (Kidokoro et al., 2009). The following

models were created in CellDesigner and then optimised using SBSIVisual:

- TOC1 inhibition of *CBF3* expression (TOC1↓)
- TOC1 and TOC1mod inhibition of *CBF3* expression (TOC1↓:TOC1mod↓)
- LHY/CCA1 up-regulation of *CBF3* expression (LHY↑)
- TOC1 inhibition and LHY/CCA1 up-regulation of *CBF3* expression (TOC1↓:LHY↑)
- Night Inhibitor, PRR7 and PRR9 inhibition of *CBF3* expression (NI↓:PRR7↓:PRR9↓)
- Night Inhibitor, PRR7 and PRR9 inhibition of *CBF3* and LHY/CCA1 up-regulation of *CBF3* expression (NI↓:PRR7↓:PRR9↓:LHY↑)
- Night Inhibitor inhibition of *CBF3* expression (NI↓)
- PRR7 inhibition of *CBF3* expression (PRR7↓)
- PRR9 inhibition of *CBF3* expression (PRR9↓)
- PRR7 and PRR9 inhibition of *CBF3* expression (PRR7↓:PRR9↓)
- Night Inhibitor and PRR9 inhibition of *CBF3* expression (NI↓:PRR9↓)

The ODEs for the above models are found in **Table 5.1**.

In this study the only models created were those representing multiplicative interactions (AND gates) between the gene inputs to regulate *CBF3* expression. This decision was carried out as the total possible combinations for creating different models of *CBF3* regulation by different components of the clock was already so vast that to then test each model as both AND gates or OR gates would be too time consuming. As such the models were created assuming that all the different regulatory components of the newly created models of *CBF3* regulation are necessary for *CBF3* regulation to occur, rather than testing whether the individual components are sufficient on their own to impart regulation.

Table 5.1: Model equations for the regulation of *CBF3* by the circadian clock, wherein c_{CBF3}^m is the concentration of *CBF3* mRNA; the parameter values n_{c1} and m_{c1} represent the rate constants for transcription and degradation respectively; $gC1 \dots gC4$ are Michaelis-Menten constants and $aC \dots dC$ are Hill coefficients. cT is the concentration of TOC1 protein, cL the concentration of LHY protein, $cP7$ the concentration of PRR7 protein, $cP9$ the concentration of PRR9 protein and cMI the concentration of NI protein.

Link to CBF3	ODE of interaction
TOC1↓	$\frac{dc_{CBF3}^m}{dt} = n_{c1} * \frac{gC1^{aC}}{gC1^{aC} + cT^{aC}} - m_{c1} c_{CBF3}^m$
TOC1↓:TOC1mod↓	$\frac{dc_{CBF3}^m}{dt} = n_{c1} * \frac{gC1^{aC}}{gC1^{aC} + cT^{aC}} * \frac{gC2^{bc}}{gC2^{bc} + cT^{bc}} - m_{c1} c_{CBF3}^m$
LHY↑	$\frac{dc_{CBF3}^m}{dt} = n_{c1} * \frac{cL^{aC}}{gC1^{aC} + cL^{aC}} - m_{c1} c_{CBF3}^m$
TOC1↓:LHY↑	$\frac{dc_{CBF3}^m}{dt} = n_{c1} * \frac{gC1^{aC}}{gC1^{aC} + cT^{aC}} * \frac{cL^{bc}}{gC2^{bc} + cL^{bc}} - m_{c1} c_{CBF3}^m$
NI↓:PRR7↓:PRR9↓	$\frac{dc_{CBF3}^m}{dt} = n_{c1} * \frac{gC1^{aC}}{gC1^{aC} + cP7^{aC}} * \frac{gC2^{bc}}{gC2^{bc} + cP9^{bc}} * \frac{gC3^{eC}}{gC3^{eC} + cNI^{eC}} - m_{c1} c_{CBF3}^m$
NI↓:PRR7↓:PRR9↓:LHY↑	$\frac{dc_{CBF3}^m}{dt} = n_{c1} * \frac{gC1^{aC}}{gC1^{aC} + cP7^{aC}} * \frac{gC2^{bc}}{gC2^{bc} + cP9^{bc}} * \frac{gC3^{eC}}{gC3^{eC} + cNI^{eC}} * \frac{cL^{dC}}{gC4^{dC} + cL^{dC}} - m_{c1} c_{CBF3}^m$
NI↓	$\frac{dc_{CBF3}^m}{dt} = n_{c1} * \frac{gC1^{aC}}{gC1^{aC} + cNI^{aC}} - m_{c1} c_{CBF3}^m$
PRR7↓	$\frac{dc_{CBF3}^m}{dt} = n_{c1} * \frac{gC1^{aC}}{gC1^{aC} + cP7^{aC}} - m_{c1} c_{CBF3}^m$
PRR9↓	$\frac{dc_{CBF3}^m}{dt} = n_{c1} * \frac{gC1^{aC}}{gC1^{aC} + cP9^{aC}} - m_{c1} c_{CBF3}^m$
PRR7↓:PRR9↓	$\frac{dc_{CBF3}^m}{dt} = n_{c1} * \frac{gC1^{aC}}{gC1^{aC} + cP7^{aC}} * \frac{gC2^{bc}}{gC2^{bc} + cP9^{bc}} - m_{c1} c_{CBF3}^m$
NI↓:PRR9↓	$\frac{dc_{CBF3}^m}{dt} = n_{c1} * \frac{gC1^{aC}}{gC1^{aC} + cNI^{aC}} * \frac{gC2^{bc}}{gC2^{bc} + cP9^{bc}} - m_{c1} c_{CBF3}^m$

Table 5.2: AICc scores for test models

Model	AICc	Weight
TOC1↓	-522.2	0.7282
TOC1↓:TOC1mod↓	-520.23	0.2718
TOC1↓:LHY↑	-472.34	0
LHY↑	-332.69	0
NI↓:PRR7↓:PRR9↓:LHY↑	-313.6	0
NI↓:PRR9↓	-276.95	0
NI↓:PRR7↓:PRR9↓	-270.85	0
NI↓	-153.7	0
PRR9↓	-150.28	0
PRR7↓	-149.88	0
PRR7↓:PRR9↓	-147	0

5.2.2 *CBF3* inhibition by TOC1 gives the best fit to biological data

To establish which of the newly created models best fits the biological data, statistical analysis of best fit was carried out in the form of AICc. The AICc here compared the simulation in four different day lengths, compared to the biological data from the Diurnal website under the same day length conditions, as seen in **Figure 5.1** in order to calculate which of the potential models best fits the biological data.

The AICc results of the different models can be seen in **Table 5.2**. TOC1 inhibition of *CBF3* expression had the best AICc score (-522.198), closely followed by the combination of TOC1 inhibition and modified TOC1 inhibition (-520.227), in third place was TOC1 inhibition combined with LHY up-regulation (-472.343) and in fourth place was LHY up-regulation on its own (-332.694). When the PRRs were incorporated into the models the scores became worse: NI↓:PRR7↓:PRR9↓:LHY↑ (-313.6); NI↓PRR9↓ (-276.95); NI↓:PRR7↓:PRR9↓ (-270.85); NI↓ (-153.7); PRR9↓ (-150.28); PRR7↓ (-149.88) and PRR7↓:PRR9↓ (-147). The good AICc scores for the models that contain TOC1 interaction implies that TOC1 regulation of *CBF3* is something that will need to be further investigated; however, the AICc does not show us how well the model matches the biological data, just which of the models tested has the best fit. The TOC1↓ model had a weight of 0.7282, strongly favouring this model (with an AICc score of -522.198) over the model with the second best AICc score (-520.277), the TOC1↓:TOC1mod↓ model with a weight of 0.2718.

5.2.3 Model simulations under different day length periods can be used to eliminate potential models

The different models that were created (**Table 5.1**) were optimised using SBSIVisual and ranked in order of best fit to the biological data (**Table 5.2**), however, whilst the AICc scores the models in order of best fit to the data, it does so only in comparison to the other models created. Therefore, the expression profiles of the different models need to be confirmed visually, so that one can confirm that the model of best fit does represent the biological expression of *CBF3* expression accurately. For a model to be selected it needs to be capable of replicating the known expression of *CBF3*. As such, the newly optimised models were simulated under the four different light conditions that were available from the DIURNAL database to compare simulated expression versus known expression: short days of only 8 hours light (8L:16D), normal days of 12 hours light (12L:12D), long days of 16 hours light (16L:8D) and constant light (24L:0D). The expression levels of the *CBF3* simulations were normalised to peaks of 1 to make them comparable to the microarray expression data (**Figure 5.2**). The wild type (biological) data for the four different light conditions shows the same period and expression pattern in all four of the different light regiments with a sharp peak 8 hours after dawn.

Only three of the models created were able to maintain the correct phase of *CBF3* expression in all of the light conditions as well as a sharp peak in expression, TOC1↓, TOC1↓:TOC1mod↓ and TOC1↓:LHY↑ (**Figure 5.2**). The three models that were able to replicate phase at 8 hours after dawn and sharp peaks were the same three models that had the best AICc scores (**Table 5.2**). The remaining models can be dismissed as potential models of *CBF3* regulation as they fail to match the biological data in several ways. LHY↑ regulation of *CBF3* had consistently early expression of *CBF3* (**Figure 5.2**). The models which had components of NI, PRR7 or PRR9 all had low amplitude, to the extent that PRR7↓:PRR9↓, PRR7↓, NI↓ and PRR9↓ barely oscillated in expression. The PRR7↓:PRR9↓:NI↓: LHY↑ and PRR9↓:NI↓ models had varying phases of expression in the different light conditions tested (**Figure 5.2**).

5 Results: Modelling the circadian clock regulation of *CBF3* expression

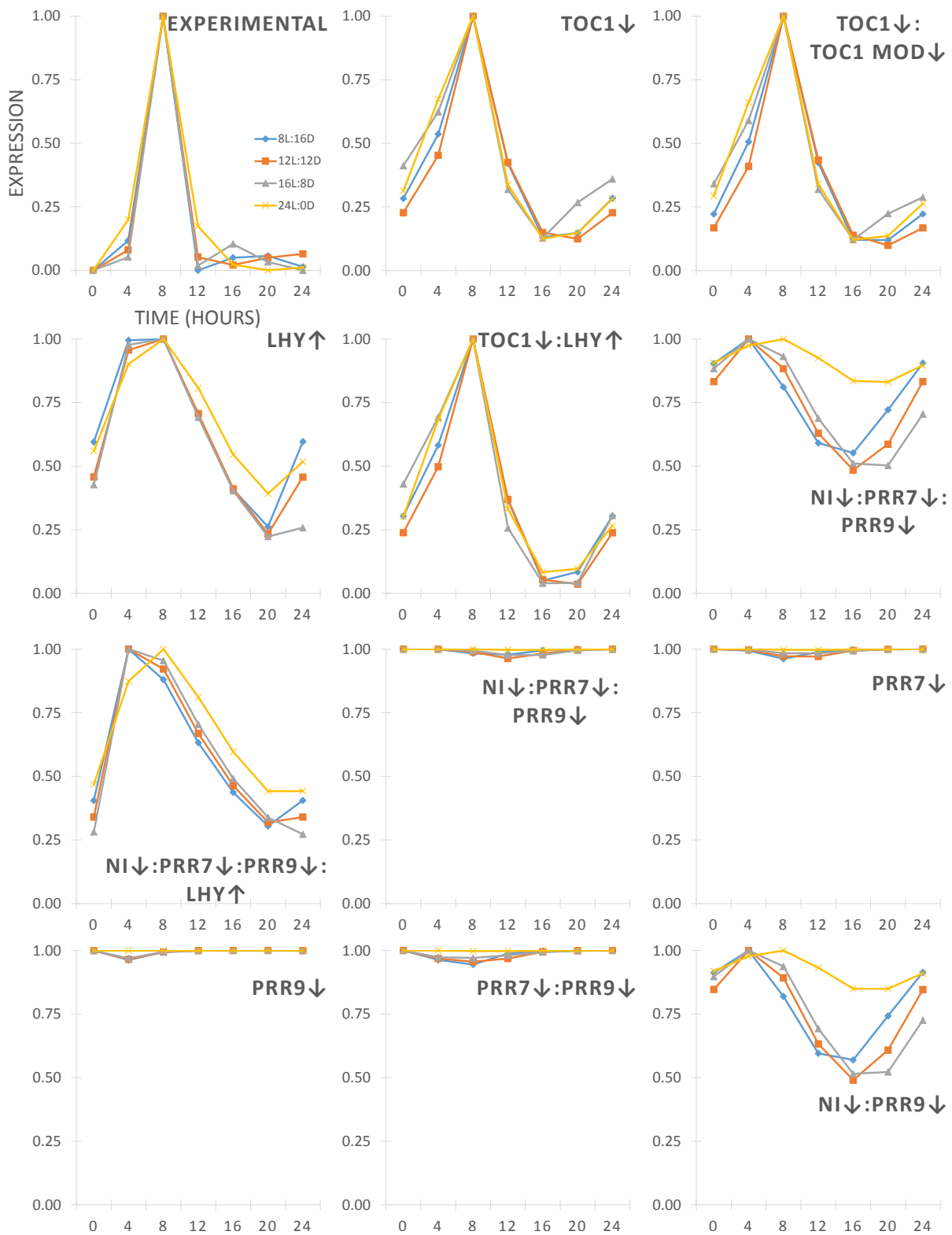


Figure 5.2: The different models built on the P2010 circadian clock model simulated under four different day length periods versus the biological data, 8L:16D (blue lines), 12L:12D (Orange lines), 16L:8D (grey lines) or 24L:0D (yellow lines).

5.2.4 The models can be made to simulate *CBF3* expression in circadian clock mutants

This study has shown how well the different models are capable of simulating *CBF3* expression in different day length conditions and thus eliminated all but the three models that had the best AICc scores as potential models of *CBF3* expression, however, the remaining models also need to be able to simulate *CBF3* expression in clock mutant plants that have been published in the literature as well.

We can mimic clock mutant plants in the model by decreasing the protein translation rates to zero for null mutants; this allows us to see how capable the models are of mimicking what occurs in *Arabidopsis* plants, which have the same mutations.

Investigating mutations to the model will also allow us to make predictions about how *CBF3* expression will be altered in mutant plants which have not yet been investigated.

In *lhy cca1* double mutants *CBF3* mRNA expression is severely reduced (Dong et al., 2011) and in the *prp5 prp7 prp9* triple mutant there is an increase in overall *CBF3* expression as well as a reduction in amplitude of oscillation (Nakamichi et al., 2009) as can be seen in **Figure 5.3A**.

In the three models of best fit (**Figure 5.3B**) all three models have a decrease in *CBF3* expression in the *lhy cca1* double mutant (**Figure 5.3C**). In the three top models there is also an increase in the levels of *CBF3* mRNA in *ni (prp5) prp7 prp9* triple mutant (**Figure 5.3C**). The *prp* triple mutant simulation has a delayed expression profile, with peak *CBF3* mRNA occurring at approximately 20 hours after dawn, rather than at the 6-12 hours that is seen in the literature suggesting that none of these models are fully capable of simulating what is occurring biologically and that there are still regulatory components of *CBF3* regulation missing from these models (Nakamichi et al., 2009).

5 Results: Modelling the circadian clock regulation of *CBF3* expression

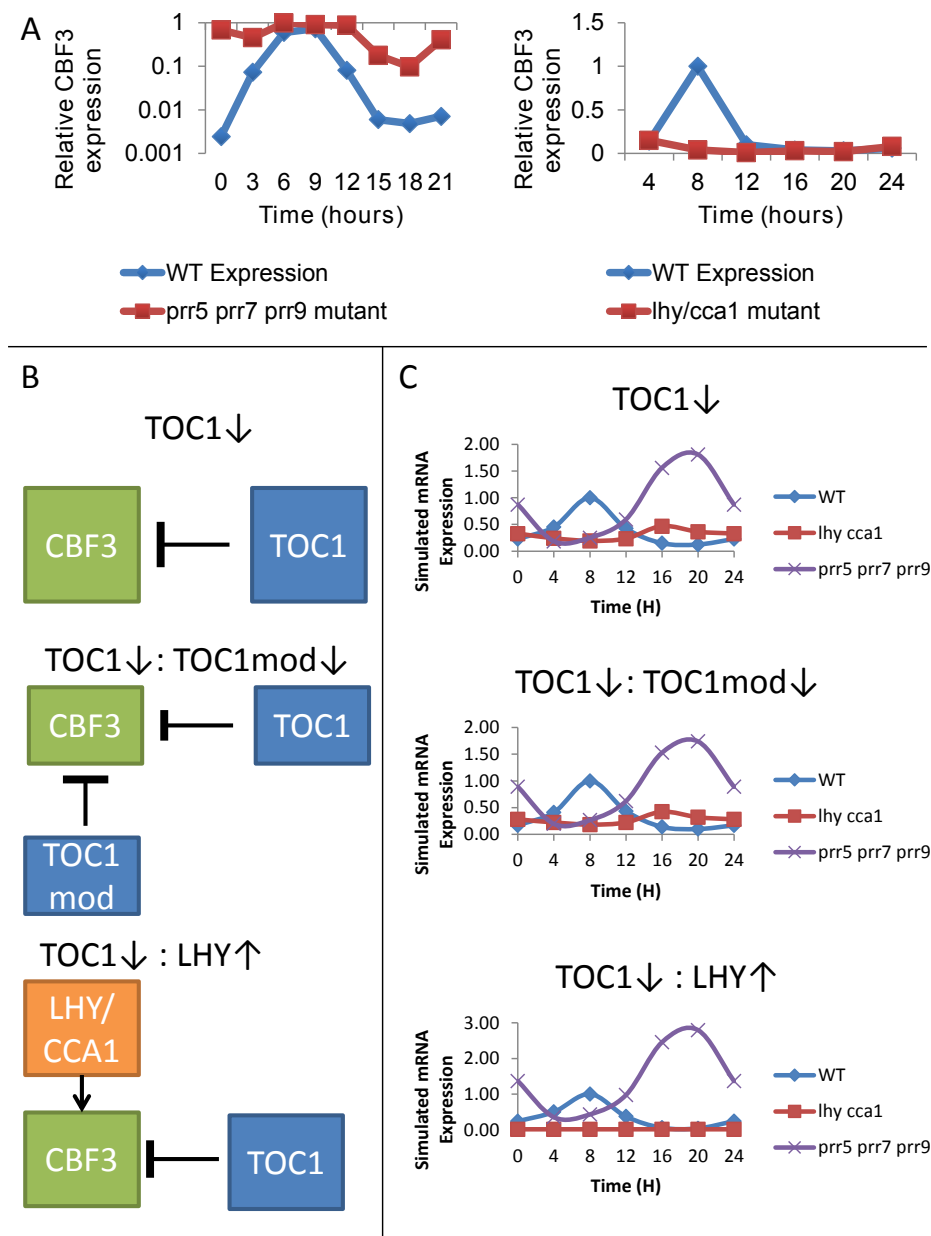


Figure 5.3: A) Relative expression of *CBF3* in *prp5 prp7 prp9* and *lhy/cca1* mutants as established experimentally: data from Nakamichi et al., 2009 and Dong et al., 2011. B) The top 3 models of best fit with *CBF3* regulatory mechanisms shown: arrows represent up-regulation and barred lines show down-regulation of *CBF3* expression. C) Mutant simulations of *CBF3* mRNA expression in *lhy cca1* double mutant (red lines) and *ni prp7 prp9* triple mutant (purple lines) in the three models with the best fit to the biological data with wild-type simulation in blue. The models were simulated for 24 hours at one hour intervals. Mutants were simulated by setting protein translation rates to zero for the relevant gene.

5.2.5 Predictions made by the models

The purpose of creating mathematical models of biological systems is so that biological predictions can be made *in silico*, which can be tested experimentally. *CBF3* expression in plants with a *toc1* mutation is currently unknown. The newly created models can be used to make predictions about how *CBF3* expression will alter in *toc1* plants compared to wild-type plants.

In the TOC1↓ and the TOC1↓:TOC1mod↓ models, when TOC1 translation is eliminated *CBF3* expression increases and flat lines at a higher level than the peak expression in the wild-type plants (**Figure 5.4**). In the LHY↑: TOC1↓ model the expression levels of *CBF3* increases and the phase of peak expression is earlier than in the wild-type plants (**Figure 5.4**). These predictions are tested and discussed in a later section.

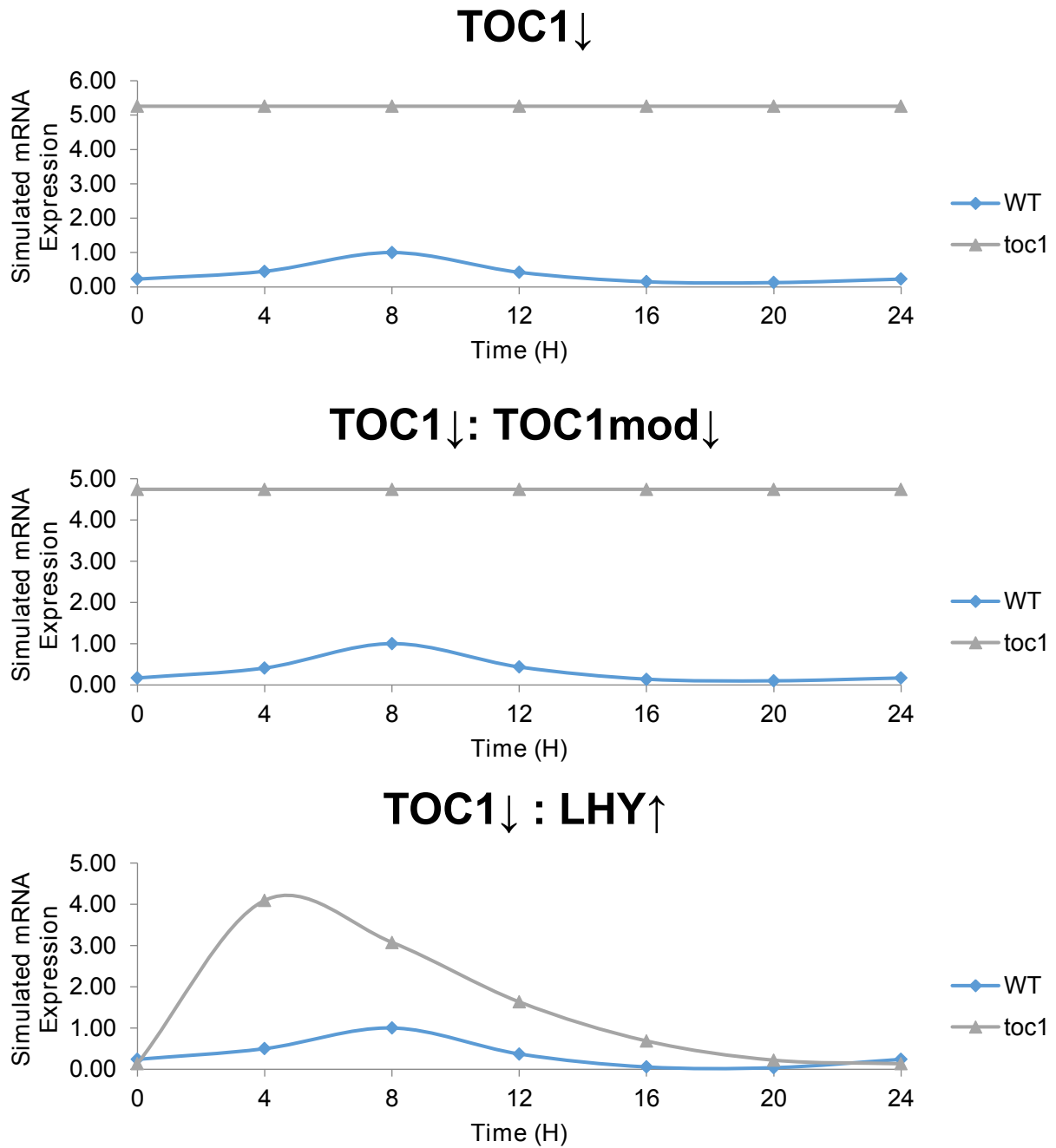


Figure 5.4: *toc1* and wild-type simulations of *CBF3* expression in the TOC1↓, TOC1↓:TOC1mod↓ and TOC1↓:LHY↑ models. *toc1* mutants were simulated by setting the transcription rate of *TOC1* to 0. Increased *CBF3* expression is observed in *toc1* mutant simulations compared to wild-type simulations in all three of the models; however, only the TOC1↓:LHY↑ model was able to maintain rhythmic *CBF3* expression. Grey lines represent *toc1* mutant simulations and the blue lines represent the wild-type simulations.

5.3 The Pokhilko 2012 circadian clock model to regulate simulated *CBF3* expression

In 2012 an updated version of the P2010 model was published which contained a number of important changes in how the circadian clock is regulated (Pokhilko et al., 2012). The Pokhilko 2012 model will hereafter be referred to as P2012. One of the biggest changes is the inclusion of the Evening Complex and its component proteins; ELF3, ELF4 and LUX (**Figure 5.5**). The Evening Complex genes replace Y in the new model based on a number of biological observations which has shown the Evening Complex to act as a repressor of *PRR9*, *TOC1* and the evening complex genes themselves (Helfer et al., 2011; Nusinow et al., 2011; Pokhilko et al., 2012). The new model publication also has a change in the way in which *TOC1* acts as a result of *TOC1-OX* and *toc1* mutant data which shows *TOC1* to have an inhibitory effect on *LHY CCA1* expression thus eliminating the need for the previous component *TOC1mod* (Pokhilko et al., 2012). The inclusion of *COP1* as a degrader of the EC through ELF3 degradation was also added into the latest model.

The large number of changes made to the Pokhilko model and the inclusion of new components such as the Evening Complex genes led to the decision to recreate the potential models in the newer P2012 model, as well as add new models to be tested, such as models that include the Evening Complex. The update to the model allowed for the creation of models that even better simulate *CBF3* expression than the models that were based on the P2010 model.

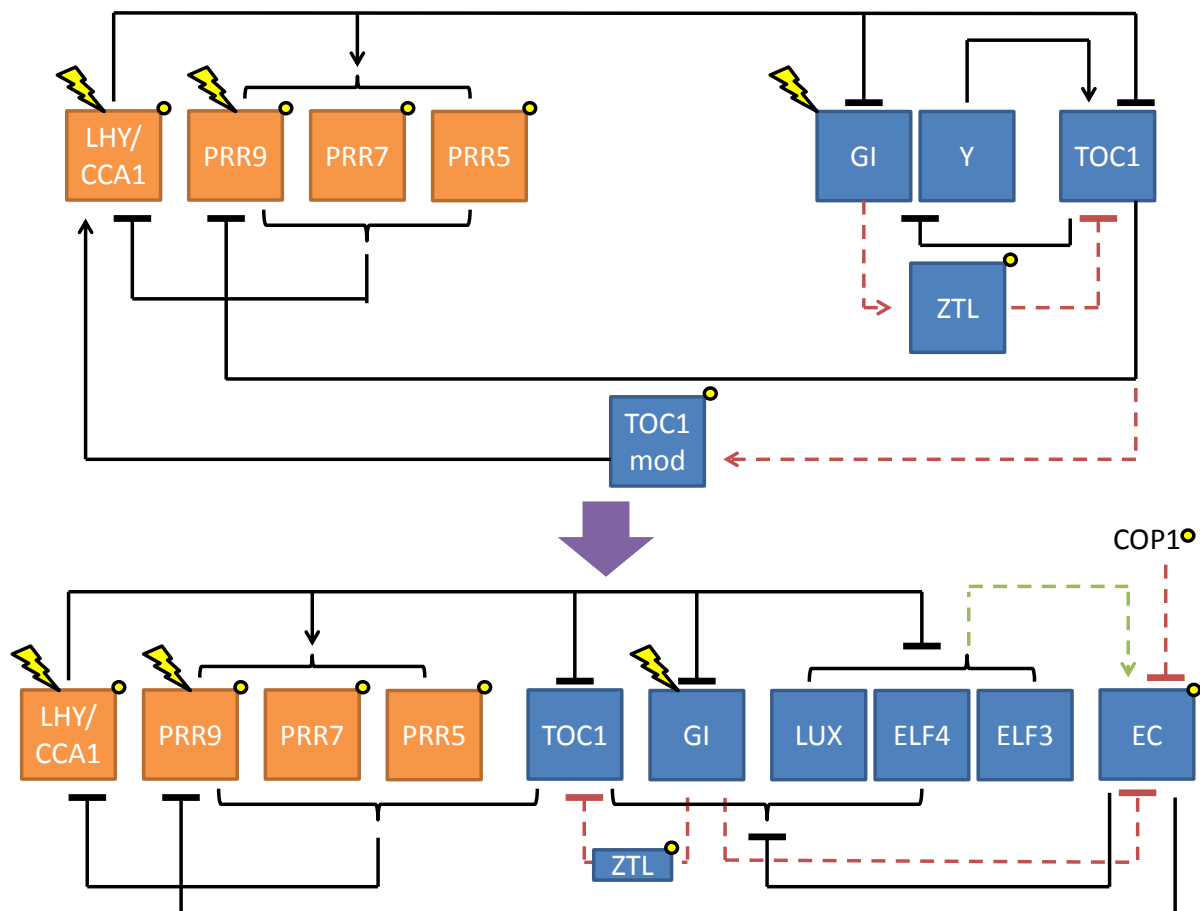


Figure 5.5: The 2010 and 2012 Pokhilko models, showing the differences between the two models. A) The Pokhilko 2010 model. Orange boxes represent the morning components and the blue boxes represent evening components. Transcriptional regulation is shown by solid lines. Flashes represent light responsive gene expression and yellow dots are post transcriptional regulation by light. B) The Pokhilko 2012 model. Orange boxes represent the morning components and the blue boxes represent evening components. Transcriptional regulation is shown by solid lines. Dashed green lines represents EC protein formation and red dashed lines represent regulation of TOC1 and EC by GI, ZTL and COP1. Flashes represent light responsive gene expression and yellow dots are post transcriptional regulation by light. Figures adapted from Pokhilko et al., 2010 and Pokhilko et al., 2012.

5.3.1 The potential models tested for *CBF3* regulation by the circadian clock

The P2012 circadian clock model no longer has some of the components that were in the P2010 model, such as TOC1mod. The newer model also has new additions to the model such as *LUX*, *ELF3* and *ELF4* which make up the Evening Complex. Results from Chapter 4 show that Evening Complex genes were required for wild-type freezing tolerance which makes them a possible candidate for a regulator of *CBF3* expression; as such Evening Complex regulation of *CBF3* expression was included in the new models.

- TOC1 inhibition of *CBF3* expression (TOC1↓)
- LHY/CCA1 up-regulation of *CBF3* expression (LHY↑)
- LHY/CCA1 up-regulation and TOC1 inhibition of *CBF3* expression (LHY↑:TOC1↓)
- Night Inhibitor, PRR7 and PRR9 inhibition of *CBF3* expression (NI↓:PRR7↓:PRR9↓)
- LHY up-regulation with Night Inhibitor, PRR7 and PRR9 inhibition of *CBF3* expression (LHY↑:NI↓:PRR7↓:PRR9↓)
- Night Inhibitor inhibition of *CBF3* expression (NI↓)
- PRR7 inhibition of *CBF3* expression (PRR7↓)
- PRR9 (inhibition of *CBF3* expression (PRR9↓)
- Evening Complex inhibition of *CBF3* expression (EC↓)
- Evening Complex up-regulation of *CBF3* expression (EC↑)
- Evening Complex and TOC1 inhibition and LHY/CCA1 up-regulation of *CBF3* expression (EC↓:TOC1↓:LHY↑)
- Evening Complex inhibition and LHY/CCA1 up-regulation of *CBF3* expression (EC↓:LHY)
- Evening Complex and TOC1 inhibition of *CBF3* expression (EC↓:TOC1↓)

- Evening Complex and LHY/CCA1 up-regulation and TOC1 inhibition of *CBF3* Expression (EC↑:TOC1↓:LHY↑)

The ODEs for the above models are found in **Table 5.3**.

As with the models created using the P2010 model, the new models of *CBF3* regulation using the P2012 circadian clock model were also built on an AND gate design as previously discussed in **Chapter 5.2.1**.

5.3.2 LHY up-regulation combined with TOC1 and EC inhibition of *CBF3* expression gives the best fit to biological data

Using the AICc package in Matlab as previously described, the AICc scores and weights were calculated for the new potential models (**Table 5.4**). The models with worst (highest) AICc scores were the models with single PRR regulation of the *CBF3* expression; PRR9↓ (-21.7049), PRR7↓ (-28.5526) and NI↓ (-29.9094). Of the models that were also previously created using the P2010 clock model and then re-created here using the P2012 model, the model with the best score was again the TOC1↓ model (-303.5916). Using the P2012 model, however, allowed for the creation of new models that were not previously possible that include the Evening Complex. The new models with the Evening Complex included as an up-regulator of *CBF3* expression had higher (worse) scores than with the EC included as an inhibitor of Evening Complex regulation: EC↑ (-44.9620) versus EC↓ (-637.7598), and EC↑:TOC1↓:LHY↑ (-276.9612) versus EC↓:TOC1↓:LHY↑ (-737.3802). The EC↓:TOC1↓:LHY↑ model was also the model that had the best AICc score (-737.3802) as well as the best weight score of 1. In fact, of the models tested, those that contained the Evening Complex as an inhibitor of *CBF3* expression had better fits to the data than the models which did not include the Evening Complex as an inhibitor of *CBF3* expression (**Table 5.4**): EC↓ (-637), EC↓:LHY↑ (-668.9001), EC↓:TOC1↓ (-681.6348) and EC↓:TOC1↓:LHY↑ (-737.3800).

Table 5.3: ODEs of the different models of $CBF3$ regulation by the circadian clock, wherein c_CBF3^m is the concentration of $CBF3$ mRNA; the parameter values n_{C1} and m_{C1} represent the rate constants for transcription and degradation respectively; $gC1gC4$ are Michaelis-Menten constants and $aCdC$ are Hill coefficients. cT is the concentration of TOC1 protein, cL the concentration of LHY protein, $cP7$ the concentration of PRR7 protein, $cP9$ the concentration of PRR9 protein cNI the concentration of NI protein, and cEC the concentration of the Evening Complex.

Link to $CBF3$	ODE of interaction
TOC1↓	$\frac{dc_{CBF3}^m}{dt} = n_{c1} * \frac{gC1^{ac}}{gC1^{ac} + cT^{ac}} - m_{c1} c_{CBF3}^m$
LHY↑	$\frac{dc_{CBF3}^m}{dt} = n_{c1} * \frac{cL^{ac}}{gC1^{ac} + cL^{ac}} - m_{c1} c_{CBF3}^m$
TOC1↓:LHY↑	$\frac{dc_{CBF3}^m}{dt} = n_{c1} * \frac{gC1^{ac}}{gC1^{ac} + cL^{bc}} * \frac{cL^{bc}}{gC2^{bc} + cL^{bc}} - m_{c1} c_{CBF3}^m$
NI↓:PRR7↓:PRR9↓	$\frac{dc_{CBF3}^m}{dt} = n_{c1} * \frac{gC1^{ac}}{gC1^{ac} + cP7^{ac}} * \frac{gC3^{cc}}{gC2^{bc} + cP9^{bc}} * \frac{gC3^{cc}}{gC3^{cc} + cNI^{cc}} - m_{c1} c_{CBF3}^m$
NI↓:PRR7↓:PRR9↓:LHY↑	$\frac{dc_{CBF3}^m}{dt} = n_{c1} * \frac{gC1^{ac}}{gC1^{ac} + cP7^{ac}} * \frac{gC2^{bc}}{gC2^{bc} + cP9^{bc}} * \frac{cL^{ac}}{gC4^{dc} + cL^{dc}} - m_{c1} c_{CBF3}^m$
NI↓	$\frac{dc_{CBF3}^m}{dt} = n_{c1} * \frac{gC1^{ac}}{gC1^{ac} + cNI^{ac}} - m_{c1} c_{CBF3}^m$
PRR7↓	$\frac{dc_{CBF3}^m}{dt} = n_{c1} * \frac{gC1^{ac}}{gC1^{ac} + cP7^{ac}} - m_{c1} c_{CBF3}^m$
PRR9↓	$\frac{dc_{CBF3}^m}{dt} = n_{c1} * \frac{gC1^{ac}}{gC1^{ac} + cP9^{ac}} - m_{c1} c_{CBF3}^m$
EC↓	$\frac{dc_{CBF3}^m}{dt} = n_{c1} * \frac{gC1^{ac}}{gC1^{ac} + cEC^{ac}} - m_{c1} c_{CBF3}^m$
EC↑	$\frac{dc_{CBF3}^m}{dt} = n_{c1} * \frac{cEC^{ac}}{gC1^{ac} + cEC^{ac}} - m_{c1} c_{CBF3}^m$
EC↓:TOC1↓:LHY↑	$\frac{dc_{CBF3}^m}{dt} = n_{c1} * \frac{gC1^{ac}}{gC1^{ac} + cT^{ac}} * \frac{cL^{bc}}{gC2^{bc} + cL^{bc}} * \frac{cL^{cc}}{gC3^{bc} + cL^{bc}} - m_{c1} c_{CBF3}^m$
EC↓:LHY↑	$\frac{dc_{CBF3}^m}{dt} = n_{c1} * \frac{gC1^{ac}}{gC1^{ac} + cEC^{ac}} * \frac{cL^{bc}}{gC2^{bc} + cL^{bc}} - m_{c1} c_{CBF3}^m$
EC↓:TOC1↓	$\frac{dc_{CBF3}^m}{dt} = n_{c1} * \frac{gC1^{ac}}{gC1^{ac} + cT^{ac}} * \frac{gC2^{bc}}{gC2^{bc} + cT^{bc}} - m_{c1} c_{CBF3}^m$
EC↑:TOC1↓:LHY↑	$\frac{dc_{CBF3}^m}{dt} = n_{c1} * \frac{gC1^{ac}}{gC1^{ac} + cT^{ac}} * \frac{cL^{bc}}{gC2^{bc} + cEC^{bc}} * \frac{cL^{bc}}{gC3^{cc} + cL^{cc}} - m_{c1} c_{CBF3}^m$

Table 5.4: AICc results for latest models including the Evening Complex. The newest models which include the evening complex have a better score than the old models. The model with the best score and weight is the model that includes LHY/CCA1, TOC1 and the EC as regulators of *CBF3* expression.

Model	AICc	Weight
EC↓:TOC1↓:LHY↑	-737.4	1
EC↓:TOC1↓	-681.6	0
EC↓:LHY↑	-668.9	0
EC↓	-637.8	0
TOC1↓	-303.6	0
LHY↑:TOC1↓	-285.6	0
EC↑:TOC1↓:LHY↑	-277	0
LHY↑	-234.5	0
LHY↑:NI↓:PRR7↓:PRR9↓	-200.3	0
EC↑	-145	0
NI↓:PRR7↓:PRR9↓	-105.2	0
NI↓	-29.91	0
PRR7↓	-28.55	0
PRR9↓	-21.7	0

5.3.3 *CBF3* Expression profiles in the new models

The AICc was used to statistically assess which of the potential models had the best fit to the biological data, however, this does not say anything about how well the models actually match the data, just which of the selected models matched it best. Therefore the different models were graphed (**Figure 5.6**) comparing them to the biological data from the DIURNAL website, the four models of best fit to the data are shown separately in **Figure 5.7** for easier visualisation. The models were simulated under the four different light conditions that biological data was available for; short days (8L:16D), normal day length (12L:12D), long day (16L:8D) and constant light (24L:0D) (**Figure 5.6**). The models containing the Evening Complex components were the only models that had sharp peaks of expression in all of the light conditions.

Of the models which contained Evening Complex as a regulator of *CBF3* expression,

only the EC↓:TOC1↓:LHY↑ model had the correct phase of expression, peaking at 8 hours after dawn in all of the different light period conditions simulated (**Figure 5.6** and **Figure 5.7**). The remaining potential models containing the Evening Complex regulation of *CBF3* included either an early phase of expression in short days with a peak occurring four hours early (EC↑:TOC1↓:LHY↑), or in constant light had a four hour later phase of expression, peaking in simulated *CBF3* expression 12 hours after subjective dawn (EC↓:TOC1↓, EC↓:LHY↑, EC↓). The EC↑ model had a peak at 0/24 hours after dawn (**Figure 5.6**). Similar to the models that used the P2010 circadian clock model, PRR-regulated *CBF3* expression was again poor at replicating the biologically observed patterns of *CBF3* expression: the NI↓:PRR7↓:PRR9↓ model of *CBF3* regulation had peak in *CBF3* expression occurring 4 hours after dawn in all of the light conditions, a four hour early phase shift. The LHY↑:NI↓:PRR7↓:PRR9↓ model was capable of maintaining a robust oscillation of *CBF3* expression under various light conditions, but had early induction of *CBF3* expression resulting in a broad peak of expression (**Figure 5.6**). The remaining PRR regulated models had constitutively high expression, with low amplitude of oscillation. The TOC1↓ and TOC1↓:LHY↑ models, which were amongst the best of the P2010 models at simulating *CBF3* expression were again good, but had an early and broad peak expression in short day and 12L:12D conditions.

5 Results: Modelling the circadian clock regulation of *CBF3* expression

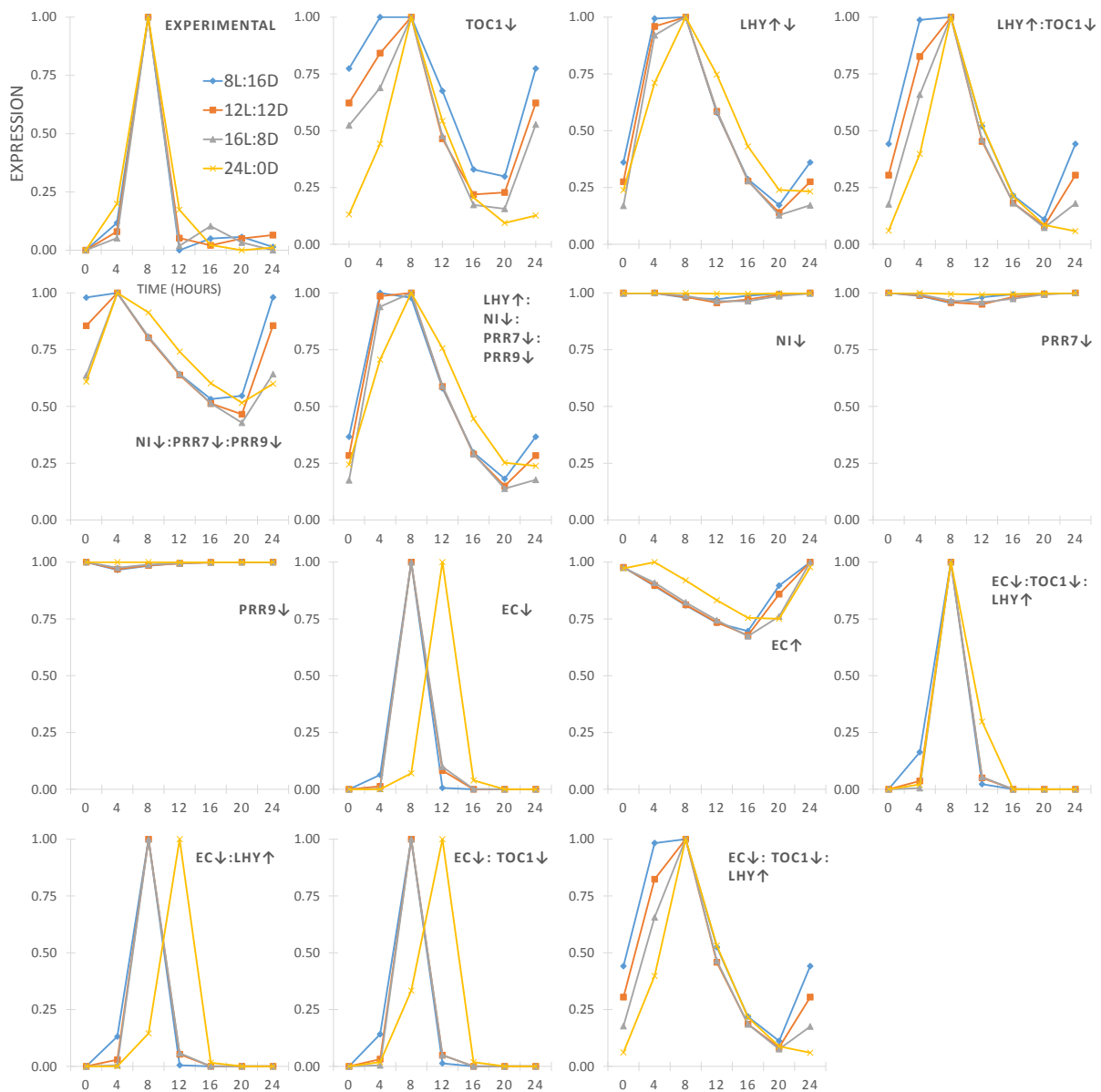


Figure 5.6: The different models built on the P2012 circadian clock model simulated under four different day length periods versus the biological data, 8L:16D (blue lines), 12L:12D (Orange lines), 16L:8D (grey lines) or 24L:0D (yellow lines)

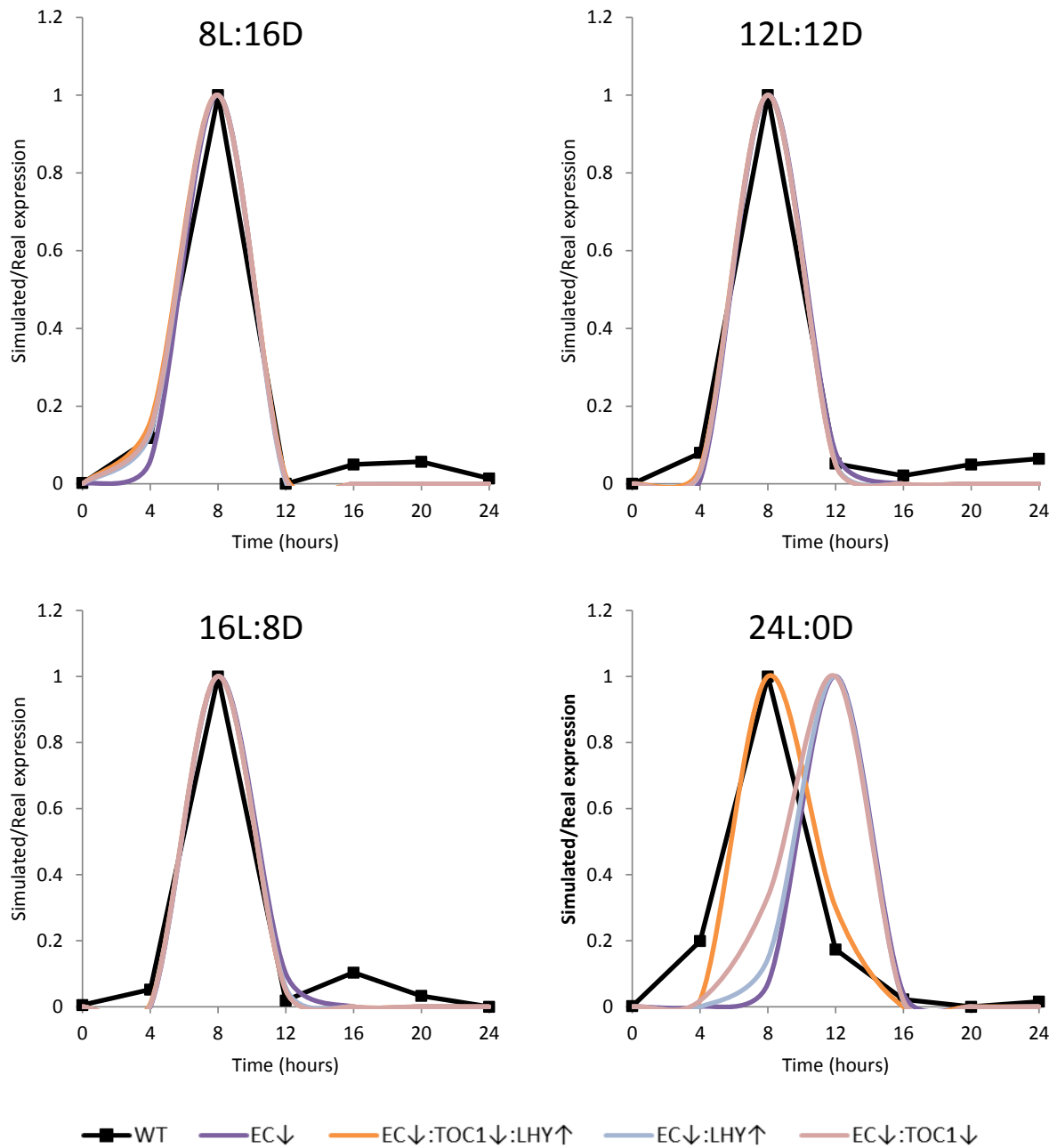


Figure 5.7: The four models of best fit built on the P2012 circadian clock model simulated under four different day length periods versus the biological data. short days (8L:16D), 12 hour light, 12 hours dark (12L:12D), long days (16L:8D) or constant light (24L:0D).

5.3.4 Day length alters peak *CBF3* expression in model simulations

In a recently published paper (Lee and Thomashow, 2012) it was shown that the period of light a plant is exposed to during the day in warm conditions has been shown to have an effect on expression levels of *CBF3* as well as the plant's ability to cope with freezing conditions. Lee and Thomashow show in their paper that in 8L:16D conditions the *CBF3* levels are three fold greater than in plants grown in 16L:8D conditions at the time of peak *CBF3* expression. Peak expression values were taken from all the potential models in short day and long day conditions and the values were normalised to an expression value of 1 for the short day simulations (**Figure 5.8**). In the models created here relative changes in *CBF3* expression levels in the models when comparing short days and long day peak expression values are shown in **Figure 5.8**. Of all the models that were tested, two had a decrease in expression in long day conditions when compared to short day conditions (NI↓:PRR7↓:PRR9↓ and EC↑). Three of the models had no change in peak expression (NI↓, PRR7↓ and PRR9↓) and the remaining models all showed increases in *CBF3* peak expression in long day conditions compared to short day conditions (**Figure 5.8**). The greatest increase observed was in the model with the best AICc score. EC↓:TOC1↓:LHY↑, which had a 1.44-fold increase in *CBF3* peak expression in short days compared to long days (**Figure 5.8**).

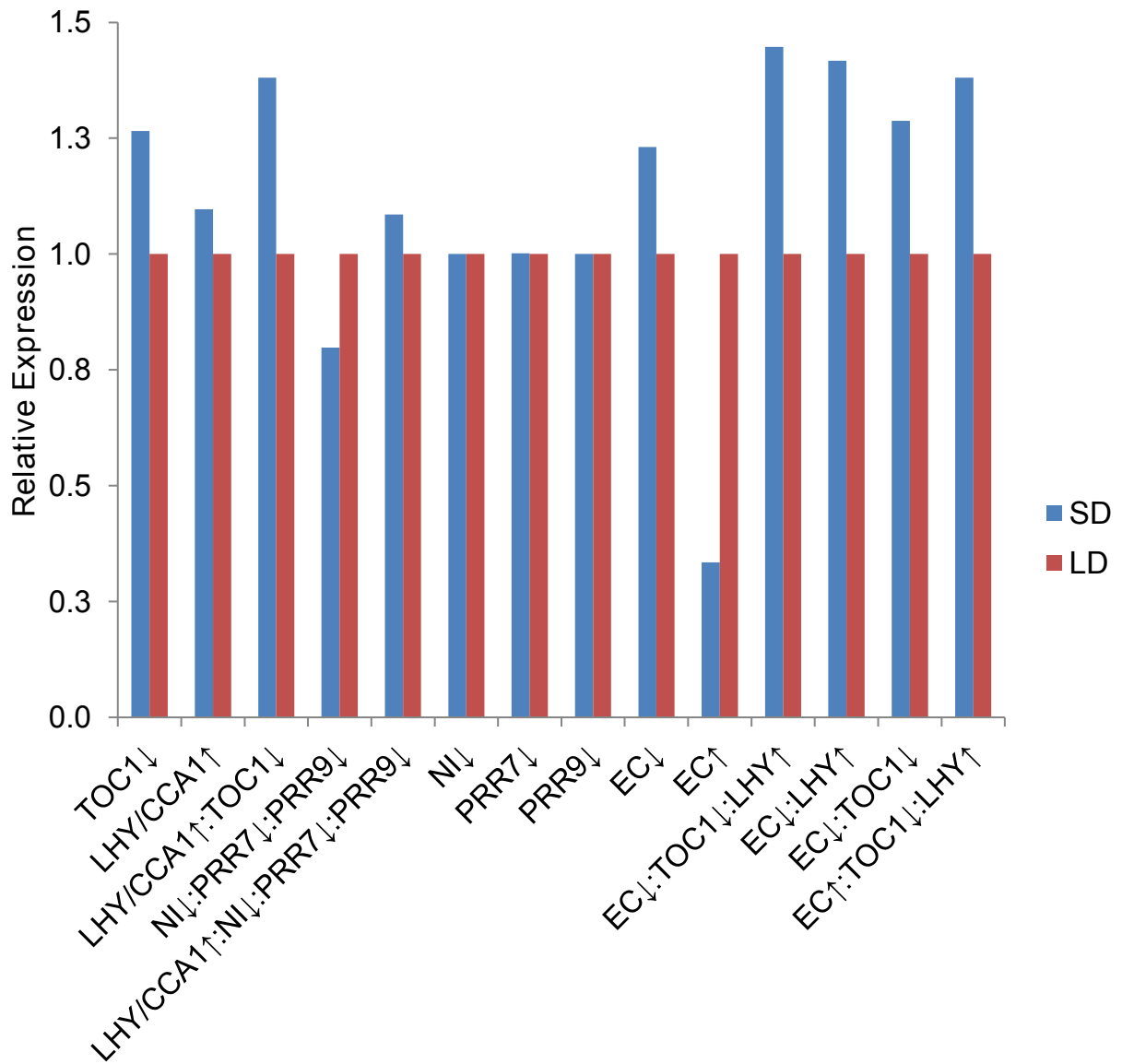


Figure 5.8: Change in expression levels in the different potential models. Peak *CBF3* expression levels were recorded from simulations running under short day (8L:16D) conditions, 8 hours of light, and long day (16L:8D) conditions, 16 hours of light.

5.3.5 How well do the models recreate known mutations from the literature?

Changes in *CBF3* expression in clock mutant plants have been reported previously in the literature (Nakamichi et al., 2009; Dong et al., 2011). For one model to be preferred over the others, it needs to be able to better replicate the changes in *CBF3* expression compared to the other models under as many different conditions as possible. Being able to replicate known clock mutant expression of *CBF3* will, therefore, add greater weight to the final selection of a preferable model of *CBF3* regulation by the circadian clock. The four models of best fit (**Figure 5.9**) were simulated in 12L:12D light conditions with *prp* triple mutant simulations and *lhy cca1* double mutant simulations.

As reported earlier *lhy cca1* double mutants have strongly reduced *CBF3* mRNA expression, whereas the *prp5 prp7 prp9* triple mutant has increased expression with a reduced amplitude and broader peak, shown in **Figure 5.10A** (Nakamichi et al., 2009). Whilst the EC↓:TOC1↓:LHY↑ was the best fit to the biological data, the top four models of best fit all had similar *CBF3* expression profiles in *lhy/cca1* and *ni (prp5) prp7 prp9* mutant simulations (**Figure 5.10B**). In *lhy/cca1* mutant simulations of the four models with the best fit to the biological data (**Figure 5.10B**), there is reduced *CBF3* expression in all model simulations. The P2012 model does not have a specifically defined *PRR5* component, instead stating that *PRR5* is likely a component of the NI (Pokhilko et al., 2010; Pokhilko et al., 2012) and as such simulating the triple mutant has to be best represented by a *ni prp7 prp9* mutant. The four models that had the best AICc scores had increased *CBF3* expression in *ni prp7 prp9* triple mutant simulations with EC↓ (108% increase), EC↓:TOC1↓:LHY↑ (254.9% increase), EC↓:LHY↑ (144% increase), EC↓:TOC1↓ (108% increase), qualitatively replicating the increase in *CBF3* expression seen biologically in *prp5 prp7 prp9* triple mutants (**Figure 5.10B**).

5 Results: Modelling the circadian clock regulation of *CBF3* expression

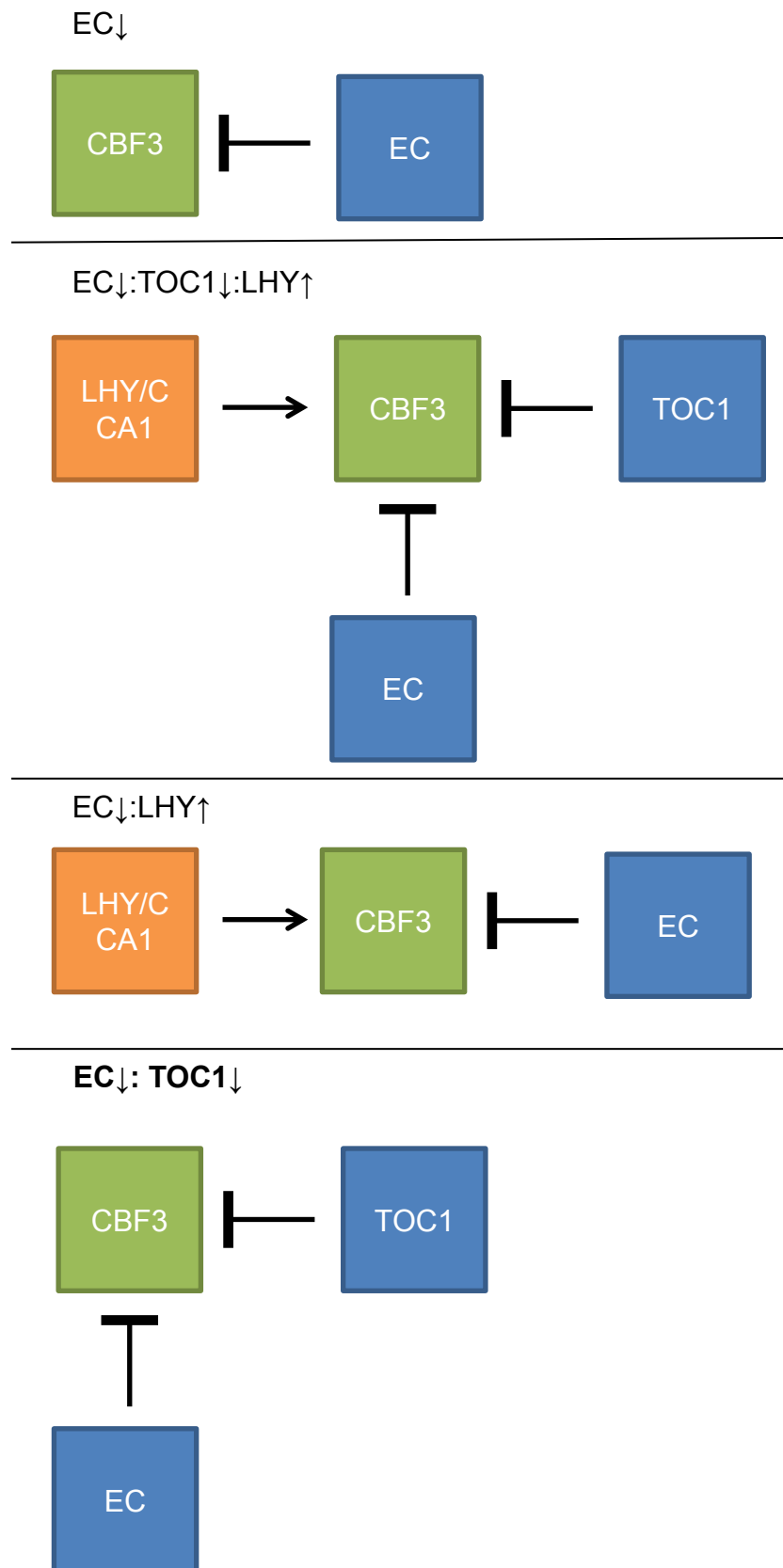


Figure 5.9: Mode of *CBF3* regulation in the top four models of best fit. Arrows represent up-regulation and barred lines show down-regulation of *CBF3* expression.

5 Results: Modelling the circadian clock regulation of *CBF3* expression

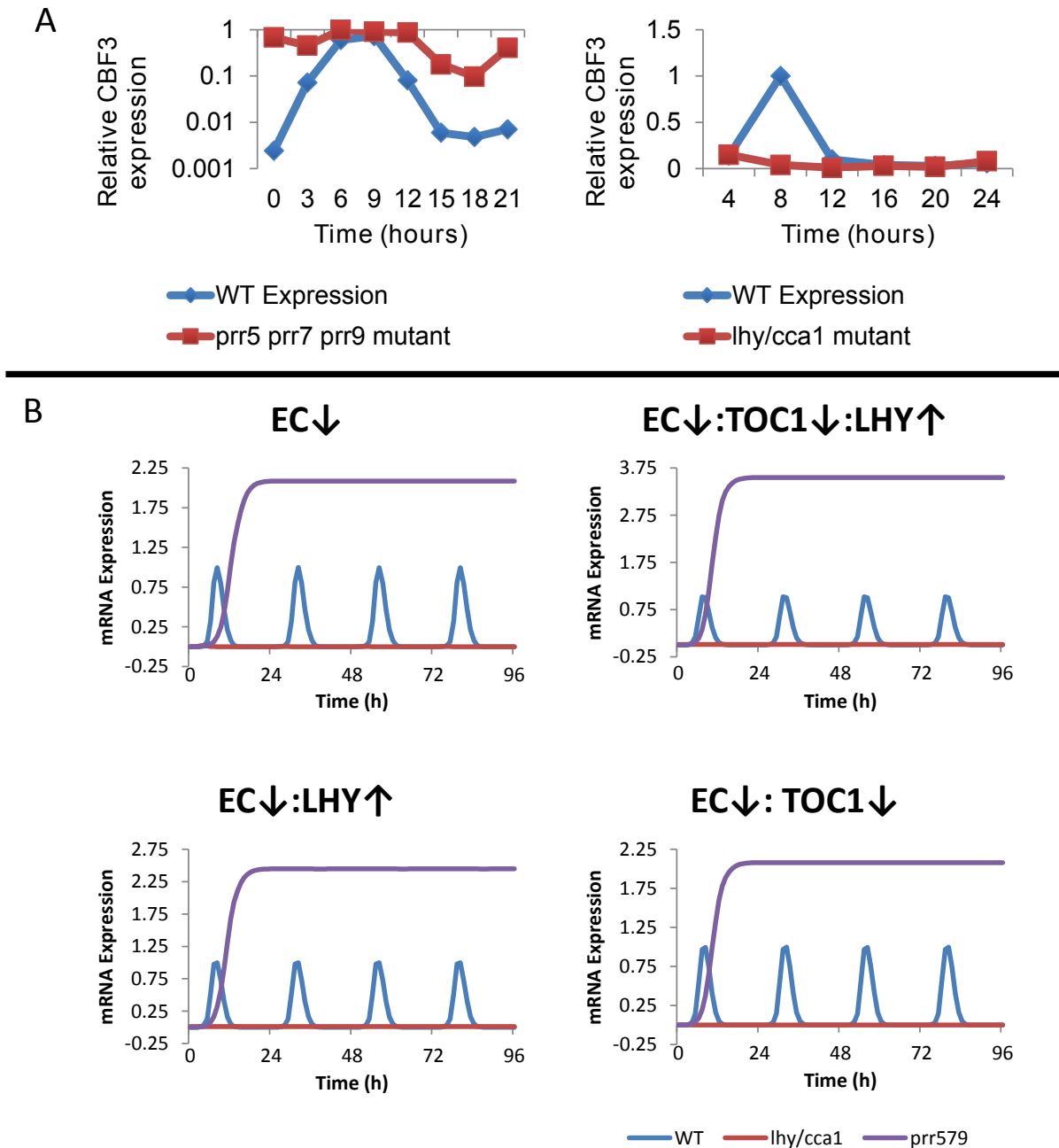


Figure 5.10: A) Relative expression of *CBF3* in *prr5 prr7 prr9* and *lhy/cca1* mutants as established experimentally: data from Nakamichi et al., 2009 and Dong et al., 2011. B) Mutant simulations in the four models of best fit, of *CBF3* mRNA expression in *lhy cca1* double mutant (red lines) and *ni prr7 prr9* triple mutant (purple lines) as well as wild-type simulations (blue lines) are shown. The models were simulated for 96 hours at one hour intervals. Mutants were simulated by setting protein translation rates to zero for the relevant gene.

5.3.6 Simulations of perturbations to the clock

Previously, in the models using the P2010 clock model, *toc1* mutants were simulated to see how this would alter *CBF3* expression as this gives a testable prediction. The same was done using the newest models created using the P2012 circadian clock model for the clock component of the model (**Figure 5.11**). The P2012 circadian clock also has the inclusion of the Evening Complex that allows for the simulation of Evening Complex mutants. LUX has previously been shown as the component of the Evening Complex that binds to other circadian clock components such as the *PRR9* promoter, and *lux* mutants were therefore simulated as well as *toc1* mutants. The four models that had the best fit to the data had *CBF3* expression simulated in *toc1* mutants. In the EC↓ model there was no change in *CBF3* expression level, in EC↓:LHY↑ there was a small increase in peak expression level, rising from a relative expression of 1 in wild-type to 1.24 in *toc1* simulations. In the EC↓:TOC1↓ model an increase from 1 in wild-type to a peak expression of 1.78 in *toc1* simulations was observed and in the EC↓:TOC1↓: LHY↑ model an increase from 1 to 2.86 was observed.

In the EC↓ *lux* simulation *CBF3* expression doubles that of the wild-type peak simulated expression and flat-lines, losing all rhythmicity. The EC↓LHY↑ *lux* mutant simulation also has increased *CBF3* expression compared to the wild-type simulation as well as a phase shift in peak expression occurring four hours before wild-type simulations. The EC↓:TOC1↓:LHY↑ model has reduced and flat expression of *CBF3* and EC↓:TOC1↓ has reduced expression with a loss of normal rhythmicity.

These simulations in *lux* and *toc1* conditions give testable predictions to help finalise the model selection and hopefully confirm the AICc model of best fit as such. If in *toc1* mutants we biologically see increased expression of *CBF3* then one can remove EC↓ as a potential model. If one observes decreased *CBF3* expression in *lux* mutants then this too will eliminate EC↓ and EC↓:LHY↑ as potential models of *CBF3* regulation and add support to the EC↓:TOC1↓:LHY↑ model.

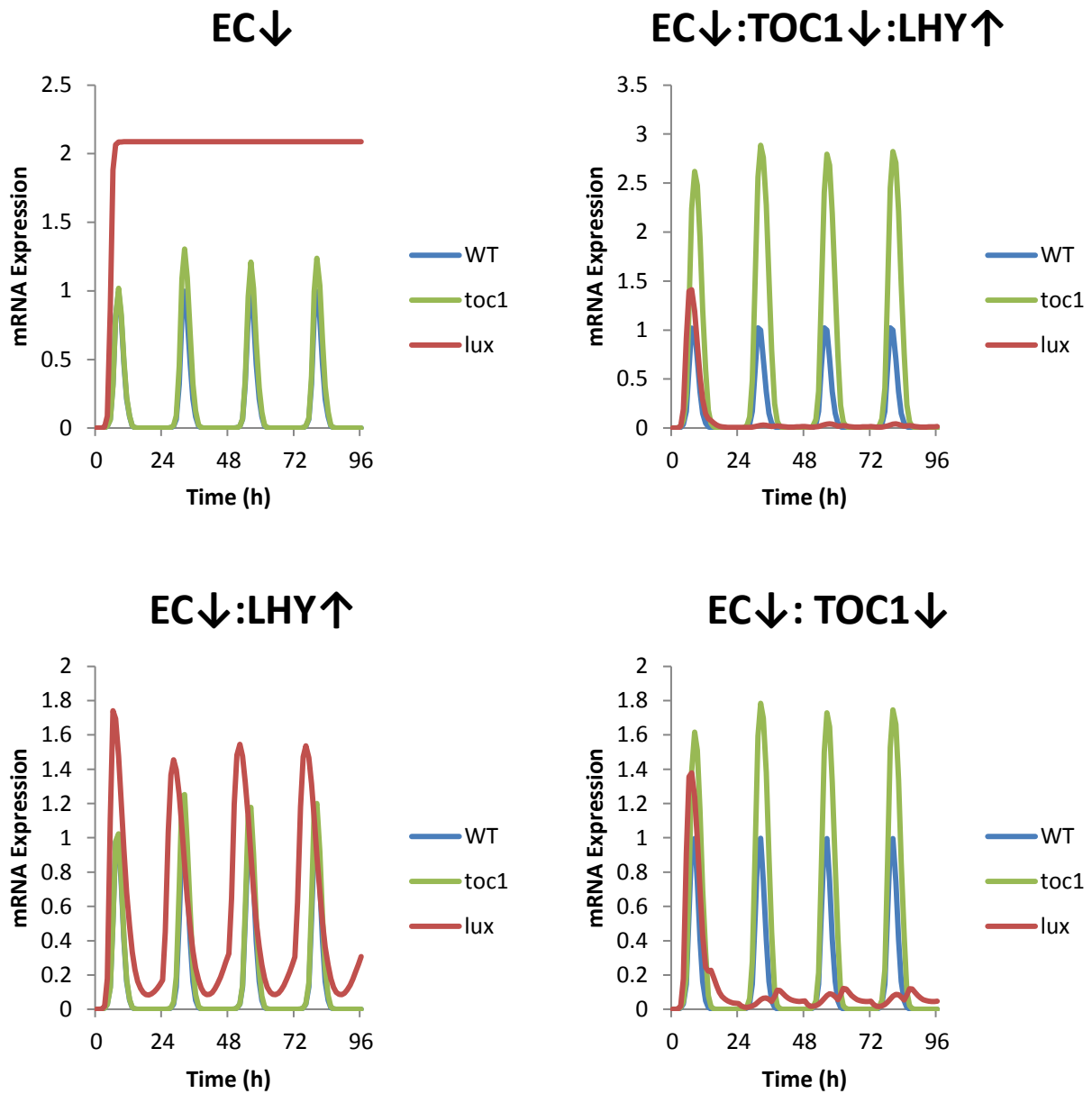


Figure 5.11: Mutant simulations of the top four models of best fit; *CBF3* mRNA expression are shown for each of the models with simulations of wild-type (dark blue lines), *lux* (red lines), and *toc1* (green lines) shown for each of the five models. The models were simulated for 96 hours at one hour intervals. Mutants were simulated by setting protein translation rates to zero for the relevant gene.

5.4 Testing the predictions made by the model

By simulating *toc1* and *lux* mutants in the various potential models, different predictions about how *CBF3* expression will be altered can be made (**Figure 5.11**). The model of best fit, EC↓:TOC1↓:LHY↑, predicts decreased *CBF3* expression in the *lux* mutant and increased expression in the *toc1* mutant. To test these predictions *CBF3* mRNA expression was studied in wild-type Col *Arabidopsis* plants and *toc1-101* and *lux-5* loss-of-function mutant plants during the morning when *CBF3* mRNA expression peaks. qRT-PCR was carried out on plants grown 22°C in 12L:12D conditions and harvested two weeks (14 days) after germination at two hour intervals throughout the morning. Three biological replicates were carried out of *CBF3* expression normalised to *ACT2* control gene expression, with the average expression of the three biological replicates and their standard error shown in (**Figure 5.12**).

5.4.1 Plants with the *toc1-101* mutation have increased peak *CBF3* expression

In the *toc1-101* mutant there is an increase in *CBF3* mRNA expression 2-10 hours after dawn, but no changes in expression at 0 or 12 hours after dawn (**Figure 5.12**). The peak of *CBF3* expression in *toc1-101*, which maintains wild-type phase, peaking eight hours after dawn, is increased by 97.56% over that of the wild-type peak expression. This data matches the prediction made by three of the four models that had the best AICc scores EC↓:TOC1↓, EC↓:TOC1↓:LHY↑ and EC↓:LHY↑. These models are good at reproducing the increase in *CBF3* expression that is seen in the *toc1* mutants (**Figure 5.11**).

5.4.2 Plants with the *lux-5* mutation have decreased peak *CBF3* expression

The *lux-5* mutants maintain rhythmicity and both maintain the same period and phase as wild type plants. In the *lux* mutant there is a decrease in *CBF3* expression after ZT 6 hours compared to wild-type plants (**Figure 5.12**). The peak in *CBF3* expression in the *lux-5* mutant plants, eight hours after dawn, is reduced by 33.2%

compared to wild-type plants. The expression level of the *lux-5* plants is reduced by an even greater amount 10 hours after dawn with a 69.1% decrease in expression compared to wild-type plants. There is a decrease in *CBF3* mRNA expression in the *lux* mutant; however, none of the four models with the best fit to the data show an exact match to this expression profile. Of the models that have a decrease in expression, the decrease is to a greater extent than is seen in the RT-PCR.

There are two models which best fit the experimental data from the RT-PCR, they are the EC↓:TOC1↓ model and the EC↓:TOC1↓:LHY↑ model. Both of these models show a decrease in *CBF3* expression in the *lux* mutant, however, the decrease in expression in the models is more extreme than that observed biologically.

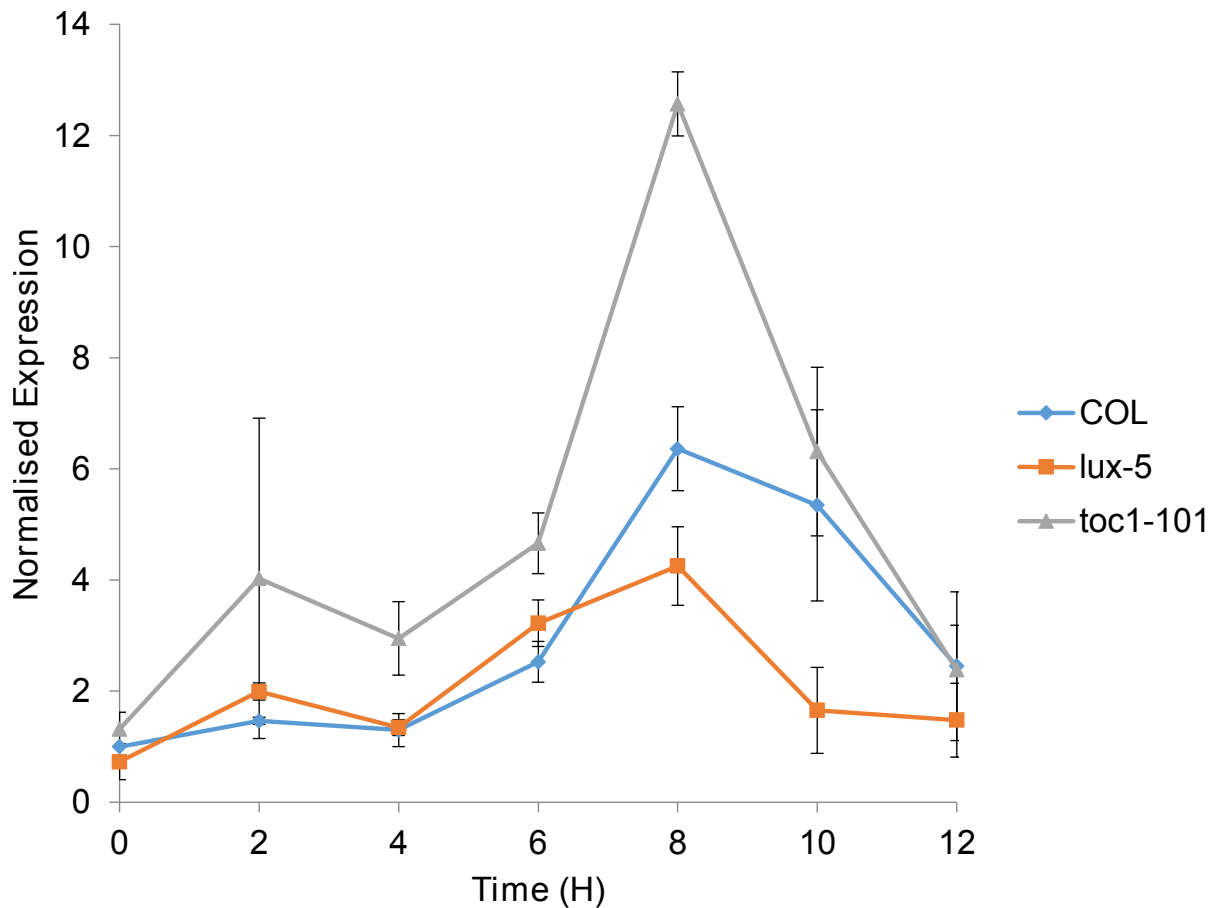


Figure 5.12: The effects of *toc1-101* and *lux-5* on the expression of *CBF3* in plants grown at 22°C with 12 hour light periods. Plants were harvested at two hour intervals and transcript levels of *CBF3* were determined by qRT-PCR. Gene expression was normalised against *ACT2*. Gene expression values were then normalised to wild type *CBF3* expression at time 0 which was set to a value of 1. Values are the average of three biological experiments, standard errors are shown.

5.4.3 The *CBF3* promoter region contains both TOC1 and LUX binding sites

The model of best fit, $EC\downarrow;TOC1\downarrow;LHY\uparrow$, predicts *CBF3* regulation by the Evening Complex and TOC1, as well as regulation by LHY/CCA1. *CBF3* regulation by LHY/CCA1 has previously been described, with CCA1 shown to directly bind to the

CBF3 promoter region (Dong et al., 2011). TOC1 and the Evening Complex have not previously been shown to have a direct regulatory role for *CBF3* expression. In order to test the hypothesis that TOC1 and the Evening Complex are involved in directly regulating *CBF3* expression a mechanism for this regulation had to be established. The *CBF3* promoter region was investigated to try and establish possible binding sites for TOC1 and the EC protein LUX (as LUX has previously been shown to be the component of the EC that binds DNA at the LUX binding site (Helfer et al., 2011)) regulation of *CBF3*.

In a recent paper, TOC1 was shown to be a DNA binding transcription factor that binds directly to a TGTG nucleotide sequence which they named T1ME (Gendron et al., 2012). The Ohio State University *Arabidopsis* Gene Regulatory Information Server (**agris**, <http://arabidopsis.med.ohio-state.edu/>), AtcisDB - Arabidopsis cis-regulatory element database, was used to search for known binding sites in the *CBF3* promoter region. The *CBF3* locus ID (At4g25480) was entered into the agris cis-regulatory database and several different binding sites were located within the *CBF3* promoter region (**Table 5.5**). The *CBF3* promoter region contains several different known protein binding site motifs. There are BHLH, homeobox, bZIP, WRKY, ARF, HB, HSF, MYB, ABI3VP1 and LFY family binding sites as well as binding sites that are not members of larger families, such as Evening Element promoter motifs and ABRE-Like binding site motifs (**Table 5.5**). Unfortunately, the T1ME motif and the LBS were not identified using the agris cis-regulatory database search as the database had not been updated to include these binding site motifs at the time of carrying out this study. As such, a manual search was carried out to try and identify any potential binding sites for TOC1 or the Evening Complex protein LUX. Using the sequence viewer in The *Arabidopsis* Information Resource website (<http://www.arabidopsis.org/>) for *CBF3* the DNA sequence preceding *CBF3* was entered copied to a word document and the T1ME motif (tgtg) and LBS motif (gatacg and gattcg) were searched. 17 putative TOC1 binding sites were also found throughout the *CBF3* promoter region with the closest found 220 bp upstream of the *CBF3* start codon (*Figure 5.13*), which lends weight to the idea that TOC1 may bind to, and regulate, *CBF3* expression. No putative LUX binding sites were located close to the transcription start sites of *CBF3*, however, LUX binding sites were observed 1.8 kb and 5 kb upstream of the *CBF3* start codon (**Figure 5.13**), offering a potential binding site for the Evening Complex.

Table 5.5: A list of the known binding sites in the *CBF3* promoter region as identified using the *Arabidopsis* Gene Regulatory Information Server

Binding site name	Sequence	Family	Reference
ABRE binding site motif	tacgtggc		(Choi, 2000)
ABRE-like binding site motif	gacgtgtc		(Shinozaki, 2000)
ABRE-like binding site motif	cacgtgga		
ABRE-like binding site motif	tacgtggc		
ABRE-like binding site motif	cacgtgtc		
ABRE-like binding site motif	cacgtgta		
ARF binding site motif	tgtctc	ARF	(Ulmasov et al., 1999)
ARF1 binding site motif	tgtctc	ARF	(Ulmasov et al., 1999)
ATB2/AtbZIP53/AtbZIP44/ GBF5 BS in ProDH	actcat	bZIP	(Sato et al., 2004)
ATHB2 binding site motif	taatcatta	HB	(Sessa et al., 1993)
AtMYC2 BS in RD22	cacatg	BHLH	(Abe et al., 1997)
Bellringer/replumless/ pennywise BS1 IN AG	aaattaa	Homeobox	(Bao et al., 2004)
DPBF1 2 binding site motif	acaccgg	bZIP	(Kim et al., 1997)
DPBF1 2 binding site motif	acacgtg	bZIP	
DPBF1 2 binding site motif	acacaag	bZIP	
DPBF1 2 binding site motif	acacggg	bZIP	
DPBF1 2 binding site motif	acacatg	bZIP	
DPBF1 2 binding site motif	acacgtg	bZIP	
DRE-like promoter motif	tgccgactt		(Chen et al., 2002)
Evening Element promoter motif	aaaatatct		(Harmer et al., 2000)
GATA promoter motif [LRE]	agataa		(Teakle et al., 2002)
GATA promoter motif [LRE]	agatag		
G-box promoter motif [LRE]	cacgtg		(Menkens and Cashmore, 1994)
GCC-box promoter motif	gccgcc		(Shinozaki, 2000)
HSEs binding site motif	agaaacttct	HSF	(Nover et al., 2001)
HSEs binding site motif	agaagtttct	HSF	
LFY consensus binding site motif	ccagtg	LFY	(Lamb et al., 2002)
LFY consensus binding site motif	ccattg	LFY	
MYB4 binding site motif	aacaaac	MYB	(Chen et al., 2002)
MYB4 binding site motif	acctacc	MYB	
RAV1-A binding site motif	caaca	ABI3VP1	(Kagaya et al., 1999)
SORLIP1	agccac		(Hudson and Quail, 2003)
SORLIP5	gagtgag		(Hudson and Quail, 2003)
T-box promoter motif	actttg		(Chan et al., 2001)
TELO-box promoter motif	aaaccctaa		(Tremousaygue et al., 1999)
W-box promoter motif	ttgacc	WRKY	(Yu et al., 2001)
W-box promoter motif	ttgact	WRKY	
W-box promoter motif	ttgacc	WRKY	
W-box promoter motif	ttgact	WRKY	

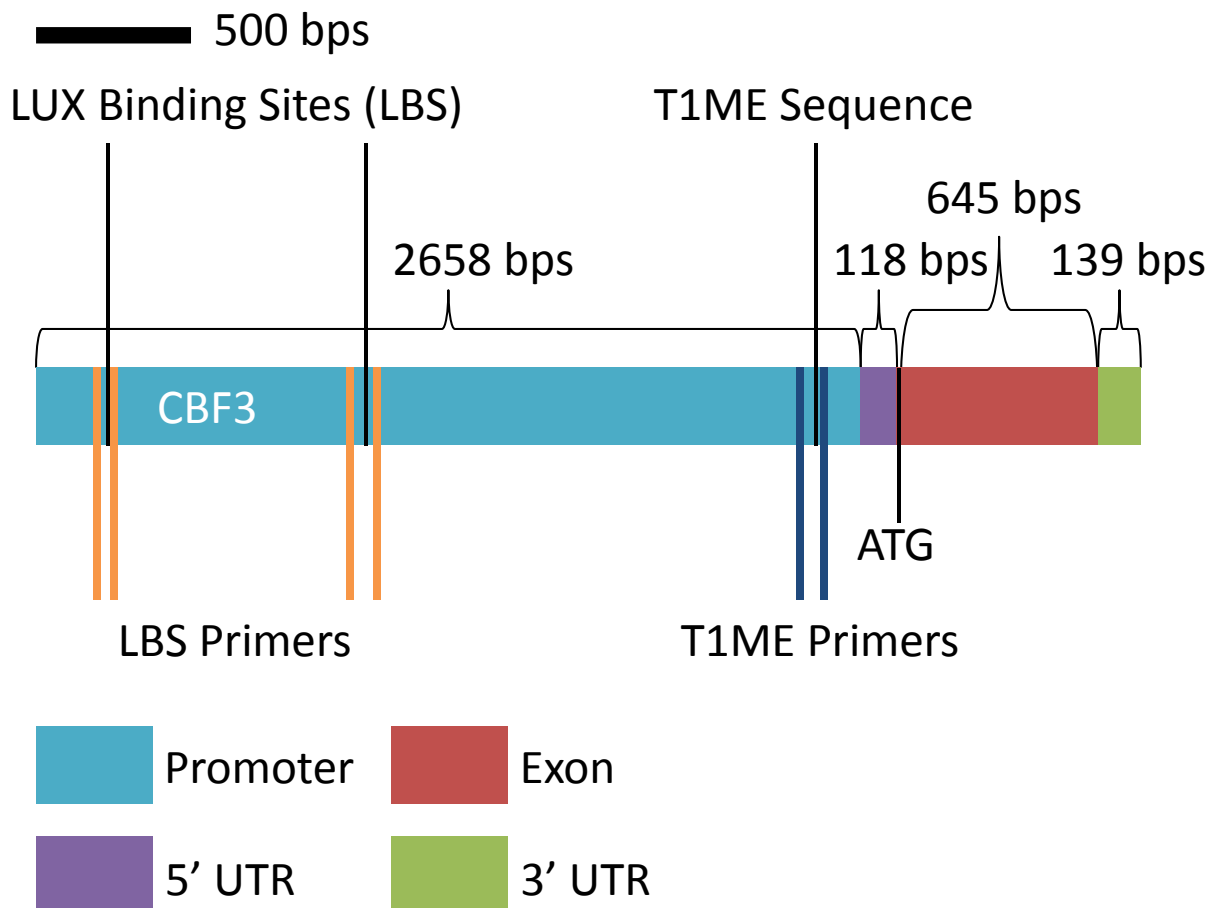


Figure 5.13: Location of T1ME binding site tested for TOC1 binding to the *CBF3* promoter region. Also shown are the two potential LUX binding sites on the *CBF3* promoter.

5.4.4 TOC1 binds directly to the *CBF3* promoter region

The model with the best fit to the biological data predicts that TOC1 is involved in regulating *CBF3* expression, a hypothesis that is backed up by the increase in *CBF3* expression that is observed in both the *toc1* mutant plants and the *toc1* mutant simulations of the EC↓:TOC1↓:LHY↑ model. In order to test whether TOC1 binds directly to the *CBF3* promoter region and is directly involved in regulating *CBF3* expression, a Chromatin Immunoprecipitation (ChIP) experiment was carried out. ChIP determines whether a protein associates with a specific region of DNA and is thus useful for showing whether a transcription factor is capable of binding to a promoter region of interest. In the *CBF3* promoter region there are several TOC1 binding site

(T1ME) motifs each with the potential for TOC1 to bind. The binding affinity of TOC1-YFP (Más et al., 2003a) to a T1ME motif region of the *CBF3* promoter in TOC1 overexpressing (*TOC1 MG*) plants was tested. A T1ME motif near the *CBF3* start codon (220bp upstream of the start codon) was selected (**Figure 5.13**) to test for TOC1 binding as well as an upstream negative control with no T1ME motif. *ACT2* was also used as a negative control for TOC1 binding. Binding was also tested for a known TOC1 binding region (*LHY* G-box) as a positive control for comparison. Plants for the ChIP experiment were grown at 22°C in 12L:12D conditions for two weeks and harvested and cross-linked 14 hours after dawn. **Figure 5.14** shows the average percent input of three biological replicates with the standard error shown.

Strong binding of TOC1 occurred in the T1ME region of the *CBF3* promoter (**Figure 5.14**).

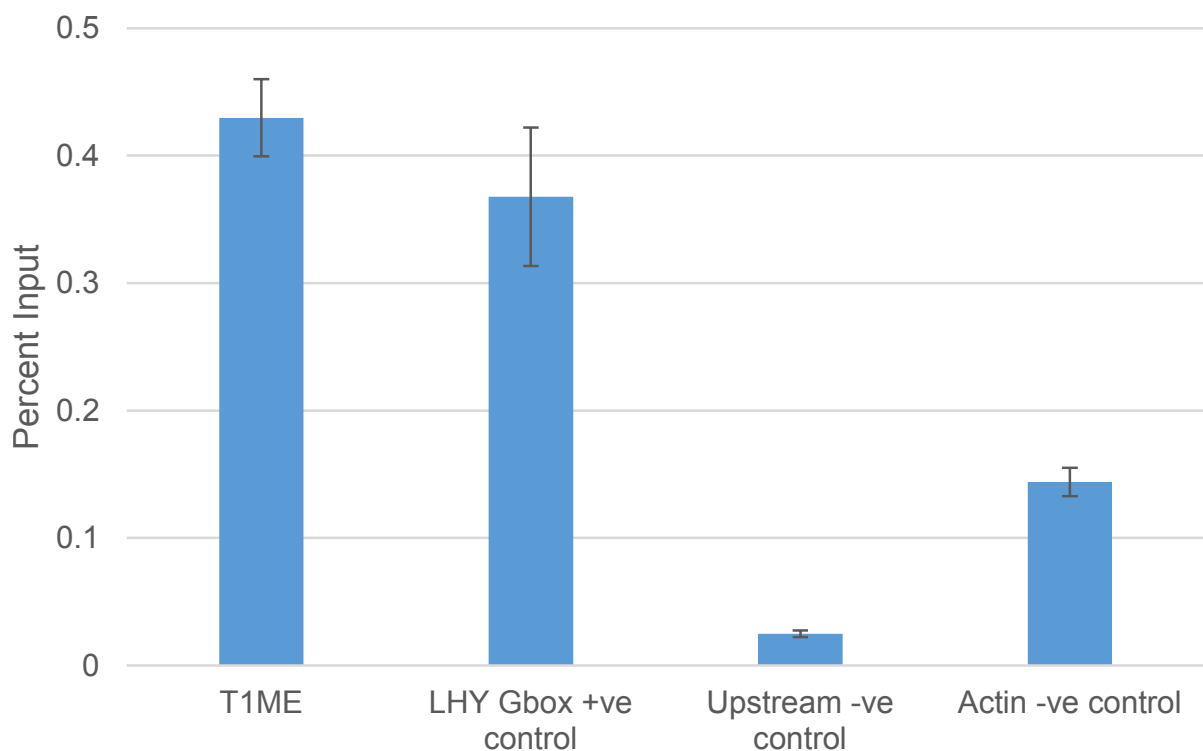


Figure 5.14: ChIP-qRT-PCR of *TOC1* minigene in a T1ME motif region of the *CBF3* promoter. A negative control from the *CBF3* promoter region with no T1ME motif, as well as an actin (*ACT2*) negative control were also tested along with a *LHY* G-box positive control. Error bars represent standard error from three biological experiments.

5.4.5 Components of the Evening Complex bind directly to the *CBF3* promoter region

This study has shown that there was direct binding of the TOC1 protein to the *CBF3* promoter region (**Figure 5.15**). Whether or not the Evening Complex was capable of binding to the *CBF3* promoter, however, had not been established. In order to test the prediction made by the modelling that the Evening Complex was regulating *CBF3* expression, ChIP was carried out by Dr Dana Macgregor and Dr Jayne Griffiths to determine if the Evening Complex was directly binding to the *CBF3* promoter like TOC1.

LUX:LUX-GFP and *ELF3:ELF3-YFP* transgenic lines were used to investigate whether the Evening Complex directly binds the *CBF3* promoter and is thus capable of directly regulating its expression. The *ELF3:ELF3-YFP* line was created and described previously in the literature (Dixon et al., 2011). The *ELF3:ELF3-YFP* line was created by first replacing *PHYA* cDNA in a *35S:PHYA-YFP* construct with *ELF3* coding sequence to create *35S:ELF3-YFP* (Dixon et al., 2011). The *35S* promoter was then replaced by the *ELF3* promoter fragment to produce *ELF3:ELF3-YFP* (Dixon et al., 2011). The *LUX:LUX-GFP* line was previously described (Helfer et al., 2011). The *LUX:LUX-GFP* line was created by cloning a 1870 bp fragment comprising the promoter region of *LUX* up to the previous gene, and the 5'UTR and coding sequence of *LUX* into pENTR/D-TOPO (Helfer et al., 2011). The construct was then recombined into pMDC107 to generate *LUX:LUX-GFP* (Helfer et al., 2011).

As mentioned previously, LUX has been shown to bind directly to clock gene promoter regions (Nusinow et al., 2011), and therefore the ability of LUX to bind to the two LUX binding sites on the *CBF3* promoter region was tested by Dr Jayne Griffiths. Similar to the TOC1 ChIP, plants were grown at 12L:12D at 22°C for 14 days and were cross-linked 14 hours after dawn. LUX binding was tested at two potential LUX binding sites (LBSi and LBSii, **Figure 5.15**) on the *CBF3* promoter as well as the TIME region that showed positive TOC1 binding. A positive control to test binding at the *PRR9* promoter was used, as was an Actin negative control. **Figure 5.15** shows the percent input of three biological experiments with the standard error shown. The ChIP experiments showed that there was no binding of *CBF3* to either of the two putative LUX binding sites (**Figure 5.15**).

ELF3 had been shown to bind to the *PRR9* promoter in the same region as LUX (Chow et al., 2012) so ELF3 was also tested by Dr Dana Macgregor to see if ELF3 would bind the *CBF3* promoter at the LBS regions. Similar to the TOC1 ChIP, plants were grown at 12L:12D at 22°C for 14 days and were cross-linked 14 hours after dawn. ELF3 binding was tested at two potential LUX binding sites (LBSi and LBSii, **Figure 5.15**) on the *CBF3* promoter as well as the T1ME region that showed positive TOC1 binding. A positive control to test binding at the *PRR9* promoter was used, as was an Actin negative control. **Figure 5.16** shows the percent input of three biological experiments with the standard error shown. There is no binding of ELF3 protein to the LBSs regions, however, there is binding of ELF3 to the *CBF3* promoter in the region that contained the T1ME motif (**Figure 5.16**).

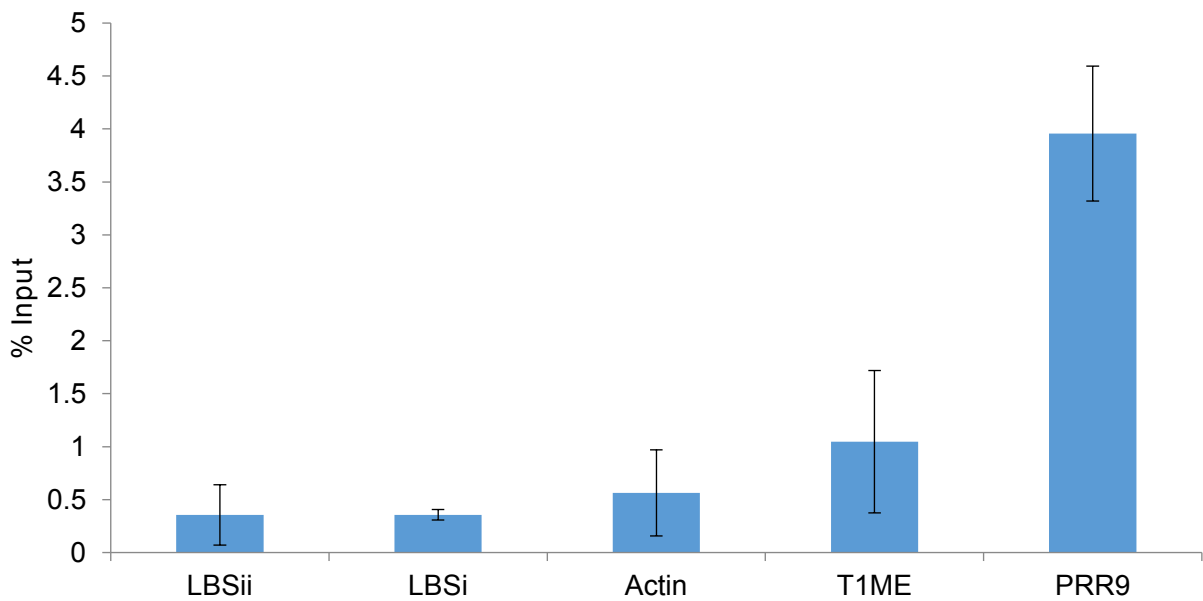


Figure 5.15: ChIP-qRT-PCR, *LUX:LUX-GFP* of Arabidopsis material taken at CT time 14 hours from plants grown at 27°C. Experiment carried out by Dr Jayne Griffiths, University of Edinburgh. Binding to the *PRR9* promoter region (positive control) is seen, but no binding is observed at either potential LUX-Binding-Site (LBSi and LBSii), or at the Actin (*ACT2*) negative control or in the T1ME (TOC1 Binding Site) region. Error bars represent standard error from three biological experiments.

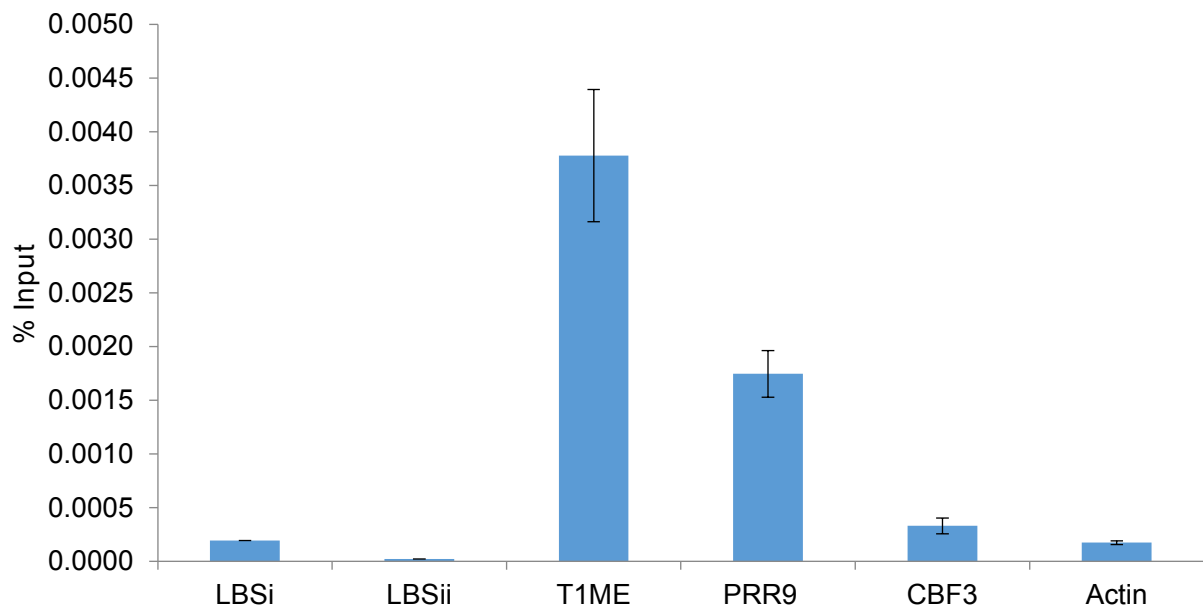


Figure 5.16: ChIP-qRT-PCR, *ELF3:ELF3-YFP* of Arabidopsis material at CT time 14 hours from plants grown at 22°C. Experiment carried out by Dr Dana Macgregor, University of Exeter. *ELF3* binding to the *CBF3* promoter region is not present at potential LUX-Binding-Site 1 (LBSi) or potential LUX-Binding-Site 2 (LBSii) but is seen in the T1ME (TOC1 Binding Site) region as well as in the *PRR9* promoter region positive control. *CBF3* primers and Actin (*ACT2*) primers, both negative controls, show no binding. Error bars represent standard error from three biological experiments.

5.4.6 In models where *CBF3* expression is up-regulated by LHY/CCA1 and inhibited by TOC1 and the Evening Complex, gating of cold signalling is possible

The effect of cold exposure on *CBF* expression varies throughout the day. Exposure to one hour of cold (4°C) is enough to increase *CBF* expression, however, the time of day at which the cold exposure occurs alters the extent of the change in *CBF* expression (Fowler et al., 2005). *CBF3* expression was shown to be induced by exposure to 4°C temperature four hours after dawn, but not when exposed to the same temperature at 16 hours after dawn (Fowler et al., 2005). It has been suggested that the circadian regulation of cold signalling occurs through the temperature controlled splicing of *CCA1*, the abundance of which is affected by temperature-controlled

splicing (Seo et al., 2012). In this scenario, a pulse of LHY/CCA1 protein (as both *LHY* and *CCA1* are represented as a single component in the P2012 model) in the models would be equivalent to a simulated pulse of cold temperature on *CBF3* expression. The model of best fit, EC↓:TOC1↓:LHY↑, was therefore tested to see whether it could replicate the cold gating seen in the literature. In order to test the gating of *CBF3* in this model *CBF3* mRNA was simulated with an LHY/CCA1 pulse occurring at different times during the day. The pulse was simulated by setting the value for LHY/CCA1 concentration to 5 at either ZT4 or ZT16 (an at least 1000% increase in LHY/CCA1 levels). The levels of *CBF3* were then observed one hour after administration of the “cold” pulse.

With a simulated cold pulse occurring at ZT4, *CBF3* simulated expression increased from 0.02128 in the simulation without the LHY/CCA1 to 0.1234 in the simulation with the LHY/CCA1 pulse (**Figure 5.17**). A pulse of LHY/CCA1 to mimic cold exposure at ZT16 resulted in no change in *CBF3* expression compared to a model without the pulse, as there was no expression of *CBF3* in either of the model simulations. Thus the selected model of *CBF3* regulation by the circadian clock was capable of simulating clock gating of cold induced *CBF3* expression.

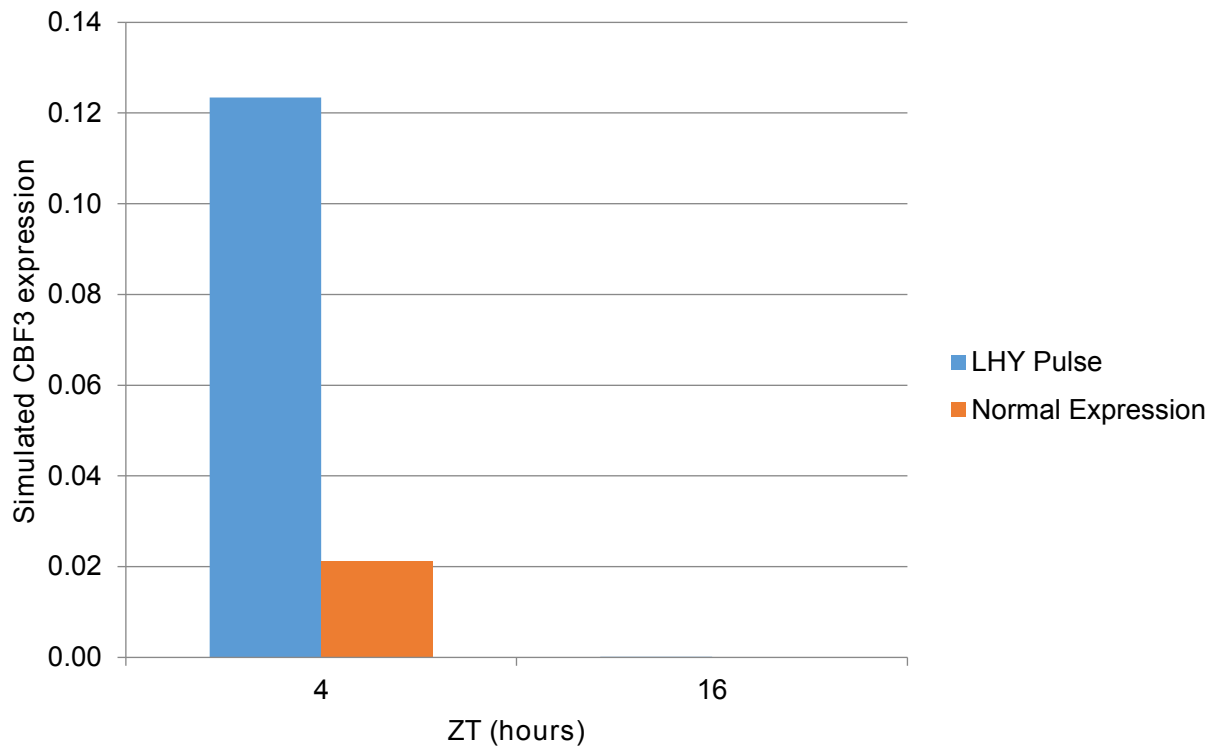


Figure 5.17: Simulated *CBF3* expression level after LHY pulse at four and ten hours after dawn, compared to normal simulated *CBF3* expression in the EC↓:TOC1↓:LHY↑ model. Simulated expression level with a LHY pulse is shown in the blue bars and normal expression without the pulse in the orange bars. Four hours after dawn, *CBF3* expression can be increased by exposure to “cold”, whereas at 16 hours after dawn there is no induction of *CBF3* expression.

5.5 Discussion

5.5.1 Modelling *CBF3* transcriptional regulation by the circadian clock

Control of temperature signalling is an important function of the plant oscillator; however, the exact structure of the transcriptional regulatory network controlling temperature by the clock is not well defined. Building on the information obtained in the freezing assay experiments and knowledge from the literature and publically

available databases, new computational models were created to help explain the control of the core cold-regulated transcription factor, *CBF3*.

Based on the data available from the literature and data obtained from the freezing tolerance experiments, models of *CBF3* transcriptional regulation by the circadian clock were created and assessed for their validity.

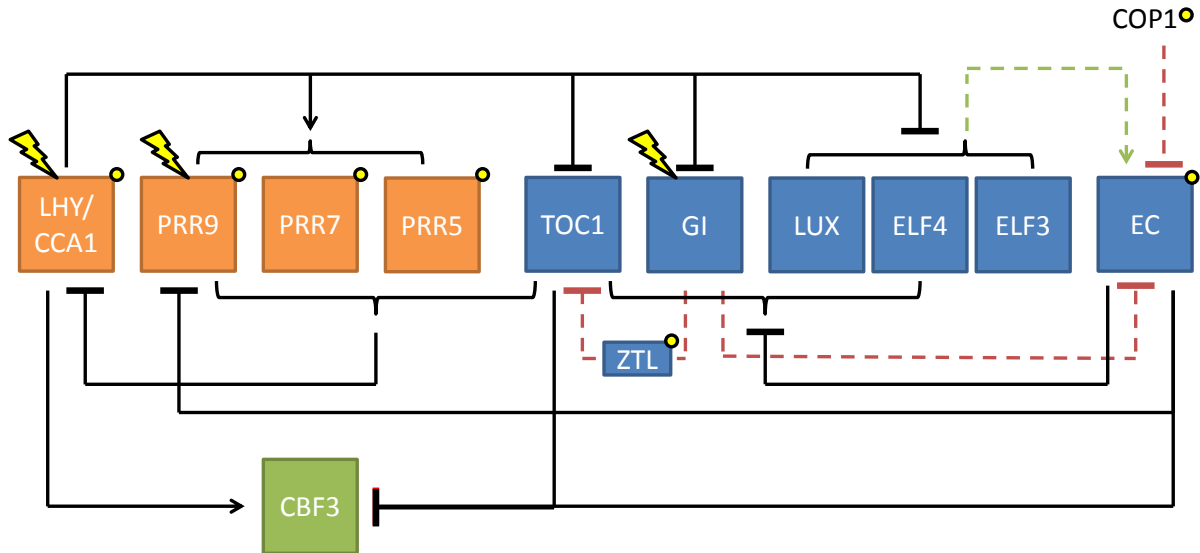


Figure 5.18: The final architecture of the Arabidopsis circadian clock model used in this study and proposed new connections to *CBF* mRNA transcription. *CBF3* transcription is inhibited by TOC1 and the Evening Complex and promoted by LHY/CCA1. Orange boxes represent the morning genes and the blue boxes represent evening genes, the green box is the newly added *CBF3* gene to the P2012 model. Transcriptional regulation is shown by solid lines. A dashed green line represents EC protein formation and red dashed lines represent regulation of *TOC1* and EC by GI, ZTL and COP1. Flashes represent light responsive gene expression and yellow dots are post transcriptional regulation by light. Figure adapted from Pokhilko 2012

5.5.2 Model construction and selection

Model selection using corrected Akaike Information Criterion

AICc scores were calculated for the various potential models and ranked in order of best fit to publicly available microarray mRNA expression data (**Figure 5.2** and **Figure 5.4**). Microarray data was used rather than producing new quantitative RT-PCR data for optimisation and model selection as there is a vast amount of microarray data available for gene in circadian and diurnal conditions (Harmer et al., 2000; Mockler et al., 2007) and by showing that this data can be used to create biologically relevant models will save both time and money in the future that would have been spent on creating new qRT-PCR expression series data.

Of the models that were created using the P2010 circadian clock, transcriptional inhibition of *CBF3* by TOC1 (**Figure 5.18**) was ranked as the model of best fit (**Table 5.2**). With the P2012 circadian clock model there were new components included that allowed for the creation of new models of *CBF3* regulation. Of the models created using the P2012 circadian clock, inhibition of *CBF3* transcription by TOC1 and the Evening Complex as well as up-regulation of *CBF3* transcription by LHY/CCA1 was ranked as the model of best fit (**Table 5.4**). The top four P2012 models all contained inhibition of *CBF3* transcription by the Evening Complex and if you eliminate these four models then the next best model of fit is the same as that observed in the P2010 model selection, inhibition of *CBF3* transcription by TOC1. The addition of the Evening Complex to the model is important as the models that included the Evening Complex are the ones with a sharp peak in *CBF3* expression that closely matches the sharp peak in expression that is seen in the biological data (**Figure 5.6**). Models that did not include Evening Complex inhibition, even if they could match the correct phase of expression, had a broader peak in expression that did not represent what was observed biologically. The publication of the P2012 circadian clock model was therefore fortuitous in allowing for the inclusion of the Evening Complex into the newer models as these simulations suggest that the Evening Complex is an essential component required for the correct expression of *CBF3*.

The PRRs are known to be important for maintaining wild-type expression of *CBF3* and wild-type rates of freezing tolerance survival, with *prr* triple mutants having increased *CBF3* expression and increased freezing tolerance (Nakamichi et al., 2009).

It is interesting, therefore, to note that the model simulations with PRR regulatory components had the worst AICc scores and bad *CBF* expression simulations in both the P2010 circadian clock models and the P2012 circadian clock models. This data suggests that the up-regulation of *CBF3* expression in the *prp5 prp7 prp9* triple mutants (Nakamichi et al., 2009) is not caused by the direct loss of inhibition of transcription by these genes; this conclusion is not obvious from the biological data available, and is a good example of the benefits of systems biology, where running model simulations can lead to non-intuitive results.

The models that had only Evening Complex inhibition or had Evening Complex inhibition in combination with LHY/CCA1 up-regulation of *CBF3* transcription maintained a sharp peak in *CBF3* expression in all four different light conditions, yet had a +4 hour phase shift when in constant light conditions. The EC↓:TOC1↓:LHY↑ model was the only model that kept the sharp peak in all the light conditions as well as the correct phase of expression. CCA1 had previously been shown to directly bind the *CBF3* promoter region to promote transcription (Dong et al., 2011), so the fact that this transcriptional regulatory component was present in the model of best fit adds credibility to the model selection technique used in this study.

This shows that in order to recreate the waveforms that are seen in *CBF3* expression in the biology the interaction of several core clock components are required: TOC1, the Evening Complex and LHY/CCA1; *CBF3* transcription that is activated by LHY/CCA1 in the morning is rapidly inhibited by TOC1 at dusk and the Evening Complex represses transcription over dawn during the early period of LHY/CCA1 expression (**Figure 5.19**).

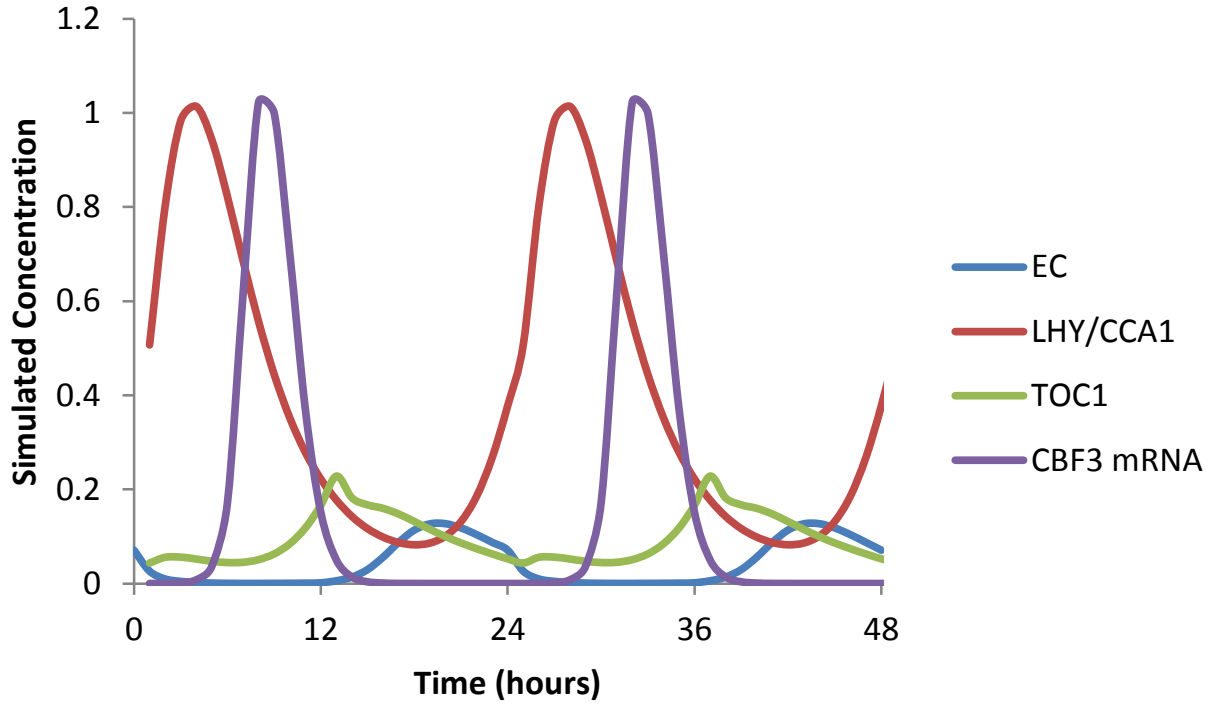


Figure 5.19: Protein concentration simulations of the proposed *CBF3* transcriptional regulatory components of the circadian clock. *CBF3* mRNA transcription is stimulated in the morning by LHY/CCA1 and inhibited rapidly by TOC1. The Evening Complex inhibition of *CBF3* transcription prevents up-regulation by LHY/CCA1 in the late evening/early morning.

5.5.3 The Pokhilko 2012 circadian clock model to regulate simulated *CBF3* expression

The model of best fit simulates *CBF3* expression in clock mutants with known *CBF3* expression and clock mutants with unknown *CBF3* expression

For the newly created model to be considered successful at simulating *CBF3* expression, it must be able to reproduce the effects of perturbations to the circadian clock. This means that the clock models must be able to reproduce the expression profile seen in *lhy cca1* double mutants (Dong et al., 2011) where *CBF3* expression is reduced to trace levels, and in the *prr5 prr7 prr9* triple mutant which shows constitutively increased *CBF3* expression with reduced amplitude of oscillation (Nakamichi et al., 2009).

In the literature, *prp5 prp7 prp9* triple mutants have increased *CBF3* expression and maintain some circadian expression, albeit with severely reduced amplitude. In the models that used the P2010 circadian clock there was a circadian rhythm maintained in the *prp* triple mutants, as well as an increase in expression; however, the phase of expression was delayed 8 hours (**Figure 5.3**). When the models were updated to the P2012 model, however, the oscillation in *CBF3* expression in the *prp* triple mutant is lost and the new model of best fit (TOC1↓:EC↓:LHY↑) shows increased *CBF3* transcription compared to wild-type, but with a flat rate of expression (**Figure 5.10**). This lack of oscillating expression of *CBF3* in the *ni(prp5) prp7 prp9* mutant simulations is likely due to the fact that in the Pokhilko 2012 model this triple mutant results in a loss of TOC1 and EC accumulation, with the expression of both of these proteins flat-lining. This means that the models that have inhibition by these components are likely to lack the rhythmicity seen in the literature (Nakamichi et al., 2009) in the *prp* triple mutant. The *prp5 prp7 prp9* triple mutant simulation also uses *ni* for the *prp5* mutant. Whilst the role of *NI* has been suggested to be that of *PRR5*, it has yet to be confirmed experimentally (Pokhilko et al., 2012) which may add to the slight differences seen in the triple mutant simulations versus the biological mutants.

Of the four models with the best fit to the biological data using the P2012 circadian clock, all produced an increase in *CBF3* expression in *prp5 prp7 prp9* triple mutants, as well as the decrease in expression in the *lhy cca1* mutant simulations reproducing the phenotypes seen in the literature (Nakamichi et al., 2009; Dong et al., 2011). This shows that there are several model constructs that are capable of mimicking *CBF3* expression in known biological mutants and that therefore the ability, or lack thereof, to mimic known *CBF3* expression in clock mutants will not help to eliminate potential models. As such perturbations to the clock with unknown *CBF3* expression had to be simulated and then tested experimentally.

As trying to replicate the effects of clock perturbations with known *CBF3* expression did not allow for the elimination of any of the models with the best AICc score, simulations of the effect of *CBF3* expression with clock perturbations with unknown *CBF3* expression were carried out.

Perturbing TOC1 production and the essential Evening Element component LUX production was therefore carried out (**Figure 5.10**). In the *lux* mutant simulations, of the four models with the best AICc scores, these models could be split broadly into

two groups. In the first group there was the models that resulted in increased *CBF3* expression, EC↓ and EC↓:LHY↑ (**Figure 5.11**). In the other group there was decreased *CBF3* expression in the *lux* mutant simulations, EC↓:TOC1↓:LHY↑ and EC↓:TOC1↓ (**Figure 5.11**). In the *toc1* mutant simulations there was increased expression in *CBF3* levels to varying degrees with the EC↓ model having very little increase in expression (**Figure 5.11**).

These simulations in *lux* and *toc1* conditions gave testable predictions to help finalise the model selection and hopefully confirm the AICc model of best fit as such. If in *toc1* mutants we biologically see increased expression of *CBF3* then one can remove EC↓ as a potential model. If one observes decreased *CBF3* expression in *lux* mutants then this too will eliminate EC↓ and EC↓:LHY↑ as potential models of *CBF3* regulation and add support to the EC↓:TOC1↓:LHY↑ model. The qRT-PCR time series of *CBF3* expression in *toc1-101* and *lux-5* mutants (**Figure 5.12**) confirmed an increase in *CBF3* expression in the *toc1-101* mutant and a decrease in expression in the *lux-5* mutant as predicted. In the *lux* simulations in **Figure 5.11** *CBF3* expression in the EC↓:TOC1↓:LHY↑ model was decreased to a greater severity than observed biologically in **Figure 5.12**. Similarly, the *toc1* EC↓:TOC1↓:LHY↑ model simulation had a greater increase in *CBF3* expression than was observed biologically in **Figure 5.12**. The reduction in severity observed in the biological experiments compared to that of the EC↓:TOC1↓:LHY↑ model could be due to the mutant allele selected for the experiments. *toc1-101* and *lux-5* are both loss-of-function mutants (Kaczorowski, 2004; Hazen et al., 2005) rather than full null mutants which could explain why the observed changes in *CBF3* expression were not as great as the model simulations as there may still be some functional protein produced.

Whilst the experiment carried out in **Figure 5.12** was good for eliminating the potential models that showed increased expression in *lux* simulations, it did pose an interesting question: if the EC is acting as an inhibitor of *CBF3* transcription, why does removing a key component of the Evening Complex result in a decrease in *CBF3* expression rather than an increase, similar to that seen in the *toc1* simulation and experimental data? Whilst the decrease in *CBF3* expression in *lux* may seem counter-intuitive, looking at the expression profiles of the clock in *lux* simulations explains this result (**Figure 5.20**). In *lux* simulations, EC production is inhibited, however, both LHY/CCA1 concentrations are decreased and TOC1 levels are increased (**Figure 5.20A**). This means that the transcriptional activation of *LHY/CCA1* is

decreased and the inhibitory effects of TOC1 are increased, thus leading to a decrease in *CBF3* expression. In the *toc1* simulations, EC levels remains at the same level whereas TOC1 expression is inhibited and LHY/CCA1 concentrations are slightly increased, thus leading to an increase in *CBF3* expression in both the *toc1* simulations (**Figure 5.20B**) and the *toc1-101* experiments (**Figure 5.12**).

This is a good example of the benefit of modelling biological systems; by modelling a system the behaviour of a network can be simulated under both normal and abnormal conditions quickly to provide non-intuitive answers to questions that may otherwise not become apparent.

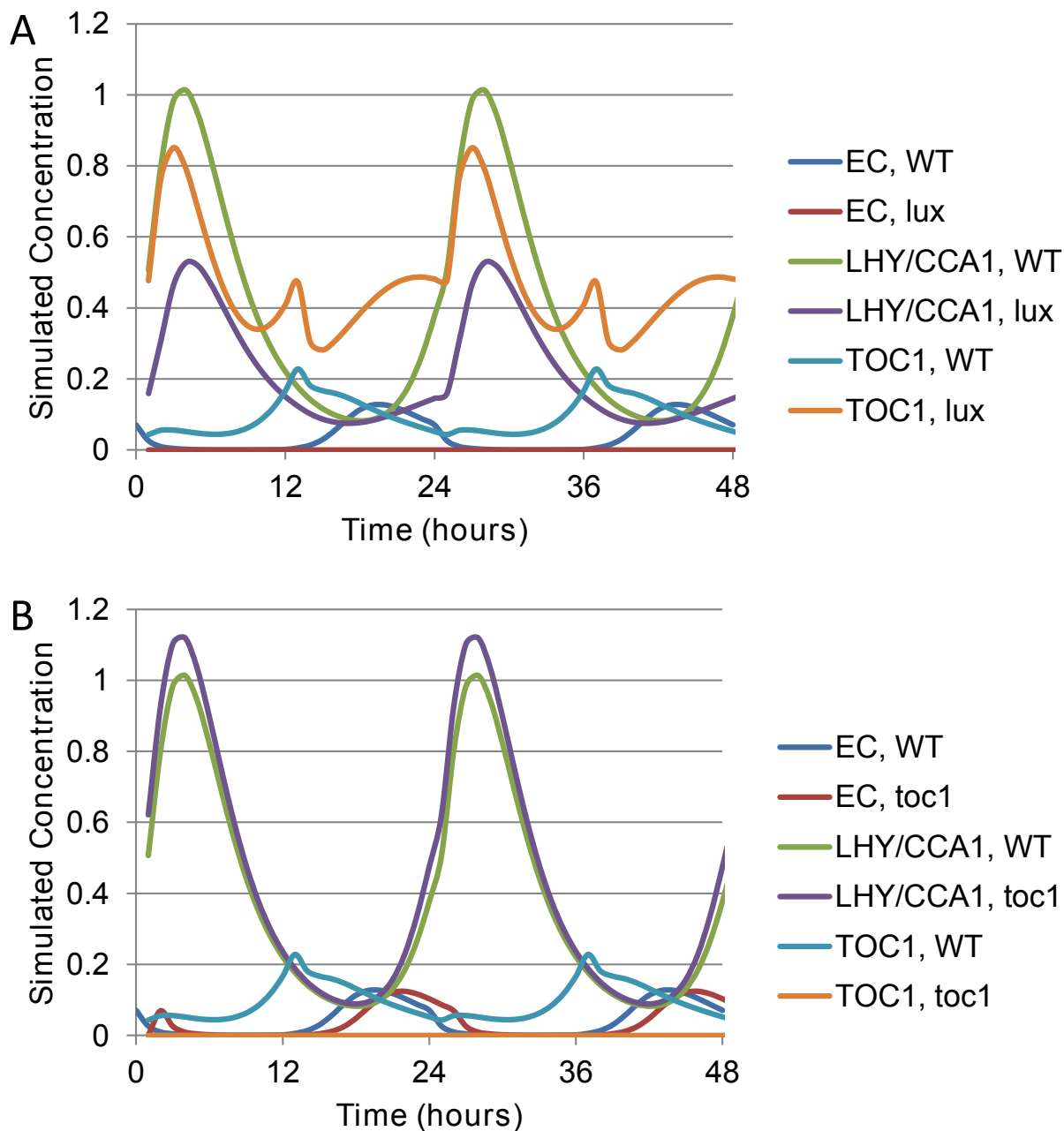


Figure 5.20: Protein accumulation in the P2012 circadian clock model in A) *lux* mutant simulations and B) *toc1* mutant simulations. The *lux* mutant results in loss of EC accumulation as well as an increase in TOC1 and LHY/CCA1 accumulations. In the *toc1* mutant simulations there is a decrease in TOC1 accumulation combined with a small increase in LHY/CCA1 accumulation and no change in EC accumulation.

5.5.4 Testing the predictions made by the model

TOC1 and the Evening Complex are direct inhibitors of *CBF3* transcription

In this study, TOC1 was shown to bind directly to the *CBF3* promoter which backs up the EC↓:TOC1↓:LHY↑ prediction that TOC1 is involved in directly regulating *CBF3* expression.

Previously, deep sequencing ChIP-Seq has been used to look at TOC1 chromatin occupancy on a genome level where TOC1 minmigeno seedlings expressing the genomic fragment of TOC1 fused to the yellow fluorescent protein in *toc1-2* mutant backgrounds was used to search for genes that contained at least one TOC1 binding region (Huang et al., 2012). The authors of this study identified 867 peak-to-gene associations corresponding to 772 potential TOC1 target genes (Huang et al., 2012). The data-set collected by Huang *et al.*, shows *CBF1* and *CBF2* TOC1 enrichment, but does not show *CBF3* TOC1 enrichment, unlike the data collected in this thesis which shows TOC1 enrichment in the *CBF3* promoter region at the putative TOC1-binding site (**Figure 5.14**).

The Evening Complex protein ELF3 was also shown to directly bind the *CBF3* promoter; however, LUX, which has previously been described as the component of the Evening Complex responsible for binding the *PRR9* promoter region to regulate gene expression (Helfer et al., 2011), was not shown to bind to the *CBF3* promoter region. This suggests the possibility of a modified Evening Complex containing ELF3 that binds to the *CBF3* promoter through ELF3 rather than the LUX protein.

Here data that shows that ELF3, an Evening Complex protein, binds directly to the *CBF3* promoter region is presented (**Figure 5.16**). ELF3 has been shown to bind to the same region of the *PRR9* promoter as LUX (Chow et al., 2012), however, both LUX and ELF3 showed no binding affinity in the LBS regions of the *CBF3* promoter. ELF3 did bind in the TIME region of the *CBF3* promoter. This suggests that the component of the Evening Complex that is involved in regulating *CBF3* expression is ELF3, rather than LUX as one may have predicted based on LUX's previously reported role in regulating gene expression (Helfer et al., 2011). The fact that ELF3 but not LUX could bind to the promoter region of *CBF3* combined with the decrease in *CBF3* expression in *lux-5* mutants suggests that Evening Complex protein LUX may not be involved in inhibiting *CBF3* transcription. Instead it is possible that there

is a role for a modified EC containing ELF3 that has similar kinetics to the EC that has previously been described but where LUX is replaced by a homologue such as BROTHER OF LUX ARRHYTHMO (NOX) (Chow et al., 2012) or a completely different complex. ELF3 is known to form complexes with other proteins that are not part of the EC, such as phytochromes (Liu, 2001). Phytochromes are known to have a role in the control of *CBF3* expression (Franklin and Whitelam, 2007) which presents the possibility another mechanism through which ELF3 is conferring transcriptional regulation of *CBF3*.

The ELF3 binding site in the *CBF3* promoter region has not been accurately determined. In the future, follow up ChIP experiments would be interesting to carry out at different regions throughout the *CBF3* promoter and on fragments of the *CBF3* promoter to ascertain a greater understanding of the binding motif of ELF3 on the *CBF3* promoter. Investigating the binding affinity of NOX to the *CBF3* promoter would also be useful to try and test the hypothesis that a NOX rather than LUX EC is binding the *CBF3* promoter.

Changes in day length simulation results in altered *CBF3* expression in the models of *CBF3* transcriptional regulation

Biologically, plants that are grown in short days (L8:D16) have a three- to five-fold increase in *CBF* expression than in plants that are grown in long days (L16:D8) at ZT8 (Lee and Thomashow, 2012). This was tested in the different models that were created using the P2012 circadian clock model and several showed an increase in *CBF3* expression in simulations run under short days compared to simulations that were run in long days (**Figure 5.8**). The largest increase was seen in the model of best fit, TOC1↓:EC↓:LHY↑, with a 1.44-fold increase in *CBF3* expression. This change in expression seen in even the best model is still less than that observed biologically. The changes in *CBF3* amplitude of expression seen experimentally under varying day light lengths was linked to inhibition of *CBF* transcription in long days by PIF4 and PIF7 (Lee and Thomashow, 2012), however, PIF4 and PIF7 regulation of *CBF* expression under long day conditions is not modelled in any of the work presented in this thesis as previously published data had shown no role for the PIFs in regulating *CBF3* expression (Kidokoro et al., 2009).

The model of *CBF3* transcriptional regulation by the clock mimics circadian gating of the cold induction of *CBF3* expression

CBF expression is gated by the circadian clock with *CBF3* expression getting stimulated by exposure to 4°C four hours after dawn but not when exposed to the same temperature change 16 hours after dawn (Fowler et al., 2005). A simulation of exposure to cold conditions was possible by adding a LHY/CCA1 pulse to the model at four and 16 hours after subjective dawn, thus mimicking the cold induced increase in LHY/CCA1 that occurs naturally (Seo et al., 2012). In the EC↓:TOC1↓:LHY↑ model, *CBF3* expression was simulated at four hours after dawn but not at 16 hours after dawn, similar to the published data on *CBF3* cold, clock, gating (Fowler et al., 2005). Unlike the previously published data on the clock gating of *CBF3* (Fowler et al., 2005) the simulations presented here had expression of *CBF3* without the cold exposure at ZT4. This is possibly due to the low expression levels not being detected in the RNA gel plots in the literature as *CBF3* has been shown to be expressed during the day in non-stressed conditions (Nakamichi et al., 2009; Dong et al., 2011). This data shows that not only was it possible to mimic a cold pulse in the models, but that the cold pulse simulation was capable of replicating the biologically observed gating of *CBF3* expression via the clock.

5.5.5 Chapter 5 summary

Several models of the potential mechanisms for *CBF3* regulation by the circadian clock were created, building on either the P2010 or the P2012 circadian clock mathematical model. The models were then optimised against publically available microarray data of *CBF3* expression in 12L:12D light conditions. The models were then ranked in order of best fit to publically available microarray data of *CBF3* expression in four different light period day lengths using AICc. In the P2010 circadian clock model the TOC1↓ model had the best fit to the biological data. In the P2012 circadian clock models the EC↓:TOC1↓:LHY↑ model had the best fit to the biological data under the four different light conditions.

lhy cca1 and *prp* triple mutant simulations for the P2010 TOC1↓ model and the P2012 EC↓:TOC1↓:LHY↑ model showed qualitative increases in *CBF3* expression in *prp* triple mutants and decreased expression in the *lhy cca1* mutant simulation, similar to

that seen biologically in the literature (Nakamichi et al., 2009; Dong et al., 2011). The EC↓:TOC1↓:LHY↑ model using the P2012 circadian clock model predicted an increase in *CBF3* mRNA expression in *toc1* mutant plants, as did the P2010 model of best fit TOC1↓. An increase in *CBF3* expression in *toc1* mutant plants was then confirmed experimentally. The EC↓:TOC1↓:LHY↑ model also predicted decreased *CBF3* expression in *lux* mutant plants a prediction that could not have been made by simply using the P2010 circadian clock model. A decrease in *CBF3* expression in *lux-5* mutant plants was then confirmed by qRT-PCR showing decreased *CBF3* mRNA expression in *lux-5* mutant plants compared to wild-type Col plants.

In order to test whether the predicted regulatory mechanisms of the clock were directly affecting the expression of *CBF3*, ChIP experiments were carried out to determine whether TOC1 and the Evening Complex were directly binding to the *CBF3* promoter region to alter expression. TOC1 was shown to bind to the *CBF3* promoter region directly. The Evening Complex component ELF3 was also shown to bind directly to the *CBF3* promoter region, however the Evening Complex component LUX was not.

Finally, the EC↓:TOC1↓:LHY↑ model was also able to produce cold gating of *CBF3* expression, with increased *CBF3* expression at ZT4 when exposed to a “cold” blast, compared to ZT16 when no increase in *CBF3* expression was observed adding further support to this model of *CBF3* regulation by the circadian clock.

6 General discussion and future work

The main aim of this thesis was to try and increase our understanding of the role of the circadian clock in regulating seed germination and cold acclimation. This led to the establishment of a few core objectives:

- To investigate the role of the circadian clock in mediating red and far-red light regulation of seed germination and dormancy
- To investigate the role of the circadian clock in regulating the cold acclimation pathway
- To model the circadian regulation of the cold acclimation pathway

These objectives have been covered and discussed in the previous three chapters of this thesis.

In this chapter a general discussion of the work carried out will take place as well as a look to any potential future work that is of interest.

6.1 The circadian clock gene *TOC1* is required for normal red light induced germination to occur

Our understanding of the circadian clock regulation of seed dormancy and germination is relatively new and incomplete; our understanding of the role of the circadian clock in regulating light-mediated germination and dormancy by red and far-red light is even less well understood. This study has shown that without *TOC1 Arabidopsis* seeds are significantly hyposensitive to red light and that the circadian clock is indeed necessary and important for normal red light induced germination to occur. In seeds with the *toc1-101* null mutant there was significant decreases observed in germination rates compared to wild-type plants after exposure to different periods of red light (**Table**

3.2, Figure 3.4). The circadian clock is known to be involved in regulating germination in *Arabidopsis* seeds (Penfield and Hall, 2009) and is important for early photomorphogenesis; *TOC1 MG* plants are hypersensitive to red light resulting in reduced hypocotyl length when grown in red light compared to wild-type plants and *toc1-2* plants are hyposensitive to red light resulting in increased hypocotyl length in comparison to wild-type plants when grown in red light (Más et al., 2003a). Therefore, this study has shown that the red light hyposensitivity that has been reported for *Arabidopsis* seedlings is also present in *Arabidopsis* seeds and confirms the hypothesis that the circadian clock is indeed involved in regulating light mediated seeds germination and dormancy, likely through the regulation of phyB via PIF3 as discussed in **Chapter 3** (Makino et al., 2002; Leivar et al., 2008).

6.2 More circadian clock genes are involved in regulating freezing tolerance than previously thought

There are circadian clock genes that have been shown to be important for freezing tolerance such as the *PRRs* and *CCA1* (Nakamichi et al., 2009; Dong et al., 2011). In order to better understand the circadian regulation of the cold acclimation pathway several circadian clock genes were investigated to try and ascertain whether there were any further clock genes that were important for regulating freezing tolerance in plants. The importance of the *PRRs* for regulating freezing tolerance had already been shown in *prrr5 prrr7 prrr9* mutants that displayed increased freezing tolerance (Nakamichi et al., 2009).

As previously discussed in **Chapter 4**, *prrr* single, double and triple mutants as well as *toc1 (prrr1)* mutants have increased freezing tolerance compared to wild-type plants when grown at 12, 17 or 22°C (**Figure 4.4**). The *PRRs* are expressed sequentially throughout the (*PRR9-PRR7-PRR5-TOC1*) thus maintaining normal circadian rhythms throughout the day (Nakamichi et al., 2005; Nakamichi et al., 2010). One might predict, therefore, that the different *PRRs* would be important for regulating freezing tolerance at different times throughout the day; is *TOC1*, an evening gene, more important for regulating freezing tolerance in the evening than the morning *PRRs*? It would be interesting, therefore, to design a time series freezing assay that could look at the effect of freezing time on freezing tolerance. There are several ways in

which this could be accomplished; one could carry out the same freezing assay as this study, but change the start time of the assay to different periods throughout the day, or one could reduce the freezing time of experiment and freeze the plants for a reduced time, but at different times during the day. The latter would be preferable as one could then match freezing time to peak mRNA concentration for the different *PRRs* but would require the development of a new protocol. One would hypothesise that whilst all of the *prp* mutants would still have increased freezing tolerance, the tolerance levels would fluctuate throughout the day relative to the wild-type expression level of the gene of interest. This would show that the sequential expression of the different *PRRs* is not only important for maintaining the clock throughout the day, but also cold acclimation.

As well as the *PRRs*, *TOC1* and *ELF3* were also shown to be important components for maintaining normal freezing tolerance levels. Being able to understand how plants are able to cope and tolerate freezing is important for future crop research; a greater understanding of how to possibly manipulate crops so that they are capable of growing in colder climates will allow for the spread and growth of crops in colder regions of the world where they were not previously able to grow and survive. This long term goal is still far away. Whilst the data presented in this study indicates that *toc1* mutants would have increased freezing tolerance that would benefit growth at colder climates, the short clock period that is caused in *toc1* mutant plants (Somers et al., 1998) may result in adverse effects to crop growth that outweigh the freezing tolerance it would imbue.

6.3 Modelling the circadian clock regulation of the cold acclimation pathway gene *CBF3*

6.3.1 Modelling methodology

One of the aims of this study was to model circadian regulation of the cold acclimation pathway. The *CBFs* are central to the cold acclimation pathway and have been shown to be circadian regulated (Fowler et al., 2005). Of the *CBFs*, *CBF3* was chosen to be modelled due to its similarity in expression profile to *CBF1* and *CBF2*, its robust expression under ambient temperatures (Mockler et al., 2007) and the previous success

in the Penfield laboratory in using *CBF3* primers.

Models were designed and created based on prior knowledge from the literature, as well as new freezing tolerance data collected in this study on possible mechanisms of *CBF3* regulation. By using publically available microarray data (Mockler et al., 2007) to optimise the new mathematical models there was no need to create new biological time series of *CBF3* expression. This is important as one of the most time consuming components of modelling biological systems is the collection of data to fit the new models to. The models were optimised to the biological data using the built in PGA optimisation of SBSI to get the parameter values for the newly created models. AICc was then used to rank the models in order of best fit to the biological data. By using this technique a model of best fit can be created without carrying out any new biological experiments and whilst this investigation looked into adding *CBF3* regulation by the circadian clock onto the current P2012 clock model, it can easily be used to model any number of other circadian clock outputs.

6.3.2 Model validation

AICc was used to rank the different models that were created in order of best fit to the microarray data (Mockler et al., 2007) of *CBF3* expression in different day length conditions. Using the P2012 model, EC↓:TOC1↓:LHY↑ regulation of *CBF3* expression was determined to be the model of best fit to the microarray data (**Table 5.4**). The EC↓:TOC1↓:LHY↑ model showed increased *CBF3* expression when simulated with *prp5 prp7 prp9* triple mutant, similar to the observed increase seen biologically (Nakamichi et al., 2009). The EC↓:TOC1↓:LHY↑ model of *CBF3* regulation by the circadian clock was also able to replicate the decrease in *CBF3* expression in *lhy cca1* mutant simulations similar to that previously reported experimentally in the literature (Dong et al., 2011). Whilst non of the models created were capable of completely, correctly, modelling *CBF3* expression in the *prp* triple mutants (there was some rhythmicity remaining in *CBF3* expression biologically (Nakamichi et al., 2009) that was not present in the models), this does not take away from the usefulness of the EC↓:TOC1↓:LHY↑ model. The EC↓:TOC1↓:LHY↑ model was still able to make biologically accurate predictions about the regulation of *CBF3*, such as the increase in *CBF3* expression that was observed in the *toc1-101* loss-of-function mutant, as well as the decrease in *CBF3*

expression that was observed in the *lux-5* loss of function mutant (**Figure 5.12**). This is one of the subjective issues of modelling biological systems; does one strive to create a perfect biological model, or does one aim simply to create a model that approximates biological systems to a sufficient degree to be useful. In this case at least, there was no need to create a model that perfectly replicated the *prp* triple mutant to be useful. Extra time could have been spent trying to modify the model so that the *prp* triple mutant better replicates *CBF3* expression, however, the benefit was not deemed worthy of the time requirement.

As well as the previously reported activation of *CBF* transcription by LHY and CCA1 (Dong et al., 2011), *CBF3* transcription is also inhibited by two evening phase components of the circadian clock, ELF3 as part of the Evening Complex and TOC1. Only the EC↓:TOC1↓:LHY↑ model was able to maintain the correct phase in different photoperiods (**Figure 5.6**) and to qualitatively simulate mutations on clock components on *CBF3* expression (**Figures 5.10 and 5.11**). TOC1 was shown to bind to the *CBF3* promoter region (**Figure 5.14**). The *toc1-101* mutation has a similar effect on *CBF1* and *CBF2* expression as it does *CBF3*, with all three of these *CBFs* having increased transcription in *toc1-101* compared to wild-type plants (Keily et al., 2013). This would suggest that TOC1 is acting to suppress the expression of all three *CBFs* not just *CBF3* as reported here; however, there is no evidence of TOC1 binding near to the *CBF1* and *CBF2* promoter. This may mean that *CBF3* is unique in the *CBFs* in its direct regulation by TOC1, or that TOC1 binding to the *CBF3* promoter, which is a neighbour of *CBF1* and *CBF2* being located immediately 3' to *CBF3* may be enough to confer TOC1 repression of *CBF1* and *CBF2* expression. Alternatively, TOC1 may be acting to repress *CBF1* and *CBF2* indirectly through another factor, such as PIF7 which interacts with TOC1 and has been shown to regulate *CBF* expression (Kidokoro et al., 2009). The Evening Complex was the final component of *CBF3* regulation by the circadian clock that was identified in this study. The very fact that the Evening Complex protein, ELF3, was shown to bind to the *CBF3* promoter (**Figure 5.16**) at a region with no LBS, and that LUX was shown not to bind to the *CBF3* promoter region (**Figure 5.15**) suggests that ELF3 may associate with other DNA binding factors. A likely target for this would be that of phytochromes. Phytochromes have been shown to form complexes with TOC1 both in yeast and *in vivo* (Liu, 2001) and phytochromes have also been shown to regulate the expression of *CBFs* (Franklin and Whitelam, 2007).

6.3.3 Further additions to the *Arabidopsis* circadian clock model of *CBF3* regulation

***CBF3* downstream genes in the model**

In this study a model of *CBF3* regulation by the circadian clock was created using only publically available microarray data of *CBF3* mRNA expression. It would be interesting to see how far we can “stretch” this method of modelling. Can further, downstream, gene regulation be correctly modelled using this technique, such as the *CBF* regulated *COR* genes such as *COR15a*. Based on the model created in this study, it would be useful to try and establish whether *COR* gene expression can be correctly modelled using the model and technique employed in this thesis. Like the *CBF3* microarray data used in this study, *COR* gene expression data under different day length conditions is also contained in the DIURNAL website (diurnal.cgrb.oregonstate.edu (Mockler et al., 2007)). Thus, using the same method as for *CBF3* one can create new models, based on the model of *CBF3* regulation by the clock, in which genes such as *COR15a* have their expression linked to regulation by *CBF3*. As with the *CBF3* models, one would then be able to perturb the model to see how this effects the expression of the *COR* gene being tested and then see how well the model matches the known *COR* gene expression or test, experimentally, to see whether the model matches the biology.

CBF feedback into the model

The circadian clock can be entrained by temperature cycles, though the mechanism by which this occurs is not well understood (Millar, 2004; Salomé and McClung, 2005). *PRR7* and *PRR9* are thought to be important components of the circadian clock for temperature responsiveness in *Arabidopsis* (Salomé and McClung, 2005). It is also known that clock gene expression levels alter greatly between plants that are grown at different temperatures (Gould et al., 2006) and that alternative splicing of genes due to temperature changes is also important for mediating the *Arabidopsis* clock responses at different temperatures (James et al., 2012). As the *CBFs* are one of the core genes that have their regulation altered by temperature changes, it would be interesting to investigate whether there was any feedback into the *Arabidopsis* circadian clock by the *CBFs* to regulate clock responses by temperature. A method to simulate the model

created in this study at different temperatures is discussed above and it would be interesting to see whether the changes seen in clock gene expression at different temperatures can be mimicked in any way by adding clock regulation by the CBFs into the model. If *CBF* expression is altered by low temperature, can adding CBF regulation of the clock genes into the model recreate the known changes in clock gene expression at lower temperatures? This could be tested by creating new models of clock regulation where the *CBF3* expression in the model created in this study feeds back into the clock.

Whilst there is no evidence for *CBFs* affecting the circadian clock, there is evidence that the CBFs are involved in regulating their own expression, as is the cold pathway protein ICE1. *CBF3* transcription is promoted by ICE1 (Chinnusamy et al., 2003) and inhibited by CBF2 (Novillo et al., 2004). In the following sections, the possibility of modelling the circadian regulation of *CBF3* at different temperatures is discussed. At low temperatures it would be beneficial to include *CBF3* regulation by ICE1 and CBF2 in order to produce a more accurate model and more accurate results. The same methodology could be applied from this study to model *CBF2* and *ICE1* expression and use this data to feed into *CBF3* expression when simulating cold temperature regulation.

Additional outputs of the *Arabidopsis* circadian clock

One of the key advantages of the modelling method used in this study is that new models of circadian output can be easily created in the same way without the need to create large time series data sets. In the future it would be interesting to see other circadian clock outputs modelled using the methods described in this study. one such output pathway that can be investigated, for example, is that of *PIF4* and *PIF5* regulation by the circadian clock. These two genes are important for plant growth and have their expression regulated by the circadian clock via LHY/CCA1 (Niwa et al., 2009) and LUX (Nusinow et al., 2011). The circadian regulation of flowering time is another example of a clock output that could simply be adapted from the methodology used here to model *FT* regulation by GI (Mizoguchi et al., 2005). There is an intermediary component of *FT* regulation by the clock in that the clock component GI regulates *CO* expression and *CO* in turn regulates *FT* expression (Mizoguchi et al., 2005). This means that one could simply model *FT* regulation by GI, or model *CO*

expression by GI followed by *FT* regulation by CO. This later modelling protocol would be similar to modelling *CBF3* downstream gene regulation by the circadian clock; as such this protocol has not yet been tested to see how accurate this type of modelling would be using the methods from this study.

6.3.4 Modelling temperature effects

The clock model at different temperatures

Cold pulses have been mimicked in the models created in this study; however, the models that were created have not been simulated at different temperatures. The models created in this study are based on the Pokhilko 2010 and the Pokhilko 2012 *Arabidopsis* circadian clock models, and as such are based on data from observations of *Arabidopsis thaliana* grown at 22°C. A previous study simulated the circadian clock at varying temperatures in a model based on the Locke 2005 circadian clock model (Gould et al., 2006) and the techniques these authors used could be applied to the models presented in this thesis. Simulating the circadian clock model at different temperatures was achieved by altering the transcription rates of core components of the clock, such as *LHY* RNA, so that they matched the altered transcription levels that are observed experimentally at different temperatures (Gould et al., 2006). By changing the transcription levels of the models presented in this thesis, in the same way as Gould et al., so that they mimicked the rates observed in *Arabidopsis* grown at different temperatures one would also be able to mimic the simulation of *CBF3* regulation by the circadian clock at different temperatures using the model present here. This would allow one to investigate the roll of the circadian clock in regulating *CBF3* expression at other temperatures than 22°C to see which genes, if any, play a more or less prominent role in regulating freezing tolerance when *Arabidopsis* is grown at different environmental temperatures. For example, it is known that *LHY*, *CCA1* and *TOC1* mRNA levels are altered in plants grown at different environmental temperatures and it would be interesting to see the effect that this has upon *CBF3* expression in the model created here and how well this mirrors experimentally observed freezing tolerance in *Arabidopsis* grown at different temperatures. To this last point, were there more time to carry out investigations into this subject, recreating the experiment carried out in **Chapter 4.3** looking at the expression of *CBF1* in *Arabidopsis* plants grown at different temperatures, but investigating the expression of

CBF3 instead would be vital data for verifying, or dismissing, the data obtained in the simulations at different temperatures.

Temperature compensation in the clock model

A recently published study has looked into modelling temperature compensation via cryptochrome signalling in the *Arabidopsis* circadian clock (Gould et al., 2013). The authors of this study identified a strong interaction between temperature and blue light signalling in the control of clock period and this resulted in the development of a temperature-compensating model of the *Arabidopsis* circadian clock. The temperature-compensating model was created by adding passive temperature effects through known blue light input pathways in the P2010 model of the circadian clock (Gould et al., 2013). The model was capable of temperature compensation and was consistent with mRNA profiles across a temperature range as well as being able to predict temperature-dependant changes in the level of LHY protein (Gould et al., 2013). Being able to incorporate this temperature compensation into the circadian clock model created in this thesis would be of use for when simulating the model at different temperatures. Therefore, the temperature compensation would have to be incorporated into the P2012 clock model.

By incorporating temperature compensation into the model, one would also be able to ascertain whether the temperature signal component important for compensation (an increase in LHY protein levels at warm temperatures (Gould et al., 2013) that had not been identified prior to the temperature compensation study) played a role in the regulation of *CBFs* at different temperatures that could explain the alterations in *CBF1* levels observed in **Figure 4.5**.

The authors of the P2010 temperature compensated model have already incorporated the temperature compensation into the P2012 model in order to test whether this would better reproduce biological observations (Gould et al., 2013). Some improvements occur when the P2012 model is used instead of the P2010 model, such as improved *LHY* mRNA fitting at 27°C, but that this would come at the expense of other components; in the case of improved *LHY* mRNA fitting, this comes at the expense of two out of *PRR9*, *TOC1* and *GI* mRNA at 27°C, depending on the choice of parameters (Gould et al., 2013). This means that if temperature compensation was to be included in the model created in the model of *CBF3* regulation by the circadian clock, then some of the simulations may not be as accurate as if the P2010 model was

used. This, however, is not a choice that can really be considered, as the P2010 circadian clock models created in this study were not only less capable of simulating *CBF3* expression, they do not have the Evening Complex included in the model, one of the core components of *CBF3* regulation as established by this study.

6.4 Further validation of the role of TOC1 in directly regulating *CBF3* mRNA transcription

The ChIP experiments carried out in this study show that TOC-YFP immunoprecipitates have enriched binding at the putative TOC1-binding site in the *CBF3* promoter T1ME element region that was tested (**Figure 5.14**). To further validate the hypothesis presented in this study that TOC1 directly binds to the *CBF3* promoter region at the T1ME binding site further experiments could be carried out to investigate whether TOC1 is able to bind to other regions of the *CBF3* promoter. Since the completion of this study further ChIP experiments have been carried out by Doctor Dana MacGregor in the Penfield laboratory at the University of Exeter in which TOC1-YFP immunoprecipitates were enriched at the *LHY* promoter T1ME element and the putative TOC1-binding site discussed in this study, but no further enrichment could be found at other sites in the *CBF3* promoter or regions that spanned all three of the *CBF* promoter regions (Keily et al., 2013). This data adds further evidence to the hypothesis that TOC1 interacts directly with the *CBF3* promoter region at the T1ME binding site to act as a transcriptional regulator of *CBF3* expression.

6.5 A systems biology approach to problem solving

This study used a systems biology approach to try and better understand how the circadian clock was involved in regulating the cold acclimation pathway via *CBF3*. **Figure 1.4** shows the basic structure of systems biology that was followed here Using our biological knowledge of *CBF3* expression (**Figure 5.1**) and circadian clock genes that are involved in regulating freezing tolerance (**Figures 4.3 and 4.4**), potential models of *CBF3* regulation were created (**Table 5.3**). These models were then used to create new hypothesis of how perturbations to the clock would affect

CBF3 expression (**Figure 5.11**). Experiments were then designed and carried out to test the hypothesis (**Figures 5.12, 5.14, 5.15 and 5.16**) which resulted in the selection of a model (EC↓:TOC1↓:LHY↑).

By using a systems biology approach, rather than a laboratory-only approach time can be saved by creating and simulating models that can result in the dismissal of potential experiments that the models show will not produce useful data. Another advantage is the discovery on non-intuitive results from models that would not, at first, seem possible; for example, removing components of the Evening Complex (which the data from this study suggests acts as an inhibitor of *CBF3* expression) results in a decrease in *CBF3* expression rather than an increase as one may predict, a problem that can be explained by simulating the clock model with perturbations to different clock components (**Figure 5.20**).

6.6 Thesis summary

To try and discover circadian clock genes that were involved in the regulation of light signalling mediated germination regulation in *Arabidopsis* seeds, several red and far-red light germination assays were carried out. None of the clock genes tested showed any altered far-red light signalling sensitivity. The *TOC1*, gene, however, was shown to be important for the circadian regulation of red light induced germination in freshly harvested imbibed seeds.

The focus of this PhD, and thus this thesis, then moved to the circadian regulation of the cold induced *CBFs*. This study wanted to establish clock components that were involved in regulating freezing tolerance that had not been shown to do so in the past and to use this information to help create a model of the clock regulation of *CBF* expression.

By using the various modelling and experimental techniques discussed in this thesis, the “best” model created was that of the EC↓:TOC1↓:LHY↑ regulation of *CBF3* expression (Figure 6.1). This model had the best AICc score compared to the other models tested as well as having by far the strongest AICc weight assigned to it. This model was also the only model that was able to not only keep the same phase and period as the biological data for *CBF3* expression in simulations of four different day length periods, but, with the inclusion of the Evening Complex as an inhibitor of

expression it was also able to mimic the sharp peak in expression that was seen in the biological data that occurred eight hours after dawn. This model was also able to qualitatively replicate an increase in *CBF3* expression in *prp5 prp7 prp9* triple mutants and a decrease in expression in *lhy cca1* double mutant simulations. The EC↓:TOC1↓:LHY↑ model also predicted that *toc1* mutant plants would have an increase in *CBF3* expression, which was experimentally validated, as well as severely decreased *CBF3* expression in *lux* mutant plants. Whilst the *CBF3* reduction seen experimentally in *lux-5* plants was not as severe as that predicted in the model, it still was a correct prediction of a reduction of *CBF3* expression, something that not all of the potential models predicted. The new connections to *CBF3* regulation that the EC↓:TOC1↓:LHY↑ predicted (TOC1 and the Evening Complex) were then further confirmed as direct regulators of *CBF3* expression via the use of chromatin immunoprecipitation which showed binding of TOC1 and the Evening Complex protein ELF3 to the *CBF3* promoter. That the model optimisation and model selection techniques used here based on publically available microarray data resulted in the successful discovery of new regulatory components validates this method for future work in creating gene regulatory networks.

This work shows that the use of publically available microarray data, rather than having to create new RT-PCR gene expression data, to optimise model parameters and for use in model selection can result in mathematical models of biological systems that can be used to make accurate predictions about the biological system they are modelling. This is exciting as there is a vast quantity of microarray data on genes that show circadian rhythmicity, which means that the approach used here can be used to help us understand the control of other circadian outputs.

Acknowledgements

I would like to thank Steven Penfield and the members of the Penfield Laboratory, especially Dana Macgregor and Kate Sidaway-Lee, Karren Halliday and the ROBuST group, especially Robert Smith, The University of York and the University of Exeter and the BBSRC for funding me.

Appendix

AICc Matlab Code. The Matlab code for simulating the AICc was coded by Robert Smith at the University of Edinburgh. It is split into five separate files that are presented below.

1) AICcU_PROB.m

```
function Q = AICcU_PROB(Simulation,tau2,tau)

nsimulation = length(Simulation);

%mu = mean(Simulation); %Straight line prior model
x = 0:(pi/3):2*pi; %sinewave prior model
sinewave = 0.5*(sin(x-pi/6)+1); %this sinewave will peak at ZT8 like the
12L:12D data

SimDiff = 0;
for j = 1:((nsimulation+1)/2)
    SimDiff = SimDiff + (Simulation(j)-sinewave(j))^2;
end

if (tau == 0)
tau2 = SimDiff/((nsimulation+1)/2);
end
    %If you want tau2 to be calculated using MLE (see Akaike_Weights.m
    %notes) then remove percent sign before tau2.
Q = log(tau2) + SimDiff/tau2;

end
```

2) Akaike.m

```
function [AICc,AICc_Endpoint] = Akaike(SimTime,Simulation,Data)
% Calculating information criterions and then summing the values due to the
% logarithmic form. Formula for AICc taken from Wu et al. (1997).

ndata = length(Data(:,1));
ndataserie = length(Data(1,:));
nsimulation = length(SimTime);
Difference = zeros(ndata-1,ndataserie-1);
RawAICc = zeros(1,ndataserie-1);
EndpointAICc = zeros(1,ndataserie-1);

for l=2:ndataserie
for i=1:nsimulation
    for j=1:(ndata-1)
        if (SimTime(i) == Data(j,1))
            Difference(j,l-1)=(Data(j,l)-Simulation(i))^2;
            %Calculates square difference between data and simulation at
            %specific time points.
        end
    end
end
resvar=(sum(Difference(:,l-1)))/(ndata-1);
RawAICc(1,l-1) = (ndata-1)*log(resvar);
EndpointAICc(1,l-1) = log(Difference(1,l-1));
%Calculates nlog(sigma^2) for one data series in one photoperiod.
end

AICc=sum(RawAICc);
AICc_Endpoint=sum(EndpointAICc);
%This sums all the AICc values from one photoperiod dataset such that we
```



```
%have n1*log(sigma1^2)+n2*log(sigma2^2)+...
```

```
end
```

3) Akaike_Weights.m

```
function
```

```
[IC,DELTA,WEIGHTS,AIC_PROBS,AICcU_DELTA,AICcU_WEIGHTS]=Akaike_Weights(LC,ta  
u)
```

```
% Code to compute Akaike Distance Matrix (ADM) and Akaike Weight Matrix  
% (AWM). n corresponds to number of days of limit cycle passed. Infomation  
% Criterion are then computed for the models, before distance and weight  
% matrices are computed to determine how good models are in comparison with  
% each other. LC is number of data limit cycles needed so  $n > k+2$ , where k  
% is the number of parameters.  
% Clock=0 if you don't want to take into account internal clock errors,  
% Clock=1 if you do.
```

```
%Load matrices of model simulations, the ordering of simulations within the  
%matrix is unimportant at this stage.
```

```
load '..\CBF Simulations\A'  
load '..\CBF Simulations\B'  
load '..\CBF Simulations\C'  
load '..\CBF Simulations\G'  
load '..\CBF Simulations\H'  
load '..\CBF Simulations\I'  
load '..\CBF Simulations\J'  
load '..\CBF Simulations\K'  
load '..\CBF Simulations\L'  
load '..\CBF Simulations\M'  
load '..\CBF Simulations\N'  
load '..\CBF Simulations\O'  
load '..\CBF Simulations\P'
```

```
if (tau == 1)
```

```
    for t = 1:51
```

```
        if (t < 12)
```

```
            tau2 = t/20 - 0.05;
```

```
        else
```

```
            tau2 = t/5 - 0.2;
```

```
        end
```

```
        IC = zeros(2,13); % Columns for Model_03 AICc, the 14 changes depending  
on how many
```

```
%models are being tested.
```

```
% [IC(1,:)] = InformationCriterion(k,model,clock,LC)
```

```
[IC(1,1) IC(2,1)] = InformationCriterion(124,A,LC,tau2,tau);
```

```
[IC(1,2) IC(2,2)] = InformationCriterion(124,B,LC,tau2,tau);
```

```
[IC(1,3) IC(2,3)] = InformationCriterion(126,C,LC,tau2,tau);
```

```
[IC(1,4) IC(2,4)] = InformationCriterion(126,G,LC,tau2,tau);
```

```
[IC(1,5) IC(2,5)] = InformationCriterion(130,H,LC,tau2,tau);
```

```
[IC(1,6) IC(2,6)] = InformationCriterion(124,I,LC,tau2,tau);
```

```
[IC(1,7) IC(2,7)] = InformationCriterion(124,J,LC,tau2,tau);
```

```
[IC(1,8) IC(2,8)] = InformationCriterion(124,K,LC,tau2,tau);
```

```
[IC(1,9) IC(2,9)] = InformationCriterion(124,L,LC,tau2,tau);
```

```
[IC(1,10) IC(2,10)] = InformationCriterion(124,M,LC,tau2,tau);
```

```
[IC(1,11) IC(2,11)] = InformationCriterion(128,N,LC,tau2,tau);
```

```
[IC(1,12) IC(2,12)] = InformationCriterion(126,O,LC,tau2,tau);
```

```
[IC(1,13) IC(2,13)] = InformationCriterion(126,P,LC,tau2,tau);
```

```

%AICc_min.
ICmin = min(IC(1,:));
AICcUmin = min(IC(2,:));

DELTA=zeros(1,13);
%Calculates Delta_Model_03 AICc = Model_03 AICc_i - Model_03 AICc_min.
for j = 1:13
    DELTA(1,j) = IC(1,j) - ICmin;
    AICcU_DELTA(t,j) = IC(2,j) - AICcUmin;
end

expsum = 0;
AICcU_expsum = 0;
%Calculates denominator of p(M).
for j=1:13
    expsum = expsum + exp(-DELTA(1,j)/2);
    AICcU_expsum = AICcU_expsum + exp(-AICcU_DELTA(t,j)/2);
end

WEIGHTS = zeros(1,13);
%Calculates p(M).
for j=1:13
    WEIGHTS(1,j) = exp(-DELTA(1,j)/2)/expsum;
    AICcU_WEIGHTS(t,j) = exp(-AICcU_DELTA(t,j)/2)/AICcU_expsum;
end

AIC_PROBS = zeros(13,13);
%Calculates how much better one model is than another in a pairwise way.
for i=1:13
    for j=1:13
        AIC_PROBS(i,j) = WEIGHTS(1,i)/WEIGHTS(1,j);
    end
end
end
elseif (tau == 0)
    tau2 = 0;
    IC = zeros(2,13); % Columns for Model_03 AICc, the 14 changes depending on
    how many
    %models are being tested.
    % [IC(1,:)] = InformationCriterion(k,model,clock,LC)
    [IC(1,1) IC(2,1)] = InformationCriterion(124,A,LC,tau2,tau);
    [IC(1,2) IC(2,2)] = InformationCriterion(124,B,LC,tau2,tau);
    [IC(1,3) IC(2,3)] = InformationCriterion(126,C,LC,tau2,tau);
    [IC(1,4) IC(2,4)] = InformationCriterion(126,G,LC,tau2,tau);
    [IC(1,5) IC(2,5)] = InformationCriterion(130,H,LC,tau2,tau);
    [IC(1,6) IC(2,6)] = InformationCriterion(124,I,LC,tau2,tau);
    [IC(1,7) IC(2,7)] = InformationCriterion(124,J,LC,tau2,tau);
    [IC(1,8) IC(2,8)] = InformationCriterion(124,K,LC,tau2,tau);
    [IC(1,9) IC(2,9)] = InformationCriterion(124,L,LC,tau2,tau);
    [IC(1,10) IC(2,10)] = InformationCriterion(124,M,LC,tau2,tau);
    [IC(1,11) IC(2,11)] = InformationCriterion(128,N,LC,tau2,tau);
    [IC(1,12) IC(2,12)] = InformationCriterion(126,O,LC,tau2,tau);
    [IC(1,13) IC(2,13)] = InformationCriterion(126,P,LC,tau2,tau);

%AICc_min.
ICmin = min(IC(1,:));
AICcUmin = min(IC(2,:));

DELTA=zeros(1,13);

```

```

AICcU_DELTA=zeros(1,13);
%Calculates Delta_Model_03 AICc = Model_03 AICc_i - Model_03 AICc_min.
for j = 1:13
    DELTA(1,j) = IC(1,j) - ICmin;
    AICcU_DELTA(1,j) = IC(2,j) - AICcUmin;
end

expsum = 0;
AICcU_expsum = 0;
%Calculates denominator of p(M).
for j=1:13
    expsum = expsum + exp(-DELTA(1,j)/2);
    AICcU_expsum = AICcU_expsum + exp(-AICcU_DELTA(1,j)/2);
end

WEIGHTS = zeros(1,13);
AICcU_WEIGHTS = zeros(1,13);
%Calculates p(M).
for j=1:13
    WEIGHTS(1,j) = exp(-DELTA(1,j)/2)/expsum;
    AICcU_WEIGHTS(1,j) = exp(-AICcU_DELTA(1,j)/2)/AICcU_expsum;
end

AIC_PROBS = zeros(13,13);
%Calculates how much better one model is than another in a pairwise way.
for i=1:13
    for j=1:13
        AIC_PROBS(i,j) = WEIGHTS(1,i)/WEIGHTS(1,j);
    end
end
end

end
end
end

```

4) InformationCriterion.m

```

function [fullAICc
fullAICcU]=InformationCriterion(k,Simulation,LC,tau2,tau)
%Program calculates values of AICc for a simulation of a model
%with k parameters. Set Clock = 0 if you do not wish to include clock
%information, Clock = 1 otherwise. LC is the number of limit cycles needed
%such that the number of data points n > k + 2, k = number of parameters.

%Loading of data files for each photoperiod being analysed.
load '..\CBF Data\CBF_SD'
load '..\CBF Data\CBF_1212'
load '..\CBF Data\CBF_LD'
load '..\CBF Data\CBF_LL'

Data1=CBF_SD;
Data2=CBF_1212;
Data3=CBF_LD;
Data4=CBF_LL;

%It is important here to know which column of the model matrices (see
%Akaike_Weights) refer to which photoperiod, this will need to be changed
%accordingly in the second entry of Akaike.

```

```

%[] = Akaike(Time column of model matrix, photoperiod simulation, datafile)
[ASD,ASDe] = Akaike(Simulation(1:7,1),Simulation(1:7,2),Data1);
[A1212,A1212e] = Akaike(Simulation(1:7,1),Simulation(1:7,3),Data2);
[ALD,ALDe] = Akaike(Simulation(1:7,1),Simulation(1:7,4),Data3);
[ALL,ALLe] = Akaike(Simulation(1:7,1),Simulation(1:7,5),Data4);

AICc = [ASD,A1212,ALD,ALL];
AICcE = [ASDe,A1212e,ALDe,ALLe];
%AICc = [A8,A12,A16,ALL];

%Since result of Akaike is logarithmic, this can be added together for each
%dataset to be used before penalised for complexity.
sumAICc = sum(AICc);
sumAICcE = sum(AICcE);
q = AICcU_PROB(Simulation(:,3),tau2,tau); %Only used for 12L:12D data since
this is what model was optimised to.

%In this loop two values may need to be changed. First, the restriction k <
%80 - the 80 has been used arbitrarily for the PIF example as no models
%featuring the Locke clock have k > 70, and no Pokhilko models have k < 90,
%so k = 80 is used to determine whether the Locke or Pokhilko clock has
%been used. The values of 98 and 180 are the number of data points being
%used from one limit cycle, these can then be extrapolated for many limit
%cycles since it doesn't affect the number coming from the Akaike program.
%If Clock = 1, then simulations and data of clock components TOC1 and CCA1
%are included, adding on to AICc values of output.
    fullAICc = LC*sumAICc + sumAICcE + 2*(LC*84+14)*(k+1)/(LC*84 + 14 - k -
2); %84 timepoints in data + 1 endpoint of 14 datasets to give full limit
cycles.
    fullAICcU = LC*sumAICc + sumAICcE + q + 2*(LC*84+14)*(k+1)/(LC*84 + 14
- k - 2);
    %fullAICc = LC*sumAICc + 2*LC*97*(k+1)/(LC*97 - k - 2);
end

```

5) Cost.m

```

function [normCost normCorr]=Cost(Simulation)
% Calculates cost functions for model. 'Simulation' should be a matrix with
% time in first column and simulations for photoperiods in further columns.

load '..\CBF Data\CBF_SD.mat'
load '..\CBF Data\CBF_1212.mat'
load '..\CBF Data\CBF_LD.mat'
load '..\CBF Data\CBF_LL.mat'

Data1=CBF_SD;
Data2=CBF_1212;
Data3=CBF_LD;
Data4=CBF_LL;

%photoperiodcost=zeros(3,1);
%photoperiodcorr=zeros(3,1);
photoperiodcost=zeros(4,1);
photoperiodcorr=zeros(4,1);

[photoperiodcost(1,1)
photoperiodcorr(1,1)]=rawCost(Simulation(:,1),Simulation(:,2),Data1);

```

```
[photoperiodcost(2,1)
photoperiodcorr(2,1)]=rawCost(Simulation(:,1),Simulation(:,3),Data2);
[photoperiodcost(3,1)
photoperiodcorr(3,1)]=rawCost(Simulation(:,1),Simulation(:,4),Data3);
[photoperiodcost(4,1)
photoperiodcorr(4,1)]=rawCost(Simulation(:,1),Simulation(:,5),Data4);
%The simulation column should be from the same photoperiod as the data it
%is being compared to!

%avgfactor = 3; %number of photoperiods used.
avgfactor = 4;
normCorr = sum(photoperiodcorr)/avgfactor;
normCost = sum(photoperiodcost)/avgfactor;

end
```

Table 1 Optimised parameter values for *CBF3* mRNA expression in the Pokhilko 2010 model.

TOC1↓ Parameter mC1: nC1: gC1:	Value 2.064122316 5 0.087795457	TOC1↓: TOC1mod↓ Parameter mC1: nC1: gC1: gC2:	Value 2.235363582 5 0.096758544 0.350039948
LHY↑ Parameter mC1: nC1: gC1:	Value 0.169585805 0.087516635 0.232468382	TOC1↓ : LHY↑ Parameter nC1: gC1: gC2: mC1:	Value 5 0.093452216 0.080170123 1.296333825
NI↓:PRR7↓:PRR9↓ Parameter mC1: nC1: gC1: gC2: gC3:	Value 0.113054588 0.038400874 5 5 0.350197497	NI↓ : PRR7↓ : PRR9↓ : LHY↑ Parameter mC1: nC1: gC1: gC2: gC3: gC4:	Value 0.096679307 2.975780682 5 5 4.408228914 3.620009136
NI↓ Parameter mC1: nC1: gC1:	Value 1.321180249 0.237142524 5	PRR7↓ Parameter mC1: nC1: gC1:	Value 0.482970113 0.086621216 5
PRR9↓ Parameter mC1: nC1: gC1:	Value 5 0.895287105 5	PRR7↓ : PRR9↓ Parameter mC1: nC1: gC1: gC2:	Value 0.563237458 0.10131118 5 5
NI↓ : PRR9↓ Parameter mC1: nC1: gC1: gC2:	Value 0.122070901 0.039119342 5 0.391315958		

Table 2 Optimised parameter values for *CBF3* mRNA expression in the Pokhilko 2012 model.

TOC1↓		LHY/CCA1↑	
Parameter	Parameter Value	Parameter	Parameter Value
mC1	0.2746	mC1	0.2176
nC1	5	nC1	0.2419
gC1	0.0081	gC1	0.7667
aC	2	aC	2
LHY/CCA1↑:TOC1↓		NI↓:PRR7↓:PRR9↓	
Parameter	Parameter Value	Parameter	Parameter Value
mC1	0.235	mC1	0.0583
nC1	4.9751	nC1	0.5224
gC1	0.0103	gC1	5
gC2	0.4754	gC2	5
aC	2	gC3	0.027
bC	2	aC	2
		bC	2
		cC	2
LHY/CCA1↑:NI↓:PRR7↓:PRR9↓		NI↓	
Parameter	Parameter Value	Parameter	Parameter Value
mC1	0.2059	mC1	0.3682
nC1	0.2608	nC1	0.0711
gC1	5	gC1	5
gC2	5	aC	2
gC3	5		
gC4	0.8186		
aC	2		
bC	2		
cC	2		
dC	2		
PRR7↓		PRR9↓	
Parameter	Parameter Value	Parameter	Parameter Value
mC1	0.2683	mC1	5
nC1	0.0511	nC1	0.9475
gC1	5	gC1	5
aC	2	aC	2
EC↓		EC↑	
Parameter	Parameter	Parameter	Parameter

	Value		Value
mC1	2.3963	mC1	0.025
nC1	5	nC1	4.7871
gC1	0.0002	gC1	1.9305
aC	2	aC	2
EC↓:TOC1↓:LHY↑		EC↓:LHY↑	
Parameter	Parameter Value	Parameter	Parameter Value
mC1	1.407	mC1	2.039
nC1	4.9967	nC1	5
gC1	0.0434	gC1	0.0003
gC2	0.0005	gC2	0.402
gC4	0.1344	aC	2
aC	2	bC	2
bC	2		
dC	2		
EC↓:TOC1↓			
Parameter	Parameter Value		
mC1	1.9056		
nC1	3.9652		
gC1	0.0004		
gC2	0.0723		
aC	2		
bC	2		

Bibliography

Abe, H., Yamaguchi-Shinozaki, K., Urao, T., Iwasaki, T., Hosokawa, D. and Shinozaki, K. (1997). Role of arabidopsis MYC and MYB homologs in drought- and abscisic acid-regulated gene expression. *The Plant cell* *9*, 1859–68.

Abe, M., Kobayashi, Y., Yamamoto, S., Daimon, Y., Yamaguchi, A., Ikeda, Y., Ichinoki, H., Notaguchi, M., Goto, K. and Araki, T. (2005). FD, a bZIP protein mediating signals from the floral pathway integrator FT at the shoot apex. *Science* *309*, 1052–6.

Adams, R., Clark, A., Yamaguchi, A., Hanlon, N., Tsorman, N., Ali, S., Lebedeva, G., Goltsov, A., Sorokin, A., Akman, O. E., Troein, C., Millar, A. J., Goryanin, I. and Gilmore, S. (2013). SBSI: an extensible distributed software infrastructure for parameter estimation in systems biology. *Bioinformatics (Oxford, England)* *29*, 664–5.

Agarwal, M., Hao, Y., Kapoor, A., Dong, C.-H., Fujii, H., Zheng, X. and Zhu, J.-K. (2006). A R2R3 type MYB transcription factor is involved in the cold regulation of CBF genes and in acquired freezing tolerance. *The Journal of Biological Chemistry* *281*, 37636–37645.

Akaike, H. (1974). A new look at the statistical model identification. *IEEE Transactions on Automatic Control* *19*, 716–723.

Alabadí, D., Oyama, T., Yanovsky, M. J., Harmon, F. G., Más, P. and Kay, S. A. (2001). Reciprocal regulation between TOC1 and LHY/CCA1 within the Arabidopsis circadian clock. *Science* *293*, 880–883.

Allen, M. D., Yamasaki, K., Ohme-Takagi, M., Tateno, M. and Suzuki, M. (1998). A novel mode of DNA recognition by a beta-sheet revealed by the solution structure of the GCC-box binding domain in complex with DNA. *The EMBO journal* *17*, 5484–96.

Ay, A. and Arnosti, D. N. (2011). *Mathematical modeling of gene expression : a guide*

Bibliography

for the perplexed biologist. *Critical Reviews in Biochemistry and Molecular Biology* 46, 137–151.

Bae, G. and Choi, G. (2008). Decoding of light signals by plant phytochromes and their interacting proteins. *Annual Review of Plant Biology* 59, 281–311.

Bao, X., Franks, R. G., Levin, J. Z. and Liu, Z. (2004). Repression of AGAMOUS by BELLRINGER in Floral and Inflorescence Meristems. *The Plant cell* 16, 1478–1489.

Baudry, A., Ito, S., Song, Y. H., Strait, A. A., Kiba, T., Lu, S., Henriques, R., Pruneda-Paz, J. L., Chua, N.-H., Tobin, E. M., Kay, S. A. and Imaizumi, T. (2010). F-box proteins FKF1 and LKP2 act in concert with ZEITLUPE to control Arabidopsis clock progression. *The Plant Cell* 22, 606–22.

Berson, D. M., Dunn, F. A. and Takao, M. (2002). Phototransduction by retinal ganglion cells that set the circadian clock. *Science* 295, 1070–3.

Bertsimas, D. and Tsitsiklis, J. (1993). Simulated annealing. *Statistical science* 8, 10–15.

Bewley, J. D. (1997). Seed germination and dormancy. *The Plant Cell* 9, 1055–1066.

Bhardwaj, V., Meier, S., Petersen, L. N., Ingle, R. A. and Roden, L. C. (2011). Defence responses of Arabidopsis thaliana to infection by Pseudomonas syringae are regulated by the circadian clock. *PloS one* 6, e26968.

Borthwick, H. A., Hendricks, S. B., Parker, M. W., Toole, E. H. and Toole, V. K. (1952). A reversible photoreaction controlling seed germination. *Proceedings of the National Academy of Sciences* 38, 662–666.

Brian, P. W. (1959). Effects of Gibberellins on Plant Growth and Development. *Biological Reviews* 34, 37–77.

Burnham, K. P. and Anderson, D. (2004). Multimodel inference: Understanding AIC and BIC in model selection. *Sociological Methods & Research* 33, 261–304.

Canella, D., Gilmour, S. J., Kuhn, L. a. and Thomashow, M. F. (2010). DNA binding by the Arabidopsis CBF1 transcription factor requires the PKKP/RAGR_xKF_xETRHP signature sequence. *Biochimica et biophysica acta* 1799, 454–62.

Bibliography

- Cao, S., Ye, M. and Jiang, S. (2005). Involvement of GIGANTEA gene in the regulation of the cold stress response in Arabidopsis. *Plant Cell Reports* 24, 683–690.
- Carpenter, C. D., Kreps, J. A. and Simon, A. E. (1994). Genes encoding glycine-rich Arabidopsis thaliana proteins with RNA-binding motifs are influenced by cold treatment and an endogenous circadian rhythm. *Plant Physiology* 104, 1015–1025.
- Casimiro, I., Beeckman, T., Graham, N., Bhalerao, R., Zhang, H., Casero, P., Sandberg, G. and Bennett, M. J. (2003). Dissecting Arabidopsis lateral root development. *Trends in plant science* 8, 165–71.
- Chan, C. S., Guo, L. and Shih, M. C. (2001). Promoter analysis of the nuclear gene encoding the chloroplast glyceraldehyde-3-phosphate dehydrogenase B subunit of Arabidopsis thaliana. *Plant molecular biology* 46, 131–41.
- Chen, W., Provar, N. J., Glazebrook, J., Katagiri, F., Chang, H.-s., Eulgem, T., Mauch, F., Luan, S., Zou, G., Whitham, S. A., Budworth, P. R., Tao, Y., Xie, Z., Chen, X., Lam, S., Kreps, J. A., Harper, J. F., Si-ammour, A., Mauch-mani, B., Heinlein, M., Kobayashi, K., Hohn, T., Dangl, J. L., Wang, X. and Zhu, T. (2002). Expression Profile Matrix of Arabidopsis Transcription Factor Genes Suggests Their Putative Functions in Response to Environmental Stresses. *The Plant cell* 14, 559–574.
- Chiang, G. C. K., Barua, D., Kramer, E. M., Amasino, R. M. and Donohue, K. (2009). Major flowering time gene, flowering locus C, regulates seed germination in Arabidopsis thaliana. *Proceedings of the National Academy of Sciences* 106, 11661–6.
- Chinnusamy, V., Ohta, M., Kanrar, S., Lee, B.-H., Hong, X., Agarwal, M. and Zhu, J.-K. (2003). ICE1: a regulator of cold-induced transcriptome and freezing tolerance in Arabidopsis. *Genes & Development* 17, 1043–1054.
- Choi, H.-i. (2000). ABFs, a Family of ABA-responsive Element Binding Factors. *Journal of Biological Chemistry* 275, 1723–1730.
- Chow, B. Y., Helfer, A., Nusinow, D. A. and Kay, S. A. (2012). ELF3 recruitment to the PRR9 promoter requires other Evening Complex members in the Arabidopsis circadian clock. *Plant Signaling & Behavior* 7, 170–173.
- Claeskens, G. and Hjort, N. L. (2003). The focused information criterion. *Journal of the American Statistical Association* 98, 900–916.

Bibliography

- Corbesier, L., Vincent, C., Jang, S., Fornara, F., Fan, Q., Searle, I., Giakountis, A., Farrona, S., Gissot, L., Turnbull, C. and Coupland, G. (2007). FT protein movement contributes to long-distance signaling in floral induction of *Arabidopsis*. *Science* *316*, 1030–3.
- Covington, M. F. (2001). ELF3 modulates resetting of the circadian clock in *Arabidopsis*. *The Plant Cell* *13*, 1305–1316.
- Covington, M. F. and Harmer, S. L. (2007). The circadian clock regulates auxin signaling and responses in *Arabidopsis*. *PLoS Biology* *5*, 1773–1784.
- Czeisler, C. A., Duffy, J. F., Shanahan, T. L., Brown, E. N., Mitchell, J. F., Rimmer, D. W., Ronda, J. M., Silva, E. J., Allan, J. S., Emens, J. S., Dijk, D.-J. and Kronauer, R. E. (1999). Stability, precision, and near-24-hour period of the human circadian pacemaker. *Science* *284*, 2177–2181.
- Daniel, X., Sugano, S. and Tobin, E. M. (2004). CK2 phosphorylation of CCA1 is necessary for its circadian oscillator function in *Arabidopsis*. *Proceedings of the National Academy of Sciences* *101*, 3292–3297.
- De Jong, H. (2002). Modeling and simulation of genetic regulatory systems : A literature review. *Journal of Computational Biology* *9*, 67–103.
- de Lucas, M., Davière, J.-M., Rodríguez-Falcón, M., Pontin, M., Iglesias-Pedraz, J. M., Lorrain, S., Fankhauser, C., Blázquez, M. A., Titarenko, E. and Prat, S. (2008). A molecular framework for light and gibberellin control of cell elongation. *Nature* *451*, 480–4.
- Devlin, P. F. and Kay, S. A. (2001). Circadian Photoperception. *Annual Review of Physiology* *63*, 677–694.
- Dixon, L. E., Knox, K., Kozma-Bognar, L., Southern, M. M., Pokhilko, A. and Millar, A. J. (2011). Temporal repression of core circadian genes is mediated through EARLY FLOWERING 3 in *Arabidopsis*. *Current Biology* *21*, 120–125.
- Dodd, A. N., Kusakina, J., Hall, A., Gould, P. D. and Hanaoka, M. (2013). The circadian regulation of photosynthesis. *Photosynthesis research* *Published*.
- Dodd, A. N., Salathia, N., Hall, A., Kevei, E., Toth, R., Nagy, F., Hibberd, J. M.,

Bibliography

- Millar, A. J. and Webb, A. a. R. (2005). Plant circadian clocks increase photosynthesis, growth, survival, and competitive advantage. *Science* *309*, 630–633.
- Doherty, C. J., Van Buskirk, H. a., Myers, S. J. and Thomashow, M. F. (2009). Roles for Arabidopsis CAMTA transcription factors in cold-regulated gene expression and freezing tolerance. *The Plant Cell* *21*, 972–984.
- Dong, C.-H., Agarwal, M., Zhang, Y., Xie, Q. and Zhu, J.-K. (2006). The negative regulator of plant cold responses, HOS1, is a RING E3 ligase that mediates the ubiquitination and degradation of ICE1. *Proceedings of the National Academy of Sciences* *103*, 8281–8286.
- Dong, M. A., Farre, E. M. and Thomashow, M. F. (2011). CIRCADIAN CLOCK-ASSOCIATED 1 and LATE ELONGATED HYPOCOTYL regulate expression of the C-REPEAT BINDING FACTOR (CBF) pathway in Arabidopsis. *Proceedings of the National Academy of Sciences* *108*, 7241–7246.
- Donohue, K., Heschel, M. S., Butler, C. M., Barua, D., Sharrock, R. a., Whitelam, G. C. and Chiang, G. C. K. (2008). Diversification of phytochrome contributions to germination as a function of seed-maturation environment. *New Phytologist* *177*, 367–79.
- Dowson-Day, M. J. and Millar, A. J. (1999). Circadian dysfunction causes aberrant hypocotyl elongation patterns in Arabidopsis. *The Plant Journal* *17*, 63–71.
- Espinoza, C., Degenkolbe, T., Caldana, C., Zuther, E., Leisse, A., Willmitzer, L., Hinch, D. K. and Hannah, M. A. (2010). Interaction with Diurnal and Circadian Regulation Results in Dynamic Metabolic and Transcriptional Changes during Cold Acclimation in Arabidopsis. *PloS One* *5*, e14101.
- Farré, E. M., Harmer, S. L., Harmon, F. G., Yanovsky, M. J. and Kay, S. A. (2005). Overlapping and distinct roles of PRR7 and PRR9 in the Arabidopsis circadian clock. *Current Biology* *15*, 47–54.
- Filichkin, S. A., Priest, H. D., Givan, S. A., Shen, R., Bryant, D. W., Fox, S. E., Wong, W.-K. and Mockler, T. C. (2010). Genome-wide mapping of alternative splicing in Arabidopsis thaliana. *Genome Research* *20*, 45–58.
- Finch-Savage, W. E., Cadman, C. S. C., Toorop, P. E., Lynn, J. R. and Hilhorst, H. W. M. (2007). Seed dormancy release in Arabidopsis Cvi by dry after-ripening, low

Bibliography

- temperature, nitrate and light shows common quantitative patterns of gene expression directed by environmentally specific sensing. *The Plant Journal* 51, 60–78.
- Finch-Savage, W. E. and Leubner-Metzger, G. (2006). Seed dormancy and the control of germination. *The New Phytologist* 171, 501–523.
- Fleming, A. J. (2005). Formation of primordia and phyllotaxy. *Current opinion in plant biology* 8, 53–8.
- Fowler, S. G., Cook, D. and Thomashow, M. F. (2005). Low temperature induction of Arabidopsis CBF1, 2, and 3 is gated by the circadian clock. *Plant Physiology* 137, 961–968.
- Franklin, K. A. and Whitelam, G. C. (2007). Light-quality regulation of freezing tolerance in Arabidopsis thaliana. *Nature genetics* 39, 1410–1413.
- Fujiwara, S., Wang, L., Han, L., Suh, S.-S., Salomé, P. A., McClung, C. R. and Somers, D. E. (2008). Post-translational regulation of the Arabidopsis circadian clock through selective proteolysis and phosphorylation of pseudo-response regulator proteins. *The Journal of Biological Chemistry* 283, 23073–23083.
- Gardner, M. J., Hubbard, K. E., Hotta, C. T., Dodd, A. N. and Webb, A. A. R. (2006). How plants tell the time. *The Biochemical Journal* 397, 15–24.
- Gendron, J. M., Pruneda-Paz, J. L., Doherty, C. J., Gross, A. M., Kang, S. E. and Kay, S. A. (2012). Arabidopsis circadian clock protein, TOC1, is a DNA-binding transcription factor. *Proceedings of the National Academy of Sciences* 109, 3167–3172.
- Gilmour, S. J., Hajela, R. K. and Thomashow, M. F. (1988). Cold acclimation in Arabidopsis thaliana. *Plant Physiology* 87, 745–750.
- Gilmour, S. J., Zarka, D. G., Stockinger, E. J., Salazar, M. P., Houghton, J. M. and Thomashow, M. F. (1998). Low temperature regulation of the Arabidopsis CBF family of AP2 transcriptional activators as an early step in cold-induced COR gene expression. *The Plant Journal* 16, 433–442.
- Gilroy, S., Read, N. D. and Trewavas, A. J. (1990). Elevation of cytoplasmic calcium by caged calcium or caged inositol triphosphate initiates stomatal closure. *Nature* 346, 769–771.

Bibliography

- Goldberg, D. E. (1989). *Genetic Algorithms in Search, Optimization and Machine Learning*. Addison Wesley.
- Goodspeed, D., Chehab, E. W., Min-Venditti, A., Braam, J. and Covington, M. F. (2012). Arabidopsis synchronizes jasmonate-mediated defense with insect circadian behavior. *Proceedings of the National Academy of Sciences of the United States of America* *109*, 4674–7.
- Gould, P. D., Diaz, P., Hogben, C., Kusakina, J., Salem, R., Hartwell, J. and Hall, A. (2009). Delayed fluorescence as a universal tool for the measurement of circadian rhythms in higher plants. *The Plant journal : for cell and molecular biology* *58*, 893–901.
- Gould, P. D., Locke, J. C. W., Larue, C., Southern, M. M., Davis, S. J., Hanano, S., Moyle, R., Milich, R., Putterill, J., Millar, A. J. and Hall, A. (2006). The molecular basis of temperature compensation in the Arabidopsis circadian clock. *The Plant Cell* *18*, 1177–1187.
- Gould, P. D., Ugarte, N., Domijan, M., Costa, M., Foreman, J., MacGregor, D., Rose, K., Griffiths, J., Millar, A. J., Finkenstädt, B., Penfield, S., Rand, D. A., Halliday, K. J. and Hall, A. J. W. (2013). Network balance via CRY signalling controls the Arabidopsis circadian clock over ambient temperatures. *Molecular systems biology* *9*, 650.
- Graf, A., Schlereth, A., Stitt, M. and Smith, A. M. (2010). Circadian control of carbohydrate availability for growth in Arabidopsis plants at night. *Proceedings of the National Academy of Sciences of the United States of America* *107*, 9458–63.
- Halberg, F. (1959). Physiologic 24-hour periodicity; general and procedural considerations with reference to the adrenal cycle. *Internationale Zeitschrift für Vitaminforschung* *10*, 225–296.
- Hanaoka, M., Kato, M., Anma, M. and Tanaka, K. (2012). SIG1, a Sigma Factor for the Chloroplast RNA Polymerase, Differently Associates with Multiple DNA Regions in the Chloroplast Chromosomes in Vivo. *International journal of molecular sciences* *13*, 12182–94.
- Harmer, S. L. (2009). The circadian system in higher plants. *Annual Review of Plant Biology* *60*, 357–377.

Bibliography

- Harmer, S. L., Hogenesch, J. B., Straume, M., Chang, H. S., Han, B., Zhu, T., Wang, X., Kreps, J. A. and Kay, S. A. (2000). Orchestrated transcription of key pathways in Arabidopsis by the circadian clock. *Science* *290*, 2110–2113.
- Harms, E., Kivimäe, S., Young, M. W. and Saez, L. (2004). Posttranscriptional and posttranslational regulation of clock genes. *Journal of Biological Rhythms* *19*, 361–373.
- Hayama, R. (2003). Shedding light on the circadian clock and the photoperiodic control of flowering. *Current Opinion in Plant Biology* *6*, 13–19.
- Hazen, S. P., Schultz, T. F., Pruneda-Paz, J. L., Borevitz, J. O., Ecker, J. R. and Kay, S. A. (2005). LUX ARRHYTHMO encodes a Myb domain protein essential for circadian rhythms. *Proceedings of the National Academy of Sciences* *102*, 10387–10392.
- Helfer, A., Nusinow, D. A., Chow, B. Y., Gehrke, A. R., Bulyk, M. L. and Kay, S. A. (2011). LUX ARRHYTHMO encodes a nighttime repressor of circadian gene expression in the Arabidopsis core clock. *Current Biology* *21*, 126–133.
- Heschel, M. S., Selby, J., Butler, C., Whitelam, G. C., Sharrock, R. A. and Donohue, K. (2007). A new role for phytochromes in temperature-dependent germination. *The New Phytologist* *174*, 735–741.
- Hindmarsh, A. C., Brown, P. N., Grant, K. E., Lee, S. L., Serban, R., Shumaker, D. E. and Woodward, C. S. (2005). SUNDIALS. *ACM Transactions on Mathematical Software* *31*, 363–396.
- Hofmann, N. R. (2012). Alternative splicing links the circadian clock to cold tolerance. *The Plant Cell* *24*, 23–24.
- Holdsworth, M. J., Finch-Savage, W. E., Grappin, P. and Job, D. (2008). Post-genomics dissection of seed dormancy and germination. *Trends in Plant Science* *13*, 7–13.
- Hornitschek, P., Lorrain, S., Zoete, V., Michielin, O. and Fankhauser, C. (2009). Inhibition of the shade avoidance response by formation of non-DNA binding bHLH heterodimers. *The EMBO journal* *28*, 3893–902.
- Huang, W., Pérez-García, P., Pokhilko, A., Millar, A. J., Antoshechkin, I., Riechmann,

Bibliography

- J. L. and Mas, P. (2012). Mapping the core of the Arabidopsis circadian clock defines the network structure of the oscillator. *Science* 336, 75–79.
- Hucka, M., Finney, A., Sauro, H. M., Bolouri, H., Doyle, J. C., Kitano, H., Arkin, A. P., Bornstein, B. J., Bray, D., Cornish-Bowden, A., Cuellar, A. A., Dronov, S., Gilles, E. D., Ginkel, M., Gor, V., Goryanin, I. I., Hedley, W. J., Hodgman, T. C., Hofmeyr, J.-H., Hunter, P. J., Juty, N. S., Kasberger, J. L., Kremling, A., Kummer, U., Le Novere, N., Loew, L. M., Lucio, D., Mendes, P., Minch, E., Mjolsness, E. D., Nakayama, Y., Nelson, M. R., Nielsen, P. F., Sakurada, T., Schaff, J. C., Shapiro, B. E., Shimizu, T. S., Spence, H. D., Stelling, J., Takahashi, K., Tomita, M., Wagner, J. and Wang, J. (2003). The systems biology markup language (SBML): a medium for representation and exchange of biochemical network models. *Bioinformatics* 19, 524–531.
- Hudson, M. E. and Quail, P. H. (2003). Identification of promoter motifs involved in the network of phytochrome A-regulated gene expression by combined analysis of genomic sequence and microarray data. *Plant physiology* 133, 1605–16.
- Hurvich, C. M. and Tsai, C.-l. (1989). Regression and time series model selection in small samples. *Biometrika* 76, 297–307.
- Ishitani, M., Xiong, L., Lee, H., Stevenson, B. and Zhu, J. K. (1998). HOS1, a genetic locus involved in cold-responsive gene expression in arabidopsis. *The Plant Cell* 10, 1151–1161.
- Ito, S., Nakamichi, N., Nakamura, Y., Niwa, Y., Kato, T., Murakami, M., Kita, M., Mizoguchi, T., Niinuma, K., Yamashino, T. and Mizuno, T. (2007). Genetic linkages between circadian clock-associated components and phytochrome-dependent red light signal transduction in Arabidopsis thaliana. 48, 971–983.
- Jaglo, K. R., Kleff, S., Amundsen, K. L., Zhang, X., Haake, V., Zhang, J. Z., Deits, T. and Thomashow, M. F. (2001). Components of the Arabidopsis C-Repeat / Dehydration- Responsive Element Binding Factor Cold-Response Pathway Are Conserved in Brassica napus and Other Plant Species. *Plant Ph* 127, 910–917.
- Jaglo-Ottosen, K. R., Gilmour, S. J., Zarka, D. G., Schabenberger, O. and Thomashow, M. F. (1998). Arabidopsis CBF1 overexpression induces COR genes and enhances freezing tolerance. *Science* 280, 104–106.

Bibliography

- James, A. B., Syed, N. H., Bordage, S., Marshall, J., Nimmo, G. a., Jenkins, G. I., Herzyk, P., Brown, J. W. S. and Nimmo, H. G. (2012). Alternative splicing mediates responses of the Arabidopsis circadian clock to temperature changes. *The Plant Cell* *24*, 961–981.
- Jang, S., Marchal, V., Panigrahi, K. C. S., Wenkel, S., Soppe, W., Deng, X.-W., Valverde, F. and Coupland, G. (2008). Arabidopsis COP1 shapes the temporal pattern of CO accumulation conferring a photoperiodic flowering response. *The EMBO journal* *27*, 1277–1288.
- Jenik, P. D. and Barton, M. K. (2005). Surge and destroy: the role of auxin in plant embryogenesis. *Development (Cambridge, England)* *132*, 3577–85.
- Kaczorowski, K. (2004). Mutants in phytochrome-dependent seedling photomorphogenesis and control of the Arabidopsis circadian clock. Phd University of California, Berkley, CA, USA.
- Kagaya, Y., Ohmiya, K. and Hattori, T. (1999). RAV1, a novel DNA-binding protein, binds to bipartite recognition sequence through two distinct DNA-binding domains uniquely found in higher plants. *Nucleic acids research* *27*, 470–8.
- Kang, H.-G., Kim, J., Kim, B., Jeong, H., Choi, S. H., Kim, E. K., Lee, H.-Y. and Lim, P. O. (2011). Overexpression of FTL1/DDF1, an AP2 transcription factor, enhances tolerance to cold, drought, and heat stresses in Arabidopsis thaliana. *Plant Science* *180*, 634–641.
- Kathryn Blackmond Laskey (2003). Population Markov Chain Monte Carlo. *Machine Learning* *50*, 175–196.
- Kato, T., Murakami, M., Nakamura, Y., Ito, S., Nakamichi, N., Yamashino, T. and Mizuno, T. (2007). Mutants of circadian-associated PRR genes display a novel and visible phenotype as to light responses during de-etiolation of Arabidopsis thaliana seedlings. *Bioscience, biotechnology, and biochemistry* *71*, 834–9.
- Keily, J., Macgregor, D. R., Smith, R. W., Millar, A. J., Halliday, K. J. and Penfield, S. (2013). Model selection reveals control of cold signalling by evening-phased components of the plant circadian clock. *The Plant Journal* *76*, 247–57.
- Kendall, S. L., Hellwege, A., Marriot, P., Whalley, C., Graham, I. a. and Penfield, S. (2011). Induction of dormancy in Arabidopsis summer annuals requires parallel

Bibliography

- regulation of DOG1 and hormone metabolism by low temperature and CBF transcription factors. *The Plant Cell* 23, 2568–2580.
- Kiba, T., Henriques, R., Sakakibara, H. and Chua, N.-H. (2007). Targeted degradation of PSEUDO-RESPONSE REGULATOR5 by an SCFZTL complex regulates clock function and photomorphogenesis in *Arabidopsis thaliana*. *The Plant Cell* 19, 2516–2530.
- Kidokoro, S., Maruyama, K., Nakashima, K., Imura, Y., Narusaka, Y., Shinwari, Z. K., Osakabe, Y., Fujita, Y., Mizoi, J., Shinozaki, K. and Yamaguchi-Shinozaki, K. (2009). The phytochrome-interacting factor PIF7 negatively regulates DREB1 expression under circadian control in *Arabidopsis*. *Plant Physiology* 151, 2046–2057.
- Kim, J.-Y., Song, H.-R., Taylor, B. L. and Carré, I. A. (2003). Light-regulated translation mediates gated induction of the *Arabidopsis* clock protein LHY. *The EMBO journal* 22, 935–944.
- Kim, S. Y., Chung, H. J. and Thomas, T. L. (1997). Isolation of a novel class of bZIP transcription factors that interact with ABA-responsive and embryo-specification elements in the Dc3 promoter using a modified yeast one-hybrid system. *The Plant journal : for cell and molecular biology* 11, 1237–51.
- Kim, W.-Y., Fujiwara, S., Suh, S.-S., Kim, J., Kim, Y., Han, L., David, K., Putterill, J., Nam, H. G. and Somers, D. E. (2007). ZEITLUPE is a circadian photoreceptor stabilized by GIGANTEA in blue light. *Nature* 449, 356–360.
- Kirkpatrick, S., Gelatt, C. D. and Vecchi, M. P. (1983). Optimization by simulated annealing. *Science* 220, 671–680.
- Kitano, H. (2002). Systems biology: a brief overview. *Science* 295, 1662–1664.
- Knight, H., Trewavas, A. J. and Knight, M. R. (1996). Cold calcium signaling in *Arabidopsis* involves two cellular pools and a change in calcium signature after acclimation. *The Plant Cell* 8, 489–503.
- Kolmos, E., Nowak, M., Werner, M., Fischer, K., Schwarz, G., Mathews, S., Schoof, H., Nagy, F., Bujnicki, J. M. and Davis, S. J. (2009). Integrating ELF4 into the circadian system through combined structural and functional studies. *HFSP journal* 3, 350–366.

Bibliography

- Koornneef, M. and Meinke, D. (2010). The development of Arabidopsis as a model plant. *The Plant Journal* 61, 909–921.
- Krishnan, N., Kretschmar, D., Rakshit, K., Chow, E. and Giebultowicz, J. M. (2009). The circadian clock gene period extends healthspan in aging *Drosophila melanogaster*. *Aging* 1, 937–948.
- Kullback, S. and Leibler, R. A. (1951). On information and sufficiency. *The Annals of Mathematical Statistics* 22, 79–86.
- Kumar, M., Husian, M., Upreti, N. and Gupta, D. (2010). GENETIC ALGORITHM : REVIEW AND APPLICATION. 2, 451–454.
- Kurkela, S. and Franck, M. (1990). Cloning and characterization of a cold-and ABA-inducible Arabidopsis gene. *Plant Molecular Biology* 15, 137–144.
- Kurkela, S., Franck, M., Heino, P., Lfing, V. and Palva, E. T. (1988). Cold induced gene expression in Arabidopsis thaliana L. *Plant Cell Reports* 7, 495–498.
- Kurosawa, G., Mochizuki, A. and Iwasa, Y. (2002). Comparative study of circadian clock models, in search of processes promoting oscillation. *Journal of Theoretical Biology* 216, 193–208.
- Kurtar, E. (2010). Modelling the effect of temperature on seed germination in some cucurbits. *African Journal of Biotechnology* 9, 1343–1353.
- Laibach, F. (1943). Arabidopsis thaliana (L.) Heynh. als object fur genetische und entwicklungsphysiologische untersuchungen. *Bot. Archiv* 44, 439–455.
- Lamb, R. S., Hill, T. A., Tan, Q. K.-G. and Irish, V. F. (2002). Regulation of APETALA3 floral homeotic gene expression by meristem identity genes. *Development* 129, 2079–86.
- Lauvergeat, V., Lacomme, C., Lacombe, E., Lasserre, E., Roby, D. and Grima-Pettenati, J. (2001). Two cinnamoyl-CoA reductase (CCR) genes from Arabidopsis thaliana are differentially expressed during development and in response to infection with pathogenic bacteria. *Phytochemistry* 57, 1187–1195.
- Leardi, R. (2007). Genetic algorithms in chemistry. *Journal of chromatography. A* 1158, 226–33.

Bibliography

- Lee, B.-h. (2002). A mitochondrial complex I defect impairs cold-regulated nuclear gene expression. *The Plant Cell* *14*, 1235–1251.
- Lee, C.-M. and Thomashow, M. F. (2012). Photoperiodic regulation of the C-repeat binding factor (CBF) cold acclimation pathway and freezing tolerance in *Arabidopsis thaliana*. *Proceedings of the National Academy of Sciences* *11*, 15054–15059.
- Lee, H., Xiong, L., Gong, Z., Ishitani, M., Stevenson, B. and Zhu, J. K. (2001). The *Arabidopsis* HOS1 gene negatively regulates cold signal transduction and encodes a RING finger protein that displays cold-regulated nucleo-cytoplasmic partitioning. *Genes & Development* *15*, 912–924.
- Lee, J. H., Yoo, S. J., Park, S. H., Hwang, I., Lee, J. S. and Ahn, J. H. (2007). Role of SVP in the control of flowering time by ambient temperature in *Arabidopsis*. *Genes & Development* *21*, 397–402.
- Leivar, P., Monte, E., Al-Sady, B., Carle, C., Storer, A., Alonso, J. M., Ecker, J. R. and Quail, P. H. (2008). The *Arabidopsis* phytochrome-interacting factor PIF7, together with PIF3 and PIF4, regulates responses to prolonged red light by modulating phyB levels. *The Plant cell* *20*, 337–52.
- Leloup, J.-C. and Goldbeter, A. (1998). A model for circadian rhythms in *Drosophila* incorporating the formation of a complex between the PER and TIM proteins. *Journal of Biological Rhythms* *13*, 70–87.
- Leloup, J.-C. and Goldbeter, A. (2003). Toward a detailed computational model for the mammalian circadian clock. *Proceedings of the National Academy of Sciences* *100*, 7051–7056.
- Leloup, J.-C., Gonze, D. and Goldbeter, A. (1999). Limit cycle models for circadian rhythms based on transcriptional regulation in *drosophila* and *neurospora*. *Journal of Biological Rhythms* *14*, 433–448.
- Leyser, O. and Day, S. (2009). *Mechanisms in Plant Development*. John Wiley & Sons.
- Liu, Q., Kasuga, M., Sakuma, Y., Abe, H., Miura, S., Yamaguchi-Shinozaki, K. and Shinozaki, K. (1998). Two transcription factors, DREB1 and DREB2, with an EREBP/AP2 DNA binding domain separate two cellular signal transduction pathways in drought- and low-temperature-responsive gene expression, respectively, in *Arabidopsis*. *The Plant Cell* *10*, 1391–1406.

Bibliography

- Liu, X. L. (2001). ELF3 encodes a circadian clock-regulated nuclear protein that functions in an Arabidopsis PHYB signal transduction pathway. *THE PLANT CELL ONLINE* 13, 1293–1304.
- Locke, J. C. W., Kozma-Bognár, L., Gould, P. D., Fehér, B., Kevei, E., Nagy, F., Turner, M. S., Hall, A. and Millar, A. J. (2006). Experimental validation of a predicted feedback loop in the multi-oscillator clock of Arabidopsis thaliana. *Molecular Systems Biology* 2, 59–64.
- Locke, J. C. W., Millar, A. J. and Turner, M. S. (2005a). Modelling genetic networks with noisy and varied experimental data: the circadian clock in Arabidopsis thaliana. *Journal of Theoretical Biology* 234, 383–393.
- Locke, J. C. W., Southern, M. M., Kozma-Bognár, L., Hibberd, V., Brown, P. E., Turner, M. S. and Millar, A. J. (2005b). Extension of a genetic network model by iterative experimentation and mathematical analysis. *Molecular Systems Biology* 1, 2005.0013.
- Lu, S. X., Webb, C. J., Knowles, S. M., Kim, S. H. J., Wang, Z. and Tobin, E. M. (2012). CCA1 and ELF3 Interact in the control of hypocotyl length and flowering time in Arabidopsis. *Plant physiology* 158, 1079–88.
- Lu, Y., Gehan, J. P. and Sharkey, T. D. (2005). Daylength and Circadian Effects on Starch Degradation and Maltose Metabolism 1. *Plant Physiology* 138, 2280–2291.
- Makino, S., Matsushika, A., Kojima, M., Yamashino, T. and Mizuno, T. (2002). The APRR1/TOC1 quintet implicated in circadian rhythms of Arabidopsis thaliana: I. Characterization with APRR1-overexpressing plants. *Plant & cell physiology* 43, 58–69.
- Más, P. (2005). Circadian clock signaling in Arabidopsis thaliana: from gene expression to physiology and development. *The International Journal of Developmental Biology* 49, 491–500.
- Más, P., Alabadi, D., Yanovsky, M. J., Oyama, T. and Kay, S. A. (2003a). Dual role of TOC1 in the control of circadian and photomorphogenic responses in Arabidopsis. *The Plant Cell* 15, 223–236.
- Más, P., Kim, W.-Y., Somers, D. E. and Kay, S. A. (2003b). Targeted degradation of

Bibliography

- TOC1 by ZTL modulates circadian function in *Arabidopsis thaliana*. *Nature* *426*, 567–570.
- Mathieu, J., Warthmann, N., Küttner, F. and Schmid, M. (2007). Export of FT protein from phloem companion cells is sufficient for floral induction in *Arabidopsis*. *Current biology : CB* *17*, 1055–60.
- Matsushika, A. (2000). Circadian waves of expression of the APRR1/TOC1 family of pseudo-response regulators in *Arabidopsis thaliana*: insight into the plant circadian clock. *Plant & Cell Physiology* *41*, 1002–1012.
- McClung, C. R. and Davis, S. J. (2010). Ambient thermometers in plants: From physiological outputs towards mechanisms of thermal sensing. *Current Biology* *20*, 1086–1092.
- McWatters, H. G., Kolmos, E., Hall, A., Doyle, M. R., Amasino, R. M., Gyula, P., Nagy, F., Millar, A. J. and Davis, S. J. (2007). ELF4 is required for oscillatory properties of the circadian clock. *Plant Physiology* *144*, 391–401.
- Medina, J. (1999). The *Arabidopsis* CBF gene family is composed of three genes encoding AP2 domain-containing proteins whose expression is regulated by low temperature but not by abscisic acid or dehydration. *Plant Physiology* *119*, 463–470.
- Mehra, A., Baker, C. L., Loros, J. J. and Dunlap, J. C. (2009). Post-translational modifications in circadian rhythms. *Trends in Biochemical Sciences* *34*, 483–490.
- Mendes, P. and Kell, D. (1998). Non-linear optimization of biochemical pathways: applications to metabolic engineering and parameter estimation. *Bioinformatics* *14*, 869–883.
- Menkens, a. E. and Cashmore, a. R. (1994). Isolation and characterization of a fourth *Arabidopsis thaliana* G-box-binding factor, which has similarities to Fos oncoprotein. *Proceedings of the National Academy of Sciences of the United States of America* *91*, 2522–6.
- Michael, T. P., Mockler, T. C., Breton, G., McEntee, C., Byer, A., Trout, J. D., Hazen, S. P., Shen, R., Priest, H. D., Sullivan, C. M., Givan, S. A., Yanovsky, M., Hong, F., Kay, S. A. and Chory, J. (2008). Network discovery pipeline elucidates conserved time-of-day-specific cis-regulatory modules. *PLoS Genetics* *4*, e14.

Bibliography

- Michael, T. P., Salomé, P. A., Yu, H. J., Spencer, T. R., Sharp, E. L., McPeck, M. A., Alonso, J. M., Ecker, J. R. and McClung, C. R. (2003). Enhanced fitness conferred by naturally occurring variation in the circadian clock. *Science* *302*, 1049–1053.
- Mihalcescu, I., Hsing, W. and Leibler, S. (2004). Resilient circadian oscillator revealed in individual cyanobacteria. *Nature* *430*, 81–85.
- Millar, A. J. (2004). Input signals to the plant circadian clock. *Journal of Experimental Botany* *55*, 277–83.
- Millar, A. J. and Kay, S. A. (1996). Integration of circadian and phototransduction pathways in the network controlling CAB gene transcription in Arabidopsis. *Proceedings of the National Academy of Sciences* *93*, 15491–1546.
- Ming Gong, A. H. v. d. L. (1998). Heat-shock-induced changes in intracellular Ca²⁺ level in tobacco seedlings in relation to thermotolerance. *Plant Physiology* *116*, 429–437.
- Mitchell, M. (1998). *An Introduction to Genetic Algorithms (Complex Adaptive Systems)*. MIT Press.
- Miura, K., Jin, J. B., Lee, J., Yoo, C. Y., Stirn, V., Miura, T., Ashworth, E. N., Bressan, R. A., Yun, D.-J. and Hasegawa, P. M. (2007). SIZ1-mediated sumoylation of ICE1 controls CBF3/DREB1A expression and freezing tolerance in Arabidopsis. *The Plant Cell* *19*, 1403–1414.
- Miyata, K., Calviño, M., Oda, A. O., Sugiyama, H. and Mizoguchi, T. (2011). Suppression of late-flowering and semi-dwarf phenotypes in the Arabidopsis clock mutant *lhy-12;cca1-101* by *phyB* under continuous light. *Plant Signaling & Behavior* *6*, 1162–1171.
- Mizoguchi, T., Wheatley, K., Hanzawa, Y., Wright, L., Mizoguchi, M., Song, H. R., Carré, I. A. and Coupland, G. (2002). LHY and CCA1 are partially redundant genes required to maintain circadian rhythms in Arabidopsis. *Developmental cell* *2*, 629–41.
- Mizoguchi, T., Wright, L., Fujiwara, S., Cremer, F., Lee, K., Onouchi, H., Mouradov, A., Fowler, S., Kamada, H., Putterill, J. and Coupland, G. (2005). Distinct roles of GIGANTEA in promoting flowering and regulating circadian rhythms in Arabidopsis. *The Plant Cell* *17*, 2255–2270.

Bibliography

- Mockler, T. C., Michael, T. P., Priest, H. D., Shen, R., Sullivan, C. M., Givan, S. A., McEntee, C., Kay, S. A. and Chory, J. (2007). The DIURNAL project: DIURNAL and circadian expression profiling, model-based pattern matching, and promoter analysis. *Cold Spring Harbor symposia on quantitative biology* *72*, 353–363.
- Moles, C. G., Mendes, P. and Banga, J. R. (2003). Parameter estimation in biochemical pathways: a comparison of global optimization methods. *Genome Research* *13*, 2467–2474.
- Morcuende, R., Osuna, D., Bla, O. E., Ho, M. and Thimm, O. (2005). Sugars and Circadian Regulation Make Major Contributions to the Global Regulation of Diurnal Gene Expression in Arabidopsis. *The Plant Cell* *17*, 3257–3281.
- Motulsky, H. and Christopoulos, A. (2003). *Fitting Models to Biological Data using Linear and Nonlinear Regression. A practical guide to curve fitting.* 4 edition, Oxford University Press, Oxford.
- Nagashima, A., Hanaoka, M., Shikanai, T., Fujiwara, M., Kanamaru, K., Takahashi, H. and Tanaka, K. (2004). The multiple-stress responsive plastid sigma factor, SIG5, directs activation of the psbD blue light-responsive promoter (BLRP) in Arabidopsis thaliana. *Plant & cell physiology* *45*, 357–68.
- Nagoshi, E., Saini, C., Bauer, C., Laroche, T., Naef, F., Schibler, U., Ansermet, Q. E., Boveresses, C. and Epalinges, C. (2004). Circadian gene expression in individual fibroblasts: Oscillators pass time to daughter cells. *Cell* *119*, 693–705.
- Nakamichi, N., Kiba, T., Henriques, R., Mizuno, T., Chua, N.-H. and Sakakibara, H. (2010). PSEUDO-RESPONSE REGULATORS 9, 7, and 5 are transcriptional repressors in the Arabidopsis circadian clock. *The Plant Cell* *22*, 594–605.
- Nakamichi, N., Kita, M., Ito, S., Yamashino, T. and Mizuno, T. (2005). PSEUDO-RESPONSE REGULATORS, PRR9, PRR7 and PRR5, together play essential roles close to the circadian clock of Arabidopsis thaliana. *Plant & Cell Physiology* *46*, 686–698.
- Nakamichi, N., Kita, M., Niinuma, K., Ito, S., Yamashino, T., Mizoguchi, T. and Mizuno, T. (2007). Arabidopsis clock-associated pseudo-response regulators PRR9, PRR7 and PRR5 coordinately and positively regulate flowering time through the

Bibliography

canonical CONSTANS-dependent photoperiodic pathway. *Plant & Cell Physiology* *48*, 822–832.

Nakamichi, N., Kusano, M., Fukushima, A., Kita, M., Ito, S., Yamashino, T., Saito, K., Sakakibara, H. and Mizuno, T. (2009). Transcript profiling of an Arabidopsis PSEUDO RESPONSE REGULATOR arrhythmic triple mutant reveals a role for the circadian clock in cold stress response. *Plant & Cell Physiology* *50*, 447–462.

Nakano, T., Suzuki, K., Fujimura, T. and Shinshi, H. (2006). Genome-Wide Analysis of the ERF Gene Family in Arabidopsis and Rice. *Plant Physiology* *140*, 411–432.

Nelson, D. C., Riseborough, J.-A., Flematti, G. R., Stevens, J., Ghisalberti, E. L., Dixon, K. W. and Smith, S. M. (2009). Karrikins discovered in smoke trigger Arabidopsis seed germination by a mechanism requiring gibberellic acid synthesis and light. *Plant Physiology* *149*, 863–873.

Ni, Z., Kim, E.-D., Ha, M., Lackey, E., Liu, J., Zhang, Y., Sun, Q. and Chen, Z. J. (2009). Altered circadian rhythms regulate growth vigour in hybrids and allopolyploids. *Nature* *457*, 327–31.

Niwa, Y., Yamashino, T. and Mizuno, T. (2009). The circadian clock regulates the photoperiodic response of hypocotyl elongation through a coincidence mechanism in Arabidopsis thaliana. *Plant & Cell Physiology* *50*, 838–54.

Noordally, Z. B., Ishii, K., Atkins, K. A., Wetherill, S. J., Kusakina, J., Walton, E. J., Kato, M., Azuma, M., Tanaka, K., Hanaoka, M. and Dodd, A. N. (2013). Circadian control of chloroplast transcription by a nuclear-encoded timing signal. *Science* *339*, 1316–9.

Nordborg, M. and Bergelson, J. (1999). The effect of seed and rosette cold treatment on germination and flowering time in some Arabidopsis thaliana (Brassicaceae) ecotypes. *American Journal of Botany* *86*, 470–475.

Nover, L., Bharti, K., Döring, P., Mishra, S. K., Ganguli, A. and Scharf, K. D. (2001). Arabidopsis and the heat stress transcription factor world: how many heat stress transcription factors do we need? *Cell stress & chaperones* *6*, 177–89.

Novillo, F., Alonso, J. M., Ecker, J. R. and Salinas, J. (2004). CBF2/DREB1C is a negative regulator of CBF1/DREB1B and CBF3/DREB1A expression and plays a

Bibliography

central role in stress tolerance in Arabidopsis. *Proceedings of the National Academy of Sciences* *101*, 3985–3990.

Novillo, F., Medina, J. and Salinas, J. (2007). Arabidopsis CBF1 and CBF3 have a different function than CBF2 in cold acclimation and define different gene classes in the CBF regulon. *Proceedings of the National Academy of Sciences* *104*, 21002–21007.

Nozue, K., Covington, M. F., Duek, P. D., Lorrain, S., Fankhauser, C., Harmer, S. L. and Maloof, J. N. (2007). Rhythmic growth explained by coincidence between internal and external cues. *Nature* *448*, 358–361.

Nozue, K., Harmer, S. L. and Maloof, J. N. (2011). Genomic analysis of circadian clock-, light-, and growth-correlated genes reveals PHYTOCHROME-INTERACTING FACTOR5 as a modulator of auxin signaling in Arabidopsis. *Plant physiology* *156*, 357–72.

Nusinow, D. A., Helfer, A., Hamilton, E. E., King, J. J., Imaizumi, T., Schultz, T. F., Farré, E. M. and Kay, S. A. (2011). The ELF4-ELF3-LUX complex links the circadian clock to diurnal control of hypocotyl growth. *Nature* *13*, 398–402.

Oliverio, K. A., Crepy, M., Martin-Tryon, E. L., Milich, R., Harmer, S. L., Putterill, J., Yanovsky, M. J. and Casal, J. J. (2007). GIGANTEA regulates phytochrome A-mediated photomorphogenesis independently of its role in the circadian clock. *Plant physiology* *144*, 495–502.

Onai, K. and Ishiura, M. (2005). PHYTOCLOCK 1 encoding a novel GARP protein essential for the Arabidopsis circadian clock. *Genes to Cells* *10*, 963–972.

O'Neill, J. S., van Ooijen, G., Le Bihan, T. and Millar, A. J. (2011). Circadian clock parameter measurement: characterization of clock transcription factors using surface plasmon resonance. *Journal of Biological Rhythms* *26*, 91–98.

Orvar, B. L., Sangwan, V., Omann, F. and Dhindsa, R. S. (2000). Early steps in cold sensing by plant cells: the role of actin cytoskeleton and membrane fluidity. *The Plant Journal* *23*, 785–794.

Ouyang, Y., Andersson, C. R., Kondo, T., Golden, S. S. and Johnson, C. H. (1998). Resonating circadian clocks enhance fitness in cyanobacteria. *Proceedings of the National Academy of Sciences* *95*, 8660–8664.

Bibliography

- Park, D. H. (1999). Control of Circadian Rhythms and Photoperiodic Flowering by the Arabidopsis GIGANTEA Gene. *Science* 285, 1579–1582.
- Penfield, S. and Hall, A. (2009). A role for multiple circadian clock genes in the response to signals that break seed dormancy in Arabidopsis. *The Plant Cell* 21, 1722–1732.
- Penfield, S., Josse, E.-m., Kannangara, R., Gilday, A. D., Halliday, K. J. and Graham, I. A. (2005). Cold and Light Control Seed Germination through the bHLH Transcription Factor SPATULA. *Current* 15, 1998–2006.
- Pokhilko, A., Fernández, A. P. n., Edwards, K. D., Southern, M. M., Halliday, K. J. and Millar, A. J. (2012). The clock gene circuit in Arabidopsis includes a repressilator with additional feedback loops. *Molecular Systems Biology* 8, 574.
- Pokhilko, A., Hodge, S. K., Stratford, K., Knox, K., Edwards, K. D., Thomson, A. W., Mizuno, T. and Millar, A. J. (2010). Data assimilation constrains new connections and components in a complex, eukaryotic circadian clock model. *Molecular Systems Biology* 6, 416–425.
- Pruneda-Paz, J. L., Breton, G., Para, A. and Kay, S. A. (2009). A functional genomics approach reveals CHE as a component of the Arabidopsis circadian clock. *Science* 323, 1481–1485.
- Radenski, A. (2012). Applications of Evolutionary Computation, vol. 7248, of Lecture Notes in Computer Science. Springer Berlin Heidelberg, Berlin, Heidelberg.
- Raikhel, N. (1992). Nuclear targeting in plants. *Plant physiology* 100, 1627–32.
- Reymond, P. and Farmer, E. E. (1998). Jasmonate and salicylate as global signals for defense gene expression. *Current opinion in plant biology* 1, 404–11.
- Robertson, F. C., Skeffington, A. W., Gardner, M. J. and Webb, A. a. R. (2009). Interactions between circadian and hormonal signalling in plants. *Plant Molecular Biology* 69, 419–427.
- Roden, L. C. and Ingle, R. A. (2009). Lights, rhythms, infection: the role of light and the circadian clock in determining the outcome of plant-pathogen interactions. *The Plant cell* 21, 2546–52.
- Rojas, R. (1996). Neutral Networks: A Systematic Introduction. Springer.

Bibliography

- Sakuma, Y., Liu, Q., Dubouzet, J. G., Abe, H., Shinozaki, K. and Yamaguchi-Shinozaki, K. (2002). DNA-binding specificity of the ERF/AP2 domain of Arabidopsis DREBs, transcription factors involved in dehydration- and cold-inducible gene expression. *Biochemical and biophysical research communications* 290, 998–1009.
- Salomé, P. A. and McClung, C. R. (2005). PSEUDO-RESPONSE REGULATOR 7 and 9 are partially redundant genes essential for the temperature responsiveness of the Arabidopsis circadian clock. *The Plant Cell* 17, 791–803.
- Sanchez, S. E., Petrillo, E., Beckwith, E. J., Zhang, X., Rugnone, M. L., Hernando, C. E., Cuevas, J. C., Godoy Herz, M. A., Depetris-Chauvin, A., Simpson, C. G., Brown, J. W. S., Cerdán, P. D., Borevitz, J. O., Mas, P., Ceriani, M. F., Kornblihtt, A. R. and Yanovsky, M. J. (2010). A methyl transferase links the circadian clock to the regulation of alternative splicing. *Nature* 468, 112–116.
- Sangwan, V., Orvar, B. L., Beyerly, J., Hirt, H. and Dhindsa, R. S. (2002). Opposite changes in membrane fluidity mimic cold and heat stress activation of distinct plant MAP kinase pathways. *The Plant Journal* 31, 629–638.
- Satoh, R., Fujita, Y., Nakashima, K., Shinozaki, K. and Yamaguchi-Shinozaki, K. (2004). A novel subgroup of bZIP proteins functions as transcriptional activators in hypoosmolarity-responsive expression of the ProDH gene in Arabidopsis. *Plant & cell physiology* 45, 309–17.
- Sauerbrunn, N. and Schlaich, N. L. (2004). PCC1: a merging point for pathogen defence and circadian signalling in Arabidopsis. *Planta* 218, 552–61.
- Sawa, M., Nusinow, D. A., Kay, S. A. and Imaizumi, T. (2007). FKF1 and GIGANTEA complex formation is required for day-length measurement in Arabidopsis. *Science (New York, N.Y.)* 318, 261–5.
- Schaffer, R., Ramsay, N., Samach, A., Corden, S., Putterill, J., Carré, I. a. and Coupland, G. (1998). The late elongated hypocotyl mutation of Arabidopsis disrupts circadian rhythms and the photoperiodic control of flowering. *Cell* 93, 1219–1229.
- Schmuths, H., Bachmann, K., Weber, W. E., Horres, R. and Hoffmann, M. H. (2006). Effects of Preconditioning and Temperature During Germination of 73 Natural Accessions of Arabidopsis thaliana. *Annals of Botany* 97, 623–634.

Bibliography

- Schwarz, G. (1978). Estimating the dimension of a model. *The Annals of Statistics* 6, 461–464.
- Seo, P. J., Park, M.-J., Lim, M.-H., Kim, S.-G., Lee, M., Baldwin, I. T. and Park, C.-M. (2012). A self-regulatory circuit of CIRCADIAN CLOCK-ASSOCIATED1 underlies the circadian clock regulation of temperature responses in Arabidopsis. *The Plant Cell* 24, 2427–2442.
- Serban, R. and Hindmarsh, A. C. (2005). CVODES: the Sensitivity-Enabled ODE Solver in SUNDIALS. *Proceedings of IDETC/CIE* 1, 25–28.
- Sessa, G., Morelli, G. and Ruberti, I. (1993). The Athb-1 and -2 HD-Zip domains homodimerize forming complexes of different DNA binding specificities. *The EMBO journal* 12, 3507–17.
- Shacklock, P. S., Read, N. D. and Trewavas, A. J. (1992). Cytosolic free calcium mediates red light-induced photomorphogenesis. *Nature* 358, 753–755.
- Shinozaki, K. (2000). Molecular responses to dehydration and low temperature: differences and cross-talk between two stress signaling pathways. *Current opinion in plant biology* 3, 217–23.
- Shinwari, Z. K., Nakashima, K., Miura, S., Kasuga, M., Seki, M., Yamaguchi-Shinozaki, K. and Shinozaki, K. (1998). An Arabidopsis gene family encoding DRE/CRT binding proteins involved in low-temperature-responsive gene expression. *Biochemical and Biophysical Research Communications* 250, 161–170.
- Somers, D. E., Kim, W.-Y. and Geng, R. (2004). The F-box protein ZEITLUPE confers dosage-dependent control on the circadian clock, photomorphogenesis, and flowering time. *The Plant Cell* 16, 769–782.
- Somers, D. E., Webb, a. a., Pearson, M. and Kay, S. a. (1998). The short-period mutant, *toc1-1*, alters circadian clock regulation of multiple outputs throughout development in *Arabidopsis thaliana*. *Development* 125, 485–494.
- Somerville, C. and Koornneef, M. (2002). A fortunate choice: the history of Arabidopsis as a model plant. *Nature reviews. Genetics* 3, 883–9.
- Spiegel, K., Leproult, R. and Cauter, E. V. (1999). Early report Impact of sleep debt on metabolic and endocrine function. *Lancet* 354, 1435–1439.

Bibliography

- Stockinger, E. J. (1997). *Arabidopsis thaliana* CBF1 encodes an AP2 domain-containing transcriptional activator that binds to the C-repeat/DRE, a cis-acting DNA regulatory element that stimulates transcription in response to low temperature and water deficit. *Proceedings of the National Academy of Sciences* *94*, 1035–1040.
- Strasser, B., Alvarez, M. J., Califano, A. and Cerdán, P. D. (2009). A complementary role for ELF3 and TFL1 in the regulation of flowering time by ambient temperature. *The Plant journal : for cell and molecular biology* *58*, 629–40.
- Suárez-López, P., Wheatley, K., Robson, F., Onouchi, H., Valverde, F. and Coupland, G. (2001). CONSTANS mediates between the circadian clock and the control of flowering in *Arabidopsis*. *Nature* *410*, 1116–20.
- Sugano, S., Andronis, C., Green, R. M., Wang, Z. Y. and Tobin, E. M. (1998). Protein kinase CK2 interacts with and phosphorylates the *Arabidopsis* circadian clock-associated 1 protein. *Proceedings of the National Academy of Sciences* *95*, 11020–11025.
- Sweeney, B. M. and Haxo, F. T. (1961). Persistence of a Photosynthetic Rhythm in Eucleated *Acetabularia*. *Science* *134*, 1361–3.
- Taherdangkoo, M., Paziresh, M., Yazdi, M. and Bagheri, M. H. (2012). An efficient algorithm for function optimization: modified stem cells algorithm. *Central European Journal of Engineering* *3*, 36–50.
- Teakle, G. R., Manfield, I. W., Graham, J. F. and Gilmartin, P. M. (2002). *Arabidopsis thaliana* GATA factors: organisation, expression and DNA-binding characteristics. *Plant molecular biology* *50*, 43–57.
- The *Arabidopsis* Genome Initiative (2000). Analysis of the genome sequence of the flowering plant *Arabidopsis thaliana*. *Nature* *408*, 796–815.
- Thomashow, M. F. (1998). Role of cold-responsive genes in plant freezing tolerance. *Plant Physiology* *118*, 1–8.
- Thomashow, M. F. (1999). Plant cold acclimation: Freezing tolerance genes and regulatory mechanisms. *Annual Review of Plant Physiology and Plant Molecular Biology* *50*, 571–599.

Bibliography

- Tremousaygue, D., Manevski, A., Bardet, C., Lescure, N. and Lescure, B. (1999). Plant interstitial telomere motifs participate in the control of gene expression in root meristems. *The Plant journal : for cell and molecular biology* 20, 553–61.
- Tsunoyama, Y., Ishizaki, Y., Morikawa, K., Kobori, M., Nakahira, Y., Takeba, G., Toyoshima, Y. and Shiina, T. (2004). Blue light-induced transcription of plastid-encoded psbD gene is mediated by a nuclear-encoded transcription initiation factor, AtSig5. *Proceedings of the National Academy of Sciences of the United States of America* 101, 3304–9.
- Turek, F. W., Joshu, C., Kohsaka, A., Lin, E., Ivanova, G., McDearmon, E., Laposky, A., Losee-Olson, S., Easton, A., Jensen, D. R., Eckel, R. H., Takahashi, J. S. and Bass, J. (2005). Obesity and metabolic syndrome in circadian Clock mutant mice. *Science* 308, 1043–1045.
- Ulmasov, T., Hagen, G. and Guilfoyle, T. J. (1999). Dimerization and DNA binding of auxin response factors. *The Plant journal : for cell and molecular biology* 19, 309–19.
- Vaistij, F. E., Gan, Y., Penfield, S., Gilday, A. D., Dave, A., He, Z., Josse, E.-M., Choi, G., Halliday, K. J. and Graham, I. a. (2013). Differential control of seed primary dormancy in Arabidopsis ecotypes by the transcription factor SPATULA. *Proceedings of the National Academy of Sciences of the United States of America* 110, 10866–71.
- Valle, Y., Member, S., Venayagamoorthy, G. K., Member, S. and Harley, R. G. (2008). Particle Swarm Optimization : Basic Concepts , Variants and Applications in Power Systems. *IEEE TRANSACTIONS ON EVOLUTIONARY COMPUTATION* 12, 171–195.
- Valverde, F., Mouradov, A., Soppe, W., Ravenscroft, D., Samach, A. and Coupland, G. (2004). Photoreceptor regulation of CONSTANS protein in photoperiodic flowering. *Science* 303, 1003–1006.
- Vinh, N. X., Chetty, M., Coppel, R., Gaudana, S. and Wangikar, P. P. (2013). A model of the circadian clock in the cyanobacterium *Cyanothece* sp. ATCC 51142. *BMC bioinformatics* 14 Suppl 2, S14.
- Wang, G.-Y., Shi, J.-L., Ng, G., Battle, S. L., Zhang, C. and Lu, H. (2011). Circadian clock-regulated phosphate transporter PHT4;1 plays an important role in Arabidopsis defense. *Molecular plant* 4, 516–26.

Bibliography

- Wang, H., Ma, L. G., Li, J. M., Zhao, H. Y. and Deng, X. W. (2001). Direct interaction of Arabidopsis cryptochromes with COP1 in light control development. *Science* 294, 154–158.
- Wang, L., Fujiwara, S. and Somers, D. E. (2010). PRR5 regulates phosphorylation, nuclear import and subnuclear localization of TOC1 in the Arabidopsis circadian clock. *The EMBO journal* 29, 1903–1915.
- Wang, Z., Triezenberg, S. J., Thomashow, M. F. and Stockinger, E. J. (2005). Multiple hydrophobic motifs in Arabidopsis CBF1 COOH-terminus provide functional redundancy in trans-activation. *Plant molecular biology* 58, 543–59.
- Wang, Z. Y. and Tobin, E. M. (1998). Constitutive expression of the CIRCADIAN CLOCK ASSOCIATED 1 (CCA1) gene disrupts circadian rhythms and suppresses its own expression. *Cell* 93, 1207–1217.
- Wigge, P. A., Kim, M. C., Jaeger, K. E., Busch, W., Schmid, M., Lohmann, J. U. and Weigel, D. (2005). Integration of spatial and temporal information during floral induction in Arabidopsis. *Science* 309, 1056–9.
- Yamaguchi-Shinozaki, K. and Shinozaki, K. (1994). A novel cis-acting element in an Arabidopsis gene is involved in responsiveness to drought, low-temperature, or high-salt stress. *The Plant Cell* 6, 251–264.
- Yamamoto, Y., Sato, E., Shimizu, T., Nakamich, N., Sato, S., Kato, T., Tabata, S., Nagatani, A., Yamashino, T. and Mizuno, T. (2003). Comparative genetic studies on the APRR5 and APRR7 genes belonging to the APRR1/TOC1 quintet implicated in circadian rhythm, control of flowering time, and early photomorphogenesis. *Plant & cell physiology* 44, 1119–30.
- Yu, D., Chen, C. and Chen, Z. (2001). Evidence for an important role of WRKY DNA binding proteins in the regulation of NPR1 gene expression. *The Plant cell* 13, 1527–40.
- Yu, J.-W., Rubio, V., Lee, N.-Y., Bai, S., Lee, S.-Y., Kim, S.-S., Liu, L., Zhang, Y., Irigoyen, M. L., Sullivan, J. A., Zhang, Y., Lee, I., Xie, Q., Paek, N.-C. and Deng, X. W. (2008). COP1 and ELF3 control circadian function and photoperiodic flowering by regulating GI stability. *Molecular Cell* 32, 617–630.
- Zeilinger, M. N., Farré, E. M., Taylor, S. R., Kay, S. A. and Doyle, F. J. (2006). A

Bibliography

novel computational model of the circadian clock in Arabidopsis that incorporates PRR7 and PRR9. *Molecular Systems Biology* 2, 58–71.

Zhang, C., Xie, Q., Anderson, R. G., Ng, G., Seitz, N. C., Peterson, T., McClung, C. R., McDowell, J. M., Kong, D., Kwak, J. M. and Lu, H. (2013). Crosstalk between the circadian clock and innate immunity in Arabidopsis. *PLoS pathogens* 9, e1003370.

Zhang, X., Fowler, S. G., Cheng, H., Lou, Y., Rhee, S. Y., Stockinger, E. J. and Thomashow, M. F. (2004). Freezing-sensitive tomato has a functional CBF cold response pathway, but a CBF regulon that differs from that of freezing-tolerant Arabidopsis. *The Plant journal : for cell and molecular biology* 39, 905–19.

Zhu, J.-K. (2002). Salt and drought stress signal transduction in plants. *Annual Review of Plant Biology* 53, 247–273.